AIRFLOW IN WAVING PLANT CANOPIES

by

J.J. FINNIGAN

A THESIS SUBMITTED TO

THE AUSTRALIAN NATIONAL UNIVERSITY

FOR THE DEGREE OF

DOCTOR OF PHILOSOPHY

SEPTEMBER 1978

Preface

The aim of the work described in this thesis was to achieve a clearer understanding of the turbulent airflow within plant canopies and its interaction with the atmospheric boundary layer. The study was motivated by the interest of the CSIRO Division of Environmental Mechanics in extending the well established theory of micrometeorology over relatively smooth, uniform surfaces to more heterogeneous situations. The study concentrates on cereal crops, of relatively simple geometry, but whose elastic properties cause them to interact dynamically with the turbulent wind.

The main body of the work is contained in Chapters 2-5 inclusive, which are presented in the form of complete research papers. Chapters 4 and 5 have been published in 'Boundary Layer Meteorology', while Chapters 2 and 3 have been submitted for publication to that journal. Although all these chapters can be read in isolation, they form a logical sequence. Chapters 1 and 6, while not designed for separate publication, have also, in the interests of uniformity, been written as self contained papers. This has inevitably led to some repetition in both content and references. The concluding remarks in Chapter 7 of course draw upon results from all the previous chapters.

Chapter 1 begins by briefly reviewing the importance of canopy flow in the context of micrometeorology in general and in particular the reasons for concentrating on the unsteady details of the turbulence rather than its mean statistics. This is shown to lead logically to the choice of flexible cereal crops as the subject of investigation. The rest of the chapter consists of a critique of the two main

theoretical frameworks which have been employed in the study of canopy turbulence, namely gradient diffusion theory and the Universal Equilibrium theory of energy spectra. The points made are illustrated by examples from published work.

Chapters 2 and 3 are concerned with the results of a field experiment, carried out in a mature wheat canopy. In Chapter 2, the mean statistics and spectra of the velocity field, within and just above the canopy, are analyzed in terms of the travelling wave type structure or 'Honami', which is observed in such crops on windy days. In Chapter 3, conditional sampling methods are employed to detail the structure of momentum transfer to the plants. In both of these chapters, results of recent investigations by several workers into the role of large or coherent structures in the momentum and energy balance of turbulent boundary layers are used to help in interpreting the data.

Because of the complexity of the data processing techniques involved in the conditional sampling methods, it is obvious that a wind tunnel model, if it could effectively duplicate the elastic behaviour of the stalks, would offer many advantages over further field experiments. In Chapter 4 therefore, criteria are advanced for simulating communities of flexible plants by an aeroelastic model. A small section of model wheat canopy, satisfying these criteria appears to reproduce the general turbulence characteristics of a prototype wheat field reasonably well. Both the research paper which forms Chapter 4 and the following one, Chapter 5, were written and accepted for publication before the analysis of the data described in Chapters 2 and 3 was complete. As a result some of the

ideas, tentatively advanced in Chapter 4, have been developed and clarified in Chapters 2 and 3. It was thought better however to present Chapter 4 in its published form and to consign to a postscript, discussion of two points which the chronologically later work has clarified.

In the course of the analysis developed in Chapter 4, it became obvious that no methods exist for predicting the effect of the spacing, drag coefficient and elasticity of individual plants in a canopy on the fluctuating airflow. Chapter 5 describes a very simple mathematical model which attempts to do this. Its qualitative predictions support the choice of stalk spacing in the small test model of Chapter 4, but its more general predictions remain to be compared with experiment.

Chapter 6 describes some preliminary wind tunnel measurements in a model canopy, constructed in precisely the same way as the small test section described in Chapter 4, but large enough for equilibrium flow conditions to be established within and above it. Profiles of mean velocity and second order moments of fluctuating velocity are shown to compare favourably with published atmospheric measurements, suggesting that a useful facility has been built in which to extend the investigations commenced in Chapters 2 and 3. Finally in Chapter 7 some points from the previous chapters, and which the author considers to be important, are reiterated and some general conclusions drawn.

Pages are numbered by chapter and a list of references is at the end of each chapter.

The work described in this thesis is my own. The joint authorship

of the papers comprising Chapters 4 and 5 reflects the usual collaboration between student and supervisor. No part of this work has been submitted for a degree at any other university.

John Finnigan

J.J. Finnigan
September, 1978

Acknowledgements

I am indebted to my supervisors, Dr P.J. Mulhearn, Dr I.R. Cowan and Dr E.F. Bradley for their advice and guidance and to my colleagues of the CSIRO Division of Environmental Mechanics for much helpful discussion. I would also like to thank Mr C.J. Hazelton, who built the apparatus for wind tunnel and field experiments and Mr O.A. Simakoff, who constructed the large model canopy.

I would particularly like to thank the editorial staff of the Division of Environmental Mechanics for their help in producing this thesis: Ms Jean Weber, who edited the manuscript, Mr Greg Heath, who produced the illustrations and Mrs Pat Jones, Mrs Joanna Daly and Mrs Veronica Popplewell who typed the manuscript.

I very much appreciate the opportunity granted me by Dr J.R. Philip, Chief of this Division to submit my work for a doctorate, and for the facilities afforded by my position with the Division of Environmental Mechanics.

J.J. Finnigan

TABLE OF CONTENTS

CHAPTER 3

TURBULENCE IN WAVING WHEAT. II. STRUCTURE OF MOMENTUM TRANSFER

CHAPTER 4

MODELLING WAVING CROPS IN A WIND TUNNEL

CHAPTER 5

A SIMPLE MATHEMATICAL MODEL OF AIRFLOW IN WAVING PLANT CANOPIES

CHAPTER 6

PRELIMINARY WIND TUNNEL MEASUREMENTS IN A LARGE AEROELASTIC MODEL CANOPY

CHAPTER 7

CONCLUDING REMARKS

Abstract

In Chapter 1, reasons are introduced for investigating the turbulent flow in plant canopies and for the choice of a field of wheat as an experimental site. A critical review of the theory of gradient diffusion in plant canopies is presented, illustrated with examples from the published literature. By using criteria derived from mixing-length arguments and dimensional reasoning, it is shown that simple gradient diffusion models should not be generally applied within canopies. Finally, dimensional arguments and published measurements are used to show that the theory of Universal Equilibrium of turbulent energy spectra has not yet been shown to be applicable to canopy turbulence.

In Chapter 2, measurements of mean and fluctuating velocity, surface pressure and stalk waving, made in a very uniform wheat canopy, are described. Features of the vertical profiles of mean turbulence quantities are discussed in the context of the resonant waving of wheat stalks. The discrete and prominent peaks in the velocity spectra measured in and above the canopy are then analyzed in the light of the organized travelling wave type structure or 'honami', observed in such crops on windy days. Prominent peaks in the spectra are identified with the arrival of gusts, the stalk waving frequency, and the frequency of oscillations in the canopy height. Two possible mechanisms are proposed to account for the observed height dependence of the peak frequencies, directly associated with stalk waving.

Chapter 3 describes the intermittent features of the turbulent velocity field within the wheat canopy, which were investigated by conditional sampling techniques and short period space-time correlations.

The velocity and shear stress profiles had qualitatively quite different forms during periods of high and low wind. Analysis of the relative importance of shear stress contributions from different quadrants of the uw plane revealed the dominant role of gusts in penetrating the canopy and transferring momentum to it from the boundary layer above. Short period space-time correlations of velocity indicated that over a significant fraction of the time, periodic velocity fluctuations pervaded the canopy-air layer. It is surmised that, while this has only a secondary effect on momentum transfer, it may be of overriding importance in heat and mass transport.

In Chapter 4, analysis of movie films of a field of barley, combined with observations of the motions of individual plants, is used to show that single stalks oscillate at a well-defined natural frequency even when stimulated by turbulent winds. Treating single stalks as resonant cantilevers allows the use of standard engineering methods to determine their elastic properties. Armed with these values, the application of similarity analysis to the equation of motion of a single stalk leads to criteria for aeroelastic modelling of wheat plants in the wind tunnel. A representative value for the spacing of stalks in a small section of model wheat field was calculated by referring to published data on momentum absorption in a variety of real and model canopies. Preliminary measurements of first and second moments of velocity in the model reveal good agreement with the prototype wheat canopy of Chapters 2 and 3.

Chapter 5 presents a simple mathematical model, which combines the effects of mean wind speed, plant spacing and the drag coefficients of individual plants to calculate the fluctuating airflow within a

waving crop canopy. The model is non-linear and is only amenable to analytical treatment when linearized; however, the full non-linear version can be solved on an electronic analogue computer.

The linear and non-linear results show unexpectedly good agreement, and the success of the linearization allows clear conclusions to be drawn about the relationship between the elasticity, geometry and mean wind speed through a stand of plants and the fluctuating components of airflow and stalk motion. Results calculated using the linearised equations are in qualitative agreement with wind tunnel results from two model canopies with different characteristics.

Chapter 6 is concerned with a large aeroelastic model canopy which has been constructed in accordance with the design criteria advanced in Chapter 4. It was installed in the CSIRO Division of Environmental Mechanics wind tunnel and preliminary tests have been performed. Measurements of turbulent velocity fluctuations with an X wire indicate that over the rear one-third of the canopy, approximately equilibrium flow has been established at all but the highest windspeeds.

Finally in Chapter 7, some general conclusions are drawn from the results of the previous chapters with particular attention being paid to the possible effects of atmospheric stability on the canopy turbulence.

CHAPTER 1

INTRODUCTORY REMARKS AND A REVIEW OF SOME CONCEPTS IN THE STUDY OF CANOPY AIRFLOWS

1. Introductory Remarks

The transfer of energy and momentum between the earth's surface and the atmosphere is the process which determines weather and climate. Four fifths of the planet lie hidden beneath the oceans, whose practically infinite capacity for heat storage has earned them the title 'the flywheel of climate'. Compared with the oceans, the land surface has almost no heat storage capacity, the surface temperature being determined from moment to moment by the balance between the net radiation, free convection and forced convection by the turbulent winds. The study of this balance is the preserve of micrometeorologists and for obvious reasons, their efforts have been concentrated in areas where measurements might be of direct benefit to people.

Of the land surface not covered with deserts, water or ice, 23% consists of forests or woods while 14% is given over to agricultural crops (Söderlund and Svensson, 1976). The importance of commercial food crops hardly needs stressing in these days of a hungry world, whilst the role of the dwindling world forests in the global carbon dioxide and nitrogen balance has only recently come under question. It comes as some surprise, then, that after about three decades of diligent work by micrometeorologists throughout the world, no reliable models of the turbulent transfer process within plant canopies have been produced.

The necessity of developing a clear understanding of turbulent airflow amongst plant communities can be demonstrated by considering the process from three different viewpoints. On the largest scale, Lettau (1959) showed that the surface roughness, acting through the medium of turbulent shear stress, plays a major role in determining

the turbulence structure throughout the lowest 1000 m of the atmosphere, while the heat transfer at the surface is an important element in both synoptic meteorology and the theory of the general circulation. Secondly, on the scale where micrometeorologists usually make their measurements, that is within the lowest 100 m of the atmosphere, the spatial distribution of plants is reflected in the uncertainty with which effective zero planes can be determined for vertical profiles of the meteorological variables, an uncertainty which seriously affects the accuracy with which the gradients and fluxes can be measured. The presence of the canopy imposes complex boundary conditions on the momentum and energy equations and, close to vegetation of any significant height or inhomogeneity, well established scaling laws break down. This is exemplified in the recent paper by Garratt (1978) and earlier work by Thom et al. (1975) while Mulhearn and Finnigan (1978) show that the depth of the atmospheric layers affected is not determined by the roughness height so much as by the generally much larger scale of the horizontal inhomogeneity.

Finally, at the smallest scale, we are interested in the microclimate of plant communities. The source and sink distributions of the quantities which influence plant growth: heat, water vapour and carbon dioxide, are determined to a large degree by the turbulent transfer processes within a canopy. Certainly, most practical methods of measuring assimilation and evapotranspiration depend upon assumptions of a particular turbulent transfer process, as we shall see in ensuing sections.

The choice of the type of canopy, in which to embark upon new investigations, is governed by several factors. In order to relate

new measurements to any substantial body of published work, a cereal canopy or a plantation of conifers must be chosen. Forest canopies, however, present a relatively complicated geometry with an open trunk space capped by a dense crown, while mature forests may be high enough for thermal stability effects to directly influence the turbulence in the canopy air spaces. On a purely practical level, their size necessitates high and expensive instrument towers, while their heterogeneity makes it difficult to ensure that a truly representative measuring station has been chosen.

Most of these problems can be avoided if a cereal, such as wheat or barley, is chosen as the experimental canopy. Although their geometry is relatively simple, the elastic properties of these plants cause them to interact dynamically with the wind, so that they form a well defined example of the behaviour of many natural surfaces. Furthermore, it has long been recognised that the wave-like motion or 'Honami', which is so obvious in these canopies on windy days, is a direct consequence of momentum transfer by large eddies in the turbulent atmospheric boundary layer. There is an obvious connection therefore between this phenomenon and the observations by several workers recently (Grass, 1971; Nakagawa and Nezu, 1977) that in fluid flows in the laboratory, the large eddies play an important role in momentum transfer to rough surfaces. The investigations referred to above form part of a large body of work concerned with the role of 'coherent structures' in the momentum and energy balance of turbulent shear flows (an excellent review is presented by Willmarth, 1975). It is reasonable to expect that many of the results and techniques arising from these investigations might be directly applicable to

canopy turbulence and might lead to an increase in understanding of canopy flows, as they have in boundary layers.

In Chapters 2 and 3, turbulence measurements in a wheat canopy will be described with particular attention paid to the unsteady character of the flow field. It will be shown that many important features of the momentum transfer are obscured by taking long time averages and that this practice can lead to erroneous physical models of the transfer process. Later chapters will be concerned with the problems of modelling a waving canopy in a wind tunnel, as it is apparent from Chapters 2 and 3 that better experimental controls than are possible in the field are needed, if the complicated problem of the canopy flow field is to be solved.

A review of the work done in the past in both real canopies and wind tunnel models will form the necessary basis for comparison for the later chapters. The review will not attempt to include everything published on the subject but will concentrate upon those papers which, in the author's opinion, have been most influential in shaping the two major themes in this research. They are the development of gradient diffusion models, which both provide a methodology for experiment and serve as a basis for prediction methods, and the application of spectral analysis to turbulence measurements.

Throughout this thesis it will be assumed that single point measurements in canopies are representative of an average over a horizontal plane, large compared with the scale of inhomogeneity of the plant parts. This should not be interpreted as an assumption that the averaging problem is unimportant or resolved; simply that the difficulties of measuring turbulence data in canopies are such that,

in general, the question has only received cursory treatment. Shaw et al. (1974) did investigate the representativeness of their measuring station in a corn crop, and Seginer et al. (1976), within the less taxing conditions of a wind tunnel model, treated the problem systematically but in most published work, the question is not addressed directly. In general eddies, with length scales similar to typical separation distances between plant parts, will be least representative of the whole flow.

This brings us to another point which must be made before commencing the review. Throughout the thesis, 'eddy' will be used as a convenient term for a velocity fluctuation with length or time scales of the same order in the three co-ordinate directions. Eddy size should not be precisely identified with for instance a given wave number in Fourier transform space. The latter provides a useful mathematical description and, while its physical interpretation is clear for definitely periodic phenomena such as vortices in a Von-Kármán vortex street, in the essentially random velocity field of truly turbulent flows, such simple interpretations should be avoided.

2. Gradient Diffusion in Plant Canopies

The avowed intention of most previous work has been to investigate heat, mass and momentum transfer to and within the plant community, in the hope of defining the nature of the turbulent transfer processes. If such investigations were to proceed, some conceptual framework had to be assumed; in analogy with many other physical situations, gradient diffusion was usually the model chosen. Before looking in detail at particular cases it is worth investigating the general validity of this approach.

All diffusion models ultimately rest upon the assumption of continual microscopic transport 'events' which, on a macroscopic scale, appear to constitute a continuum process. The class of hypotheses leading to gradient diffusion formulae are usually described as 'mixing-length' theories. In the following section, a mixing-length theory is developed and its various assumptions examined in the context of canopy and boundary-layer flow.

Consider the diffusion of any conserved quantity whose concentration is $\Gamma(z,t)$, where z is a space co-ordinate and t is time. The flux, F, through a plane, z = constant, of a property, Γ, is defined by

$$- F(z,t) = \frac{\partial}{\partial t} \int_{-\infty}^{z} \Gamma(z',t)\, dz' . \qquad (1)$$

If the transport of Γ is effected by statistically homogeneous and sationary random motion of particles having 'mean free path', ℓ, and not mean square velocity, V, then the mean flux can be estimated by asuming that all particles travel with the r.m.s. speed over ℓ.

It is assumed that particles arrive at z from z+ℓ and z-ℓ tagged with Γ values appropriate to their respective planes of departure and give up their excess or deficiency in Γ immediately upon arriving at z (see Fig. 1).

Fig. 1

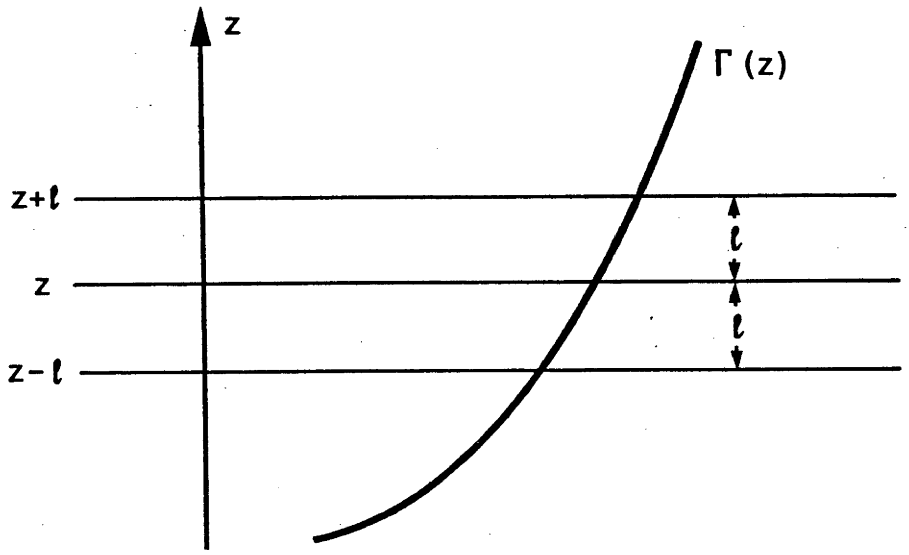

If n/2 particles per unit time cross unit area in each direction, the net mean flux of Γ is

$$\overline{F} = \frac{1}{2} n V \left\{\overline{\Gamma}\ (z-\ell) - \overline{\Gamma}\ (z+\ell)\right\} \quad . \tag{2}$$

Expanding the Γ terms as Taylor series about z leads to

$$\overline{F}\ (z,t) = -n V \left\{\ell\ \Gamma_z + (\ell)^3 \frac{1}{3!} \Gamma_{zzz} + (\ell)^5 \frac{1}{5!} \Gamma_{zzzzz} + - - -\right\} \tag{3}$$

where $\Gamma_z \equiv \frac{\partial \Gamma}{\partial z}$. All even derivatives have cancelled out.

If the second and higher order terms of the expansion can be neglected compared to the first, (3) simplifies to the gradient transport model,

$$\overline{F}\ (z,t) = - K_\Gamma \Gamma_z$$

$$\text{where} \qquad K_\Gamma = n V \ell \ . \tag{4}$$

If ℓ and V are functions of time and space, then the transporting mechanism is no longer symmetrical and the simple formulation set out above is not strictly applicable.

Corrsin (1974) has considered this point in a formal manner by representing Γ, ℓ and V at $z+\ell$ and $z-\ell$ by their Taylor series expansions in time and space about z and substituting these expressions into (2). The resulting equation for the flux up to second order becomes:

$$\frac{1}{n}\overline{F}\,(z,t) = -\ell\, V\, \overline{\Gamma}_z - \ell\, \overline{\Gamma}\, V_z + 2\ell\, \ell_z\, \overline{\Gamma}_t + (2\ell\, \ell_z \frac{\overline{\Gamma}}{V})\, V_t + 2\ell\, \ell_t\, \overline{\Gamma}_z$$

$$+ (2\ell\, \ell_t \frac{\overline{\Gamma}}{V})\, V_z + 2\ell^2\, \overline{\Gamma}_{zt} + (2\ell^2 \frac{\overline{\Gamma}}{V})\, V_{zt} + - - - \quad . \tag{6}$$

Using (6), conditions for neglecting terms of higher order than the first on the RHS can be separated into limiting conditions on the stationarity and homogeneity of the concentration field and transporting mechanism.

Many fluid mechanics textbooks avoid this complication by deriving the condition for valid truncation of the series expansion separately for contributions from the +z and -z directions; see for example Hinze (1959), Tennekes and Lumley (1972). In this case terms in even derivatives must be considered and the condition for retaining the gradient transport term only is:

$$\left| \frac{\Gamma_{zz}}{\Gamma_z} \right| \left(\frac{\ell}{2}\right) \ll 1 \tag{7}$$

This approach is perfectly valid and leads to a useful condition with which to test the applicability of the gradient diffusion model.

The mixing-length approach was first applied to transport of momentum in turbulent flows by Prandtl (1925) and Taylor (1932), while Von Kármán (1930) derived equivalent formulae by dimensional reasoning.

Their argument was that the particles can be replaced by 'lumps' of fluid which retain their identity or conserve their properties on average over a distance ℓ. Taylor developed his 'vorticity transport' theory upon the assumption that in a two dimensional fluid flow, vorticity is conserved but the model of Prandtl, in which momentum is the conserved property, has found more favour among micrometeorologists. In Prandtl's model, the concentration field, $\Gamma(z,t)$ is the mean velocity $U(z,t)$ and (2) is rewritten as

$$\tau = \rho V \{U(z-\ell) - U(z+\ell)\} \qquad (8)$$

where τ is the turbulent shear stress and ρ the fluid density.

Prandtl and Taylor fully realised that there is no exact analogy between say the transfer of momentum by the collisions of elastic molecules in the kinetic theory of perfect gases and the mixing of turbulent eddies. Momentum is transferred by turbulent motion only over distances where the orthogonal velocities of the fluid particles are well correlated. The measure of this distance is the Lagrangian integral length scale, a quantity which is unfortunately almost impossible to extract experimentally from real turbulent flows. In high Reynolds Number turbulence, Corrsin (1963) has suggested that it should be of the same order as the Eulerian Integral scale, which can be estimated from the conveniently measured autocorrelation coefficient. If L_w is the Eulerian integral scale of vertical fluctuations, then

$$L_w = w' \int_0^\infty R_w(\hat{t})\, d\hat{t}$$

where $R_w = \dfrac{\overline{w(t)\, w(t+\hat{t})}}{\overline{w(t)^2}}$ is the autocorrelation coefficient

and $w' = (\overline{w^2})^{\frac{1}{2}}$,

w being the fluctuation in vertical velocity, $\hat{t}$ is the time delay and $\overline{\quad}$ denotes a long time average. (Since in boundary layers, $R_w(\hat{t})$ usually contains a negative loop, the vertical integral scale is sometimes defined as $L_w = w' \int_0^{T'} R_w(\hat{t})\, d\hat{t}$ where T' is the time delay corresponding to the first zero crossing.) In homogeneous turbulence without shear, Snyder and Lumley (1971) showed that the Lagrangian and integral scales are related by the variance of velocity fluctuations. At this stage, however, it is debatable whether their formulae can be applied without modification to inhomogeneous shear flows. For the order of magnitude arguments used in this and subsequent sections, the simpler equivalence will be adequate.

In the lower part of equilibrium atmospheric boundary layers, $L_w \simeq 0.4z$ (Counihan, 1975) and in this region the mean velocity profile is well represented by

$$\frac{U}{u_*} = \frac{1}{\kappa} \ell n\, z + \text{constant} \qquad (9)$$

where κ is a universal constant $\simeq 0.4$ and $u_* = \left(\frac{\tau}{\rho}\right)^{\frac{1}{2}}$.

Taking $\ell = L_w$, condition (7) can be applied resulting in

$$\left|\frac{U_{zz}}{U_z}\right| \left(\frac{\ell}{2}\right) \equiv \left|\frac{-\frac{u_*}{\kappa}\cdot\frac{1}{z^2}}{\frac{u_*}{\kappa}\cdot\frac{1}{z}}\right| \left(\frac{0.4z}{2}\right) \simeq 0.2 \ .$$

Within a crop of rice, 0.8 m high, Inoue et al. (1975) found that the mean velocity profile was adequately represented by a profile of the form,

$$U = U_H \exp \alpha\left(\frac{z}{H} - 1\right) \qquad (10)$$

where $\alpha = 2.3$ and U_H was the value of U at $z = H$, the top of the canopy. L_w, measured by sonic anemometer, was about 0.2H in the top 30% of the canopy. Applying condition (7) once again,

$$\left|\frac{U_{zz}}{U_z}\right| \left(\frac{\ell}{2}\right) \equiv \frac{\alpha}{H} \frac{0.2H}{2} \simeq 0.23 \ .$$

It appears that the requirements for using a gradient transport model on the basis of mixing-length arguments are not really met in either the logarithmic region of atmospheric boundary layers or within canopies. Condition (7) is not always reliable however. This is demonstrated by the pathological case of $U_{zz} = 0$. This invariably occurs just above the canopy in the region of transition between the exponential and logarithmic profiles.

Corrsin has applied the more formal conditions arising from equation (6) to measurements in a smooth wall turbulent boundary layer by Blackwelder and Kovaszny (1972). He found that the requirements of stationarity upon the mean velocity field and the transporting mechanism are adequately met, that the homogeneity condition on the mean velocity gradient is only roughly fulfilled in the inner part of the boundary layer, and that the requirement of homogeneity of the transporting mechanism is emphatically violated.

The gradient transport mixing-length hypothesis is apparently not strictly applicable to the inner region of a turbulent boundary layer ($z < 0.2\delta$ where δ is the boundary-layer thickness) but it is in this region where the logarithmic velocity profile, the theory's most successful prediction, is observed to be a universal feature and the inferred success of mixing-length theories in this region has led to their application to the canopy layer (see for example, Inoue et al., 1962).

It can be shown however that a relationship of the form $\tau = \rho C U_z$, where C is a constant, is a dimensional necessity in a

flow with only one length and one velocity scale. Following Tennekes and Lumley (1972), we can say that if eddies of length scale ℓ and velocity scale u' (where ' denotes an rms velocity fluctuation) derive their energy from the mean flow, then

$$\frac{u'}{\ell} \propto \frac{dU}{dz} \quad ; \tag{10}$$

and if the eddies which interact with the mean gradient in this way are of comparable dimension to the flow width, then

$$\frac{u'}{\ell} = C_1 \frac{dU}{dz} \quad , \tag{11}$$

where C_1 is a constant of order 1. Let

$$C_2 = \frac{\overline{uw}}{u'w'} \quad ,$$

where u is the fluctuating part of the streamwise velocity. Then $\tau = - \rho C_2 u'w'$, and if u' and w' of the same order of magnitude, then

$$\tau = - \rho C_3 u'^2 \quad . \tag{12}$$

In practice, in turbulent flows driven by shear, u' and w' are always well correlated in eddies which can absorb energy from the mean flow by vortex stretching so that C_2 and C_3 are of order 1 (Tennekes and Lumley, 1972). If no other length and time scales are present, C_1 should be of order 1 also. This merely implies that the time scale of the large eddies is the same as the time scale of the mean flow, since they are the fluctuating part of the flow. Substituting for one of the u's in (12) by (11) gives

$$\tau = - \rho C_3 C_1 u' \cdot \ell \frac{dU}{dz} \tag{13}$$

which is equivalent to (4).

No assumptions about momentum conservation or gradient transport were made in deriving (13); it follows merely from the assumption that single length and velocity scales govern the flow.

In an equilibrium boundary layer above a uniform surface, the only length scale available is the height z so that $\ell = C_4 z$, where C_4 is a constant. Substituting for u' in (13) by (11) leads to

$$u_* = \kappa \, z \, \frac{dU}{dz} \quad \text{where} \quad \kappa = -C_4 C_1 \sqrt{C_3}$$

and integrating we get (with assumption of constant u_*, which in the absence of sources or sinks for momentum is required by conservation of momentum)

$$\frac{U}{u_*} = \frac{\ell n \, z}{\kappa} + \text{constant}, \tag{14}$$

the familiar logarithmic profile. A phenomenological argument has been used to arrive at (14). The same result however follows from formal dimensional analysis.

The reason for the success of flux-gradient relationships in the log layer appears to be dimensional necessity. In the case of the canopy, however, it seems unlikely that assumptions of single length and velocity scales can be made, certainly not in times of strong wind. In general eddies within the canopy will have length scales derived from the mean shear, $\frac{\partial U}{\partial z}$, the wakes of plant elements and scales appropriate to stalk waving. This last effect is particularly important in cereal crops since (as will become clear in later chapters) over half a waving cycle, stalks absorb momentum from large eddies, storing it as strain energy and then release it to the flow over the second half cycle with time scales determined by the waving period. In particular, in this situation one cannot write $\frac{u'}{\ell} \simeq \frac{dU}{dz}$.

Even if all the derivatives of the mean velocity field were known, there are more serious doubts about the applicability of mixing-length models to canopy flows. The model must assume that the diffused property is conserved over a length, ℓ. However the size of ℓ typical of turbulent canopy flows is larger than average plant spacing so that there are distributed sources and sinks - leaves, stalks and branches - within a mixing-length. The transported quantity is not conserved and equation (2) cannot be applied. To take this argument a little further, if two species have different source distributions they will be 'not conserved' to differing degrees over a typical mixing-length and their apparent diffusivities, derived from the mixing-length model will differ. Finally Corrsin (1974) has pointed out that as a general principle, fluxes should only be expected to be a <u>function</u> of the gradients of quantities at a point in space rather than involving their histories up to that time, if the transporting mechanism is fairly localized. It will be shown in Chapter 3 however, that much of the momentum transport in a wheat canopy is accomplished by eddies with length scales much larger than those of the local canopy geometry.

Having established some necessary concepts in diffusion models, we can progress to consider the behaviour of ℓ and V in real flows. Mathematical models will not be treated explicitly; they rest upon the same concepts as are used in interpreting field data, relying upon plausible assumptions about the behaviour of ℓ and V for their development. The papers of Thom (1972), Cionco (1965), Cowan (1968) and Philip (1964) might be mentioned, however, as exemplifying some different approaches.

Analytical derivations of canopy wind profiles depend upon parameterizing the characteristic velocity, V, in (2). The expression commonly used is (11)

with the constant C_1 absorbed in ℓ so that $V = \ell \frac{dU}{dz}$. Inoue et al. (1962) used this relationship with the further assumption that the sink strength for momentum is equal to the aerodynamic drag, F, to obtain the following equation,

$$\frac{d\tau}{dz} = \frac{d}{dz}\left(\rho\, \ell^2 \frac{dU}{dz}\right)\frac{dU}{dz} = F = \rho\, C_d\, A(z) U^2 \quad , \tag{15}$$

where C_d is a dimensionless drag coefficient and A(z) is the area of vegetation per unit volume of space. (15) can be integrated with the assumption of constant ℓ,C and A to yield the familiar exponential velocity profile

$$U = U_H \exp \alpha \left(\frac{z}{H} - 1\right) \tag{16}$$

where $U = U_H$ at $z = H$ and $\alpha = H\,(C_d\, A/2\ell^2)^{1/3}$. Inoue et al. apparently assumed that ℓ could be taken as constant on the grounds that i_u, the turbulent intensity within the canopy, was approximately constant (see Inoue, 1963) and constancy of C and A seemed reasonable assumptions. Equation (15), moreover, is rather intractable when these parameters are functions of z, and both Cionco (1965) and Ordway et al. (1960) made similar assumptions to derive (16). Following their pioneering work, the exponential profile for uniform canopies has acquired the status of dogma. It is interesting to see therefore that there is little or no experimental evidence of a constant length scale within canopies; certainly the few measured values of L_w available do not behave in this way.

Inoue et al. (1975) measured an increase of L_w with height in a rice crop while Allen (1968), from measurements in a plantation of Japanese Larch, showed the strong height dependance of the horizontal Eulerian length scale, L_u [$= u' \int R_u(t)\, dt$, and which we would expect to be simply related to L_w].

Wright and Lemon (1966) report different vertical distributions of L_u with different values of U_H in a corn crop while Saito et al. (1970) provide a plot of a monotonically increasing L_w, also in corn.

Other estimates of ℓ in real canopies have relied upon measuring τ, either directly or indirectly, and then using u_* as a velocity scale, writing $\ell = \frac{u_*}{dU/dz}$.

Unfortunately the most common means of calculating τ, the so called 'aerodynamic method', is itself prone to error and contains internal inconsistencies; these will be dealt with in the next section. Using this method however, Uchijima and Wright (1964) measured a linear relationship between ℓ and z in the lower part of a corn crop followed by an abrupt decrease in ℓ at the top of the canopy. Inoue et al. (1975) observed a similar but less abrupt profile in a rice field and Saito et al. (1970) showed a similar profile in the same corn crop where they measured a smoothly increasing L_w.

More reliable estimates were obtained for both ℓ ($= u_*/\frac{dU}{dz}$) and L_w by Seginer et al. (1976) in a wind tunnel model canopy of rigid spikes. They found that while $\frac{u_*}{dU/dz}$ was roughly constant, L_w increased with z so that

$$L_w \simeq 0.31\ z.$$

Cionco (1972a) attempted to generalise the concept of the exponential profile by allowing α to vary with z and identifying various aspects of its variation with measured distributions of A and inferred C_d's. At this point however the exponential profile loses its theoretical basis and application of equation (18) with variable α must be regarded simply as a curve fitting exercise.

This point had been recognized by Saito (1964) who had derived an expression

$$U = U_H \exp\left(- \int_z^H p(z)\, dz \right) \qquad (19)$$

where p(z) is a proportionality factor combining the height dependance of the various factors affecting momentum absorption. Since p(z) is quite arbitrary, the adoption of the exponential form in (19) merely imposes certain conditions upon U such as a positive sign.

The velocity scale, V, appropriate to the mixing-length model is the r.m.s. Lagrangian vertical velocity fluctuation. As in the case of the length scale, the best estimate available for this is the Eulerian equivalent, usually expressed as the vertical turbulence intensity, i_w [$= \left[\overline{w^2}\right]^{\frac{1}{2}}/U$]. Although there are a great deal of data on the behaviour of i_u (the longitudinal turbulence intensity) in a variety of real and model canopies, there are relatively few measurements of i_w available. Cionco (1972b) summarized most of the reliable data available at that time and concluded that in simple canopies (those with A(z) essentially constant) i_u was also constant with one or two exceptions. Finnigan and Mulhearn (1978) (Chapter 4) suggested that in canopies where stalks were waving strongly, i_u would increase with height even if A(z) were constant, while in both the rigid model canopy of Seginer et al. (1976) and the flexible model of Finnigan and Mulhearn, i_w increased almost linearly with height.

The relationship, $V = \ell \frac{dU}{dz}$ is obviously only strictly true for U proportional to exp(z), which in turn depends upon ℓ being constant. In this case, $V = \frac{\ell\alpha}{H} U$ [using (16)], and if $V = w' = i_w U$, then

$$i_w = \frac{\ell\alpha}{H} \qquad (20)$$

In the rice canopy of Inoue et al. (1975), taking $\ell = L_w \simeq 15$ cm (appropriate to the top 30% of the canopy), H = 80 cm and $\alpha = 2.3$, then $i_w \simeq 0.43$. The measured value of i_w in the top 30% of the canopy was roughly 0.23, not a particularly good agreement.

To summarize, the mixing length-gradient diffusion model leads to a momentum diffusivity which is the product of characteristic length and velocity scales, ℓ and V. These should be Lagrangian integral scales but their Eulerian equivalents are substituted through necessity.

Measured Eulerian integral scales and vertical turbulent intensities in real and model canopies however lend no support to the assumptions of constant ℓ and i_u, necessary for the only analytically derivable velocity profile for canopy flow, the exponential profile. In cases where both directly measured L_w's and mixing-lengths derived from $\ell = u_*/\frac{dU}{dz}$ can be compared, the agreement is not particularly good, derived ℓ's often showing bulges or abrupt jumps in mid-canopy which are difficult to attribute to any physical process. On the other hand, the exponential velocity profile does appear to collapse a good deal of canopy data and, given the shaky foundation of the gradient diffusion model, it is perhaps more appropriate to be agreeably surprised at the success of the theory rather than censorious over its shortcomings.

3. The concept of drag in canopy flows and the aerodynamic method of finding the diffusivity

Once a gradient diffusion model has been accepted, some further assumptions are necessary to apply it usefully in calculating fluxes of heat, carbon dioxide and water vapour, these being the species of most interest to micrometeorologists. Writing the general diffusion relationship as

$$F_\Gamma = K_\Gamma \frac{d\Gamma}{dz} \quad , \tag{21}$$

the first assumption is equality of K_Γ between different species. The argument usually advanced to support this is that passive scalars are all transported by the same turbulent fluctuations and should therefore have the same eddy diffusivities. While this may indeed be true in the canopy air spaces, diffusivities derived from mixing length formulations are subject to the caveat expressed earlier, that different source distributions over a mixing length may lead to different apparent K_Γ's. Equality of K_Γ's for heat, water vapour and CO_2 is the only requirement of the 'energy balance' method which equates the net vertical radiation flux at a height z to the energy equivalents of water vapour and sensible heat flux and CO_2 fixation by photosynthesis. This method has been used by, amongst others, Denmead (1964) in a pine plantation and Brown and Covey (1966) in a cornfield. The details of the method are clearly set out by Thom (1975). We are going to concern ourselves here, however, with the aerodynamic method of evaluating the fluxes. This approach employs streamwise momentum as a tracer for the diffusion of the scalars and therefore rests upon an assumption of the equality of K_M, the momentum diffusivity and the other K_Γ's. This correspondence is less likely than that of the scalar diffusivities since there is no counterpart

in the transfer of the scalar species of the role of pressure gradients in momentum transport.

The method is usually developed in the following way. The vertical gradient of shear stress within the canopy equated to the sink strength for momentum, that is the aerodynamic drag of the leaves, stems and branches:

$$\frac{d\bar{\tau}}{dz} = \frac{d}{dz}\left[\rho K_M \frac{dU}{dz}\right] = \rho C_d A \overline{\tilde{u}|\tilde{u}|} \quad . \tag{22}$$

It is assumed that the drag force can be parameterized in the way shown, the drag coefficient, C_d, and the foliage area per unit volume, A, both being in general functions of z, while the modulus sign ensures that the drag force is always in the direction of the instantaneous velocity. If the foliage can wave, then $\tilde{u}$ must be replaced by the relative velocity of air and stalk. The right hand side of (22) is normally written as $\rho C_d A U^2$. Integrating (22), we obtain

$$\rho K_M \frac{dU}{dz} = \tau(z) = \tau(H) - \int_z^H \rho C_d A U^2 \, dz \quad . \tag{23}$$

If the value of the shear stress at H, the top of the canopy, is known (for example by measuring the log profile some way above the canopy and inferring d and z_o, the zero plane displacement and the roughness length, by an iteration process) and if U and A can be measured, then, with the assumption of constant C_d,

$$C_d = \tau(H) \Big/ \left[\rho \int_o^H A(z) \, U^2 \, dz\right]; \tag{24}$$

and finally, from (23) and (24),

$$\rho K_M(z) = \left[\tau(H) - C_d \int_z^H A(z)\, U^2(z)\, dz\right] / \left[\frac{dU}{dz}\right] \quad . \qquad (25)$$

Let us examine the inbuilt assumptions of this process in detail, first of all that $F = C_d A U^2$, F being the aerodynamic drag. Early measurements of the effect of free stream turbulence on the drag coefficient of bluff bodies (where C_d is defined for an arbitrary bluff body as $F/(\rho a U^2)$, a being some representative area), such as the results quoted by Hoerner (1965) or McLaren et al. (1969), suggested that increasing intensity of free stream turbulence always leads to a reduction in drag. This was supported by the observation that the drag coefficients of cylindrical rods in simple model canopies were about 40% of the value measured in steady air streams (Seginer et al., 1976). Other, generally more recent measurements, however, on circular cylinders (Surry, 1972), angular bluff bodies (Robertson et al., 1969), rectangular cylinders and plates (Bearman and Trueman, 1971; Bearman, 1969) and square prisms (Lee, 1975/76) show that the effect of turbulence scale cannot be ignored. All of these measurements are at lower turbulent intensities ($i_u \simeq 10\%$) than are typically encountered in canopies, where i_u values in excess of 50% are common, but they reveal a pattern of drag coefficients, steadily increasing from their initially reduced values once the Eulerian length scale, L_u, exceeds about 3 body diameters (or an equivalent body dimension). At smaller length scales, the behaviour is complicated, with C_j a maximum when L_u equals the body diameter and passing through a minimum at $L_u \simeq 2$ diameters (Lee, 1975/76). The behaviour at large L_u/D (D being body diameter) is to be expected from the quadratic nature of the drag term. Writing $\tilde{u} = U + u$ where $U = \bar{\tilde{u}}$, if $U \geqslant u$

$$\bar{F} = \rho C_d A U^2 (1 + i_u^2) \quad . \tag{26}$$

(26) would be true if all of the fluctuations contributing to $\overline{u^2}$ had length scales much larger than a body dimension. In the model canopy of Seginer et al. (1976), consisting of aluminium rods 2.38 mm in diameter, L_u varied from 2.5 cm at the bottom of the canopy to 7.5 cm at the top. More crudely, it can be inferred from the spectra of Figure 2, reproduced from Seginer et al. (1976), that most of the contribution to the total variance, $\overline{u^2}$, comes from eddies with time scales much greater than D/u' (where $u' = i_u U$; and $i_u \simeq 0.5$). To take account of the partitioning of the eddies into various length scales, (26) should be rewritten

$$\bar{F} = \rho C_d A U^2 (1 + s i_u^2) \tag{27}$$

where s is less than 1 and represents that fraction of the eddies which have length scales much greater than the body size. Substituting (27) into (24) we see that the drag coefficient inferred from (24) has absorbed the coefficient $(1 + s\, i_u^2)$ and is that much larger than the 'true' drag coefficient. In equation (23), the flux of mean momentum, $\rho K_M\, dU/dz$, is equated to the absorption of mean momentum, $\int_z^H \rho\, Cd\, A\, U^2\, dz$, with the assumption implicit in this formulation that the RHS represents the sink of the property, ρU, whose concentration gradient drives the diffusion. The result is that, if diffusion of ρU is regarded seriously as a tracer for heat, CO_2 and water vapour, then the diffusivity, K_M, derived from (25) is too large by a factor $(1 + s\, i_u^2)$. In the experiment of Seginer et al. (1976), $d\tau/dz$ as a function of height was known from X wire anemometer measurements, as was U(z) and A(z). With this information $C_d(z)$ could be calculated from (22). The results are presented in Figure (3)

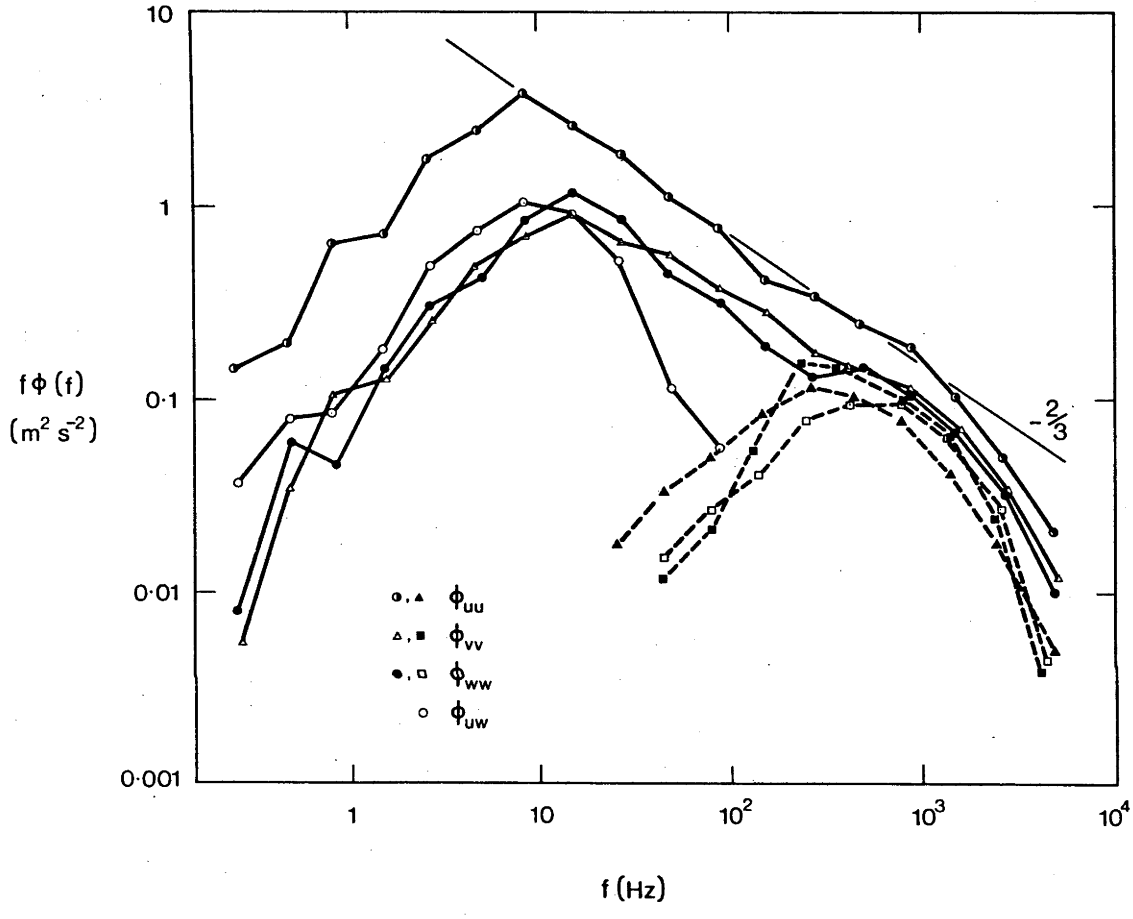

Fig. 2. Power spectra of streamwise, ϕ_{uu}, vertical, ϕ_{ww}, and cross-stream, ϕ_{vv}, velocity fluctuations and cross spectra of streamwise and vertical fluctuations, ϕ_{uw} from Seginer et al. (1976). Broken lines denote the contribution of the stalks alone to the total power. The straight line marked -2/3 is equivalent to the -5/3 law dependence for spectra presented as $f\phi(f)$ vs. log(f).

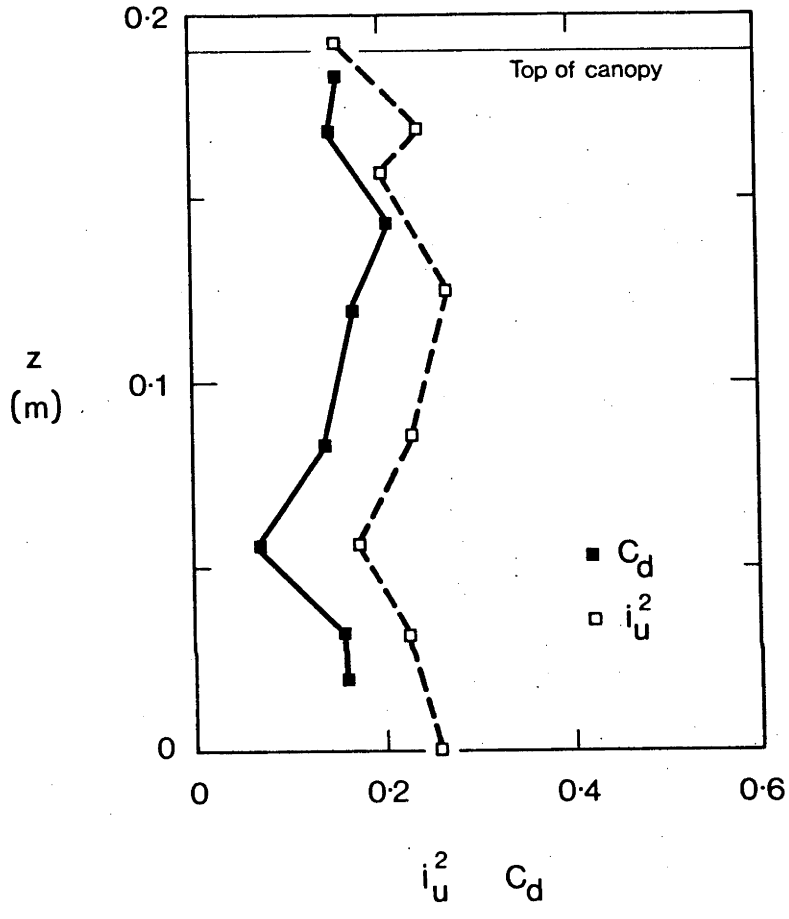

Fig. 3. Comparison of the drag coefficient, C_d, derived from Equation (22), using results of Seginer et al. (1976), and the square of the measured turbulence intensity, i_u^2, in the same experiment.

together with the profile of i_u^2. Although the correlation is not exact, due possibly to errors in graphically differentiating τ, there is an obvious correspondance between the profiles of i_u and C_d.

Moving from this basic conceptual problem of 'what exactly is being diffused?', one can go on to consider the assumption of C_d constant with height. This is certainly untrue for the lower regions of simple canopies where, using Reynolds Numbers based upon typical stalk diameters of 0.5 cm and wind speeds of about 1 m s^{-1}, it is obvious that even bluff bodies such as cylinders are in an aerodynamic regime where their drag coefficient varies significantly with windspeed. This point will be developed in Chapter 3 in the context of the unsteady flow regime of the lower canopy. For the moment it suffices to refer to the paper of Thom (1971). In a model canopy of cylindrical spikes, he calculated $K_M(z)$ from (23) using C_d's proportional to those of two dimensional cylinders at a Reynolds Number given by the local U(z) and compared the result with values with $K_M(z)$ obtained from the assumption of constant C_d. His results are reproduced in Figure (4).

The data of Seginer et al. (1976) provide an opportunity to compare values of τ calculated by the aerodynamic method with direct measurements.

Within the canopy

$$U = U(H) \exp \alpha \left[\frac{z}{H} - 1\right] \qquad \alpha = 1.634$$

$$H = 0.19 \text{ m}$$

$$A = 5.29 \text{ m}^2 \text{ m}^{-3}$$

and

$$\tau(H) = \rho u^{*2}(H) \qquad u^*(H) = 1.82 \text{ m s}^{-1} .$$

From (24) $C_d = \rho u^{*2}/\rho A \int_o^H U^2 \, dz$

$$= u^{*2}/A U^2 (H) \int_o^H \exp 2\alpha \left[\frac{z}{H} - 1\right] dz$$

$$= u^{*2}/A U^2 (H) \left[\frac{H}{2\alpha}\left(1 - \frac{1}{\exp 2\alpha}\right)\right]$$

$$C_d = 3.3/\left[5.29 \times 81 \times \frac{0.19}{3.268} \times 0.962\right] = \underline{0.138} \; .$$

This is lower than the average value of C_d obtained from equation (22) or from a pressure tapped stalk which gave an average value of $C_d \simeq 0.151$. The distribution of $-\overline{uw}$ obtained by substituting $C_d = 0.138$ into equation (23) is plotted in Figure (5) together with measurements of $\overline{uw}$ from an X wire anemometer. It is apparent that for the case of a simple uniform canopy with constant A and exponential velocity profile, the predictions of the model are quite accurate. Equations (22) to (26) ensure that the canopy shear stress is bounded from above by the limiting value of $\tau(H)$ so that the predicted $\tau(z)$ within the canopy must be of the correct order; in the worked example above, the availability of a directly measured $\tau(H)$ has improved the accuracy of the calculation. Unfortunately, for the reasons already mentioned, such good agreement cannot be expected in more heterogeneous situations. It is in fact an interesting comment upon the self consistency of the method, that such good agreement would not have been achieved had more accurate values of C_d obtained from the pressure tapped stalk or from equation (22) been used in calculating $\tau(z)$ from (24).

From (24) $C_d = \rho u^{*2}/\rho A \int_o^H U^2 \, dz$

$$= u^{*2}/A U^2 (H) \int_o^H \exp 2\alpha \left[\frac{z}{H} - 1\right] dz$$

$$= u^{*2}/A U^2 (H) \left[\frac{H}{2\alpha}\left(1 - \frac{1}{\exp 2\alpha}\right)\right]$$

$$C_d = 3.3/\left[5.29 \times 81 \times \frac{0.19}{3.268} \times 0.962\right] = \underline{0.138} \; .$$

This is lower than the average value of C_d obtained from equation (22) or from a pressure tapped stalk which gave an average value of $C_d \simeq 0.151$. The distribution of $-\overline{uw}$ obtained by substituting $C_d = 0.138$ into equation (23) is plotted in Figure (5) together with measurements of $\overline{uw}$ from an X wire anemometer. It is apparent that for the case of a simple uniform canopy with constant A and exponential velocity profile, the predictions of the model are quite accurate. Equations (22) to (26) ensure that the canopy shear stress is bounded from above by the limiting value of $\tau(H)$ so that the predicted $\tau(z)$ within the canopy must be of the correct order; in the worked example above, the availability of a directly measured $\tau(H)$ has improved the accuracy of the calculation. Unfortunately, for the reasons already mentioned, such good agreement cannot be expected in more heterogeneous situations. It is in fact an interesting comment upon the self consistency of the method, that such good agreement would not have been achieved had more accurate values of C_d obtained from the pressure tapped stalk or from equation (22) been used in calculating $\tau(z)$ from (24).

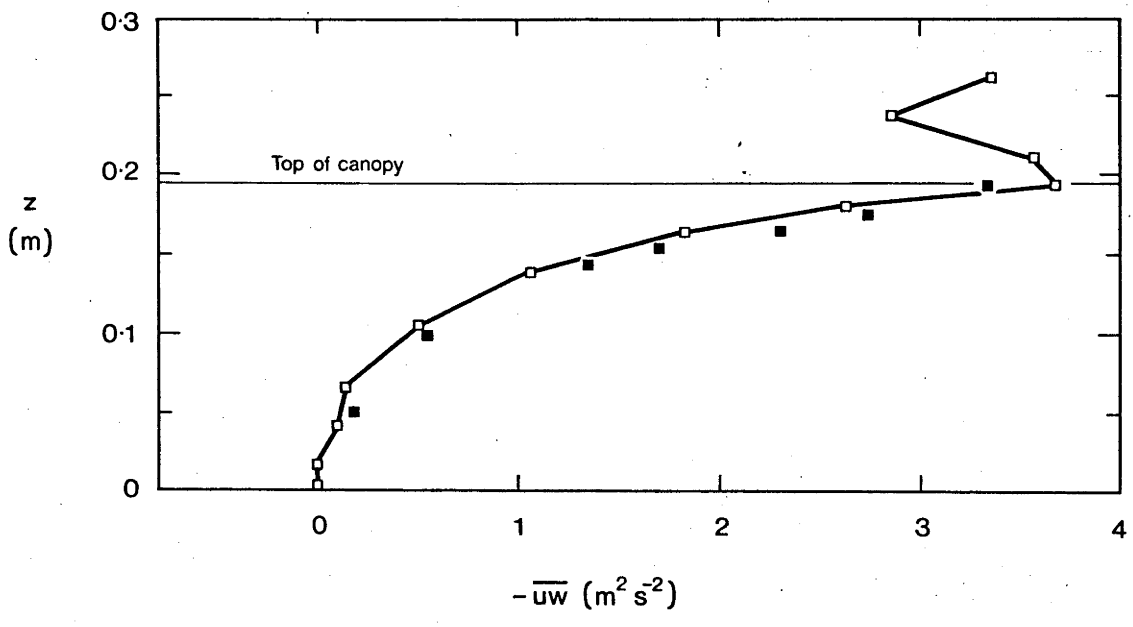

Fig. 5. Comparison between directly measured values of shear stress, $-\overline{uw}$ and values calculated by aerodynamic method, taken from data of Seginer *et al.* (1976). □ $-\overline{uw}$ measured by X wire; ■ $-\overline{uw}$ calculated by aerodynamic method.

4. Turbulent Energy and Spectral Theory

The loss of information which occurs when terms in the Navier-Stokes equations are decomposed into mean and fluctuating parts and then time averaged leads to the 'closure' problem of turbulence. Equations for mean moments of a given order always contain terms in higher order moments. Plausible relationships between them, usually based on empirical observations, are required to reduce the number of unknowns to the number of equations so that they form, in principle at least, a solvable set.

In the previous sections we have been discussing 'first order' closure schemes where the covariance, $\overline{uw}$, which appears in the equations for moments of the first order, the mean velocities, is equated to a scalar eddy diffusion coefficient multiplied by the mean velocity gradient. It was realized early in the study of turbulence, however, that to describe the interactions between eddies of different sizes, the equations for general two point correlations at least are required. Employing tensor notation for brevity we can write one equation,

$$\frac{\overline{\partial u_i u_j'}}{\partial t} = -\left[\overline{u_j' u_\ell \frac{\partial u_i}{\partial x_\ell}} + \overline{u_i u_\ell' \frac{\partial u_j'}{\partial x_\ell'}}\right]$$

$$-\frac{1}{\rho}\left[\overline{u_j' \frac{\partial p}{\partial x_i}} + \overline{u_i \frac{\partial p'}{\partial x_j'}}\right]$$

$$+\nu\left[\overline{u_j' \frac{\partial^2 u_i}{\partial x_\ell^2}} + \overline{u_i \frac{\partial^2 u_j'}{\partial x_\ell'^2}}\right] \qquad (28)$$

where the subscripts i, j, ℓ can take values 1, 2, 3 corresponding to the three co-ordinate directions and u_i is the velocity at a point, P, with position vector $\underset{\sim}{x}$ while u_i' is the velocity at a point P' with position vector $\underset{\sim}{x} + \underset{\sim}{r}$ (Bradshaw, 1976). ν is the kinematic viscosity.

When the separation, $\underset{\sim}{r}$, becomes zero, Equation (28) expresses the rate of change of the covariance, $\overline{u_i u_j}$ at a single point. The second order tensor $\overline{u_i u_j}$ has six independent components since $\overline{u_i u_j} = \overline{u_j u_i}$. The three equations for the on diagonal terms, $\overline{u_i u_i}$, are usually combined into a transport equation for the turbulent kinetic energy per unit mass, $\frac{1}{2}\overline{q^2}$, where $\overline{q^2} = \overline{u_1 u_1} + \overline{u_2 u_2} + \overline{u_3 u_3}$. Reverting to our earlier u, v, w notation, where v now represents a cross stream horizontal velocity fluctuation, we can write the equations for $\frac{1}{2}\overline{q^2}$ and the covariance $\overline{uw}$ for the case of a steady, two dimensional boundary layer flow:

$$(U\frac{\partial}{\partial x} + W\frac{\partial}{\partial z})\,\frac{1}{2}\overline{q^2} = -\overline{uw}\,\frac{\partial U}{\partial z} - \frac{\partial}{\partial z}\,(\overline{pw} + \frac{1}{2}\overline{q^2 w}) - \varepsilon \qquad (29)$$

$$(U\frac{\partial}{\partial x} + W\frac{\partial}{\partial z})\,(\overline{-uw}) = \overline{w^2}\,\frac{\partial U}{\partial z} - \overline{p\left(\frac{\partial u}{\partial z} + \frac{\partial w}{\partial x}\right)} + \frac{\partial}{\partial x}\left(\overline{pu} + \overline{uw^2}\right) \qquad (30)$$

U + u and W + w are the sums of the mean and fluctuating parts of the streamwise and vertical velocities respectively. p is the fluctuating pressure and ε, the viscous dissipation term; $\varepsilon = \frac{1}{2}\nu\overline{\left(\frac{\partial u_i}{\partial x_j} + \frac{\partial u_j}{\partial x_i}\right)^2}$. Terms representing viscous transport have been ignored since they are usually negligible in high Reynolds Number flows. Information about the spatial variation of the turbulence has disappeared in moving from Equation (28) to (29) and (30) and length scales must be derived in some way if (29) and (30) are to be usefully interpreted.

Taylor (1938) first showed rigorously that the second and higher order correlations, occuring in Equations (28-30), could be represented

by their Fourier transforms in wave number or frequency space. Fourier transforming Equations (28-30) has the advantage of converting spatial differentiation to simple multiplication by wave number or frequency. Although the closure problem remains, the transformed equations have some advantages for mathematical manipulation and a considerable amount of effort has been expended in modelling the equations in that form. For further references the reader is referred to Leslie (1973). Information about the behaviour of the correlations $\overline{u_i u_j}$ with space or time delay is conveniently displayed in the form of co-spectra or energy spectra and this has become a conventional way of presenting turbulence data.

The spectral representation can be demonstrated by writing the one dimensional wave number spectrum of $\overline{u_i u_j'}$ (where we have reverted temporarily to tensor notation for convenience) for a wave number component in the x_1 direction

$$\phi_{ij}\ (k_1) = \frac{1}{2\pi} \int_{-\infty}^{\infty} \overline{u_i u_j'} \exp\ (-ik_1 r_1)\ dr_1 \qquad (31)$$

and its inverse

$$\overline{u_i u_j'}\ (r_1) = \int_{-\infty}^{\infty} \phi_{ij}\ (k_1) \exp\ (ik_1 r_1)\ dk_1 \qquad (32)$$

where k_1 is the component in the x_1 direction of the wave number $\underset{\sim}{k}$ and $\underset{\sim}{r}$ is the separation between u_i and u_i'. $\phi_{ij}(k_1)$ is the spectral density due to all motions of wave number k_1 whatever their values of k_2 and k_3. $i = \sqrt{-1}$. In practice it is more often the autocorrelation, $\overline{u_i(t)\ u_i(t+\hat{t})}$ and its corresponding frequency spectrum, $\phi(f)$, which is measured, but if Taylor's hypothesis can be invoked, the representations are equivalent, with a wave number, k_1, replaced by a frequency Uk_1.

When spectra obtained in boundary layers are plotted against wave number or frequency, they are seen to be reasonably smooth functions. This observation has led to the concept of the 'Energy Cascade' and to the dimensional arguments of Kolmogorov (1941). The notion of the energy cascade is that the largest turbulent eddies derive their energy from the mean velocity gradient through a mechanism of vorticity amplification. Lines of vorticity aligned with the direction of maximum strain in a shear flow are stretched and their vorticity amplified at the expense of the vorticity components at right angles to them. Since, in a boundary layer, the principle axes of the strain rate have definite orientations, the eddies which interact directly with the mean shear are anisotropic. Their energy is passed to higher wave numbers by the vortex stretching process and, at these higher wave numbers, eddies are in turn stretched by the fluctuating velocity fields of the larger eddies. At the same time, as Hinze (1959) has persuasively argued, fluctuating pressures in the flow field act to redistribute the energy among $\overline{u^2}$, $\overline{v^2}$ and $\overline{w^2}$ components so as to tend to minimise their differences. Eventually eddies are of sufficiently high wave number or frequency that they can be destroyed by the action of viscosity, their kinetic energy being dissipated directly to heat.

If the Reynolds Number of the flow is high enough, there should be a range of eddy sizes which are small enough or alternatively have been 'scrambled' enough to have 'forgotten' the initial orientation of the large eddies. The small eddies have become isotropic. Furthermore, in flows with very high Reynolds Numbers, there should exist a range of wave numbers sufficiently far removed from the large eddies as to be isotropic, but too large for viscosity to act upon them

directly. This is the 'inertial sub-range' where the only important parameters can be the rate at which energy passes from eddy to eddy, a quantity determined by the dissipation at the high wave number end of the spectrum or equally well by the 'feeding' at the low wave number end.

Kolmogorov (1941) used dimensional arguments to show that, in the inertial sub-range, the spectrum must have the form,

$$\phi = \text{constant} \times \varepsilon^{2/3} k^{-5/3} . \qquad (33)$$

where ε is the rate of energy dissipation.

This '-5/3 law' is regarded as one of the most useful relationships in turbulence theory and has been applied in many situations where the rather stringent conditions assumed by Kolmogorov in its derivation cannot be expected to apply. It should be mentioned at this stage also, that in the light of recent experimental results, some of the arguments used in the formal derivation of (33) have been shown to be untenable (see Leslie, 1973). Nevertheless the -5/3 law continues to be universally applied.

Let us examine the conditions for the existence of an inertial sub-range. Kolmogorov stated that in the range where the spectral density, ϕ, is only a function of wave number, k, dissipation rate, ε, and kinematic viscosity, ν, only one length scale, η', can be formed:

$$\eta' = \left(\frac{\nu^3}{\varepsilon}\right)^{\frac{1}{4}}$$

and if eddies in this range are isotropic it is possible to define an eddy size or inverse wave number below which 90% of the dissipation should take place as

$$\eta = 15\left(\frac{\nu^3}{\varepsilon}\right)^{\frac{1}{4}} . \qquad (34)$$

In flows in local equilibrium, the production of turbulent energy by the action of the Reynolds stress upon the mean shear is equal to the rate of dissipation by viscosity so that we can write (for a two dimensional shear flow)

$$-\overline{uw}\,\frac{\partial U}{\partial z} = \varepsilon \ . \tag{35}$$

It will be shown below that this assumption almost certainly does not apply to canopies, however a value of η obtained using (34) ought to be of the correct order of magnitude.

A length scale, L_e, representative of the anisotropic large eddies, can be obtained directly as

$$L_e = u_*/\frac{\partial U}{\partial z} \ .$$

From the foregoing discussion, we would expect eddies in the inertial sub-range to satisfy the condition

$$L_e \gg \frac{1}{k_{isr}} \gg \eta \tag{36}$$

where k_{isr} is the wave number of a typical inertial sub-range eddy. We can use the data from a wheat canopy presented in Chapters 2 and 3 to calculate L_e and η for a typical canopy flow, and we find:

$$L_e \simeq 0.20 \text{ m}$$

$$\eta \simeq 0.015 \text{ m} \ .$$

Condition (36) can hardly be satisfied in this case; moreover if we relax condition (36) sufficiently to allow L_e and η to delimit a possible inertial sub-range, we can make two observations. Firstly, throughout this range of wave numbers or eddy sizes, energy is being fed into the spectrum directly from the wakes of individual plants and plant parts. This effectively negates the assumption that only feeding from lower wave numbers is important. In fact we would expect the

spectral density to decrease at a slower rate than $k^{-5/3}$. Secondly the assumption of isotropy requires that the orientations of the fluctuating velocity gradients (which, by acting on smaller eddies, continue the energy cascade) are randomly disposed in space by the time the inertial sub-range is reached. Within the canopy, however, the velocity gradient fields of plant wakes will have preferred orientations right into the dissipation range.

It appears that there are no a priori reasons to expect the predictions of the universal equilibrium theory to hold in canopy turbulence. It should be pointed out however that, this theory aside, spectra can provide a reasonably easy-to-interpret picture of periodic phenomena such as stalk waving.

The terms on the RHS of Equation (29) can be interpreted as production, dissipation and spatial transport of turbulent kinetic energy. The latter integrate to zero over the whole flow field and serve to transfer energy from the site where it is produced by the terms like $\overline{uw}\ \partial U/\partial z$ to regions where it is dissipated. If dissipation and production at a point are equal (and opposite), the flow is said to be in local equilibrium and should obey simple scaling laws. The inner region of smooth wall turbulent boundary layers, where the logarithmic law applies, is the classic example of local equilibrium. In boundary layers over rough walls however, both Antonia and Luxton (1971b) and Mulhearn and Finnigan (1978) found that a substantial portion of the production of $\frac{1}{2}\overline{q^2}$ at small z is diffused out from the wall by turbulent fluctuations. Within a canopy, the production term, $u_*^2\ \partial U/\partial z$, exhibits a strong peak at the canopy top (Uchijima and Wright, 1964; Baines, 1972; Seginer et al., 1976) and we would expect both the lower regions of the

canopy, where production is small, and the boundary layer above the canopy to be sinks for $\frac{1}{2}\overline{q^2}$. To measure the triple correlations involved in the diffusion terms like $\partial\,\overline{q^2 w}/\partial z$ of Equation (29) requires better instrumental accuracy than has so far been obtained in the field. In the model canopy of Seginer et al. (1976), however, one of the turbulent diffusion terms, $\partial\overline{w^3}/\partial z$ was measured and it was apparent that this term at least was diffusing energy from the peak of production at the canopy top to the regions below.

Both Baines (1972), studying turbulence in a wheat crop, and Uchijima and Wright (1964) in corn, made the assumption that dissipation equals production throughout the canopy, which probably invalidates some of their conclusions. Despite this reservation, Uchijima and Wright presented a good deal of valuable information. They presented their data both as power spectra, ϕ, and structure functions, B_{uu} where,

$$B_{uu} = \overline{[u(x) - u(x+r)]^2} \quad . \tag{37}$$

Since data were only measured at a single point, Taylor's hypothesis was invoked to calculate B_{uu}; Hinze (1959) has shown, however, that this assumption is unreliable when the r.m.s. turbulent velocities are a substantial fraction of the mean, a circumstance which invariably accompanies canopy flows. B_{uu} should therefore be treated with some caution, certainly at large values of r. In the inertial subrange, the structure function obeys a relationship equivalent to Equation (33):

$$B_{uu} = \text{constant} \times \varepsilon^{2/3}\, r^{2/3} \tag{38}$$

Uchijima and Wright's measured B_{uu}'s showed reasonable agreement with (38) at small r but the power spectra of streamwise fluctuations, ϕ_{uu},

decayed more slowly than the -5/3 law predicts. The spectra measured by Inoue et al. (1975), using sonic anemometers in a rice canopy, also appear to fall off more slowly than $k^{-5/3}$ as do the corn canopy data of Isobe (1972), but in both these cases the spectra are very ragged in the high frequency range and only general trends can be estimated.

Surprisingly, the most accurate canopy measurements available to date do show excellent agreement with the -5/3 law over a limited frequency range of 0.4 to 2.0 Hz. These measurements, made by Shaw et al. (1974) within a corn canopy with a fast response hot wire anemometer, produced power and co-spectra of u, v and w. With their data, they were able to test the prediction of the Universal Equilibrium theory, that within the isotropic range, the streamwise and cross stream spectral densities should be in the ratio $\phi_{uu}/\phi_{ww} = \phi_{uu}/\phi_{vv} = 0.75$. They found instead that $\phi_{uu}/\phi_{ww} \simeq 1.05$ and $\phi_{uu}/\phi_{vv} = 1.1$. In other words, within the -5/3 law wave number range, the eddies were not isotropic.

The Reynolds Number of wind tunnel experiments is normally too low for a true inertial sub-range to exist but the power spectra measured by Seginer et al. (1976) in their model canopy of rods showed a reasonable agreement with the -5/3 law over one decade. The conditions for isotropy, however, were not present there either. The experimental setup in their model canopy allowed the contribution to the total energy spectrum by the turbulence energy generated by the wakes of the rods alone to be identified (see Figure 2). Although the rod turbulence was probably underestimated because of the spatial averaging effect of the hot wires (Sheih et al., 1978), it was far outweighed by the production from the action of turbulent shear stress on the mean velocity gradient.

Both Baines (1972) and Uchijima and Wright (1964) calculated the total dissipation throughout the canopy (assuming it equalled the production) and compared it with the net radiation at the canopy top. They concluded that ε contributes a negligible amount to the sensible heat flux budget, being of the order of 0.1% of the radiation flux.

Two other important experiments where results have been presented in spectral form should be mentioned. Isobe (1972) measured two point statistics using two sonic anemometers with different vertical separations in and above a corn canopy. His spectra show a good deal of variability when presented in terms of Coherence and Phase (See Lumley and Panofsky, 1964, for definitions of these terms). They suggest, however, that fluctuations of low wave number move down in the canopy while there is a characteristic frequency band, 0.11 Hz to 0.18 Hz, where fluctuations are propagating upwards. Space time correlations presented in the same paper are more informative and reveal that the large eddies, which contribute most to the correlations at large time delay, are being convected downstream more rapidly than the mean velocity at the sensors. This particular point will be taken up in Chapters 2 and 3.

Allen (1968) used heated thermocouple anemometers in and above a Japanese larch plantation to measure power spectra and Eulerian length scales. The latter measurements have been discussed in an earlier section; his spectra, however, while not extending to a high enough frequency range to properly test the Universal Equilibrium hypotheses, enabled him to identify the average frequency of arrival of large gusts. This appeared to vary directly with the mean wind speed. This point also will be expanded in Chapters 2 and 3.

The equation for the covariance, (30) is somewhat different to the

kinetic energy budget of (29). Contributions to the time mean covariance can only be from anisotropic eddies so that viscous dissipation is unlikely to be important. The main sink terms are the pressure-velocity gradient correlations, $\overline{p\left(\frac{\partial u}{\partial z}+\frac{\partial w}{\partial x}\right)}$ which act to smooth out anisotropy. Where co-spectra have been calculated (Shaw et al., 1974; Seginer et al., 1976) they have cut off points at frequencies substantially lower than the power spectra. To date, measurements of terms in the covariance budget (30) have not been presented in the literature, but Shaw (1977) and Wilson and Shaw (1977) have produced a second order closure scheme based upon this equation, which avoids some of the anomalies of the simpler gradient diffusion models. Some direct measurements therefore would obviously be very useful.

To summarize this section, it appears that although the classic prediction of Universal Equilibrium spectral theory, the -5/3 law, appears to fit some of the measurements within canopies, most of the assumptions leading to its derivation can be shown to be emphatically violated. Like the logarithmic and exponential profiles, it is remarkably tolerant. This tolerance, however, severely limits its usefulness and we are bound to say that, so far at least, the Universal Equilibrium theory has not been shown to be applicable within canopies. The universal constant in Equation (33) has now been determined with some confidence in the atmospheric boundary layer and enables the dissipation to be derived directly from spectral results. Within the canopy it seems unlikely that any consensus would be reached on its value or whether indeed it has any validity.

Direct measurements of the terms of (29) and (30) would be of great value if reliable three dimensional sensors could be employed. In the

first case the production/dissipation ratio and its spatial variation is a fairly sensitive test of whether simple scaling laws can adequately describe the flow field (Townsend, 1976). If second order closure models of the type proposed by Wilson and Shaw (1977) are to be developed then more information must be obtained on the terms of both Equations (29) and (30). At a more practical level, this information can be used to assess the range of approximate validity of the simpler first order theories described in the earlier sections.

References

Allen, L.H., Jr.: 1968, 'Turbulence and Wind Speed Spectra Within a Japanese Larch Plantation', J. Appl. Meteorol. 7, 73-78.

Antonia, R.A. and Luxton, R.E.: 1971, 'Energy Balance in a Turbulent Boundary Layer on a Rough Wall', Phys. Fluids. 14, 1027-1029.

Baines, G.B.K.: 1972, 'Turbulence in a Wheat Crop', Agric. Met. 10, 93-105.

Bearman, P.W.: 1969, An Investigation of the Forces on Flat Plates in Turbulent Flow, NPL Aero Report 1296 ARC 31 125.

Bearman, P.W. and Trueman, D.M.: 1971, An Investigation of the Flow around Rectangular Cylinders, Imperial College of Science and Technology, I.C. Aero Report 71-15.

Blackwelder, R.F. and Kovaszny, L.S.G.: 1972, 'Time Scales and Correlations in a Turbulent Boundary Layer', Phys. Fluids 15, 1545-1554.

Bradshaw, P.(Ed.): 1976, Topics in Applied Physics: Turbulence, Springer-Verlag, Berlin, 335 pp.

Brown, K.W. and Covey, W.: 1966, 'The Energy-budget Evaluation of the Micro-meteorological Transfer Processes Within a Cornfield', Agric. Met. 3, 127-149.

Cionco, R.M.: 1965, 'A Mathematical Model for Airflow in a Vegetative Canopy', J. Appl. Meteorol. 4, 517-22.

Cionco, R.M.: 1972a, 'A Wind Profile Index for Canopy Flow', Boundary-Layer Meteorol. 3, 255-263.

Cionco, R.M.: 1972b, 'Intensity of Turbulence Within Canopies with Simple and Complex Roughness Elements', Boundary-Layer Meteorol. 2, 453-465.

Counihan, J.: 1975, 'Adiobatic Atmospheric Boundary Layers: A Review and Analysis of Data from the Period 1880-1972', Atmos. Environ. 9, 871-905.

Corrsin, S.: 1963, 'Estimation of the Relations between Eulerian and Lagrangian Scales in Large Reynolds Number Turbulence', J. Atmos. Sci. 20, 115.

Corrsin, S.: 1974, 'Limitations of Gradient Transport Models in Random Walks and Turbulence. Adv. Geophys. 18A, 25-60.

Cowan, I.R.: 1968, 'Mass, Heat and Momentum Exchange between Stands of Plants and their Atmospheric Environment', Quart. J. Roy. Meteorol. Soc. 94, 523-544.

Denmead, O.T.: 1964, 'Evaporation Sources and Apparent Diffusivities in a Forest Canopy', J. Appl. Meteorol. 3, 383-389.

Finnigan, J.J. and Mulhearn, P.J.: 1978, 'Modelling Waving Crops in a Wind Tunnel', Boundary-Layer Meteorol. 14, 253-277.

Garratt, J.R.: 1978, 'Transfer Characteristics for a Heterogeneous Surface of Large Aerodynamic Roughness', Quart. J. Roy. Meteorol. Soc. 104, 243-256.

Grass, A.J.: 1971, 'Structural Features of Turbulent Flow over Smooth and Rough Boundaries', J. Fluid Mech. 50, 233-235.

Hinze, J.O.: 1959, Turbulence: an Introduction to its Mechanism and Theory, McGraw-Hill.

Hoerner, S.F.: 1965, Fluid Dynamic Drag, Published by the author.

Inoue, E.: 1963, 'On the Turbulent Structure of Airflow Within Crop Canopies', J. Met. Soc. Japan, Ser. II, 41, 317-326.

Inoue, E., Lemon, E.R. and Denmead, O.T.: 1972, 'A Preliminary Investigation into the Air Flow within Crop Canopies', Unpublished Material.

Inoue, K., Uchijima, Z., Horie, T. and Iwakiri, S.: 1975, 'Studies of Energy and Gas Exchange within Crop Canopies (10) Structure of Turbulence in Rice Crop', J. Agric. Meteorol. (Japan) 31, 71-82.

Isobe, S.: 1970, 'A spectral analysis of turbulence in a corn canopy', Bull. Nat. Inst. Agr. Sci. (Japan) Ser. A. No. 19, 101-112.

Kolmogorov, A.N.: 1941, 'The local Structure of Turbulence in Incompressible Viscous Fluid for Very Large Reynolds Numbers', In Friedlander, S.K. and Topper, L. (Eds.) Turbulence, Classic Papers on Statistical Theory (1961), Interscience, New York.

Lee, B.E.: 1975/6, 'Some effects of Turbulence Scale on the Mean Forces on a Bluff Body', J. Indust. Aerodynamics 1, 361-370.

Leslie, D.C.: 1973, Developments in the theory of Turbulence, Oxford University Press, London.

Lettau, H.H.: 1959, 'Wind Profile, Surface Stress and Geostrophic Drag Coefficients in the Atmospheric Surface Layer', Adv. Geophys. 6, 241-259.

Lumley, J.L. and Panofsky, H.A.: 1964, The Structure of Atmospheric Turbulence, Wiley-Interscience, New York.

McLaren, F.G., Sherratt, A.F.C., Morton, A.S.: 1969, 'Effect of Free Stream Turbulence on the Drag Coefficient of Bluff, Sharp-edged cylinders', Nature 224, 908-909.

Mulhearn, P.J. and Finnigan, J.J.: 1978, 'Turbulent Flow over a very Rough, Random Surface', Boundary-Layer Meteorol. (in press).

Nakagawa, H. and Nezu, I.: 1977, 'Prediction of the Contributions to the Reynolds Stress from Bursting Events in Open-Channel Flow', J. Fluid Mech. 80, 99-128.

Ordway, D.E., Ritter, A., Spence, D.A. and Tan, E.S.: 1960, Effects of Turbulence and Photosynthesis on CO_2 Profiles in the Lower Atmosphere. Therm Advanced Research Report, TAR-IR. 601, Ithaca, New York.

Philip, J.R.: 1964, 'Sources and Transfer Processes in the Air Layers Occupied by Vegetation', J. Appl. Meteorol. 3, 390-395.

Prandtl, L.: 1925, Zeitschr.Angew. Math. Mech. 5, 137-138.

Robertson, J.A. and Rutherford, G.S.: 1969, 'Turbulence Effect on Drag of Angular Blunt Bodies', Proc. Am. Soc. Civ. Eng. 95, 781-785.

Saito, T.: 1964, On the Wind Profile within Plant Communities', Bull. Nat. Inst. Agr. Sci. (Japan) Ser. A, 11, 67-73.

Saito, T., Nagai, Y., Isobe, S., and Horibe, Y.: 1970, 'An Investigation of Turbulence within a Crop Canopy', J. Agr. Meteorol. (Japan), 25, 205-215.

Seginer, I., Mulhearn, P.J., Bradley, E.F., and Finnigan, J.J.: 1976, 'Turbulent Flow in a Model Plant Canopy', Boundary-Layer Meteorol. 10, 423-453.

Shaw, R.H.: 1977, 'Secondary Wind Speed Maxima Inside Plant Canopies', J. Appl. Meteorol. 16, 514-521.

Shaw, R.H., Silversides, R.H., and Thurtell, G.W.: 1974, 'Some Observations of Turbulence and Turbulent Transport Within and Above Plant Canopies', Boundary-Layer Meteorol. 5, 429-449.

Sheih, C.M. and Finnigan, J.J.: 1978, 'An Experimental Determination of the Probe Length Requirements for the Study of the Turbulent Wake behind a Cylinder', J. Fluid. Mech. (Submitted for publication).

Snyder, W.H. and Lumley, J.L.: 1971, 'Some Measurements of Particle Velocity Autocorrelation Functions in a Turbulent Flow', J. Fluid Mech. 48, 41-71.

Söderlund, R. and Svensson, B.H.: 1976, 'The Global Nitrogen Cycle', In Svensson, B.H. and Söderlund, R. (Eds.) Nitrogen, Phosphorus and Sulphur - Global Cycles. SCOPE Report 7, Ecol. Bull. (Stockholm) 22, 23-75.

Surry, D.: 1972, 'Some Effects of Intense Turbulence on the Aerodynamics of a Circular Cylinder at Subcritical Reynolds Number', J. Fluid. Mech. 52, 543-563.

Taylor, G.I.: 1932, 'The Transport of Vorticity and Heat through Fluids in Turbulent Motion', Proc. Roy. Soc. A, 135, 697-700.

Taylor, G.I.: 1938, 'The Spectrum of Turbulence', In S.K. Friedlander and L. Topper (Eds.) Turbulence - Classic Papers on Statistical Theory, Interscience, New York.

Tennekes, H., and Lumley, J.L.: 1972, A First Course in Turbulence, MIT Press, Cambridge, Mass., 300 pp.

Thom, A.S.: 1971,'Momentum Absorption by Vegetation', Quart. J. Roy. Meteorol. Soc. 97, 414-428.

Thom, A.S.: 1972, 'Momentum, Mass and Heat Exchange of Vegetation', Quart. J. Roy. Meteorol. Soc. 98, 124-134.

Thom, A.S.: 1975, 'Momentum, Mass and Heat Exchange of Plant Communities', In Monteith, J.L. (Ed.) Vegetation and the Atmosphere, Academic Press , London.

Thom , A.S., Stewart, J.B., Oliver, H.R., and Gash, J.H.C.: 1975, 'Comparison of Aerodynamic and Energy Budget Estimates of Fluxes over a Pine Forest', Quart. J. Roy. Meteorol. Soc. 101, 93-105.

Townsend, A.A.: 1976, The Structure of Turbulent Shear Flow, Cambridge Univ. Press, Cambridge.

Uchijima, Z. and Wright, J.L.: 1964, 'An Experimental Study of Air Flow in a Corn Plant-air Layer', Bull. Nat. Inst. Agric. Sci. (Japan) Ser. A. 11, 19-65.

Von Kármán, T.: 1930, Nachr. Ges. Wiss. Göttingen, Math.-Phys. Kl. pp 58-76.

Willmarth, W.W.: 1975, 'Structure of Turbulence in Boundary Layers', In Yih, C.S. (ed.), Advances in Applied Mechanics 15, pp. 159-253, Academic Press, New York.

Wilson, N.R. and Shaw, R.H.: 1977, 'A Higher Order Closure Model for Canopy Flow', J. Appl. Meteorol. 16, 1197-1205.

Wright, J.L. and Lemon, E.R.: 1966, 'Photosynthesis under Field Conditions. VIII. Analysis of Windspeed Fluctuation Data to Evaluate Turbulent Exchange Within a Corn Crop', Agron. J. 58, 255-261.

CHAPTER 2

TURBULENCE IN WAVING WHEAT.

I. MEAN STATISTICS AND HONAMI

Abstract. Measurements of mean and fluctuating velocity, surface pressure and stalk waving have been made in a very uniform wheat canopy. Features of the vertical profiles of mean turbulence quantities are discussed in the context of the resonant waving of wheat stalks. The discrete and prominent peaks in the velocity spectra measured in and above the canopy are then analyzed in the light of the organized travelling wave type structure or 'honami', observed in such crops on windy days. Prominent peaks in the spectra are identified with the arrival of gusts, the stalk waving frequency, and the frequency of oscillations in the canopy height. Two possible mechanisms are proposed to account for the observed height dependence of the peak frequencies, directly associated with stalk waving.

Symbols

x streamwise co-ordinate positive downwind

y cross stream co-ordinate

z vertical co-ordinate positive upwards

$\tilde{u}$ instantaneous streamwise velocity

$\tilde{v}$ instantaneous cross stream velocity

$\tilde{w}$ instantaneous vertical velocity

$\tilde{u} = U + u; \quad U = \bar{\tilde{u}}; \quad \bar{u} = 0$

$\tilde{v} = V + v; \quad V = \bar{\tilde{v}}; \quad \bar{v} = 0$

$\tilde{w} = W + w; \quad W = \bar{\tilde{w}}; \quad \bar{w} = 0$

$\tilde{p}$ instantaneous pressure

$\tilde{p} = P + p; \quad P = \bar{\tilde{p}}; \quad \bar{p} = 0$

$$\bar{q} = \lim_{T\to\infty} \frac{1}{T} \int_0^T q\,(t)\,dt$$

$\hat{h}$ characteristic height of hill in theory of Jackson and Hunt (1974)

$\hat{L}$ characteristic length of hill in theory of Jackson and Hunt (1974)

$C_d(z)$ Dimensionless drag coefficient of foliage

$A(z)$ Area of foliage per unit volume of space

u_* friction velocity $= (-\overline{uw})^{\frac{1}{2}}$

i_u streamwise turbulence intensity $= \left(\overline{u^2}\right)^{\frac{1}{2}}/U$

i_w vertical turbulence intensity $= \left(\overline{w^2}\right)^{\frac{1}{2}}/U$

ϕ_{uu} power spectral density of streamwise velocity fluctuations

ϕ_{ww} power spectral density of vertical velocity fluctuations

ϕ_{uw} cross spectral density of streamwise and vertical velocity fluctuations

ξ instantaneous displacement of wheat stalk from its mean position in the x direction

ξ_o amplitude of periodic displacement

λ wavelength of honami waves

f frequency of honami waves

θ phase velocity of homani waves = λf

f_g frequency of arrival of gusts at the surface

R_{pu} pressure velocity correlation coefficient

$$R_{pu} = \frac{\overline{u(z,t+\tau) \cdot p(t)}}{\left[\overline{u^2(z,t+\tau)} \cdot \overline{p^2(t)}\right]^{\frac{1}{2}}}$$

$'$ values relevant to velocity waves rather than honami waves

S Strouhal Number

D typical dimension of canopy element

Other symbols are defined as they are encountered in the text.

1. Introduction

Over the last decade, a great deal of experimental work has been directed at determining the role of 'large' or 'coherent' structures in the transport of momentum in turbulent boundary layers. It has become accepted that momentum transport is a very intermittent process and is usually accompanied by a velocity field considerably different from the mean (Mollo-Christensen, 1973), whilst gusts or 'downsweeps' of high momentum fluid, randomly distributed in time and the x-y plane, have been shown to be the dominant mechanism of momentum transfer very close to the surface in rough wall turbulent boundary layers (Grass, 1971; Nakagawa and Nezu, 1977). Such gusts or downsweeps are now known to be manifestations of large eddies with length scales of the order of the boundary layer thickness (Brown and Thomas, 1976). In the atmospheric boundary layer above and within plant canopies a few isolated results [for example, those of Allen (1968) in Japanese Larch and of Isobe (1972) in corn] have suggested that the character of the turbulence within the canopy might owe more to the properties of the boundary layer several plant heights above the foliage than to wakes of leaves, stems, branches or even individual trees. The phenomena of 'homani', or patches of coherent waving in cereal crops (Inoue, 1955), and 'catspaws' on open water (Dorman and Mollo-Christensen, 1973) are particular examples of the intermittency of momentum transfer to the earth's surface.

However, most of the published measurements of turbulence in plant canopies have been concerned with providing the essential background knowledge of the behaviour of mean turbulence statistics without which more detailed investigations cannot be attempted. This has necessitated long averaging periods in order to obtain the desired statistical

confidence; but as a result, the unsteady details of the flow have been obscured. The theoretician has been left with the task of relating these mean statistics to the observed boundary conditions of the flow field, the surface geometry and some reference mean velocity. Foliage flexibility has invariably been ignored in formal analyses but is sometimes invoked qualitatively in the form of appeals to 'streamlining' to explain some observed dependence of drag upon windspeed, although it is relatively simple to show that the contribution to the mean aerodynamic drag in a waving cereal canopy from the motion of the plants directly is of the same order as that of the mean and fluctuating velocities (Finnigan and Mulhearn, 1978a).

The present work is an attempt to detail the intermittent nature of the turbulence in a flexible plant canopy, a stand of wheat. It is divided into two parts. In this paper the mean turbulence statistics of the flow will be established and some of the observed features of the measured velocity spectra will be explained in terms of the interaction between the stalks' motion and the turbulent velocity field. In Finnigan (1978), hereafter referred to as 'Part II', a more detailed analysis of the structure of momentum transfer will be attempted using techniques of conditional sampling.

2. Description of Experimental Site

The measurements were made between 9 and 18 December 1976 at the CSIRO Ginninderra Experiment Station, Canberra, Australia. The data were collected in a very uniform stand of wheat forming a rectangle 700 m by 300 m, with its long axis aligned at 310°. The measuring station was about 500 m downwind of the short edge of the canopy and 50 m in from one of the long sides. Therefore measurements could be made when the wind was

between -6° and +26° of the long axis of the canopy without encountering edge effects. In fact throughout the experiments the mean wind blew steadily from the West North West (295°) with a variation of ±5° which was well within these limits. The measuring site was at the crest of a very slight hill (maximum slope ≈1°). The profile of this hill measured by theodolite and staff is shown in Figure 1.

The principal reason for the choice of the site was the very uniform character of the canopy, which consisted of mature wheat about one month from harvest. The stalk height averaged 1.25 m throughout the canopy, and the leaf area/unit volume, estimated photographically, was about 0.83 $m^2\ m^{-3}$, with little apparent variation with height over the upper 90% of the canopy. The wheat was planted in rows at right angles to the long axis of the canopy. The row spacing was 0.2 m and the spacing of tillers within rows averaged 0.07 m. At the stage of crop development, however, the row structure could not be detected by 0.25 m above the soil surface. A general view of the site is provided by Figure 2.

3. Instrumentation

Measurements of turbulent velocities were made with single and X configuration hot wire anemometer probes. The probes were mounted on a vertical mast with the single wire fixed at a height of 2 m, whereas the height of the X wire was variable. Both sensors were mounted on damped wind vanes with a time constant of 1 s, free to rotate about a vertical axis, and these vanes in turn were fixed to arms which projected 0.5 m from the mast. The single wire of the reference probe was aligned horizontally while the 'X' of the X configuration probe was in a vertical plane. DISA 55P61 and 55P01 miniature wire probes were used as the

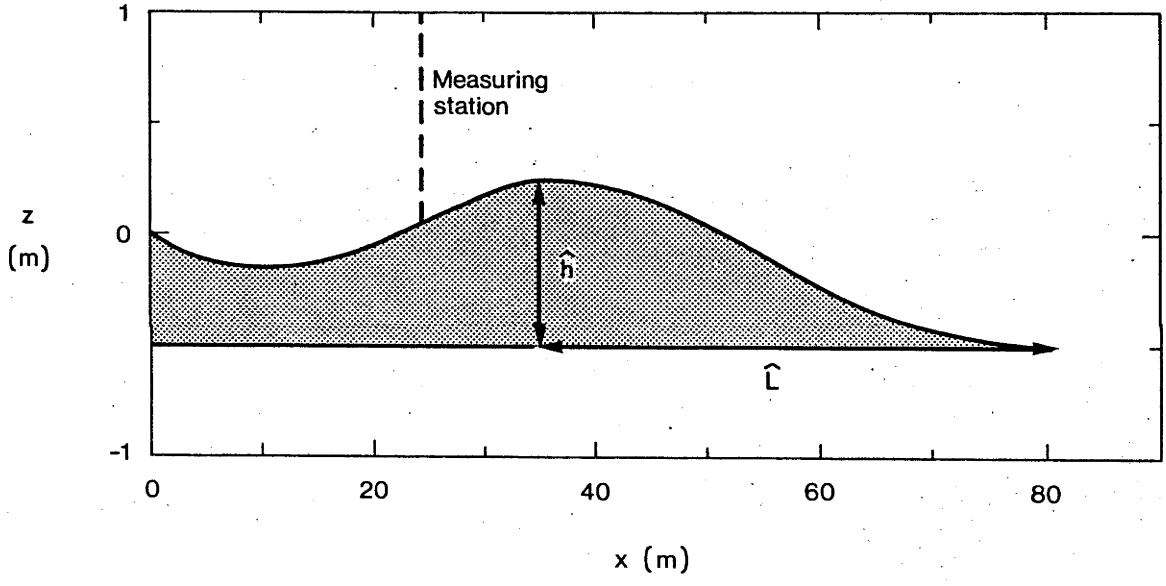

Fig. 1. Profile of field site. $\hat{h}$ and $\hat{L}$ are characteristic height and length scales of the hill.

Fig. 2. General view of mast and canopy.

sensors. An open 'cage' of 22 SWG piano wire was used to protect the X probe from flailing stalks when it was traversed into the canopy. The hot wire and mast arrangement is detailed in Figure 3.

All hot wires, which were driven by Thermo Systems Inc. Model 1050 hot wire bridges, were operated at an overheat ratio of 1.5 and were initially calibrated in the CSIRO Division of Environmental Mechanics Wind Tunnel. In the field, two points on the calibration curve were fixed by placing the wires in a DISA 55D41 miniature wind tunnel immediately before an experimental run. It was established that the form of the calibration curve remained constant, the effect of ambient temperature variation being, to first order at least, to simply scale the curve. No other temperature corrections were made.

The outputs from the sensors were offset and scaled to vary between ±5 volts on an EAI TR20 analogue computer, low pass filtered below 250 Hz by Rockland model 1042F 4-pole filters with Butterworth response, and then recorded on a Hewlett Packard type 3955 analogue tape recorder. The records were processed on a Digital Equipment Corporation PDP 11/40 computer.

The static pressure at the ground surface, vertically below the hot wires, was measured with a Validyne DP15TL pressure transducer, whose dynamic response was flat between 0 and 300 Hz. The 25.4 mm diameter circular membrane of the transducer formed one wall of a cylindrical cavity which was open to the atmosphere via a 4.76 mm diameter hole in a thin brass sheet. This sheet was set flush with the ground surface. The reference pressure to the reverse side of the membrane was provided by a leak to atmosphere through a pinhole in a 2 mm wall thickness neoprene tube. This hole had an empirical time constant of 0.05 s^{-1}.

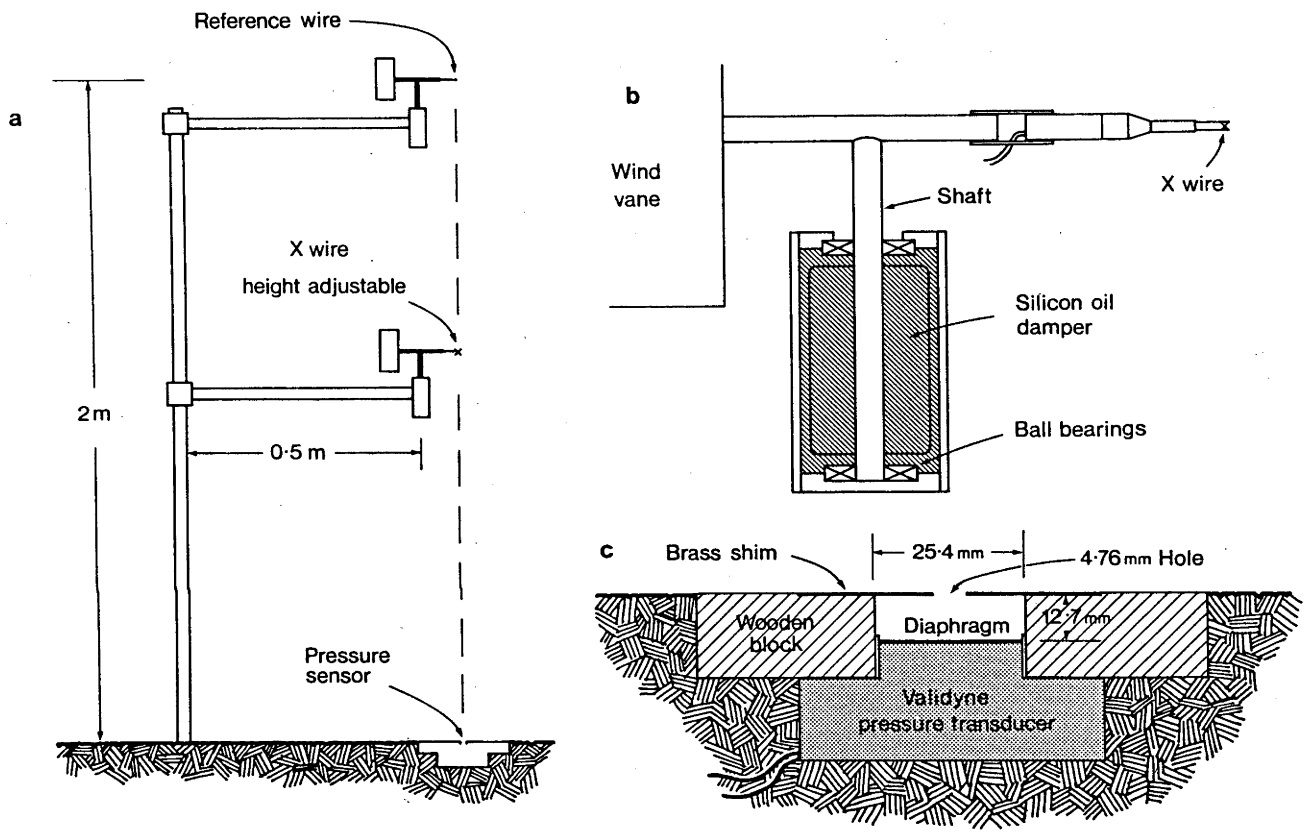

Fig. 3. (a) arrangement of hot wire sensors on mast; (b) details of wind vane; (c) details of pressure sensor installation.

If the cavity containing the membrane and sensing hole were regarded as a Helmholtz resonator, it would have had a natural frequency of the order of 4.5 KHz and would have had no effect in the frequency range of the present measurements. The output of the transducer was low pass filtered below 250 Hz by the Rockland filter, resulting in a system with a dynamic response to fluctuations essentially flat between .07 Hz and 250 Hz. The transducer was calibrated against an inclined manometer after the experiment and had a linear static response. The details of the installation are shown in Figure 3c.

In order to determine the phase and frequency of stalk waving, two Philips Type PR 9833K/01 miniature strain gauges were cemented on opposite sides of the bases of each of five individual stalks. Pairs of gauges were connected in bridge circuits to eliminate the effects of temperature drift; their outputs were recorded on the analogue tape recorder.

The sensors described were all located at a single station on the field site. To obtain the overall picture of the turbulent flow in the canopy, necessary for an appreciation of honami, the waving wheat was filmed for 10 minutes during each experimental run with a Super 8 movie camera and the film later played back at a lower speed for analysis. Apart from the digital computer, all recording instruments were located in a caravan parked downwind of the field site.

4. Errors in Hot Wire Measurement

Assuming that all probes have a cosine response to wind direction, and neglecting for the moment other sources of error, the X wire measures a mean velocity equal to $(U^2 + V^2)^{\frac{1}{2}}$ and the single wire measures

$(U^2 + V^2 + W^2)^{\frac{1}{2}}$. Throughout the measuring periods, however, the vanes deviated less than ±15° from their mean position so that the X wire overestimated U by a maximum amount $(1 + \tan^2 15°)^{\frac{1}{2}} \simeq 3.5\%$.

Weiss and Allen (1976) have measured fluctuating velocities above a vine crop using 3 component propeller anemometers and found that during strong gusts the inclination to the horizontal of the wind vector was always less than 15°. We can say then that the reference wire would overestimate U by at most $(1 + 2\tan^2 15°) \simeq 7\%$.

The most serious error in the wire measurements, however, is a consequence of employing an oversimplified transfer equation between the effective cooling velocity at the wire and the true velocity vector. For the case of an X wire with wires at angles of α_1 and α_2 to the probe axis, the effective cooling velocity C_{eff} is given by

$$C_{eff_i} = \left|\left\{(\tilde{u} \sin \alpha_i + \tilde{w} \cos \alpha_i)^2 + \ell^2 v^2 + k^2 (\tilde{u} \cos \alpha_i - \tilde{v} \sin \alpha_i)^2\right\}^{\frac{1}{2}}\right| \quad (1)$$

where ℓ, the pitch factor, represents the sensitivity of the wires to the v component and k their sensitivity to axial cooling. ℓ is normally taken to be of order 1 while for the X wires used in this experiment k is given as 0.12 by Champagne and Sleicher (1967). The modulus sign recognizes the rectifying property of the hot wires. $\tilde{u}$, $\tilde{v}$ and $\tilde{w}$ are instantaneous streamwise, cross-stream and vertical velocity components, respectively.

In practice equation (1) is usually approximated by

$$C_{eff_i} = \tilde{u} \sin \alpha_i + \tilde{w} \cos \alpha_i \quad (2)$$

and the modulus sign is ignored. This is a valid procedure in low intensity turbulence since it involves neglecting terms of order

u^2/U^2, w^2/U^2, v^2/U^2 and k^2, and rectification is unlikely to be a problem. In the large turbulent intensities typical of canopy flow, however, use of equation (2) can lead to large errors in measured moments of velocity.

Tutu and Chevray (1975) have calculated the distortion which would appear in a jointly normal probability density distribution of $\tilde{u}$, $\tilde{v}$ and $\tilde{w}$ if it were sampled by a perfectly matched X wire and equation (2) were used as the transfer function. They found that for a true $\left(\overline{u^2}\right)^{\frac{1}{2}}/U$ of 50%, and $\left(\overline{w^2}\right)^{\frac{1}{2}}/U = \left(\overline{v^2}\right)^{\frac{1}{2}}/U$ of 40%, U would be overestimated by 20%, whereas $\left(\overline{u^2}\right)^{\frac{1}{2}}/U$, $\left(\overline{w^2}\right)^{\frac{1}{2}}/U$ and $\overline{uw}/U^2$ would be underestimated by -26%, -32% and -64% respectively. These errors were a combination of ignoring the effects of the $\tilde{v}$ component and of rectification. Rectification alone $\left[\left(\overline{v^2}\right)^{\frac{1}{2}}/U = 0\right]$ produced errors in U, $\left(\overline{u^2}\right)^{\frac{1}{2}}/U$, $\left(\overline{w^2}\right)^{\frac{1}{2}}/U$ and $\overline{uw}/U^2$ of +3.6%, -12.9%, -11.8% and -42.1% respectively. Rectification is the main source of error in $\overline{uw}/U^2$ but its effect will be mitigated if instead of being distributed normally, u fluctuations are positively skewed, particularly at times of large contributions to $\overline{uw}$.

Grass (1971) and Nakagawa and Nezu (1977) have shown that the downsweep-burst cycle, observed by many workers in turbulent flows over smooth surfaces, is also a feature of rough wall boundary layers and channel flows. Close to a rough wall, however, Nakagawa and Nezu showed that the dominant mechanism transferring momentum to the surface is the downsweep or gust (u positive, w negative) rather than the burst (u negative, w positive). In Part II, it will be shown that close to and within the canopy, practically all of the momentum transfer is associated with large positive u fluctuations. Tutu and Chevray's calculations show that the Gaussian joint p.d.f., which in reality had zero skewness, appeared to have a skewness of +0.28 due to the effects of rectification

and neglect of $\tilde{v}$ fluctuations. Reference to Figure 4, in which profiles of skewness from three runs (R1, R2, R4) are plotted, shows that the measured skewnesses are between two and a half and fourteen times larger than this, indicating that a large positive skewness is a real feature of the flow. It can be assumed, therefore, that, at least during the time when most momentum is being transferred, rectification is unimportant.

The remaining source of major error is the neglect of $\tilde{v}$ in equation (2). Since most gusts have time scales much larger than 1 s, the vanes should keep the wires aligned so that in the reference frame of the probes, $\tilde{v} = 0$. There is no doubt that fluctuations with scales of 1 s or smaller will affect the measured moments. It is worth pointing out, however, that most of the contributions to $\overline{u^2}$ and $\overline{w^2}$ come from fluctuations with frequencies less than 1 Hz (see Figures 10, 11, 12).

The errors involved in the analogue and digital processing of the hot wire signals have been checked by replacing the hot wire bridge outputs with accurately known test signals and are about 1%.

5. Experimental Procedure

In order to obtain a profile, the X wire was moved to different heights whilst the reference wire recorded continuously. Data for each point were recorded for 5 min. When the X wire is very close to the reference wire ($z = 1.95$ m) their cross-correlation coefficient, R_{uu_R}, defined as

$$R_{uu_R} = \frac{\overline{u(t)u_R(t+\tau)}}{\left[\overline{u^2}(t)\ \overline{u_R^2}(t+\tau)\right]^{\frac{1}{2}}}$$

should closely approximate the autocorrelation coefficient of u at $z = 1.975$ m, that is $R_{uu}(1.975)$. Given R_{uu_R} as a function of time delay, τ,

an estimate can be made of the Eulerian time scale $\mathcal{L}$, where $\mathcal{L} = \int_0^\infty R_u(\tau)d\tau$. From data presented in Part II, $\mathcal{L}(1.975) \simeq 1.5$ s. With knowledge of $\mathcal{L}$ and assumption of Gaussian distributions of u and w, the averaging time, T, necessary to determine second moments to an accuracy of ε% (that is, to within ε% of the expected value as $T \to \infty$) can be roughly determined (Lumley and Panofsky, 1964). With an averaging time of 300 s, ε is approximately 14% while tripling the averaging time to 900 s reduces ε to 6%. The errors are of the same order and the larger value is no greater than the uncertainties associated with use of X wires which were discussed in the previous section. Since it was felt desirable to obtain profiles with the minimum possible change in ambient conditions if intermittent features were to be studied and, short of employing an array of sensors, this demanded the shortest possible averaging time at any height, five minutes, which represents $\simeq$ 200 cycles of stalk waving, was felt to be an acceptable compromise.

Not all sensors were operated throughout each profile. Details of the experimental configuration for each run are given in Table I. It will be noticed that the order in which different heights were sampled is apparently random. This was done deliberately to avoid adding any smooth long-term variations in the measurements to the profile. If ambient conditions changed markedly at any time, such as a drop in mean wind speed, a profile was curtailed, so that profiles have differing numbers of sample points. Finally, during some ten minute period in the course of obtaining a profile, the waving canopy was filmed with a Super 8 movie camera.

TABLE I.

Summary of experimental conditions

Date	Profile No.	Sensors Operating	$z^{\dagger}$ m	U m s^{-1}	U_R m s^{-1}
9/12/76	R1	X wire only	1.55	4.035	-
			1.25	4.096	-
			.75	1.588	-
			.35	1.475	-
10/12/76	R2	X wire and reference wire	1.00	1.774	3.07
			0.70	1.18	2.633
			1.50	3.368	4.025
			0.40	1.001	3.575
			1.95	3.235	3.043
			0.10	0.891	3.208
14/12/76	R4	X wire and reference wire	0.4	1.301	5.562
			0.7	1.687	5.192
			1.0	2.090	7.404
			1.3	3.63	8.805
18/12/76	R5	X wire, reference wire, pressure sensor, strain gauges	1.4	5.272	6.229
			1.2	4.670	6.293

†z values are given in the order in which profile was measured.

6. Results and discussion

6.1 MEAN STATISTICS

The profiles of first and second moments of velocity, described below, were obtained from 300-second averages at each height. An algebraic rotation of axes of $-\alpha$ was applied to the measured velocity vectors, where $\alpha = \tan^{-1} W/U$, so that in the transformed co-ordinate system $W = 0$. Before the transformation was applied, α was observed to be distributed randomly between $\pm 4.0°$, no coherent trend being discernable in any one profile or between profiles, so it was assumed that α was the result of probe misalignment.

The profiles of a given moment resulting from different runs have not been combined into composite averages. The particular ambient conditions pertaining to each run can be obtained from Table I.

In Figure 5 are presented profiles of $U(z)$, normalized with the reference velocity U_R at 2 m. The profiles fall generally into the familiar concave form characteristic of uniform canopies. No attempt has been made to fit them to an exponential profile as has commonly been done in the past, since the physical reasoning behind such a form relies upon the existence of an essentially constant mixing length within the canopy and assumes implicitly that there exists a momentum diffusivity related to local canopy geometry which is the principal determining factor in the profile shape. Of more interest is the fact that the profiles appear to be approaching a constant, non-zero value in the lower regions of the canopy. This behaviour is unexpected although reference to earlier published work, which has been summarized by Shaw (1977), reveals that it is by no means uncommon, even in uniform canopies. In the absence of substantial mean velocity shear of the correct sign, one is forced to

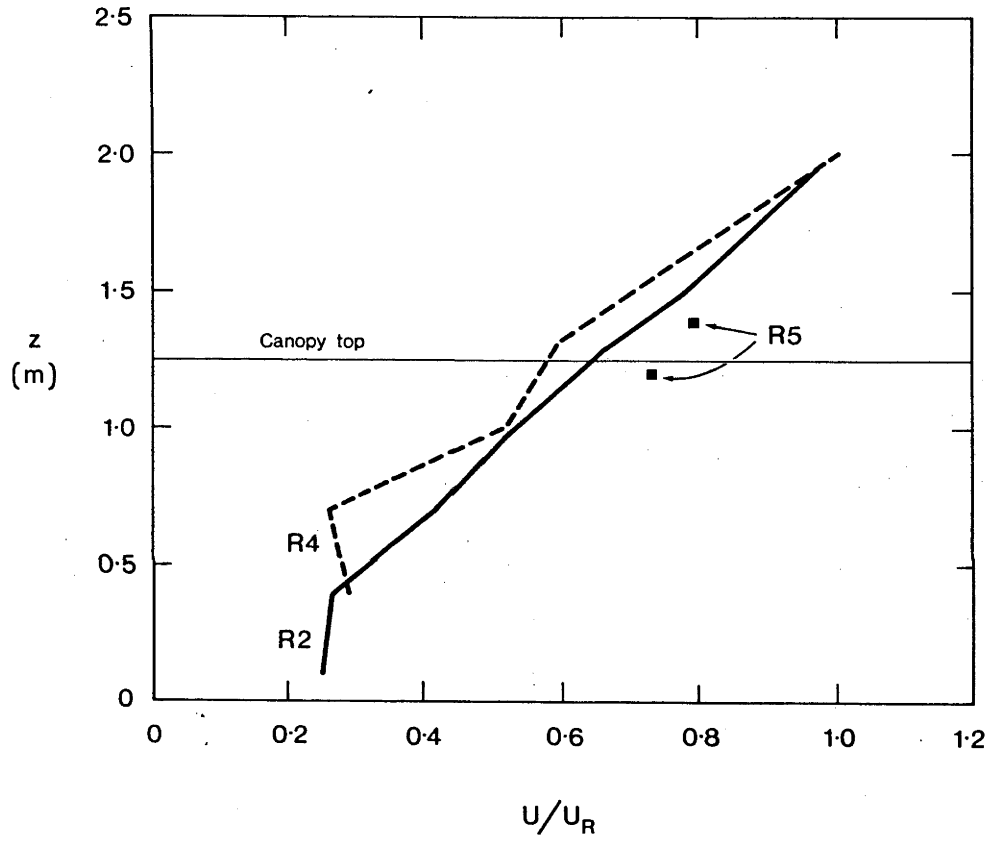

Fig. 5. Normalized mean velocity, U/U_R, versus height, z.

consider carefully the mechanism by which the drag upon the plant parts in the lower region of the canopy can be sustained.

The time average momentum equation in the streamwise direction, neglecting viscous terms and variations in the x and y directions compared with variations in the z direction, can be written as

$$0 = -\frac{1}{\rho}\frac{\partial P}{\partial x} - \frac{\partial \overline{uw}}{\partial z} - \frac{1}{2} C_d A U^2 \qquad (3)$$

where $\partial P/\partial x$ is the steady streamwise pressure gradient, $\overline{uw}$ is the remaining component of the Reynolds stresses, and C_d is the average dimensionless drag coefficient of the vegetation, whose projected area per unit volume of space is A.

In Figure 6, the profiles of friction velocity, $u_* [= (-\overline{uw})^{\frac{1}{2}}]$, normalized by the mean velocity U, are presented for R2, R4 and R5. With the use of the mean value of U_R for the whole profile and Figures 5 and 6, the order of magnitude of the last two terms in equation (3) can be calculated.

Since the experimental site was not perfectly flat, the pressure gradient $\partial P/\partial x$ will not be zero. A theory of turbulent flow over a low hill, taking into account the effects of surface roughness, has been proposed by Jackson and Hunt (1975); it enables an order of magnitude calculation to be made of the perturbation to the longitudinal pressure gradient caused by the slope. With a height to characteristic length ratio of 1:100 (Jackson and Hunt's definition; see Figure 1) for the present hill, and an assumed upstream roughness length, z_o, of 0.1 m (where 0.1 m is a typical value taken from published results over similar canopies), the normalized perturbation to the local static pressure $\Delta P/\rho u_*^2$ is of order 2.0. Assuming a value of u_* of 0.3 m s^{-1} (which is an average value for runs R2 and R4 at a height of 2 m at the measuring

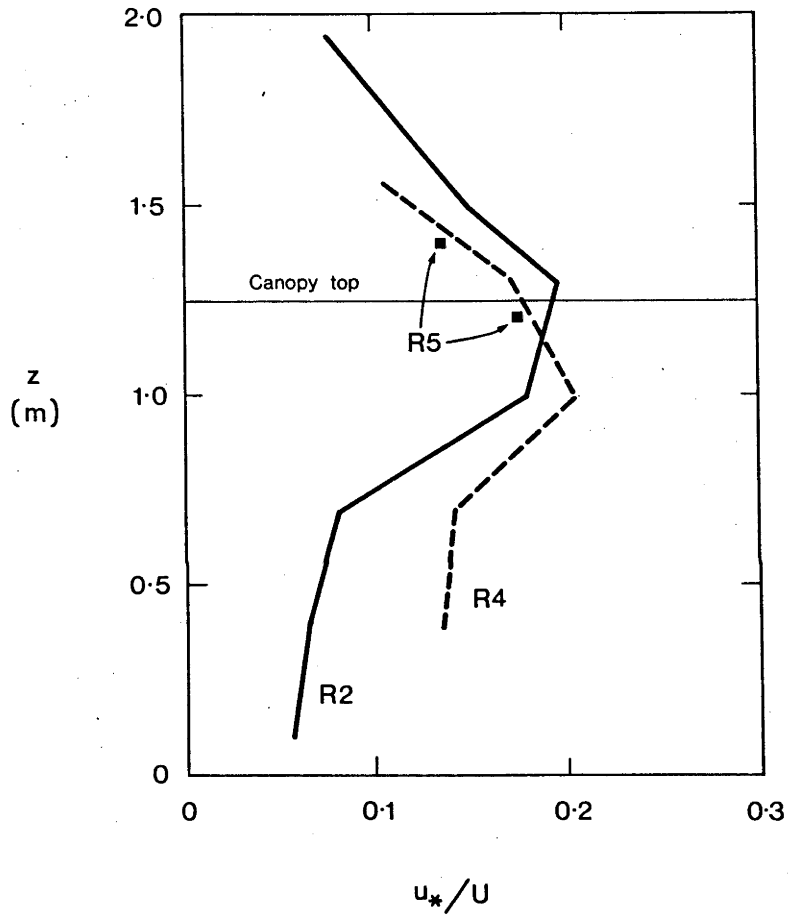

Fig. 6. Normalized friction velocity, u_*/U, versus height, z.

station), $\Delta P = 0.22$ Pa. With a characteristic length for the hill of 50 m (see Figure 1), the mean longitudinal pressure gradient resulting from the slope is of order 4.4×10^{-3} Pa m^{-1}.

A has been estimated from photographs of the canopy as 0.83 m^{-1} and C_d is taken as 0.3 following direct measurements of C_d in a wind tunnel model canopy by Seginer et al. (1976). From R2, $U = 0.875$ m s^{-1}, at $z = 0.75$ m, so that

$$\frac{1}{2} C_d A U^2 = 9.57 \times 10^{-2} \text{ m s}^{-2},$$

$$\frac{\Delta(-uw)}{\Delta z} = 8.6 \times 10^{-2} \text{ m s}^{-2} \text{ (Figure 6 profile R4) at 0.75 m,}$$

and

$$\frac{1}{\rho} \frac{\partial P}{\partial x} = 3.7 \times 10^{-3} \text{ m s}^{-2} .$$

Substituting these values into equation (3), the RHS becomes $[-0.37 + 8.6 - 9.57] \times 10^{-2}$. Within the limits of accuracy which are assumed to apply to our measurements, and the arbitrary assumption of $C_d = 0.3$, this is close to zero. Two conclusions may be drawn. Firstly, in comparison to the drag and shear stress gradient terms, the pressure gradient is negligible and cannot contribute substantially to the momentum balance in the middle regions of the canopy. Secondly, the apparent balance between the terms of equation (3) supports the interpretation of the time mean statistics in an essentially one-dimensional framework.

Shaw (1977) and Wilson and Shaw (1977) have shown that the existence of a vertical momentum flux combined with a zero or negative velocity gradient does not violate the momentum equation, (3). It means, however, that there cannot exist a simple first order or 'k theory' flux-gradient relationship for momentum. These points are discussed in detail in the last two references.

In Figure 7 profiles of streamwise and vertical turbulence intensities, i_u and i_w [where $i_u = \left(\overline{u^2}\right)^{\frac{1}{2}}/U$ and $i_w = \left(\overline{w^2}\right)^{\frac{1}{2}}/U$] are plotted for three profiles: R1, R2 and R4. Both i_u and i_w peak at the top of the canopy, and both show a strong increase with height up to this peak. Measurements collected by Cionco (1972) and Inoue et al. (1975) show that in general, canopies with constant vertical distribution of leaf area density, A(z) [simple canopies], also have constant $i_u(z)$ with certain notable exceptions. Flexible cereal canopies such as wheat, rice and barley show an increase of i_u with height when windy conditions cause the stalks to wave. This behaviour has also been observed in a flexible wind tunnel model canopy by Finnigan and Mulhearn (1978a). On reflection, an increase in i_u with constant A can be expected if the waving motion of the stalks is particularly important, since waving amplitude of course increases with height. The data summarized by Inoue et al. (1975) indicate that the absolute values of i_u profiles in certain crops may be dependent on both mean wind speed and thermal stability. For this reason, the curves presented in Figure 7 have not been combined into composite averages.

An increase in i_w with z in moderately tall canopies, both rigid and flexible, is reported by most workers whether in the field or in wind tunnels (see for example Seginer et al., 1976). The presence of the ground surface presumably acts to restrict the scale of vertical fluctuations. The curves of Figure 7b fit into this general picture.

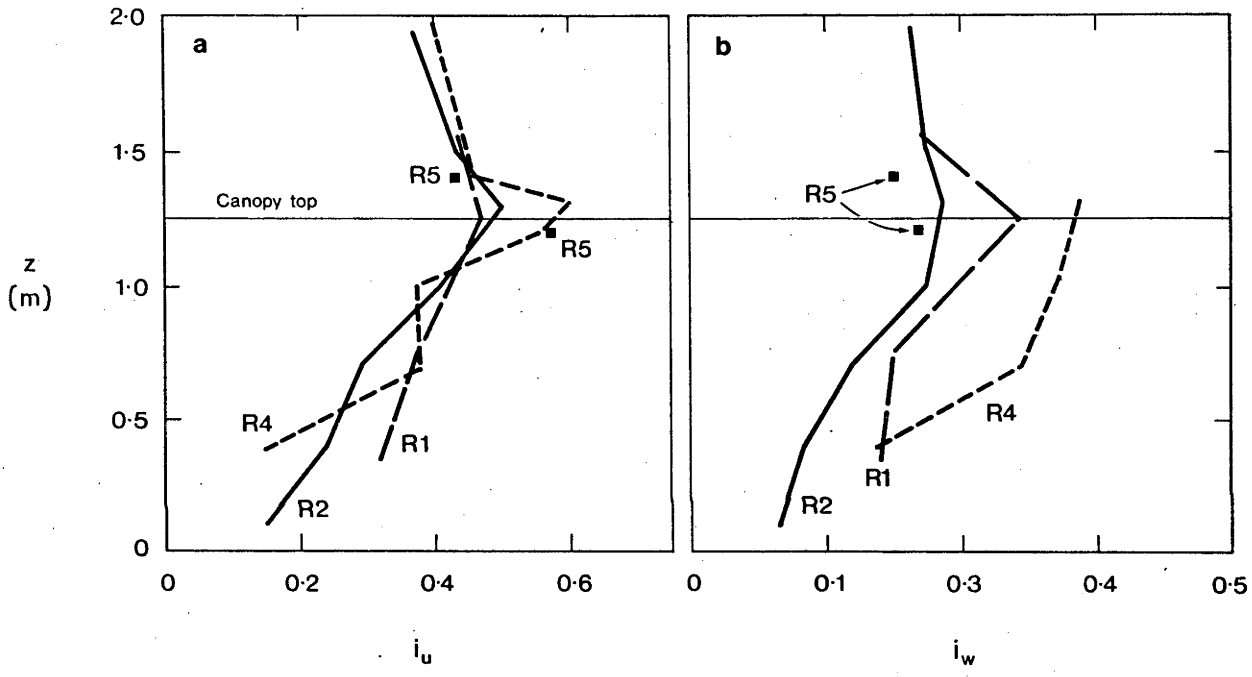

Fig. 7. Profiles of (a) streamwise, i_u, and (b) vertical, i_w, turbulence intensities versus height, z.

6.2 WAVING STALKS, HONAMI AND VELOCITY FLUCTUATIONS

Most of the results discussed in this section come from R2, where a very complete profile was obtained. The conclusions drawn are corroborated by analysis of profile R4, but the R4 results have been omitted to avoid the confusion of referring to a different set of velocity scales. When other profiles are being used, they will be referred to explicitly. Spectra of velocity, pressure and strain gauge output were obtained by transforming 2^{17} points, equivalent to 262 s of data on the PDP 11/40, using a Fast Fourier transform routine developed by Fraser (1978). The data are presented as power spectra of u, w, strain gauge output and pressure fluctuation, or co-spectra of uw. The power and co-spectral density functions are defined by the relationships

$$\left.\begin{aligned} \int_o^\infty \phi_{uu}(f)\ df &= \overline{u^2} \\ \int_o^\infty \phi_{ww}(f)\ df &= \overline{w^2} \\ \int_o^\infty \phi_{uw}(f)\ df &= -\overline{uw} \end{aligned}\right\} \qquad (4)$$

with analogous formulae for spectra of stalk waving, ϕ_{sg}, and surface pressure, ϕ_{pp}. The spectra have been smoothed using a narrow band moving average of 0.1 Hz (50 pts) so that details of the waving motion would not be obscured and, because of this minimal smoothing, the initial time series were tapered before transformation with a 'Hanning window' or cosine bell function to reduce leakage.

The spectrum of strain gauge output is shown in Figure 8 for one of the strain gauged stalks recorded during R5. The units of power/unit frequency, ϕ_{sg}, are arbitrary. If the stalk can be regarded as essentially an elastic cantilever, then the strain on the stalk surface

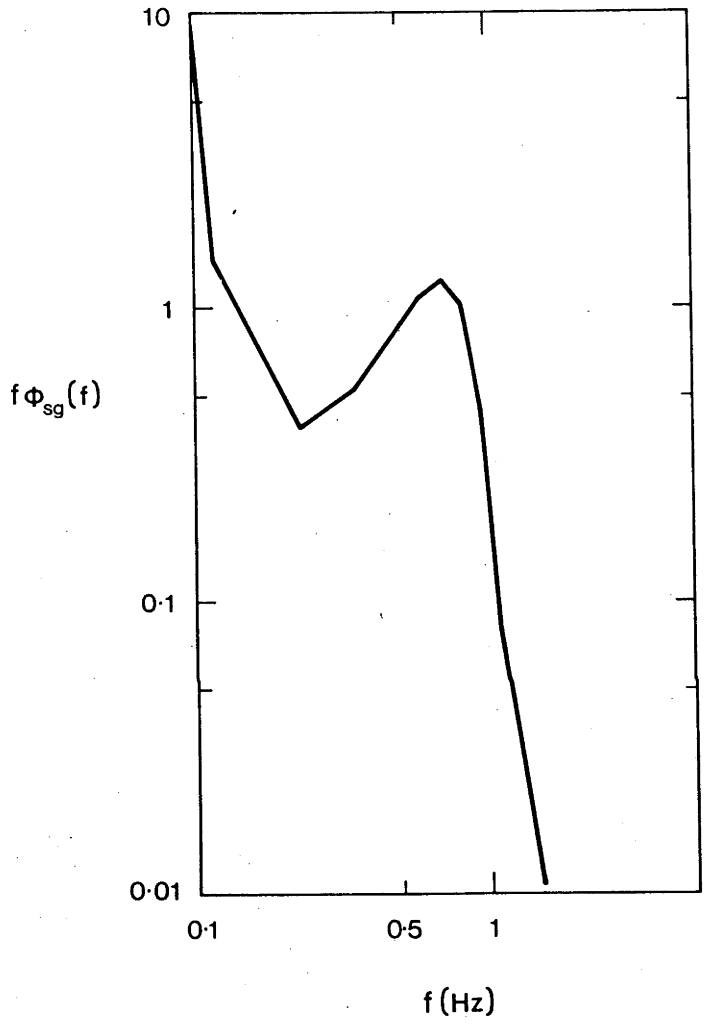

Fig. 8. Power spectrum of displacement of a waving stalk (strain gauge output), ϕ_{sg}, from R5.

is directly proportional to the deflection of the ear. The waving frequencies of five strain gauged stalks, with a height range of 1.15 to 1.30 m, were identical, a result of the mutual interference of the stalks in the canopy. In isolation, the vibrational frequency of the stalks would be proportional to, amongst other things, the inverse square of their lengths. The value of 0.7 Hz for the vibrational frequency, f, obtained from Figure 8 is close to the value of f = 0.67 ± .08 Hz obtained by timing many waving stalks in the movie film of R5. The value of f for R2, again obtained from film, is slightly lower being 0.625 ± 0.1 Hz. This discrepancy is ascribed to the drying out of the crop as the experiment progressed.

The phenomenon of honami, the organized and persistent ocean-like waving motions so striking in cereal crops on windy days, has been analyzed in a series of papers by Inoue, for example Inoue (1955). Finnigan and Mulhearn (1978a) have proposed that honami waves are records of the passage of gusts of air with high streamwise momentum, which sweep down to the surface from an outer part of the boundary layer, bending over a succession of stalks in their downwind passage. The stalks then spring back and vibrate with a streamwise phase difference.

It was apparent from analysis of the movie films that when honami took place, the field was divided into patches of coherent waving, elongated downstream with abrupt and arbitrary phase differences between adjacent patches. Within patches, individual plants vibrated at their common natural frequency, f, while the small phase difference between adjacent plants, smoothly varying in the streamwise direction, gave the impression of waves moving through the canopy. Individual patches were of the order of 20 m in downwind extent by 7 m crosswind and retained

their identity for about 5 s on average. The picture fits in exactly with that reported for a field of barley under similar conditions (Finnigan and Mulhearn, 1978a). Honami waves appear to be analogous to 'catspaws' on open water with the additional property of the plants' elasticity conferring some persistence and regularity.

The displacement of the stalks in the canopy can be approximated by a harmonic travelling compression wave

$$\xi = \xi_o \exp 2\pi i \left(\frac{x}{\lambda} - ft\right)$$

where $\xi(x)$ is the x-direction displacement of the stalk from its mean position, $\xi_o(x)$ is the vibration amplitude, λ is the wavelength and f the frequency of stalk vibration. $i = \sqrt{-1}$. Care should be taken when applying this formulation to the elevation of the canopy top. Since the height of a stalk passes through a maximum twice a cycle, the surface elevation should strictly be represented by a transverse wave of wavelength $\lambda/2$ and frequency 2f. In practice, this double frequency 'transverse' wave has a large effect upon the vertical velocity fluctuations.

It is a simple matter to obtain θ, the phase velocity ($\theta = \lambda f$), or λ directly from the movie films. Figure 9 presents a histogram of the distribution of values of θ for R2; 42 determinations of θ are included in this plot. Of particular note is the fact that the average phase velocity, 3.76 m s^{-1}, is 80% higher than the mean velocity at the top of the canopy, 2.32 m s^{-1}, and that the distribution of θ has a marked positive skewness. This phase velocity distribution can also be regarded as a distribution of the velocity of gusts at the crop surface.

Figures 10, 11 and 12 present power and co-spectra of u, w and uw respectively, plotted as $f\phi(f)$ against log f [where $\phi(f)$ is defined in

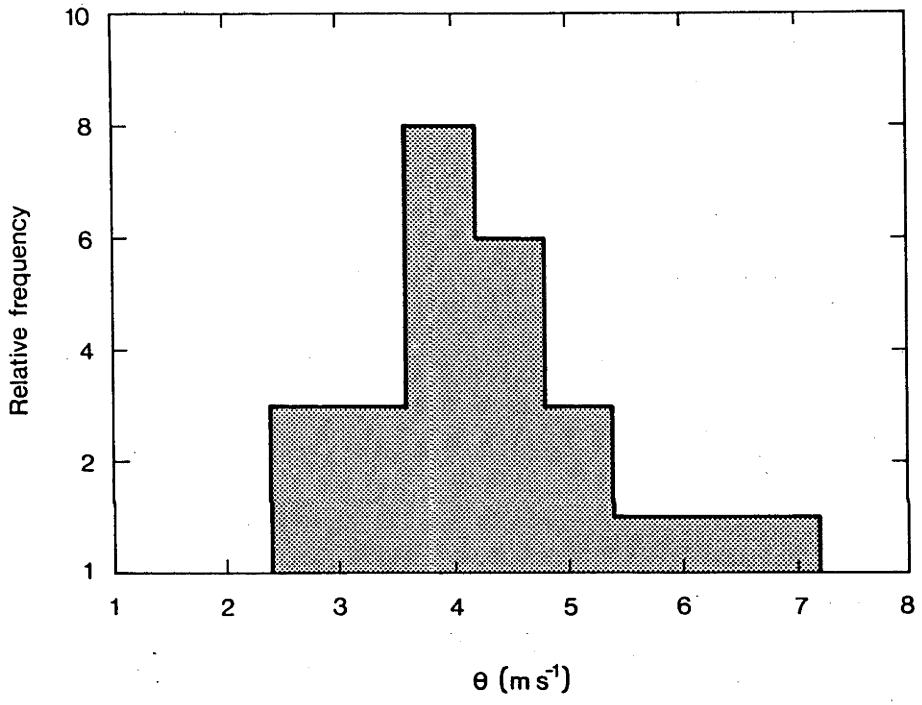

Fig. 9. Relative frequency of honami phase velocities, θ, measured from movie film of R2.

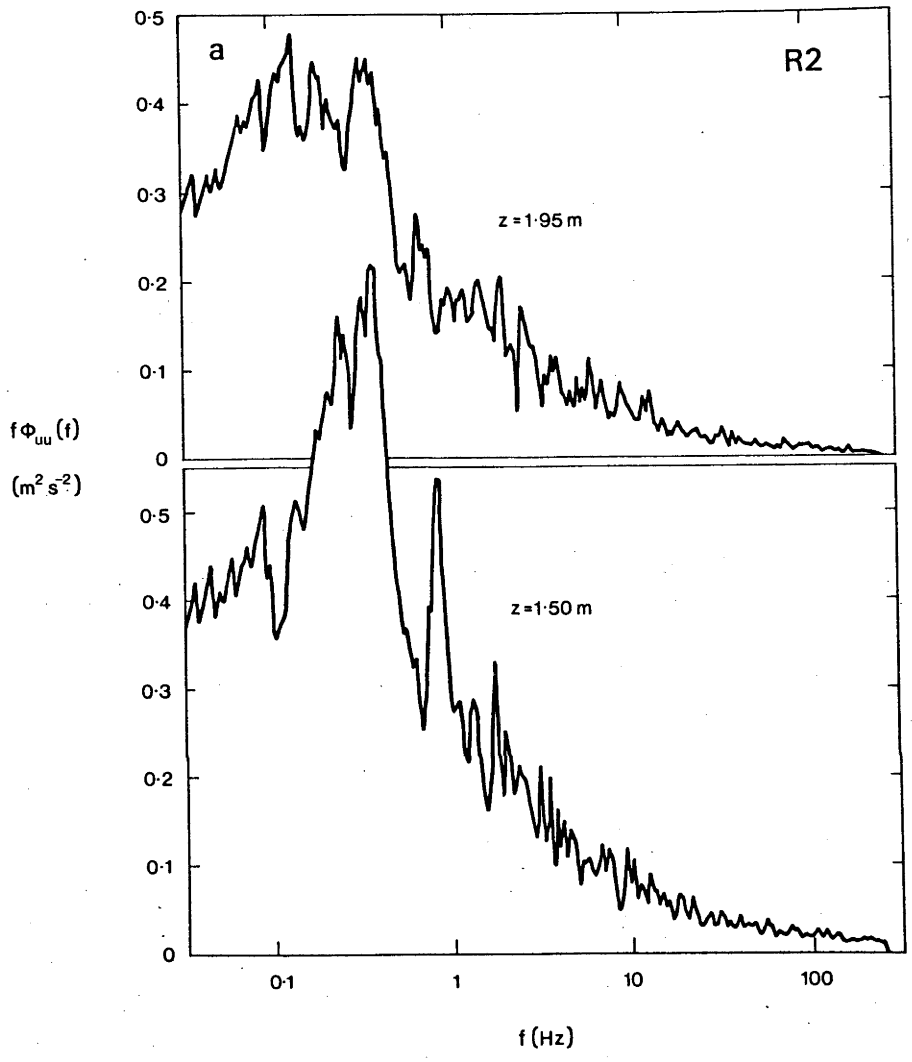

Fig. 10. Power spectra of streamwise velocity fluctuations, ϕ_{uu}. (a,b) R2; (c) R5.

b

R2

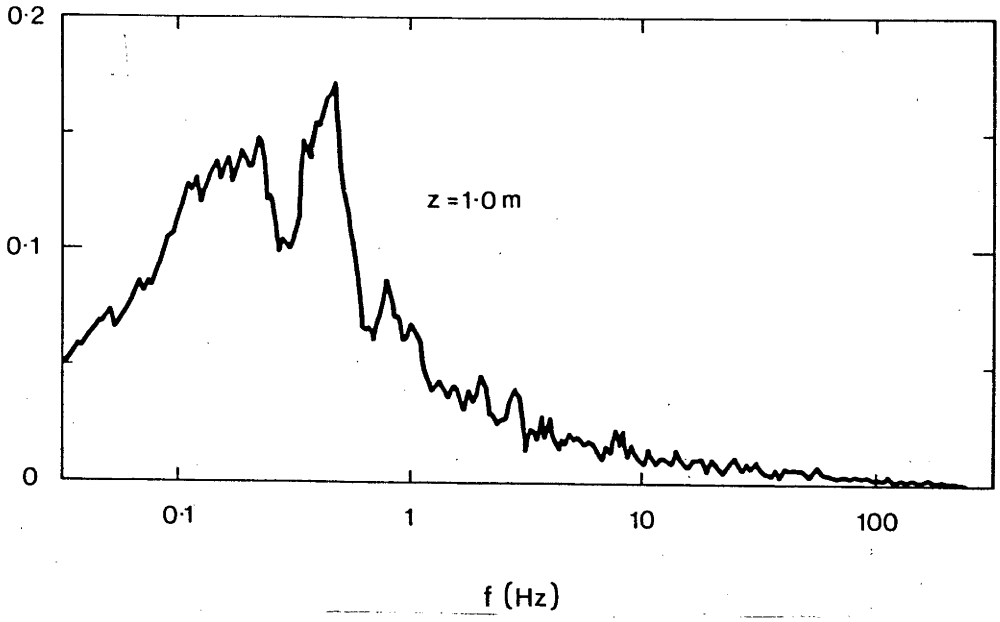
0·2
0·1
0
z = 1·0 m
0·1
1
10
100
f (Hz)

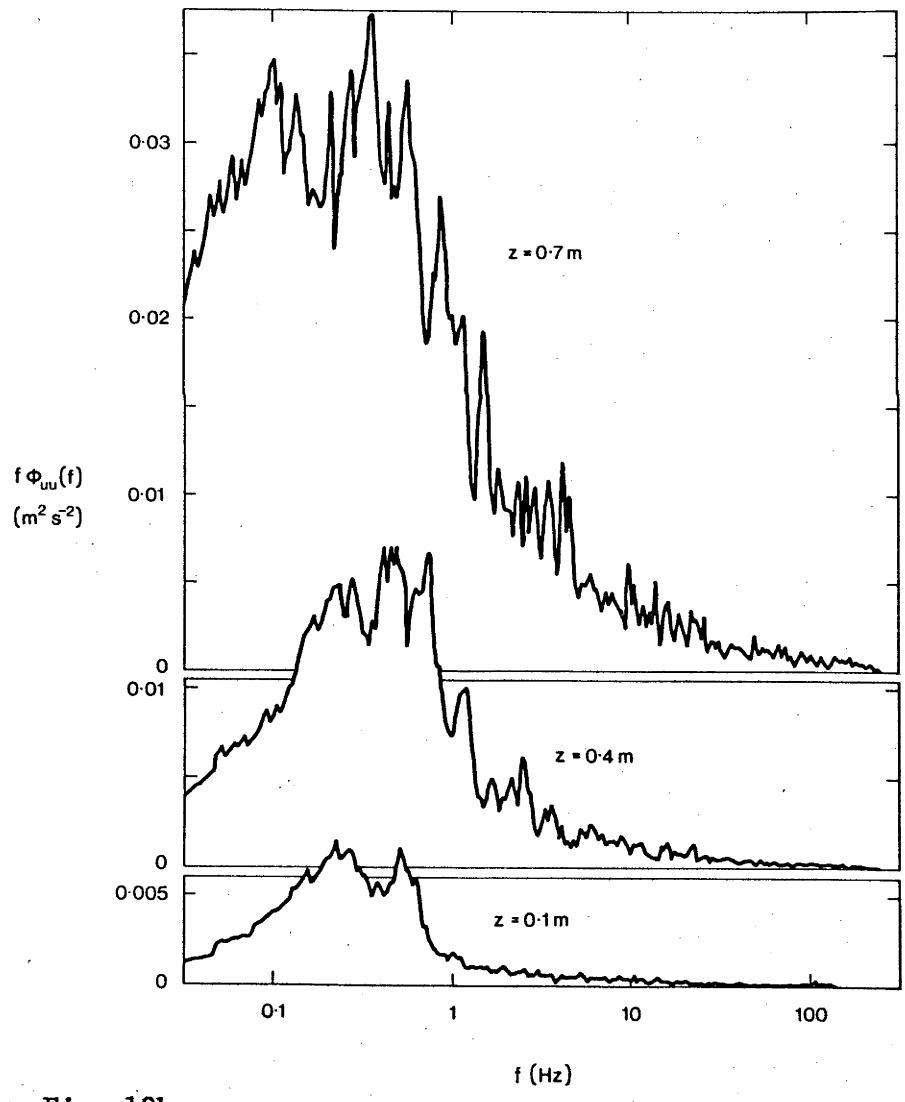
f Φuu(f)
(m² s⁻²)
0·03
0·02
0·01
0
z = 0·7 m
0·01
0
z = 0·4 m
0·005
0
z = 0·1 m
0·1
1
10
100
f (Hz)

Fig. 10b.

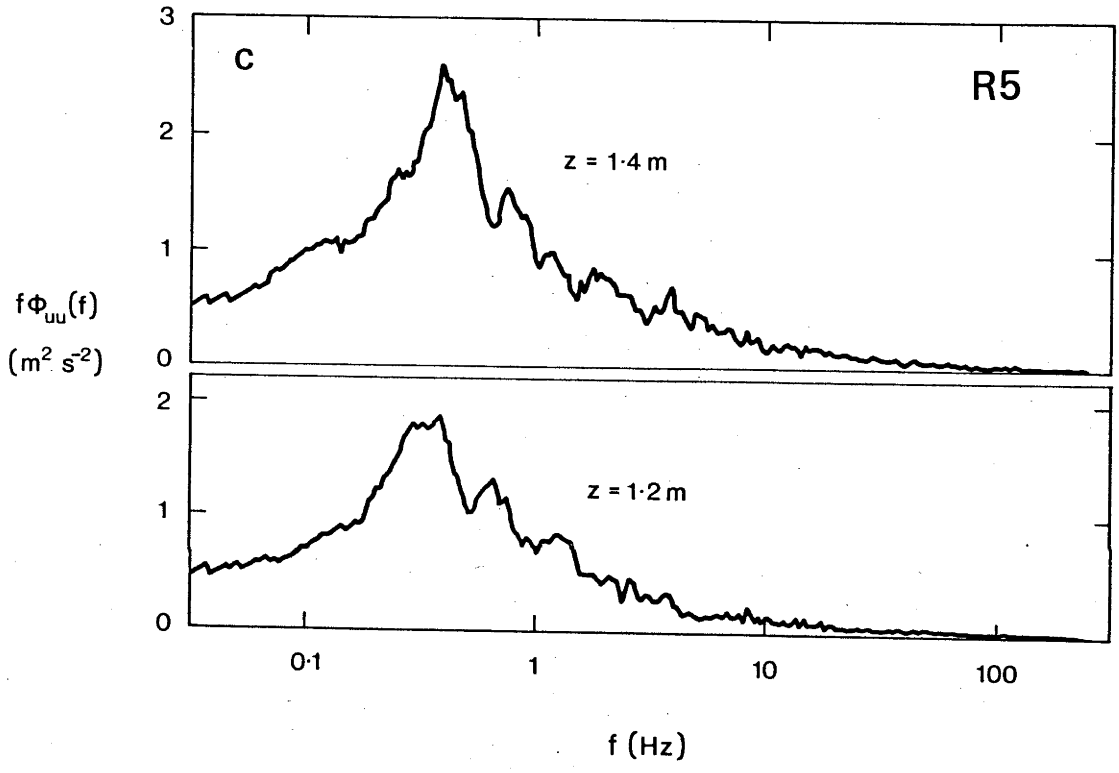

Fig. 10c.

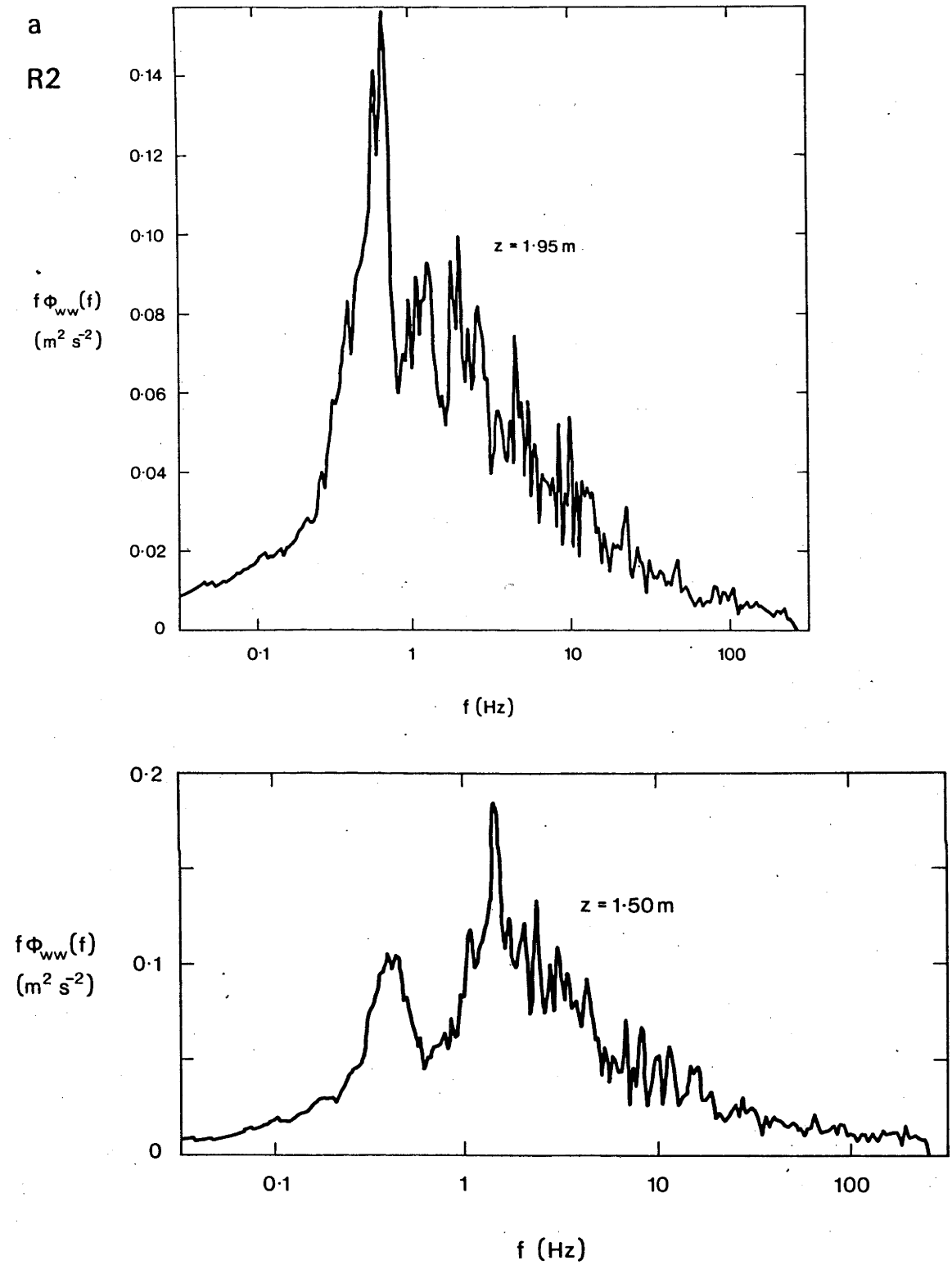

Fig. 11. Power spectra of vertical velocity fluctuations, ϕ_{ww}.
(a,b) R2; (c) R5.

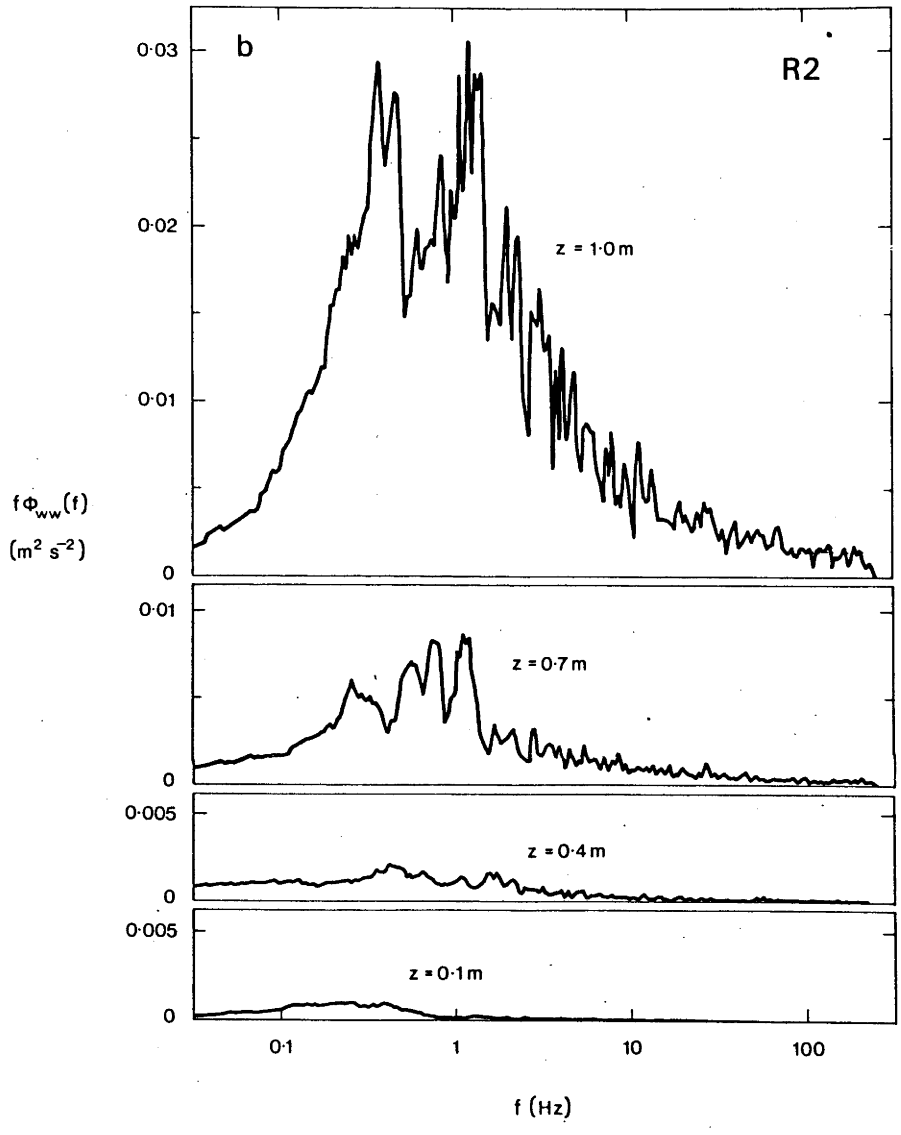
b
R2
0·03
0·02
0·01
0
z = 1·0 m
0·01
0
z = 0·7 m
0·005
0
z = 0·4 m
0·005
0
z = 0·1 m
0·1
1
10
100
f (Hz)
fΦww(f)
(m² s⁻²)

Fig. 11b.

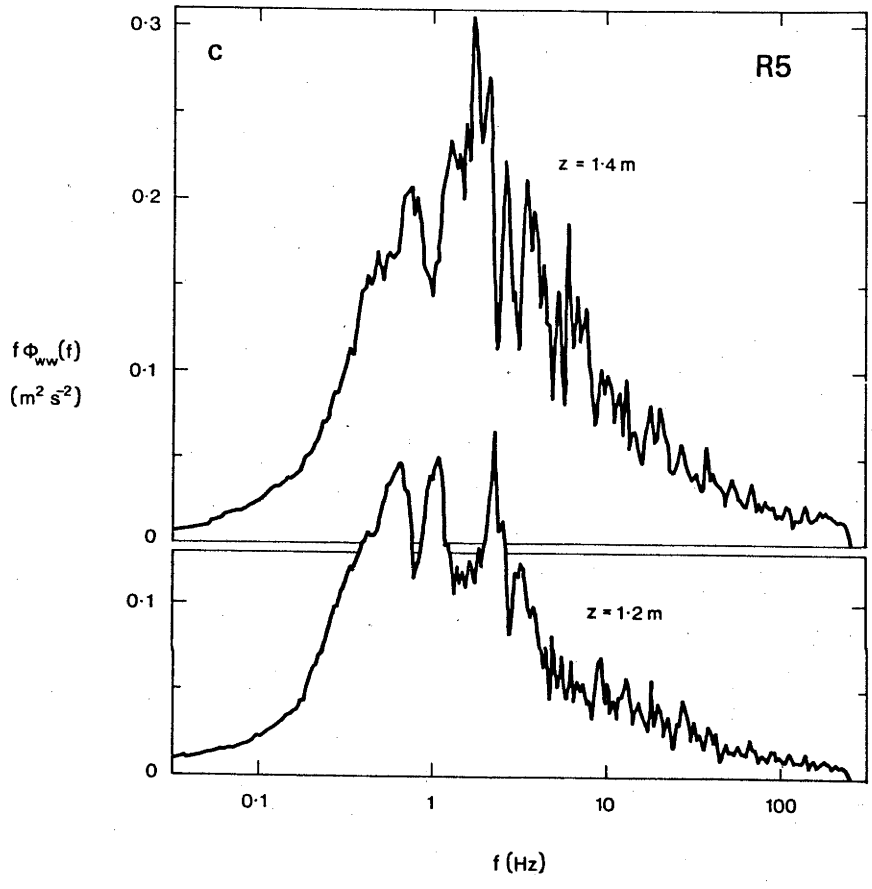

Fig. 11c.

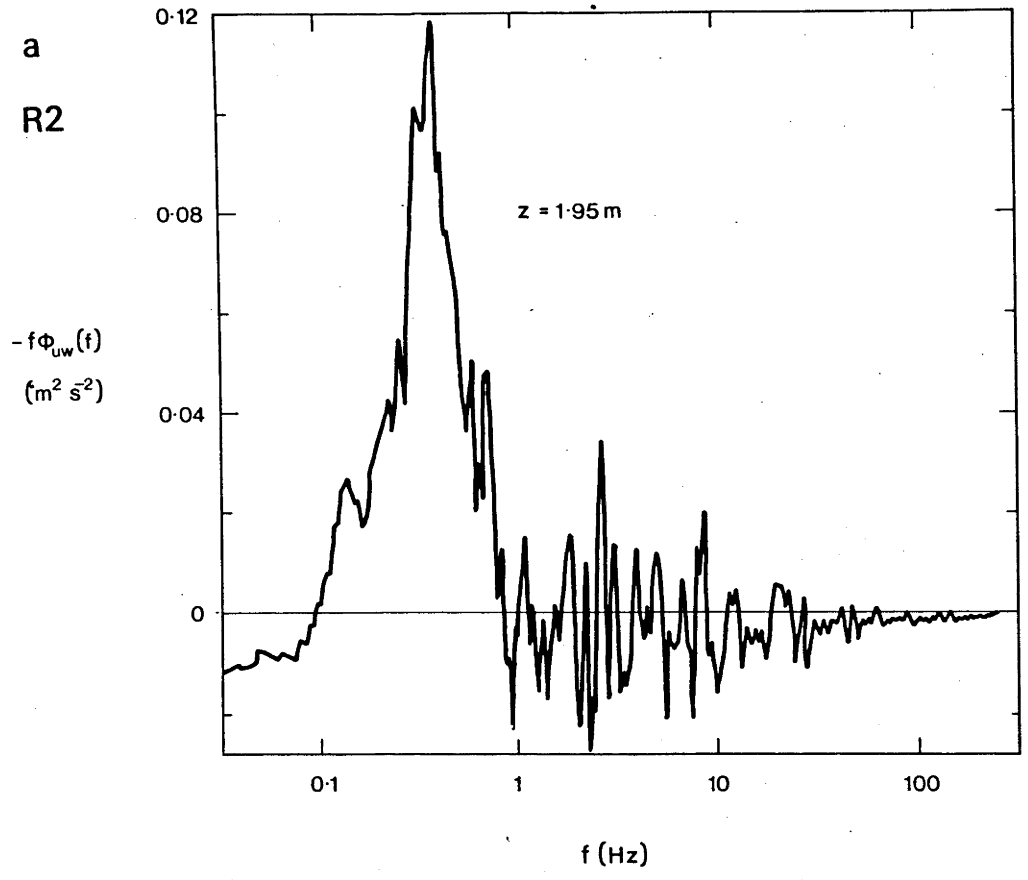

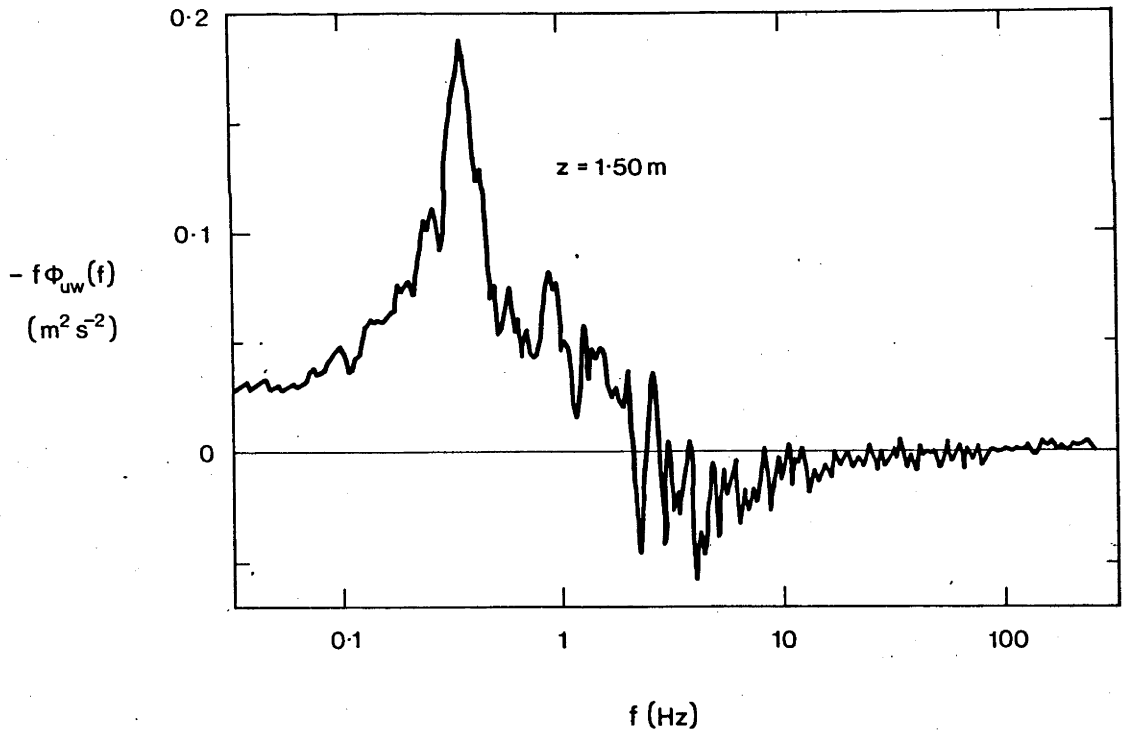

Fig. 12. Cross spectra of streamwise and vertical velocity fluctuations, ϕ_{uw}. (a,b) R2; (c) R5.

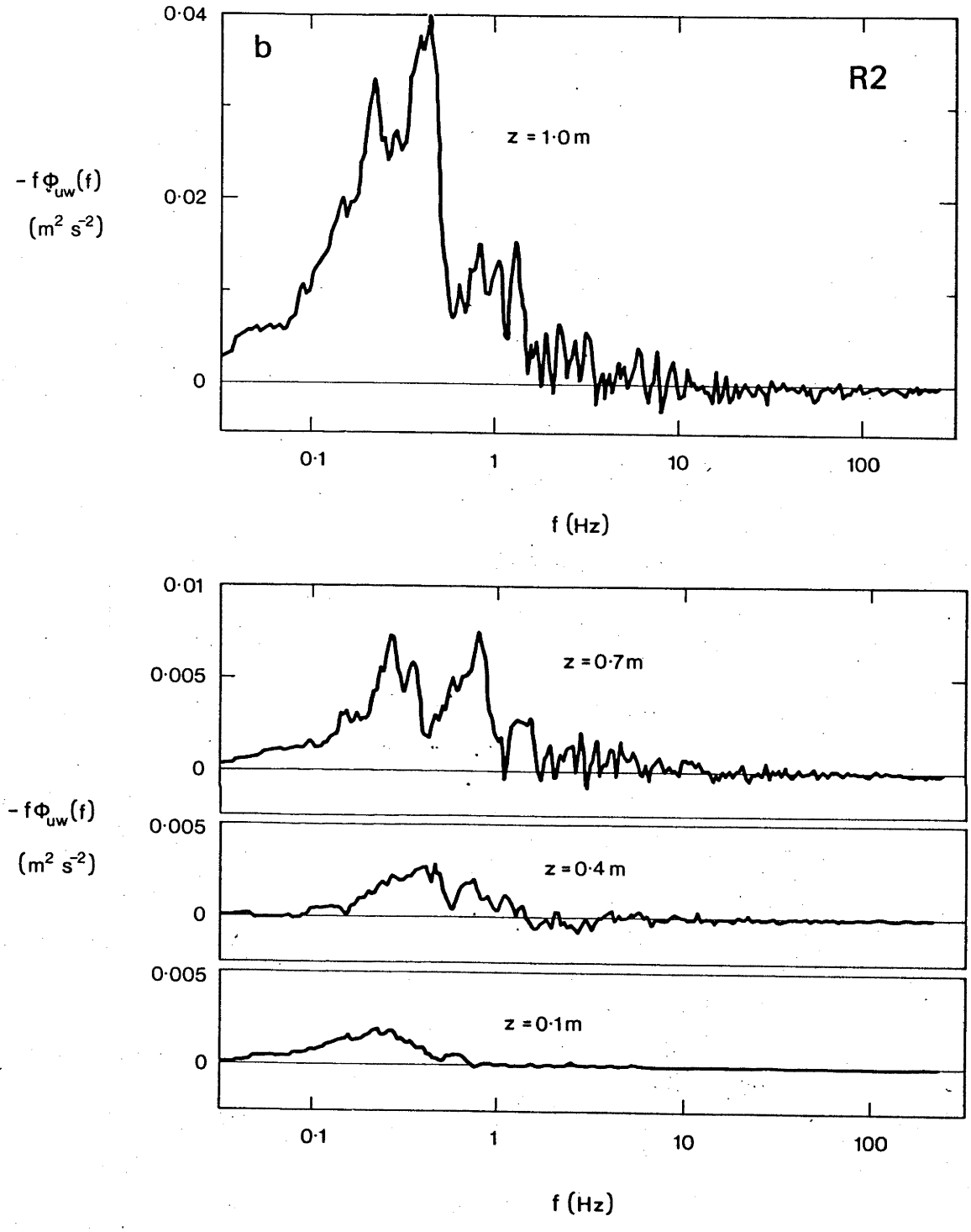
b
R2
z = 1·0 m
0·04
0·02
0
- fΦuw(f)
(m² s⁻²)
0·1
1
10
100
f (Hz)
z = 0·7m
z = 0·4 m
z = 0·1m
0·01
0·005
0
0·005
0
0·005
0
- fΦuw(f)
(m² s⁻²)
0·1
1
10
100
f (Hz)

Fig. 12b.

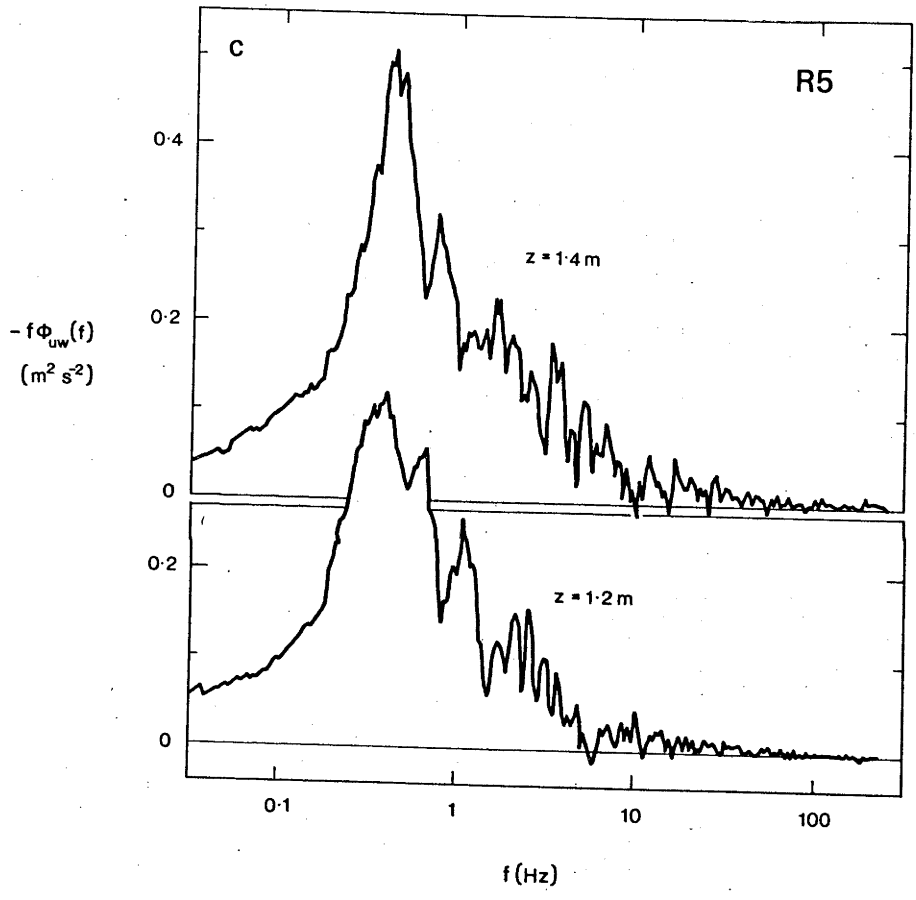

Fig. 12c.

equation (4)] so that the variance is equal to the area under the curve. No attempt has been made to collapse the different curves since, as will become apparent, no single length or time scale adequately encompasses the several mechanisms which determine the velocity structure within the canopy. The spectral values should be divided by the square of the mean reference velocity over the transformed period if the magnitudes of the various curves are to be directly compared.

Three prominent peaks appear in the various spectra at frequencies of roughly 0.35, 0.6 and 1.2 Hz, but the precise frequency of the peaks appears to depend upon the height, z. Concentrating initially upon the spectra for z = 1.0 and 1.5 m, just below and just above the top of the canopy, where we might expect the influence of waving to be strongest and the features of the spectra clearest, we can see that a peak, which is close to twice the waving frequency, dominates the ϕ_{ww} spectra at z = 1.5 m and is very important at z = 1.0 m; while in ϕ_{uu}, the two lower frequency peaks at roughly .35 and .6 Hz are larger. In the co-spectra of $\overline{uw}$, the low frequency and waving frequency peaks are most striking. In Figure 13 computer printouts of $\tilde{u}_R$, $\tilde{u}$, $\tilde{w}$ and -uw versus time from R2 at z = 1.0 and 1.5 m reveal characteristic features which have average frequencies close to those of the spectral peaks. We will return to these time series to consider specific features but for the moment it suffices to point out that the periodic sections of the traces occur intermittently. The Fourier transform representation in such a case is not perfectly appropriate and the spectra should be compared with the time series if they are to be interpreted correctly.

The variation with height of the frequencies of the spectral peaks in ϕ_{uu}, ϕ_{ww} and ϕ_{uw} have been plotted in Figure 14. Averages from two

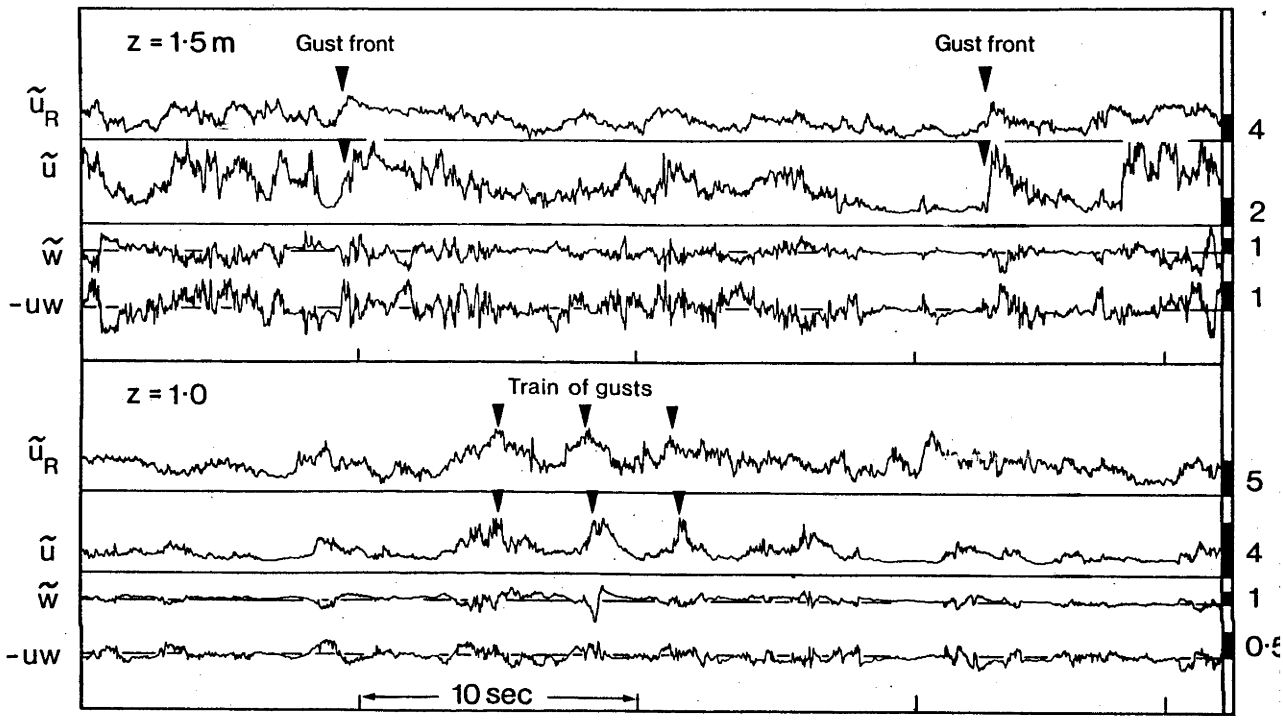

Fig. 13. Computer plots of typical sections of $\tilde{u}_R$, $\tilde{u}$, $\tilde{w}$ (m s^{-1}) and -uw (m^2 s^{-2}) versus time from R2. Scales are given at right of plots. Significant events are marked on the traces.

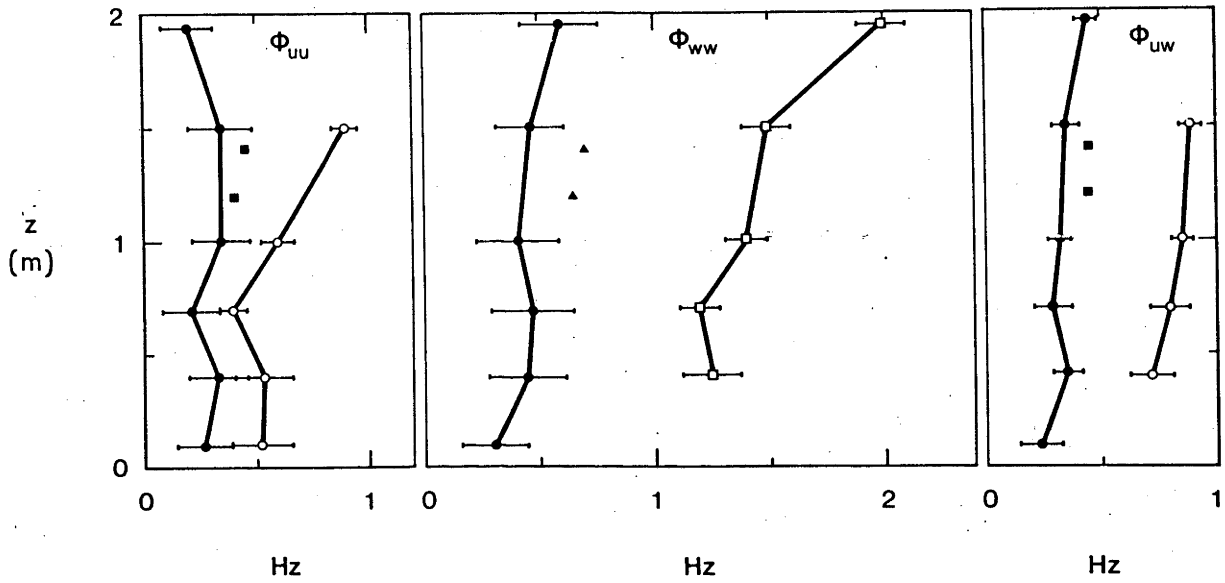

Fig. 14. Frequency of prominent spectral peaks in ϕ_{uu}, ϕ_{ww}, ϕ_{uw} versus height, z, from R2 and R5. ● R2, low frequency peak; ○ R2, waving requency peak; □ R2, 2 × waving frequency peak; ■ R5, low frequency peak; ▲ R5, waving frequency peak.

spectra were used at each height, the 262 s period for one spectrum starting at t = 0 and for the second, ending at t = 300 s.

Error bars indicate the uncertainty which results from the finite width of the spectral peaks. The frequency of the lowest peak shows a very slight trend with height in each case, while the peaks at roughly the waving frequency and its first harmonic show a pronounced increase with height. In the case of the ϕ_{ww} spectrum, no curve for the middle frequency can be drawn with confidence, while the curve representing the middle frequency in ϕ_{uw} is only tentative and must be treated with caution.

Let us consider first the significance of the lowest frequency. Reference to Figure 13 shows that the velocity fluctuations of this frequency in the reference wire trace seem to be echoed, after some time delay, in the $\tilde{u}$ signal at both 1.5 m and 1.0 m. It seems probable therefore that this lowest frequency represents the frequency of arrival of gusts. It is now accepted that gusts or downsweeps of high momentum fluid to the surface are manifestations of large coherent structures or eddies which are randomly distributed in time and in the x-y plane and which essentially have a vortex-like structure (see for example, Brown and Thomas, 1976). Lu and Willmarth (1973; reported in Willmarth, 1975) have shown that the mean period between gusts depends upon length and velocity scales representative of the outer part of the boundary layer, but they did not report any periodicity in gust arrival as appears to be the case here.

During profile R5, the mean wind speed at 2 m was substantially higher than during R2. In Figure 14, the peak frequencies from R5 spectra are included and actual spectra from R5 are presented in Figures

10c, 11c and 12c, so a direct comparison between the position of the spectral peaks can be made. There is in fact a pronounced shift to higher frequencies of the first spectral peak. Taking the mean gust frequency, f_g, as that of the lower frequency peak and using U_R as an 'outer flow' scale, we have:

from R2 $$\frac{U_R}{f_g} = \frac{3.52}{0.35} = 10.06 \text{ m} ;$$

from R5 $$\frac{U_R}{f_g} = \frac{5.5}{0.50} = 11.0 \text{ m} .$$

Although the velocity scale used is not strictly an outer flow variable, and the periodicity of gust arrival rather than a conditional sampling procedure was used, the indication is that the period between gusts in regular trains does seem to vary directly with mean velocity. Inoue (1955) presented results for a rice canopy which suggest the same kind of behaviour for a range of U(H) between 1 and 3 m s^{-1}, H being the canopy height. At higher windspeeds [U(H) = 3 to 5 m s^{-1}], his measurements show no decrease of gust period with U. Unfortunately, the accuracy of his gust detection method is not clear from the English summary of the Japanese paper. On a larger scale, Allen (1968) used the low frequency peak of ϕ_{uu} spectra measured over Japanese larch to show that the period between gusts, $1/f_g$ was approximately proportional to U for values of U between 3.5 and 8.7 m s^{-1}.

It was apparent from the movie film of R5 and from the time trace of R5 including the strain gauge response (see Figure 15) that waving or honami is much more pronounced during this time of stronger wind. This of course is not unexpected since as the primary forcing function of the stalk waving, the gusts, approaches the natural frequency of the stalks, a resonant interaction will result in more pronounced waving. It is

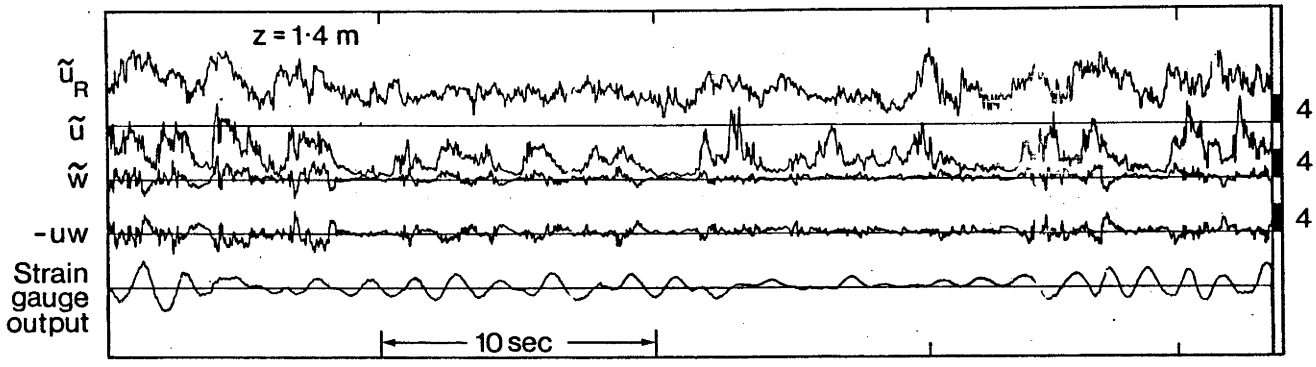

Fig. 15. Computer plot of typical section of $\tilde{u}_R$, $\tilde{u}$, $\tilde{w}$ (m s^{-1}), -uw (m^2 s^{-2}) and strain gauge output versus time from R5. Scales are given at right of plots.

fortunate for farmers that strong damping ensures a very flat resonant peak for cereal crops!

Returning now to the height dependence of those peaks, which are related directly to the waving motion, the motion of the stalks is coupled with that of the air layers in the upper part of the canopy, through the fluctuating drag term

$$\frac{1}{2}\rho C_d A\,(\tilde{u} - \partial\xi/\partial t)\,|\tilde{u} - \partial\xi/\partial t| \quad . \tag{5}$$

We assume that the drag is proportional to the square of the relative velocities of the air and foliage and the modulus sign recognizes the fact that the direction of the instantaneous wind and drag vectors coincide. The effect of pressure gradients accompanying changes in $\tilde{u}$, the so-called 'added mass' term, is probably small at the frequencies where most energy in u is concentrated and has been ignored. The stalks in effect, having temporarily stored some of the momentum of a gust as strain energy, impart it to the relatively low velocity air behind the gust front as they commence to wave. As the $\tilde{u}$ component of the airflow through the canopy is periodically accelerated and decelerated, continuity ensures fluctuations in $\tilde{w}$ also so that a transverse travelling wave motion is impressed upon a layer of fluid centred around the top of the stalks. The situation is complicated, however, by the oscillations in the mean height of the canopy. Although oscillations at this frequency affect both u and w, as can be seen from Figure 13, they appear relatively more important in the w spectra, being swamped by the much larger u fluctuations in ϕ_{uu}. It should be emphasized that this is not a manifestation of the quadratic nature of the drag term (5), since the effect of the modulus sign is to suppress the non-linearity (Finnigan and Mulhearn, 1978b).

The wavelike motion of the air layers contributes to the instantaneous momentum transfer in two ways. Firstly, the inclination of the velocity vector ($= \tan^{-1} \tilde{w}/\tilde{u}$) is periodic; and secondly, as pointed out by Reynolds and Hussain (1972), the background Reynolds stresses (as distinct from the organized wave motion) are modulated by the velocity wave. The quantitative results of Reynolds and Hussain unfortunately are for a wave of small amplitude relative to the background fluctuations and are not directly applicable to the present case of large amplitude waves, so that it is not clear whether the net momentum flux resulting from this latter effect would be close to zero when averaged over many cycles. Peaks in the ϕ_{uw} spectra at the waving frequency are most probably a consequence of a change in effective drag coefficient between a retreating and advancing stalk. Since the ϕ_{uw} spectra are dominated by peaks at the gust arrival frequency, it is obvious that these largely control the mean transfer of momentum to the canopy. The relative importance of gusts and waving in momentum transfer will be treated in a more quantitative fashion in Part II.

The precise form of the velocity wave is obviously rather complicated and probably cannot be adequately represented by a harmonic wave simply related to the stalks' motion. The following discussion therefore is necessarily rather speculative but may serve to illustrate some possible mechanisms for the observed features of the spectra.

Once initiated by a localized patch of coherently waving stalks, the velocity waves can propagate through a region of fluid by means of their pressure fields and by momentum transfer (turbulent shear stress) between adjacent fluid layers. (We will show in the next section that the second mechanism appears to be the more important.) At the same

time, regions of fluid containing travelling velocity waves may be accelerated by pressure gradients associated with eddies or gusts whose length scales are much greater than the honami wave length. Such an acceleration of a region of fluid would result in its associated wave motion (as recorded by the hot wire fixed in space) changing frequency through a Doppler shift. The connection between the stalks' motion and the velocity fluctuations expressed by (5), suggests that wavelike velocity fluctuations should have similar wavelengths to those in the honami waves, at least when the fluctuations are first impressed upon the air layers in the canopy. With this assumption, the local phase velocity, $\theta'(z)$, of the velocity waves can be calculated. $\theta' = \lambda f'_{peak}$, where λ(= 5.37 m for the peaks around 0.6 Hz, the waving frequency, and 2.68 m for the peaks at 1.2 Hz) is the wavelength of the stalks' motion, and ' denotes values associated with the velocity waves rather than the honami waves. $\theta'(z)$, calculated from the waving dependent peak frequencies of Figure 14 and normalized with the local mean velocity, $U(z)$, is plotted in Figure 16. $\theta'/U = 1$ denotes a velocity wave propagating at the local mean velocity. It is apparent from Figure 16 that θ' exceeds the local mean velocity, at least between z = 1.5 and 0.4 m. The shape of the curve is reminiscent of the skewness profile of u (see Figure 4). If the assumption of constant wavelength is valid, it appears that velocity waves throughout the canopy are associated with times of higher than average streamwise velocity, the effect becoming more marked as one proceeds deeper into the canopy. Penetration of 'parcels' of air, 'marked' with velocity waves from their contact with the stalks at the canopy top, into the lower canopy where they are decelerated or above the canopy where, free of the direct influence of stalk drag, they

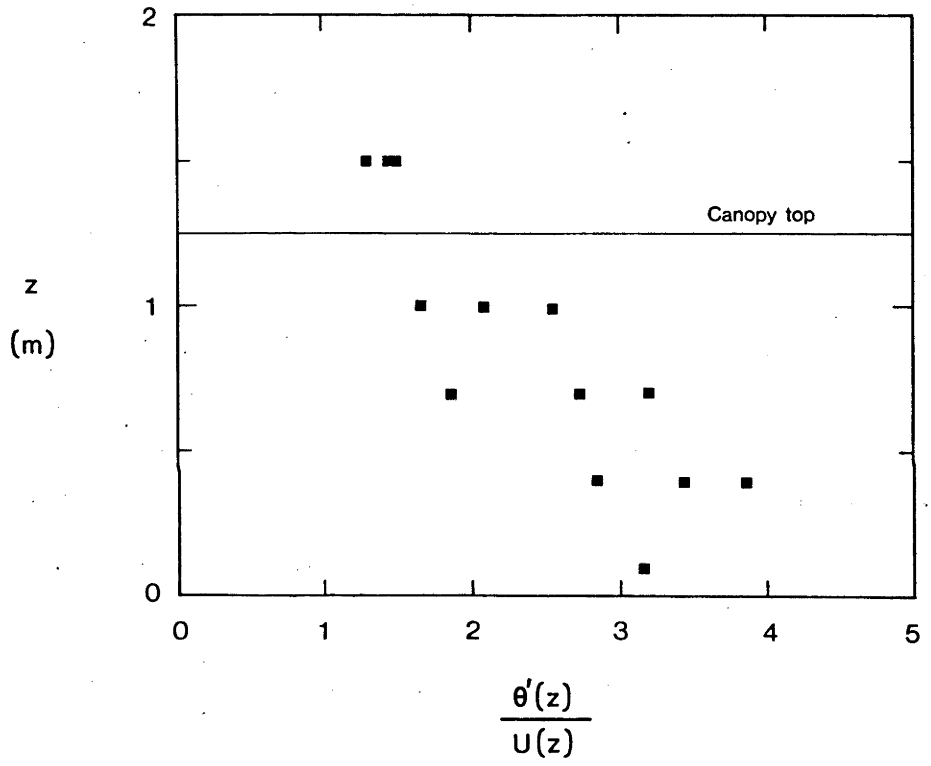

Fig. 16. Normalized velocity wave phase velocities, $\theta'(z)/U(z)$, versus height, z, from R2.

accelerate, conveniently explains the observed height dependence of the spectral peaks. Unfortunately it is probably a considerable over-simplification. In Part II, results will be presented which suggest that, during a gust, the velocity profile throughout the upper region of the canopy has a greater shear than the mean profile ($\partial U/\partial z$ larger) so that any waving motion imparted to the penetrating gust by the stalks is itself rapidly sheared, possibly distorting both the wavelength and the frequency of the velocity waves. To completely resolve the question of whether the wavelength is essentially constant during the lifetime of a train of velocity waves, it would be necessary to compare the measured velocity fluctuations with the motion of the patch of stalks which initiated that particular wave train.

6.3 PRESSURE FLUCTUATIONS

The power spectrum of surface static pressure fluctuations, measured during profile R5, is presented in Figure 17. The spectral peak coincides exactly with that of the stalk waving, 0.7 Hz, which can be derived from Figure 8. This frequency is also the same as the waving peak in the R5 velocity spectrum, ϕ_{uu}, at z = 1.2 m which can be seen in Figure 10c. Unfortunately, velocity spectra from R5 were not obtained at small values of z, but the spectra of R4, which had similar values of U_R to R5, exhibited the same shift of the waving spectral peaks to lower frequencies with decreasing z, as appears in R2. It is probable that the pressure fluctuations at the ground surface owe more to velocity fluctuations at the top of the canopy than to those immediately above the ground, which in any case have a mean variance only about 4% of those at the canopy top.

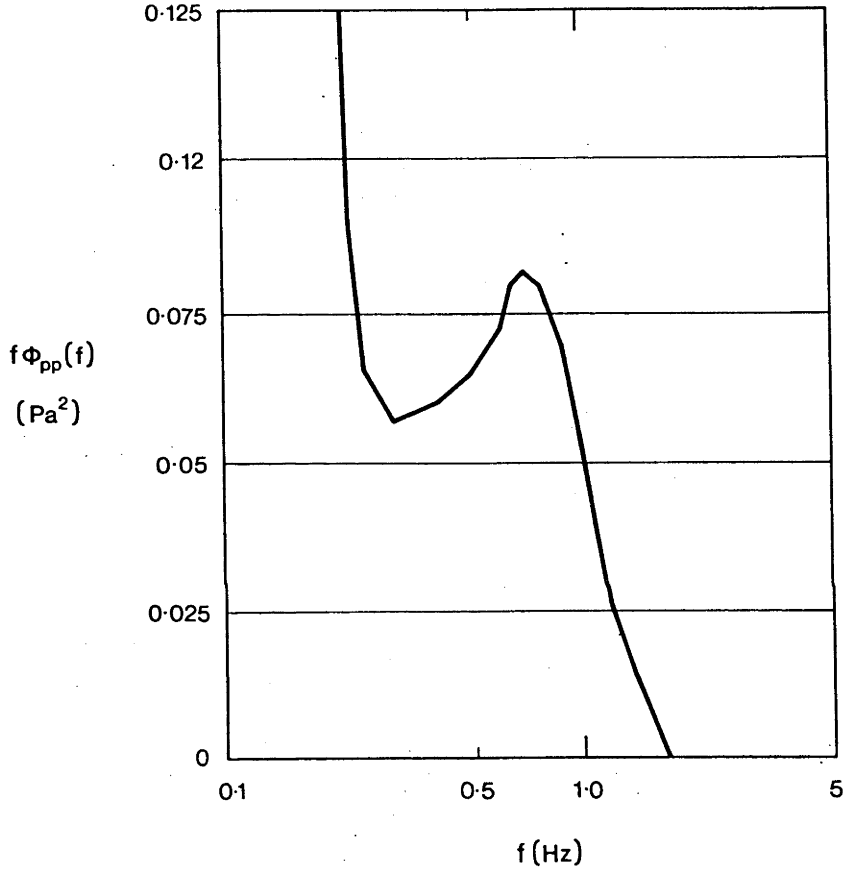

Fig. 17. Power spectrum of surface pressure fluctuations, ϕ_{pp}, from R5; z = 1.2 m.

A considerable body of data has been collected upon the ratio $\left(\overline{p^2}\right)^{\frac{1}{2}}/\rho u_*^2$ in smooth wall turbulent boundary layers. This work has been reviewed by Willmarth (1975) and the measured ratio varies between about 2.6 and 3.4 although the actual value may be somewhat higher since most of the transducers employed did not properly resolve small scale fluctuations in $\tilde{p}$. Over very rough walls, however, this should not be so great a problem as the smallest intense pressure fluctuations should have length scales at least of the scale of the roughness elements. Blake (1970) measured surface pressure in a rough wall turbulent boundary layer and results over his roughest wall indicated that $\left(\overline{p^2}\right)^{\frac{1}{2}} = 3.4\ \rho u_*^2$ whilst Burton's (1971) measurements over a very rough wall suggest a value somewhere between 3.4 and 2.6. The average value of $\left(\overline{p^2}\right)^{\frac{1}{2}}$ for the two runs of R5 was 4.49 Pa whilst ρu_*^2 was 0.425 Pa, giving $\left(\overline{p^2}\right)^{\frac{1}{2}} = 10.56\ \rho u_*^2$. The smallest scale fluctuations which might contribute substantially to the r.m.s. pressure within the canopy will be of order D/S where D is a typical dimension of a plant element (= 0.01 m) and S is an average Strouhal number taken as 0.2, giving a length scale $\simeq$ 0.05 m. Fluctuations with this length scale are substantially larger than the diameter of the sensing hole (0.00476 m) and should be adequately resolved by the pressure transducer.

Figure 18 presents the correlation coefficient, R_{pu}, between streamwise velocity fluctuations at z = 1.2 m in run R5 and surface pressure, where

$$R_{pu} = \frac{\overline{u[z,(t+\tau)] \circ p(t)}}{\left(\overline{u^2[z,(t+\tau)]} \circ \overline{p^2(t)}\right)^{\frac{1}{2}}} .$$

R_{pu} is strongly period in τ, the time delay, with a frequency equal to the stalk waving frequency, f. The significance of periodic

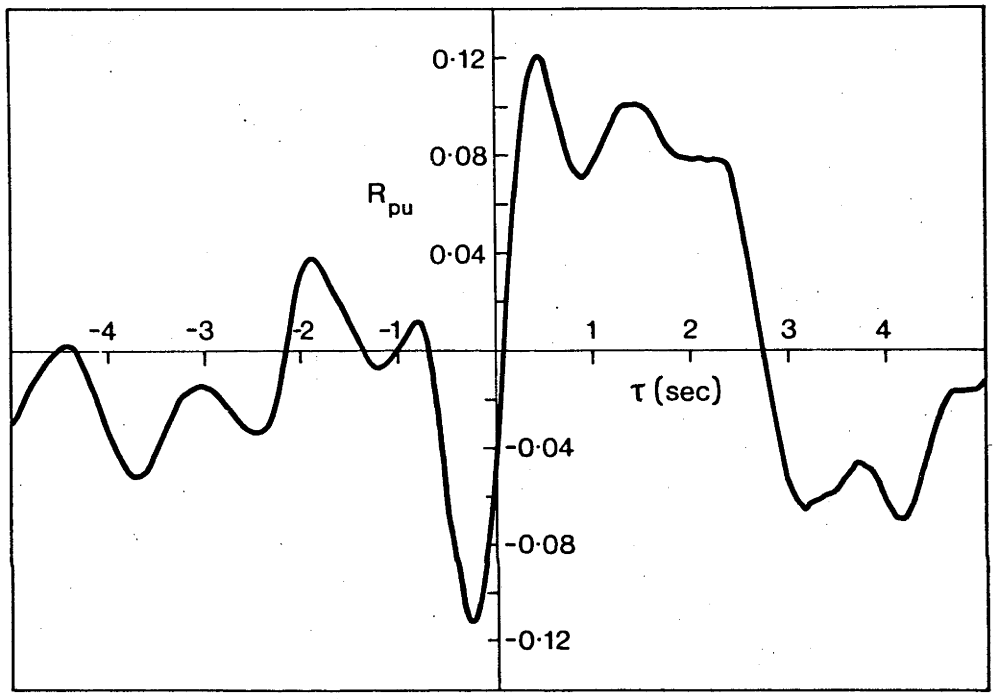

Fig. 18. Pressure velocity correlation coefficient, $R_{pu}(\tau)$ versus time delay, τ. From R5; $\bar{z}$ = 1.2 m.

correlation coefficients will be discussed in detail in Part II. For the moment it suffices to say that a periodic R_{pu} is a strong indication that the well correlated sections of u(t) and p(t) are those simultaneously periodic, with a common frequency.

Burton (1971) measured R_{pu} over a very rough wall. His results have essentially the same form as Figure 18 with maximum positive correlation at positive time delay (p leads u) and vice versa, but Burton's results lack the strong periodicity of the present values. The maximum value of $R_{pu} = +0.12$ from Figure 18 is about twice the maximum value ($R_{pu} = +0.07$) measured by Burton at the minimum vertical separation of his hot wire probe and pressure sensor.

The importance of the pressure fluctuations in momentum transfer is not clear however, since, although the fluctuations seem to have a relatively large magnitude and be well correlated with velocity fluctuations at the canopy top, the wavelike velocity fluctuations close to the ground have a lower frequency and are obviously not simply connected with the local pressure field.

Mulhearn's (1975) theoretical treatment and Burton's (1971) experimental results both indicate that R_{pu} passes through a maximum and then approaches zero as time delay and spatial separation decrease to zero. Since recent second order closure models of the canopy turbulence (e.g. Wilson and Shaw, 1977) neglect terms like $\overline{up}$ and $\overline{wp}$ in their general stress budget, a more detailed investigation of the behaviour of R_{pu} is indicated.

7. Conclusions

Despite the difficulties inherent in using hot wire anemometers in high intensity turbulence, it is proposed that the observed large positive skewness of u will mitigate the errors, at least during times of large contributions to the Reynolds stress. The normalized mean velocity profiles exhibit a fairly constant region ($dU/dz = 0$) in the bottom 30% of the canopy; and the estimated mean pressure gradient, which could result from the topography of the field site, is insufficient to balance the drag of the foliage in this region. The implication is that shear stress is maintained by a mechanism other than simple gradient diffusion. From (3), a reversal in sign of $\partial(U^2)/\partial z$ implies a reversal in sign of $-\partial^2\overline{uw}/\partial z^2$, the curvature of the shear stress profile. Unfortunately the resolution of the $\overline{uw}$ results is not sufficient to draw any worthwhile conclusions about the behaviour of $-\partial^2\overline{uw}/\partial z^2$. The reader is referred to Wilson and Shaw (1977) for a detailed discussion of the whole question, but two conclusions can be drawn: the common assumption of a single-valued flux-gradient relationship within the canopy fails in the present case and the observed balance between the foliage drag and the shear stress gradient permits a one-dimensional framework to be adopted when considering the time mean statistics.

The power and co-spectra of velocity are dominated by prominent peaks which show a consistent variation with height. Inspection of the original time traces of velocity forces the lowest frequency peak of about 0.35 Hz (in R2) to be interpreted as the characteristic frequency of gusts which appear to arrive in trains of up to three or four at the canopy. This is an unexpected and somewhat surprising result. The

observed phase velocity of honami waves in the crop can be interpreted as 'frozen histories' of gust velocity or the convection velocity of the large eddies with which the gusts are associated; they show a strong positive skewness reminiscent of the velocity traces measured by the hot wires. Once a region of the canopy has been set into motion by the passage of a gust, the waving stalks modulate the velocity field through their aerodynamic drag; in addition, the fluctuation in canopy height, which occurs at twice the waving frequency, strongly affects the velocity components, being most apparent in the vertical fluctuations. The observed variation with height of the frequency of velocity spectral peaks directly connected with stalk waving, has been tentatively ascribed to two mechanisms, not mutually exclusive. Acceleration by large scale pressure gradients of regions of fluid, already containing propagating velocity waves through their interaction with the stalks, would result in a Doppler shift of the wave frequency measured by a fixed hot wire. This mechanism assumes that the wavelength of the velocity wave is conserved. At the same time the rapid shear experienced by a region of fluid at the top of the canopy might result in both the wavelength and frequency becoming height dependent. Without experimental controls, not possible in a field experiment, the relative importance of these two effects is impossible to resolve.

The ratio of r.m.s. surface pressure fluctuations below the canopy, $\left(\overline{p^2}\right)^{\frac{1}{2}}$, to ρu_*^2 is about three times larger than values measured in other atmospheric or rough wall boundary layers. The pressure fluctuations exhibit a strong peak at the waving frequency, not at the frequency of the velocity fluctuations close to the ground, and appear to result from the velocity field at the top of the canopy. The form of the pressure

velocity correlation, R_{pu}, with a vertical separation equal to the canopy height is similar to that measured over a very rough wall by Burton (1971) but has a strongly periodic character (suggesting that it is the wavelike velocity fluctuations which contribute most to R_{pu}) and the maximum value of R_{pu} is about twice that measured by Burton.

Acknowledgements

The author thanks Dr E.F. Bradley, Dr A.R.G. Lang and Dr C.J. Barnes of this laboratory for much helpful discussion and particularly Dr P.J. Mulhearn of the Royal Australian Naval Research Laboratory, Sydney, whose enthusiasm and guidance made this work possible.

References

Allen, L.H. Jr.: 1968, 'Turbulence and Wind Speed Spectra within a Japanese Larch Plantation', J. Appl. Meteorol. 7, 73-78.

Blake, W.K.: 1970, 'Turbulent Boundary-layer Wall-pressure Fluctuations on Smooth and Rough Walls', J. Fluid Mech. 44, 637-660.

Brown, G.L. and Thomas, A.S.W.: 1976, Large Structure in a Turbulent Boundary Layer, Univ. of Adelaide, Dept of Mech. Eng. Report TN 16/76.

Burton, T.E.: 1971, On the Generation of Wall Pressure Fluctuations for Turbulent Boundary Layers over Rough Walls, Acoustics and Vibration Lab. Report No. 70208-4, Massachusetts Institute of Technology.

Champagne, F.H. and Sleicher, C.A.: 1967, 'Turbulence Measurements with Inclined Hot-wires', J. Fluid Mech. 28, 177-182.

Cionco, R.M.: 1972, 'Intensity of Turbulence Within Canopies with Simple and Complex Roughness Elements', Boundary-Layer Meteorol., 2, 453-465.

Dorman, C.E. and Mollo-Christensen, E.: 1973, 'Observation of the Structure on Moving Gust Patterns over a Water Surface ("Cat's Paws")', J. Phys. Oceanogr. 3, 120-132.

Finnigan, J.J.: 1978, 'Turbulence in Waving Wheat. II. Structure of Momentum Transfer'. Boundary-Layer Meteorol. (submitted for publication).

Finnigan, J.J. and Mulhearn, P.J.: 1978a, 'Modelling Waving Crops in a Wind Tunnel', Boundary-Layer Meteorol. 14, 253-277.

Finnigan, J.J. and Mulhearn, P.J.: 1978b, 'A Simple Mathematical Model of Airflow in Waving Plant Canopies', Boundary-Layer Meteorol. 14, 415-431.

Fraser, D.: 1978, 'An Optimised Mass Storage FFT', Assoc. of Comp. Mach. Trans. on Math. Software (in press).

Grass, A.J.: 1971, 'Structural Features of Turbulent Flow over Smooth and Rough Boundaries', J. Fluid Mech. 50, 233-255.

Inoue, E.: 1955, 'Studies of the Phenomena of Waving Plants ("HONAMI") Caused by Wind. Part 1. Mechanism and Characteristics of Waving Plants Phenomena', J. Agric. Meteorol. (Japan) 11, 18-22.

Inoue, K., Uchijima, Z., Horie, T. and Iwakiri, S.: 1975, 'Studies of Energy and Gas Exchange within Crop Canopies (10) Structure of Turbulence in Rice Crop', J. Agric. Meteorol. (Japan) 31, 71-82.

Isobe, S.: 1972, 'A Spectral Analysis of Turbulence in a Corn Canopy', Bull. Nat. Inst. Agric. Sci. (Japan) Ser. A, No. 19, 101-112.

Jackson, P.S. and Hunt, J.C.R.: 1975, 'Turbulent Wind Flow over a Low Hill', Quart. J. Roy. Meteorol. Soc. 101, 929-955.

Lu, S.S. and Willmarth, W.W.: 1973, 'Measurements of the Structure of the Reynolds Stress in a Turbulent Boundary Layer', J. Fluid Mech. 60, 481-511.

Lumley, J.L. and Panofsky, H.A.: 1964, The Structure of Atmospheric Turbulence, Wiley-Interscience, New York, 239 pp.

Mollo-Christensen, E.: 1973, 'Intermittency in Large Scale Turbulent Flows', Ann. Rev. Fluid Mech. 5, 101-118.

Mulhearn, P.J.: 1975, 'On the Structure of Pressure Fluctuations in Turbulent Shear Flow', J. Fluid Mech. 71, 801-813.

Nakagawa, H. and Nezu, I.: 1977, 'Prediction of the Contributions to the Reynolds Stress from Bursting Events in Open-channel Flows', J. Fluid Mech. 80, 99-128.

Reynolds, W.C. and Hussain, A.K.M.F.: 1972, 'The Mechanics of an Organized Wave in Turbulent Shear Flow. Part 3. Theoretical Models and Comparisons with Experiments', J. Fluid Mech. 54, 263-288.

Seginer, I., Mulhearn, P.J., Bradley, E.F., and Finnigan, J.J.: 1976, 'Turbulent Flow in a Model Plant Canopy', Boundary-Layer Meteorol. 10 423-453.

Shaw, R.H.: 1977, 'Secondary Wind Speed Maxima Inside Plant Canopies', J. Appl. Meteorol. 16, 514-521.

Tutu, N.K. and Chevray, R.: 1975, 'Cross-wire Anemometry in High Intensity Turbulence', J. Fluid Mech. 71, 785-800.

Weiss, A. and Allen, L.H. Jr.: 1976, 'The Flux-angle Distribution of Momentum as Determined from Propeller Anemometer Measurements', Quart. J. Roy. Meteorol. Soc. 102, 775-779.

Willmarth, W.W.: 1975, 'Structure of Turbulence in Boundary Layers', in Yih, C.-S. (ed.), Advances in Applied Mechanics, Vol. 15, Academic Press, New York, pp. 159-254.

Wilson, N.R. and Shaw, R.H.: 1977, 'A Higher Order Closure Model for Canopy Flow', J. Appl. Meteorol. 16, 1197-1205.

CHAPTER 3

TURBULENCE IN WAVING WHEAT.

II. STRUCTURE OF MOMENTUM TRANSFER

Abstract. The intermittent features of the turbulent velocity field within a wheat canopy were investigated by conditional sampling techniques and short period space-time correlations. The velocity and shear stress profiles had qualitatively quite different forms during periods of high and low wind. Analysis of the relative importance of shear stress contributions from different quadrants of the uw plane revealed the dominant role of gusts in penetrating the canopy and transferring momentum to it from the boundary layer above. Short period space-time correlations of velocity indicated that over a significant fraction of the time, periodic velocity fluctuations pervaded the canopy-air layer. It is surmised that, while this has only a secondary effect on momentum transfer, it may be of overriding importance in heat and mass transport.

Symbols

x streamwise co-ordinate positive downwind

y cross stream co-ordinate

z vertical co-ordinate positive upwards

$\tilde{u}$ instantaneous streamwise velocity

$\tilde{v}$ instantaneous cross stream velocity

$\tilde{w}$ instantaneous vertical velocity

$\tilde{u} = U + u; \quad U = \bar{\tilde{u}}; \quad \bar{u} = 0$

$\tilde{w} = W + w; \quad W = \bar{\tilde{w}}; \quad \bar{w} = 0$

$\tilde{v} = V + v; \quad V = \bar{\tilde{v}}; \quad \bar{v} = 0$

$\tilde{p}$ instantaneous pressure

$\tilde{p} = P + p; \quad P = \bar{\tilde{p}}; \quad \bar{p} = 0$

$$\bar{q} = \lim_{T\to\infty} \frac{1}{T} \int_0^T q(t)\, dt$$

$\bar{}$ denotes long time average

$=$ denotes short time average

$\hat{}$ denotes conditional average.

subscript R denotes reference wire ($z = 2.0$ m)

Other symbols are defined as they are encountered in the text.

1. Introduction

This paper is the second part of an investigation into the turbulence structure of a wheat canopy, conducted with the primary aim of establishing those features of momentum transfer which are masked by long time averages. A body of data, collected in smooth and rough wall turbulent boundary layers, has emphasized the essential intermittency in time and space of Reynolds stress (for a review of some of these results see Willmarth, 1975). The results of Dorman and Mollo-Christensen (1973), obtained over an open water surface, showed that intermittent periods of high momentum transfer were accompanied by instantaneous velocity profiles very different from the mean. At the same time, a few isolated results from field experiments in plant canopies (Allen, 1968; Isobe, 1972) have suggested that air motions with length scales much larger than those typical of the canopy might make very important contributions to the velocity field.

Most mathematical models of canopy flow have, however, attempted to relate the canopy geometry and time-averaged momentum absorption by a process of continuous diffusion by turbulent eddies, expressed as a flux-gradient relationship and characterised by a single valued diffusivity or mixing length (see for example Cowan, 1968; Thom, 1972). This approach has been criticized on general theoretical grounds by Corrsin (1974); it has also become apparent that it is inadequate to account for observations in many simple canopy-flow situations (Shaw, 1977). It is hoped in this paper to determine the degree of uniformity (or otherwise) of momentum transfer to and within the canopy, in order to test the basic premise of the conventional approach.

In the first part of this investigation (Finnigan, 1978), hereafter referred to as 'Part I', results were analyzed in the conventional manner: time-average, single point statistics and spectra of the turbulent velocity and surface pressure were presented. The features of the velocity spectra were interpreted in terms of the organised wave motion or 'honami', so prominent in cereal canopies on windy days. It was established that the honami waves were records of the passage of gusts of air with high streamwise momentum, which sweep down to the surface from an outer part of the boundary layer, bending over a series of stalks in their downwind passage. These stalks then spring back and vibrate at their natural frequency, but the small but smoothly varying phase difference between adjacent stalks gives the impression of waves moving through the canopy.

The areas of coherently waving stalks impress a velocity wave upon the air moving through the top of the canopy and the waving frequencies form prominent peaks in the velocity spectra. At the top of the canopy, these peaks are seen to be identical to the waving frequency but move to lower frequencies as one descends into the canopy and higher frequencies as one rises above it. This height dependence of the frequency peaks is ascribed to a combination of a Doppler effect, as regions of fluid containing propagating velocity waves are accelerated past the fixed hot wire, and distortion of the wavelength of the velocity waves by rapid shear of these same regions. For a more detailed discussion of these observations see Part I.

The errors in hot wire measurements, unavoidable in high intensity turbulence, were shown to be mitigated to some extent in the present experiment by the strong positive skewness of streamwise velocity within the canopy.

2. Experimental Site and Instrumentation

The measurements were made in a very uniform crop of wheat, 1.25 m high, at the CSIRO Ginninderra Experiment Station, Canberra, Australia between 9 and 18 December 1976. The primary sensors were single and X wire anemometer probes mounted on damped wind vanes on a vertical mast. The single wire was fixed at a height of 2 m to provide a reference signal, while the X wire could be moved vertically to obtain profile measurements. Supplementary instrumentation included a pressure sensor arranged to record pressure at the ground surface, miniature strain gauges glued to wheat stalks to measure their waving directly, and an 8 mm movie camera used to record the waving motion of the field. A detailed description of the instrumentation and field site can be found in Part I.

3. Results and Discussion

The results described in the next three sections were obtained from 5 min records of sensor output at each height in the profile. Data were recorded on an analogue tape recorder after first being low pass filtered at 250 Hz by 4 pole filters with a Butterworth response. The signals were subsequently digitized and linearized using predetermined calibration data on a Digital Equipment Corp. PDP 11/40 computer. Spectra were obtained digitally using a Fast Fourier transform routine, the time series being tapered before transformation with a 'Hanning window'. Analysis of the possible aerodynamic mean pressure gradients resulting from inhomogeneities in the site, revealed that the time mean measurements could be interpreted in an essentially one-dimensional framework.

Details of the particular experimental conditions pertaining to each run can be found in Table I. Because of the considerable computing time involved in analyzing the data by conditional methods, only the results of Run R2 have been completely processed. However, sufficient spot checks were done on the rest of the data to support the conclusions presented here.

TABLE I.

Summary of experimental conditions

Date	Profile No.	Sensors Operating	$z^{\dagger}$ m	U $m\ s^{-1}$	U_R $m\ s^{-1}$
9/12/76	R1	X wire only	1.55	4.035	-
			1.25	4.096	-
			.75	1.588	-
			.35	1.475	-
10/12/76	R2	X wire and reference wire	1.00	1.774	3.07
			0.70	1.18	2.633
			1.50	3.368	4.025
			0.40	1.001	3.575
			1.95	3.235	3.043
			0.10	0.891	3.208
14/12/76	R4	X wire and reference wire	0.4	1.301	5.562
			0.7	1.687	5.192
			1.0	2.090	7.404
			1.3	3.63	8.805
18/12/76	R5	X wire, reference wire, pressure sensor, strain gauges	1.4	5.272	6.229
			1.2	4.670	6.293

†z values are given in the order in which profile was measured.

3.1 CONDITIONALLY SAMPLED MEAN PROFILES

Typical time traces of the streamwise velocity, $\tilde{u}$, vertical velocity, $\tilde{w}$, and shear stress, $-\overline{uw}$, at various heights in the canopy, together with the simultaneous record of streamwise velocity at z = 2 m, $\tilde{u}_R$, are shown in Figure 1. It is immediately obvious that as one descends into the foliage, the turbulent signal begins to acquire an intermittent character until at z = 0.4 and 0.1 m, the trace is reminiscent of the outer wake region of a turbulent boundary layer, with periods of strong turbulence separated by quiescent periods. It can be seen that periods of strong turbulence within the canopy are associated with higher than average velocity above the canopy. In an attempt to quantify this relationship, the turbulence statistics were conditionally sampled in the following way. An indicator function, $I(\tilde{u}_R)$, was defined such that

$$I = 1 \; ; \quad 2 \text{ m s}^{-1} > \tilde{u}_R \geq 0$$

$$I = 2 \; ; \quad 3 \text{ m s}^{-1} > \tilde{u}_R \geq 2 \text{ m s}^{-1}$$

$$I = 3 \; ; \quad 4 \text{ m s}^{-1} > \tilde{u}_R \geq 3 \text{ m s}^{-1}$$

$$I = 4 \; ; \quad 5 \text{ m s}^{-1} > \tilde{u}_R \geq 4 \text{ m s}^{-1}$$

$$I = 5 \; ; \quad \tilde{u}_R \geq 5 \text{ m s}^{-1} \; .$$

The conditional average of the turbulence moment of interest, $\hat{\mu}(I)$, (where $\hat{}$ denotes a conditional average, $\bar{}$ a normal average) within the canopy was then computed according to the value of the indicator function such that

$$\hat{\mu}(I) = \frac{1}{m(I)} \sum_{j=1}^{n} \mu_j \, \delta(I - I_j)$$

where n is the number of digitized values of μ, μ_j and I_j being the jth values of μ and I.

$$\delta(I - I_j) = \begin{cases} 1 \text{ if } I_j = I \\ 0 \text{ if } I_j \neq I \end{cases}$$

and m(I) is the number of times $I = I_j$.

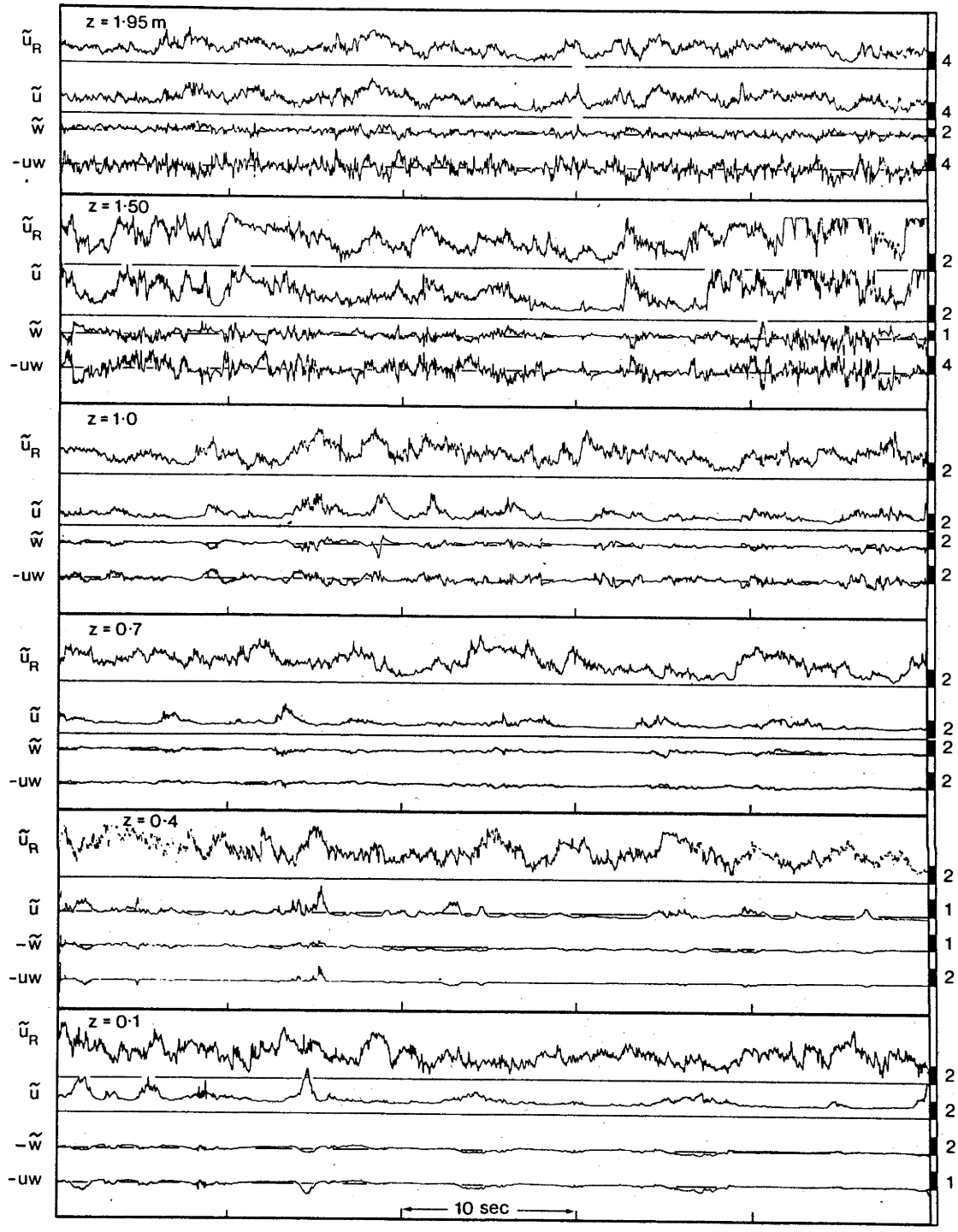

Fig. 1. Computer plots of typical sections of $\tilde{u}_R$, $\tilde{u}$, $\tilde{w}$ (m s^{-1}) and -uw (m^2 s^{-2}) versus time from R2 at various heights, z. The large amplitude fluctuations were truncated by the plotter. This does not imply that the measured signals were truncated.

The conditional sampling process is shown schematically in Figure 2.

The averages were then normalized using the central value of the reference velocity according to their condition so that

$\hat{M}(1)$ normalized with 1 m s^{-1}

$\hat{M}(2)$ " " 2.5 m s^{-1}

$\hat{M}(3)$ " " 3.5 m s^{-1}

$\hat{M}(4)$ " " 4.5 m s^{-1}

$\hat{M}(5)$ " " 5.5 m s^{-1}.

The final non-dimensional moments are assumed to indicate the appearance of the moment field if the conditions appropriate to each average obtained all the time. The author realizes that the effect of a change in velocity at 2 m will not be reflected instantly within the canopy but felt that to impose some height dependent time delay, so that averages at z depended upon the value of I some time earlier, was equivalent to an implicit assumption of some mechanism of propagation.

Reference to Figure 11, where the variation with height of the time delay of peak correlation between u_R and u(z) is plotted, reveals that the time taken for a change in velocity at z = 2.0 m to be felt at z = 0.10 m was about 1.40 s, so a compromise was reached by smoothing the relevant signals with a 2-second moving average before the conditional sampling operation.

The mean velocity profiles appropriate to $\tilde{u}_R < 2$ m s^{-1} and $5 > \tilde{u}_R \geq 4$ m s^{-1} are plotted in Figure 3; the long time average profile U/U_R is included for comparison. Within the upper 50% of the canopy, the shapes of the two conditionally averaged profiles are qualitatively different; stronger winds or gusts appear able

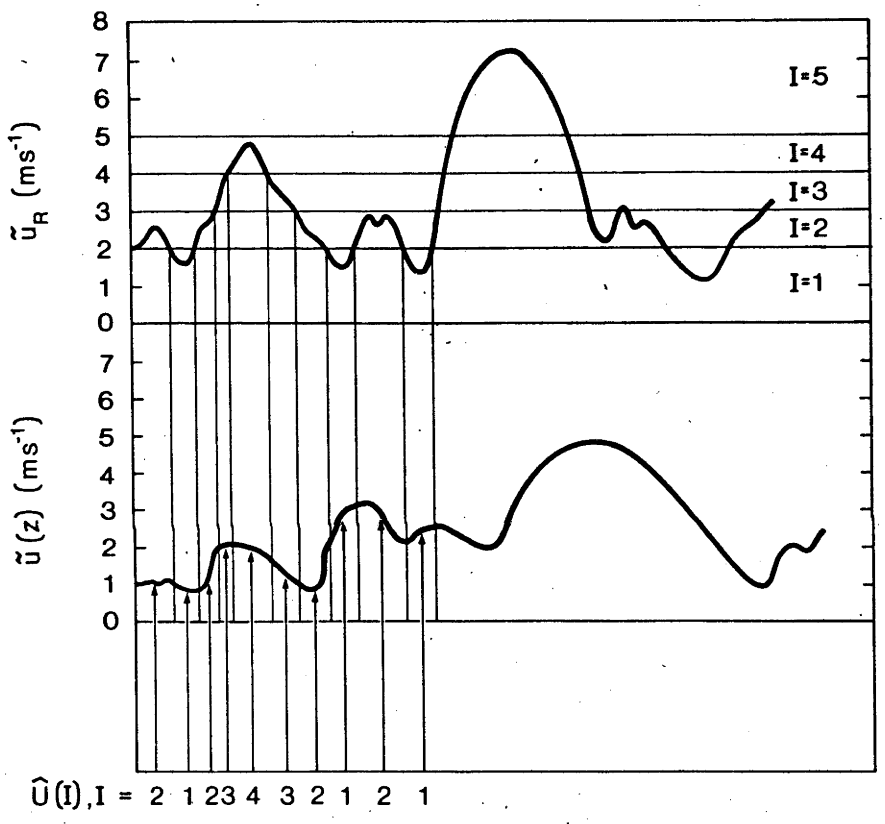

Fig. 2. Diagram of the conditional sampling process forming $\hat{U}(I)$.

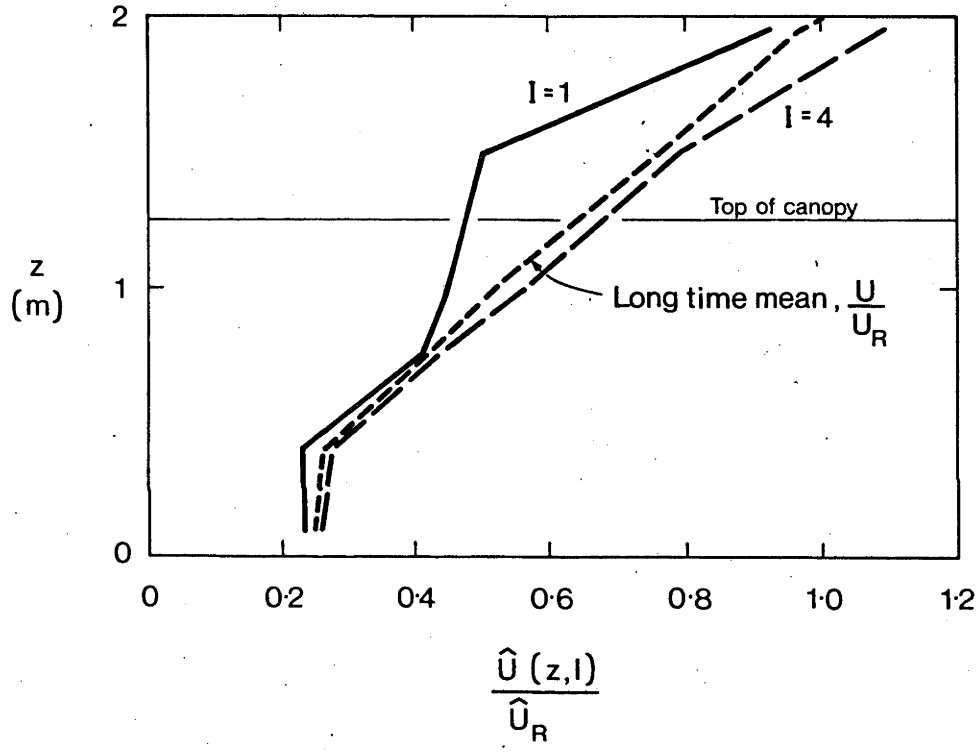

Fig. 3. Normalized conditionally sampled mean velocity, $\hat{U}(z,I)/\hat{U}_R$, versus height, z.

to penetrate much better into the foliage and the strong wind profile exhibits a much stronger shear in the upper canopy, presumably a result of the stronger absorption of momentum during times of higher wind by the aerodynamic drag of the foliage which increases as $\tilde{u}^2$. The similarity between the strong wind profile and the time mean profile simply reflects the fact that despite their relatively more frequent occurrence, weak winds make a smaller contribution to the mean than strong winds. Some caution is needed in interpreting these profiles. It should be realized that profiles obtained by this conditional process are no more representative of instantaneous velocity profiles than is the conventional long time mean.

The conditionally averaged shear stress profiles of Figure 4 appear to be more sensitive to I than are the velocity profiles. They are presented as curves of $\hat{u}_*$ [= $(-\widehat{uw})^{\frac{1}{2}}$] normalized as before with the appropriate $\hat{U}_R$; the long time mean profile u_*/U_R is included for comparison. It is apparent that, as with the velocity profile, the form of the shear stress profile is qualitatively quite different during periods of low and high wind. $\hat{u}_*/\hat{U}$ at the top of the canopy for $\tilde{u}_R > 5$ m s^{-1} is about 3 times $\hat{u}_*/\hat{U}$ for $\tilde{u}_R < 2$ m s^{-1}. The mean profile, at least to 1.5 m, appears to coincide with $\hat{u}_*/\hat{U}_R$ for $\tilde{u}_R > 5$ m s^{-1}, suggesting that the dominant contribution to the shear stress profile comes from times of high wind.

It is a useful aid to interpreting these profiles to consider the situation of $\tilde{u}$ or $\overline{uw}$ simply proportional to $\tilde{u}_R$ with a height dependant proportionality constant. In this case it can be shown simply that identical profiles would be obtained for each value of I. Departures from this case reflect the degree to which the profiles depend upon $\tilde{u}_R$ also.

The <u>intensity</u> of contributions to momentum transfer in each regime can be obtained by dividing the fractional contribution to total shear

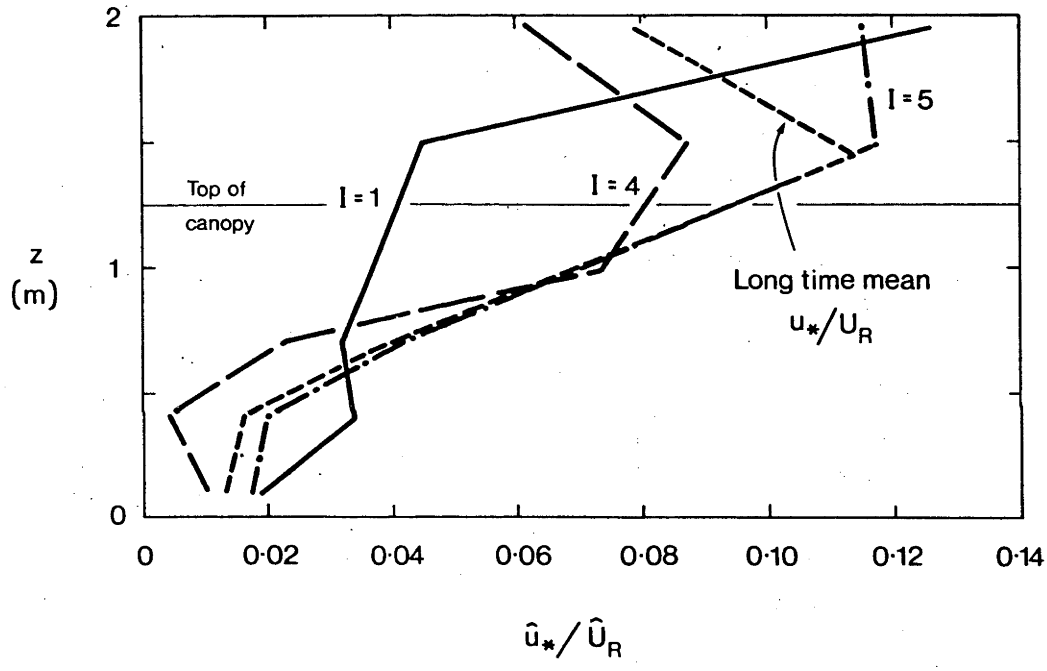

Fig. 4. Normalized conditionally sampled friction velocity, $\hat{u}_*/\hat{U}_R$, versus height, z.

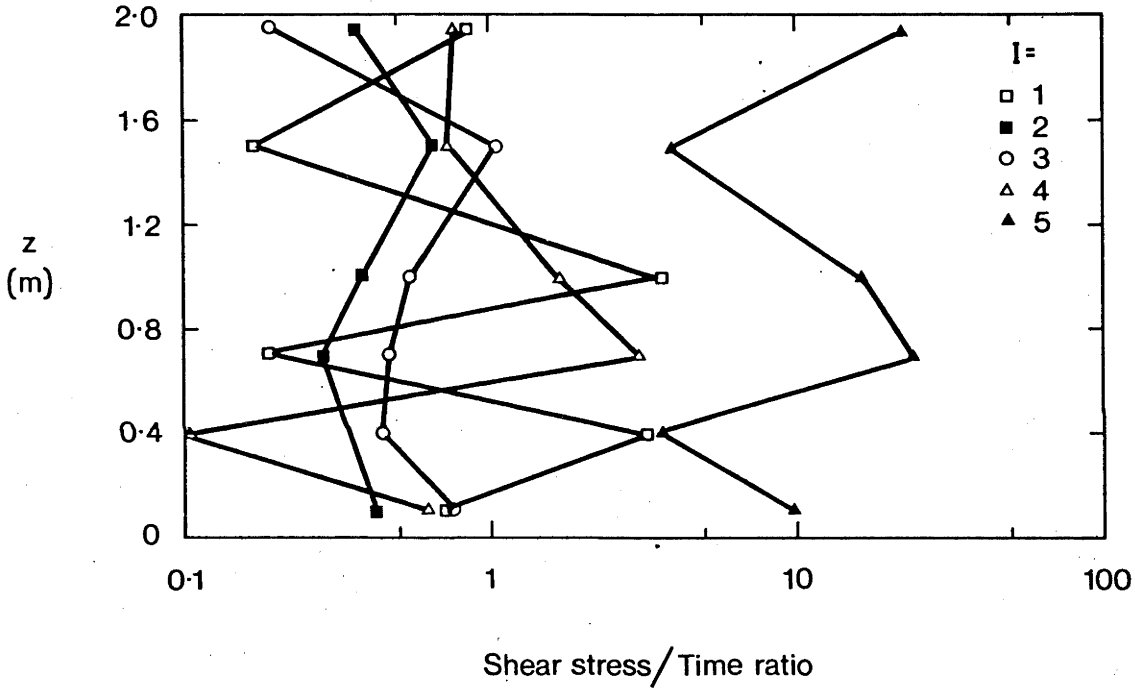

Fig. 5. Fractional contribution to shear stress from each conditional average, $(\widehat{uw}(I)/\overline{uw})$ divided by fraction of total time I had that value, $\left(\frac{m(I)}{n}\right)$.

stress for a given indicator value by the fraction of the total time that I had that value. This quantity is plotted against height in Figure 5 (i.e. $[\widehat{uw}(I)/\overline{uw}]/[m(I)/n]$ vs. z). Once again it is useful to imagine the situation u_* independent of I, when all the profiles would have a value of 1 irrespective of I. In fact it is obvious from Figure 5 that the relatively short lived periods when $\tilde{u}_R$ exceeds 5 m s^{-1} are times of very intense momentum transfer.

These observations suggest an alternative explanation for the commonly observed dependence upon mean wind speed of the total drag coefficient or any other parameter of a tall cereal crop which is a function of mean momentum absorption, such as the roughness length, z_o, or the zero plane displacement of the logarithmic wind profile (see Inoue et al., 1975; Maki, 1975a, b). A decreasing total drag coefficient, C (where $C = -2\overline{uw}/U^2$ at some height above the crop) with increasing mean wind speed is usually ascribed to streamlining of the crop as it bends before the wind. These observations, however, may well be a result of an inappropriate normalizing function, U^2, for the drag regime in the canopy. In light winds, the present results indicate that few gusts would penetrate the canopy and winds would be low in the lower part of the foliage. The aerodynamic regime at these levels would then be primarily laminar. Taking a cylinder as representing a typical canopy element, at Reynolds numbers lower than about 10^3, corresponding to a stalk diameter of .01 m and a wind speed of 1.5 m s^{-1}, typical of lower canopies in light winds, the drag coefficient based on cylinder diameter and U^2 rises rapidly as U decreases (Hoerner, 1965). This is a result of using incorrect scaling criteria for the low Reynolds number regime; wetted surface area and $U^{3/2}$ are the correct scales. It has been pointed out in Part I that the period between gusts decreases with U_R so that the total time that a given depth of the canopy contributes

to momentum absorption primarily through laminar skin friction decreases rapidly as U_R increases. Contributions to drag in the lower canopy from form drag during intermittent periods of high wind would outweigh the laminar contribution, so that the drag coefficient, C, of the whole canopy would decrease as the mean velocity increased.

3.2 QUADRANT REPRESENTATION OF SHEAR STRESS

The results presented in the preceding section indicate that momentum transfer is an intermittent process, occurring at times when gusts penetrate into the canopy and the velocity profile differs from its form in light winds. To proceed, further information about the instantaneous features of the velocity field which contribute to the average shear stress, $-\overline{uw}$ is needed. This can be obtained by sorting the contributions to $\overline{uw}$ into four parts depending upon the quadrant of the uw plane in which the correlation occurred (Lu and Willmarth, 1973). The four conditional averages are defined as:

$\widehat{uw}_1$ when $u > 0$, $w > 0$: outward interaction

$\widehat{uw}_2$ when $u > 0$, $w < 0$: gust or sweep

$\widehat{uw}_3$ when $u < 0$, $w < 0$: inward interaction

$\widehat{uw}_4$ when $u < 0$, $w > 0$: burst.

$\widehat{uw}_1$ and $\widehat{uw}_3$ make positive contributions to the mean, and $\widehat{uw}_2$ and $\widehat{uw}_4$ negative contributions. It is useful to define normalized versions of these conditional averages so $RS_n = \widehat{uw}_n / |\overline{uw}|$ and $\sum_{n=1}^{4} RS_n = -1$.*

In Figure 6, the normalized averages, RS_n, are plotted against height for three different profiles, R2, R4 and R5. Within the canopy the resultant $\overline{uw}$ is the relatively small difference between the large negative and positive contributions from sweeps and outward interactions respectively. It has been established that in smooth wall turbulent boundary layers in the laboratory, the average frequency of gust arrival at the surface scales with the mean velocity and the boundary layer thickness (Lu and Willmarth,

* This expression also serves as a definition of $\widehat{uw}_n$

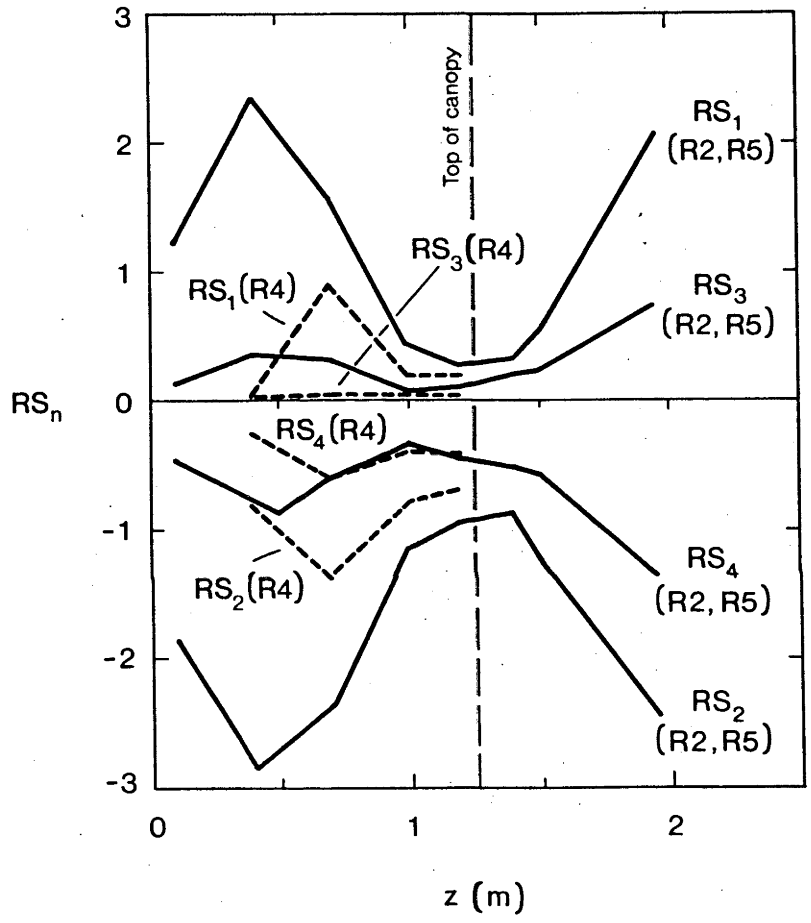

Fig. 6. Normalized contribution to $\overline{uw}$ from each quadrant, RS_n, versus height, z. Data from runs R2, R4, R5.

1973). In Part I, results were presented which suggested similar behaviour over the wheat canopy, at least over the Reynolds number range of this experiment. The large values of RS_1 and RS_2 from R2 reflect the increased intermittency of Reynolds stress arrival which is associated with a lower mean wind speed than in R4 and R5. Relatively few gusts are available to penetrate to the middle reaches of the canopy and their contributions to the stress budget are several times the mean.

Within the canopy, bursts and outward interactions are negligible; but above the canopy, bursts start to increase in importance until at $z = 1.95$ m, $RS_4 \simeq RS_1$. There are not many published results with which these observations can be directly compared. Only Nakagawa and Nezu (1977) have analyzed Reynolds stress over a rough wall using the quadrant representation. Their results, obtained in an open channel flow, show that, as the wall is approached, sweeps take over from bursts as the principal mechanism of momentum transfer and this effect is more pronounced as the surface roughness increases. In the outer 90% of the boundary layer bursts outweigh sweeps and both are two or three times as large as contributions from the other two quadrants. Grass (1971) deduced this same behaviour from flow visualization in an open rough wall channel flow; however, both these experiments were conducted at considerably lower Reynolds numbers than the present study.

The only work at comparable Reynolds numbers is that of Weiss and Allen (1976), who measured the flux angle distribution of momentum $\phi(\alpha)$ above vine rows where $\phi(\alpha)$ was defined by the relation

$$\frac{1}{T}\int_{-\pi}^{\pi} \phi(\alpha)\, d\alpha = -\overline{uw} \quad ,$$

T being the averaging time and $\alpha = \tan^{-1} w/u$ so that

$$RS_1 = \frac{1}{|\overline{uw}|}\frac{1}{T}\int_0^{\pi/2} \phi(\alpha)\, d\alpha \quad ;$$

$$RS_2 = \frac{1}{|\overline{uw}|}\frac{1}{T}\int_0^{-\pi/2} \phi(\alpha)\, d\alpha \quad ;$$

$$RS_3 = \frac{1}{|\overline{uw}|}\frac{1}{T}\int_{-\pi/2}^{\pi} \phi(\alpha)\, d\alpha \quad ;$$

$$RS_4 = \frac{1}{|\overline{uw}|}\frac{1}{T}\int_{\pi/2}^{\pi} \phi(\alpha)\, d\alpha \quad .$$

Their measurements were made at heights of 6.4 m and 4.1 m above the ground with vine rows 2 m high. Figure 7, which is redrawn from Weiss and Allen (1976), shows the relative intensity of gusts (RS_2) compared to bursts (RS_4) over their surface.

Both sweeps and bursts are manifestations of the large eddies or 'coherent structures' which are the characteristic feature of turbulent boundary layers. In a very simplified picture, these eddies have the general form of spanwise vortices (but are of limited spanwise extent) with a rotation in the sense of a ball rolling downwind along the surface when viewed from a co-ordinate system moving with the eddy. Sweeps or gusts are identified with the downwind face of the eddy which carries high momentum fluid from the outer part of the boundary layer to the surface (Brown and Thomas, 1976). As the rearward face of the eddy moves upwards, it lifts the highly sheared layer of fluid close to the surface into the outer part of the layer, causing intense, localized 'bursts' of turbulence (Laufer, 1972). (This idealized description only applies to the plane of symmetry of these complex structures, which in reality

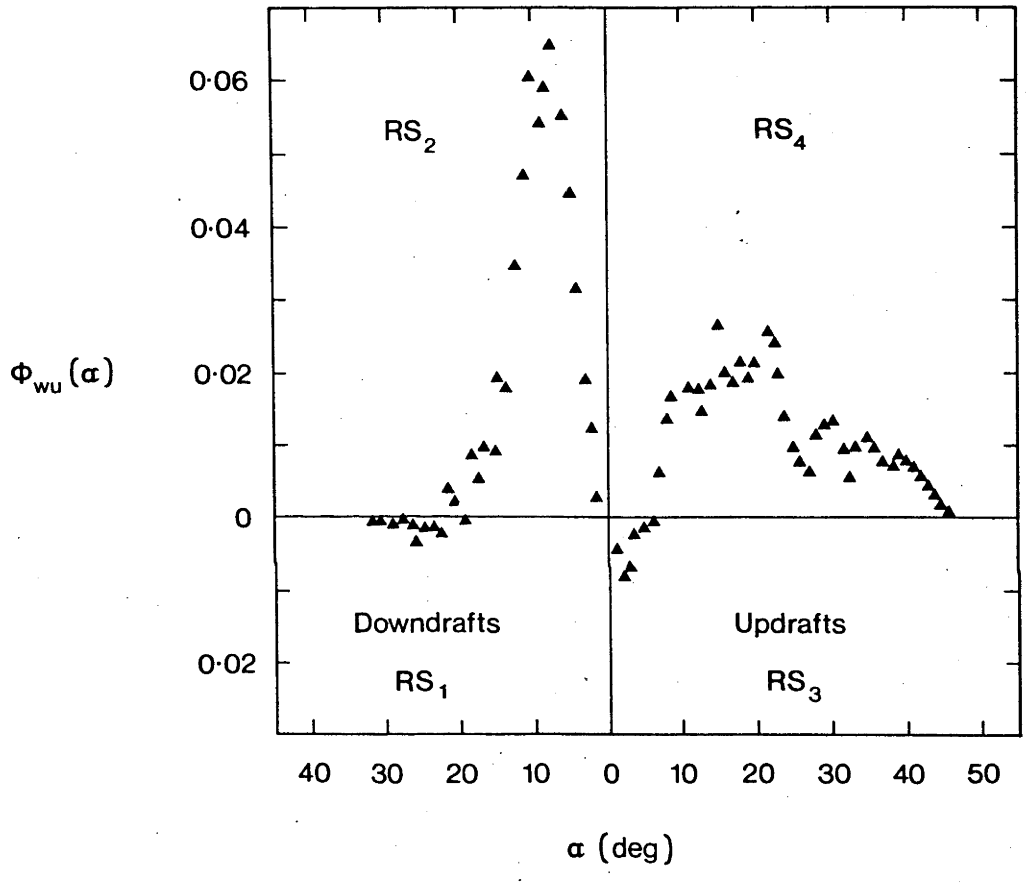

Fig. 7. Flux angle distribution of momentum, $\phi_{wu}(\alpha)$, over vine rows, redrawn from Weiss and Allen (1974).

probably exhibit some features of the 'Double roller' eddy proposed by Townsend, 1976.)

In Part I it was shown that when a gust arrives at the canopy surface it initiates a period of strong waving in the stalks and that the stalks' displacement in the x direction, ξ, can be described by a travelling wave of the form

$$\xi = \xi_o \exp 2\pi i\left(\frac{x}{\lambda} - ft\right) \quad , \qquad (1)$$

where ξ_o is the amplitude of the waving, λ the wavelength and f the frequency. $i = \sqrt{-1}$. θ $(= \lambda f)$, the phase velocity of the waves, is a record of the velocity of the gust as it passed over the surface. On average, θ was about 1.8 times the mean velocity at the top of the canopy. The motion of the stalks in the wake of a gust modulates the airstream in the upper canopy through the medium of aerodynamic drag, and continuity ensures that fluctuations in streamwise velocity are accompanied by $\tilde{w}$ fluctuations so that a transverse wavelike motion is imposed upon the background turbulent paths of the fluid particles.

It is suggested that this wavelike particle path is the reason for large values of RS_2 and RS_1 in the mid canopy, since times of strong waving are associated with larger than average streamwise velocity (see Part I) and w at a point is alternately positive and negative as the wave progresses.

More information about the relative intermittency of the various contributions, RS_n, can be obtained by adding a fifth region, the 'hole', to the quadrant representation of shear stress. The hole is delimited by the curves $|uw| = \text{constant}$, where $|uw| = H\ |\overline{uw}|$. The five regions are defined in Figure 8. With this scheme we can extract large contributions to $\overline{uw}$ from each quadrant by defining $\widehat{uw}_i^*$ such that

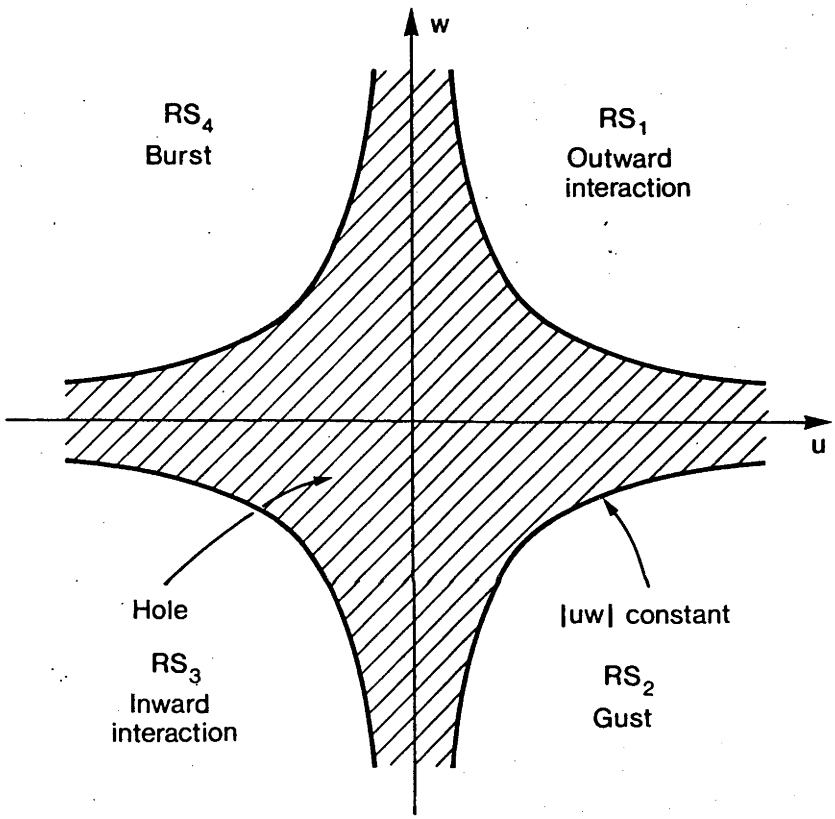

Fig. 8. Schematic drawing of the five regions of the 'quadrant and hole' representation in uw space.

$$\widehat{uw}_i^*(H) = \frac{1}{m}\sum_{k=1}^{m} \widehat{uw}_{ik} \cdot Y(k,H)$$

where $\widehat{uw}_{ik}$ is the kth member of the m digitized values of $\widehat{uw}_i$ in the ith quadrant and

$$Y(k,H) = \begin{cases} 1 \text{ if } \left|\widehat{uw}_{ik}\right| \geq H \cdot |\overline{uw}| \\ 0 \text{ if } \left|\widehat{uw}_{ik}\right| < H \cdot |\overline{uw}| \end{cases} .$$

In Figure 9, the dependence of $\widehat{uw}_i^*$ upon H for each quadrant is plotted for each height in the R2 profile. At the top of and above the canopy, the contributions $RS_i^* = \widehat{uw}_i^*/|\overline{uw}|$ for the two most important quadrants, sweeps and outward interactions, decrease relatively rapidly with changing H, $RS_i^*/RS_i\big|_{i=1,2}$ being less than 0.1 by the time H = 20. Within the canopy, however, $RS_i^*/RS_i\big|_{i=1,2}$ is still about 0.4 at H = 40. In other words, throughout and just above the canopy contributions to shear stress are generally very much greater than the mean but this feature is emphasized deep within the canopy by the more infrequent penetration of gusts to these regions. The corresponding dependence of RS_3^* and RS_4^* upon H, plotted in Figure 9, shows that these events make their contributions to the shear stress budget at only a few multiples of $|\overline{uw}|$.

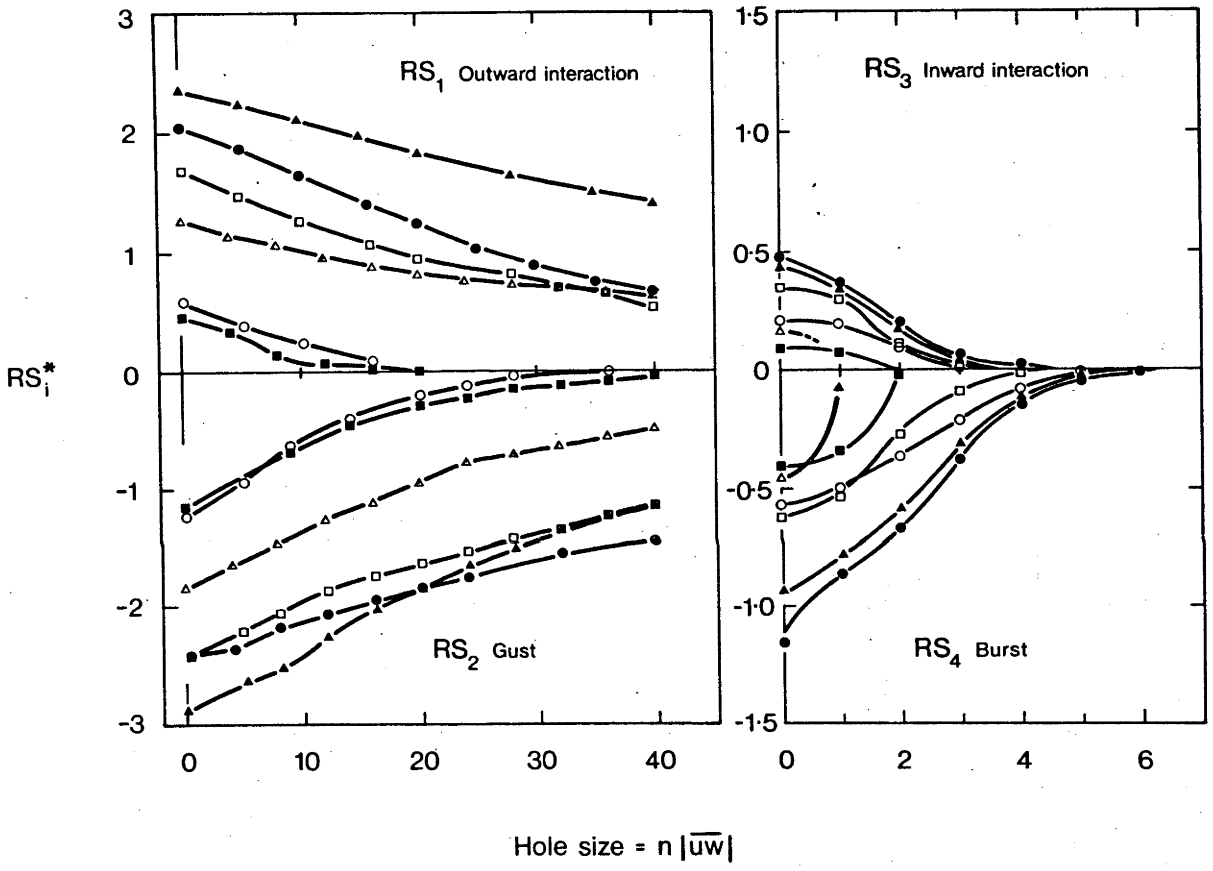

Fig. 9. Normalized contributions of RS_i^* to $\overline{uw}$ versus hole size, $H|\overline{uw}|$, at various heights, z(m): ● 1.95, ○ 1.5, ■ 1.0, □ 0.7, ▲ 0.4, △ 0.1.

3.3 CORRELATIONS

The obvious way to investigate the dependence of the velocity within the canopy upon that above is to compute the space, time correlation coefficient, $R_{uu_R}(z,\tau)$ where

$$R_{uu_R} = \frac{\overline{u(z,t - \tau/2) \cdot u_R(t + \tau/2)}}{\left[\overline{u^2}(z,t - \tau/2) \cdot \overline{u_R^2}(t + \tau/2)\right]^{\frac{1}{2}}} \qquad (2)$$

Curves of $R_{uu_R}(z,\tau)$ against time delay τ are presented in Figure 10 for profile R2. The correlation diminishes from a value of 0.8 at a vertical separation of .05 m to 0.16 at a separation of 1.90 m. Figure 11 presents the time delay of the peak of maximum correlation as a function of height, $\tau_p(z)$. With the exception of that at 0.7 m, the points fall upon a smooth curve. If we define the vertical convection velocity of the peak correlation as $(d\tau_p/dz)^{-1}$, the speed with which a streamwise velocity fluctuation at z = 2 m propagates towards the surface, we see that the convection velocity decreases as one descends into the canopy, to become approximately constant below z = 1.0 m. The curve of Figure 11 can be compared with similar data obtained in a rigid wind tunnel model canopy by Seginer and Mulhearn (1977). They suggest that their curve of time delay against separation approaches asymptotically the level of zero plane displacement within the canopy, although it is not clear why this should be so. In the light of the present results, it seems more likely that their curve should be extrapolated linearly to the level, z = 0.

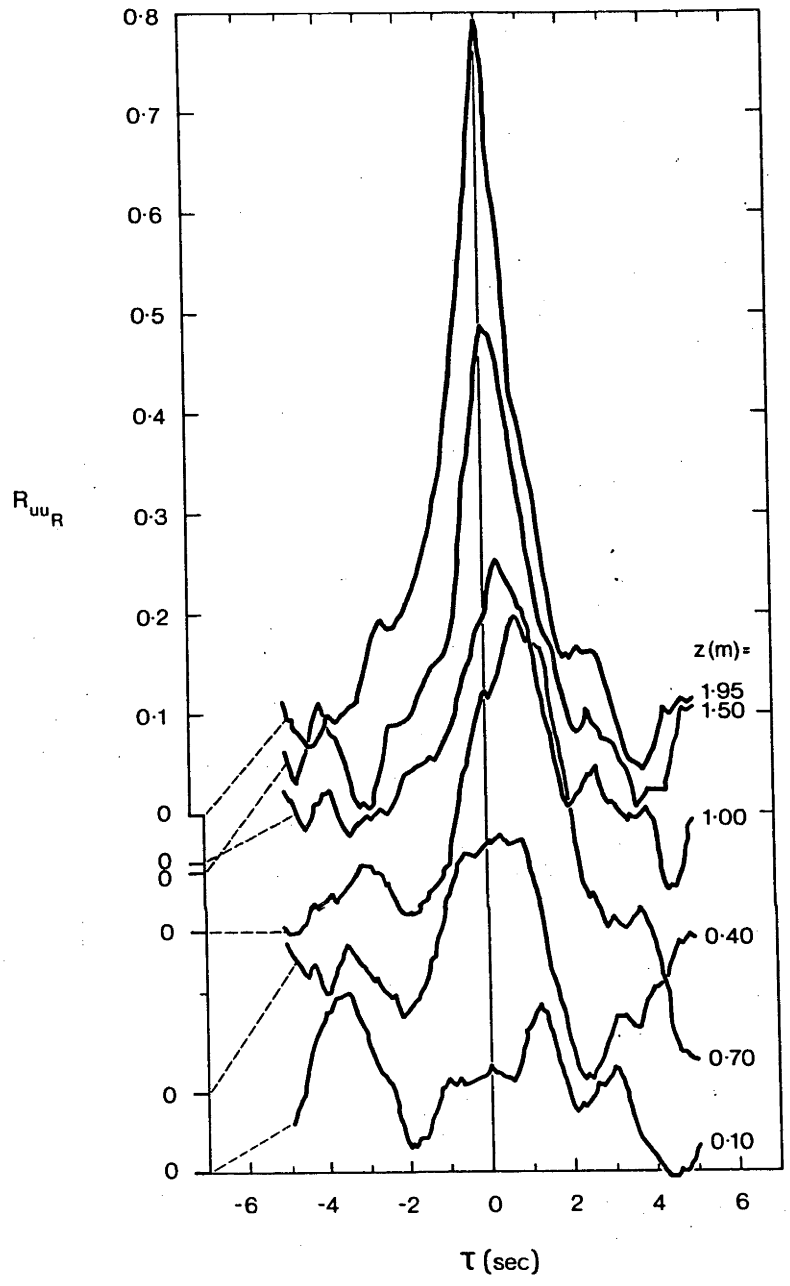

Fig. 10. Long period space-time correlations R_{uu_R} of u_R and u from R2.

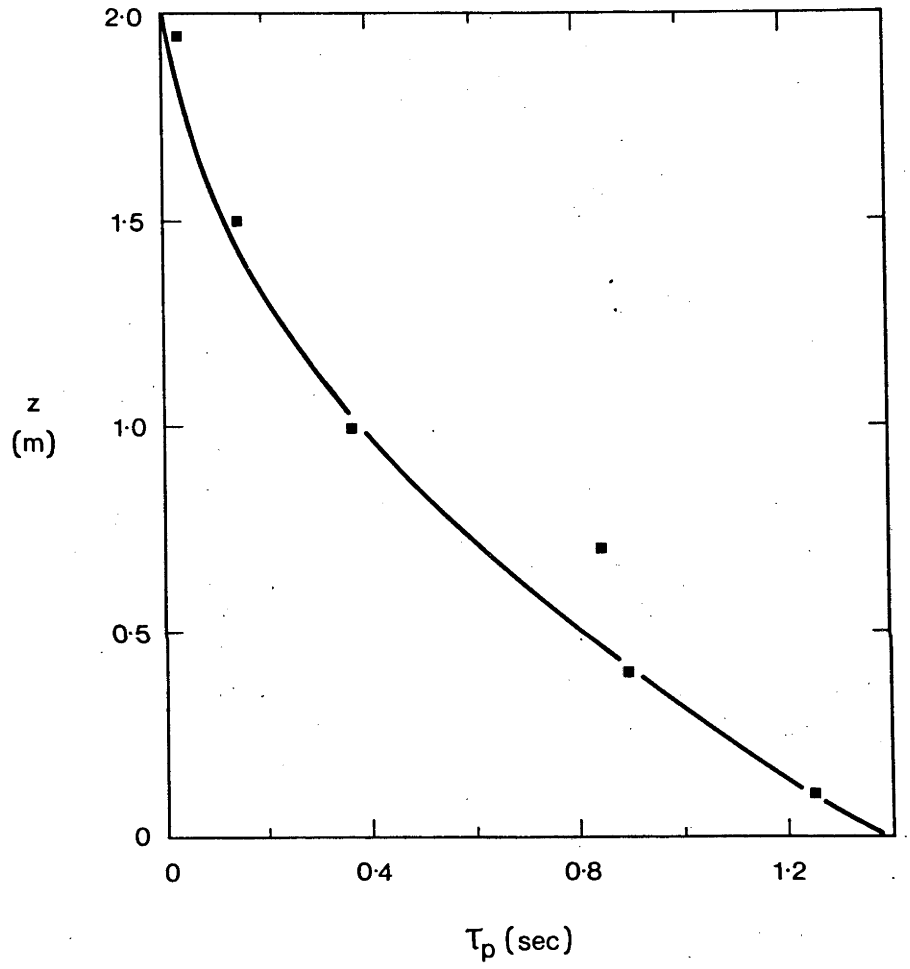

Fig. 11. Time delay, τ_p, of peak of R_{uu_R} versus height, z, from R2.

In Part I, it was observed that the patches of coherent waving (honami) which appear in the canopy in the wake of gusts are randomly distributed in space and time. The long time averaging involved in computing the correlation R_{uu_R} will tend to smooth out the contributions of this coherent motion to R_{uu_R} as randomly spaced events are superimposed.

Accordingly a series of short period space-time correlations was calculated for successive ten second intervals of the various time traces of R2 and R5. The short period time-space correlation is defined as

$$R^{*}_{uu_R}(z,\tau) = \frac{\overline{\overline{u'(t+\tau/2)\cdot u'_R(t-\tau/2)}}}{\left[\overline{\overline{(u')^2}(t+\tau/2)}\cdot\overline{\overline{(u'_R)^2}(t-\tau/2)}\right]^{\frac{1}{2}}} \qquad (3)$$

and $$\overline{\overline{g}}(t) = \frac{1}{T}\int_{-T/2}^{T/2} g(t)\,dt \quad ,$$

where τ = 5 seconds.

u' and u'_R are fluctuating components of $\tilde{u}$ and $\tilde{u}_R$ derived by subtracting the short time means obtained by averaging over the 5 s periods of the correlation. Figure 12 presents a diagram of the relationship of the sections of the time traces in correspondence as τ changes.

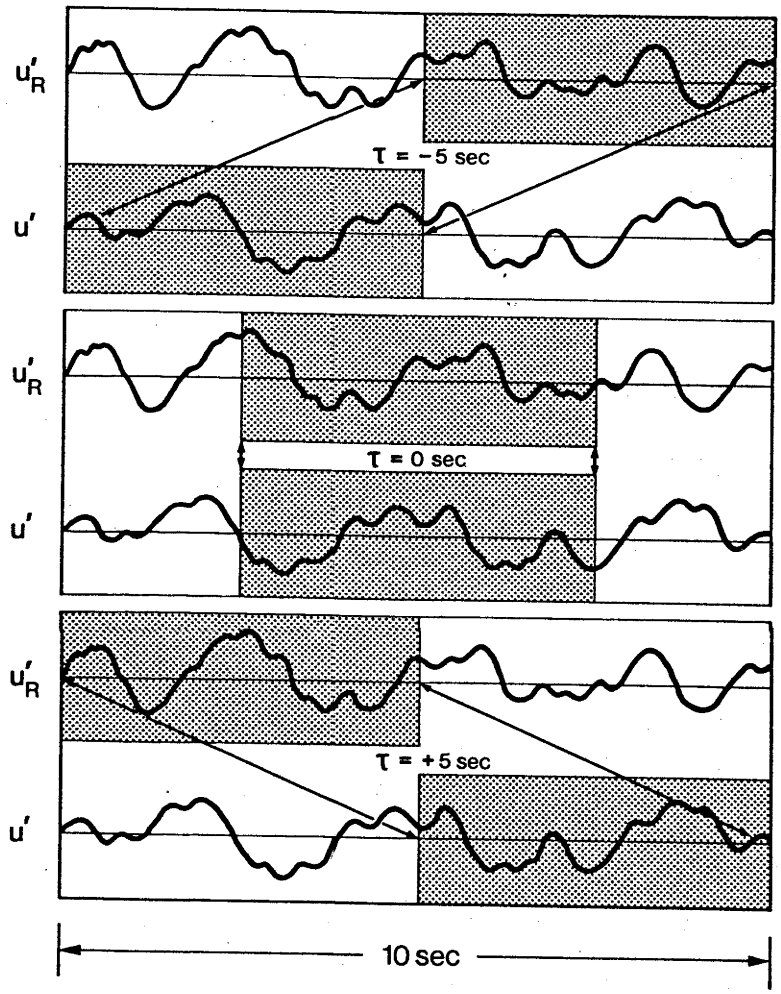

Fig. 12. Relationship between 5 second intervals of $\tilde{u}_R$ and $\tilde{u}$ during formation of short period space-time correlations, $R^*_{uu_R}$.

A typical series of successive values of $R^*_{uu_R}$ is shown in Figure 13 for R2, z = 1.0 m. The immediately striking feature of the correlations is their strong periodicity; two periods are predominant, approximately 0.65 Hz, the stalk waving frequency, and 0.35 Hz, the average arrival frequency of gusts at the surface. Unlike their observed behaviour in normal rough wall turbulent boundary layers, gusts tended to arrive over the waving wheat in trains of 3 or 4 with a well defined period, which appeared to scale upon U_R (see Part I).

To interpret the periodic behaviour of these short time correlations, it is useful to consider the result of correlating two harmonic signals, $\sin \omega_1 t$ and $\sin \omega_2 t$. It can be shown that, if

$$R^*(\tau) = \frac{1}{2T} \int_{-T}^{T} \sin \omega_1(t+\tau/2) \sin \omega_2(t-\tau/2)dt ,$$

then:

$$R^*(\tau) = \frac{1}{2} \left\{ \cos(\omega_1+\omega_2)(\tau/2) \operatorname{sinc}[(\omega_1-\omega_2)T] - \cos(\omega_1-\omega_2)(\tau/2)\operatorname{sinc}[(\omega_1+\omega_2)T] \right\} , \qquad (4)$$

where $\operatorname{sinc}(\psi) = \frac{\sin \psi}{\psi}$.

$R^*(\tau)$ therefore acts selectively to distinguish contributions from two signals with the same periodicity since sinc(0) = 1, but sinc(ψ) falls off rapidly with increasing ψ. If $\omega_1 = \omega_2 = \omega$, then $R(\tau) = \frac{1}{2} \cos \omega\tau$ - sinc $2\omega T$. If ω = 4.4 rad/sec (stalk waving frequency) and T = 5 sec, sinc $2\omega T$ = .0158, so that $R^*(\tau) \simeq \frac{1}{2} \cos \omega\tau$.

Bearing these results in mind we can interpret the traces exhibiting strong periodicity at the waving or gust arrival frequency as times when, within one 10 second interval, velocity fluctuations at this frequency were present at both hot wires. In Figure 14 examples of

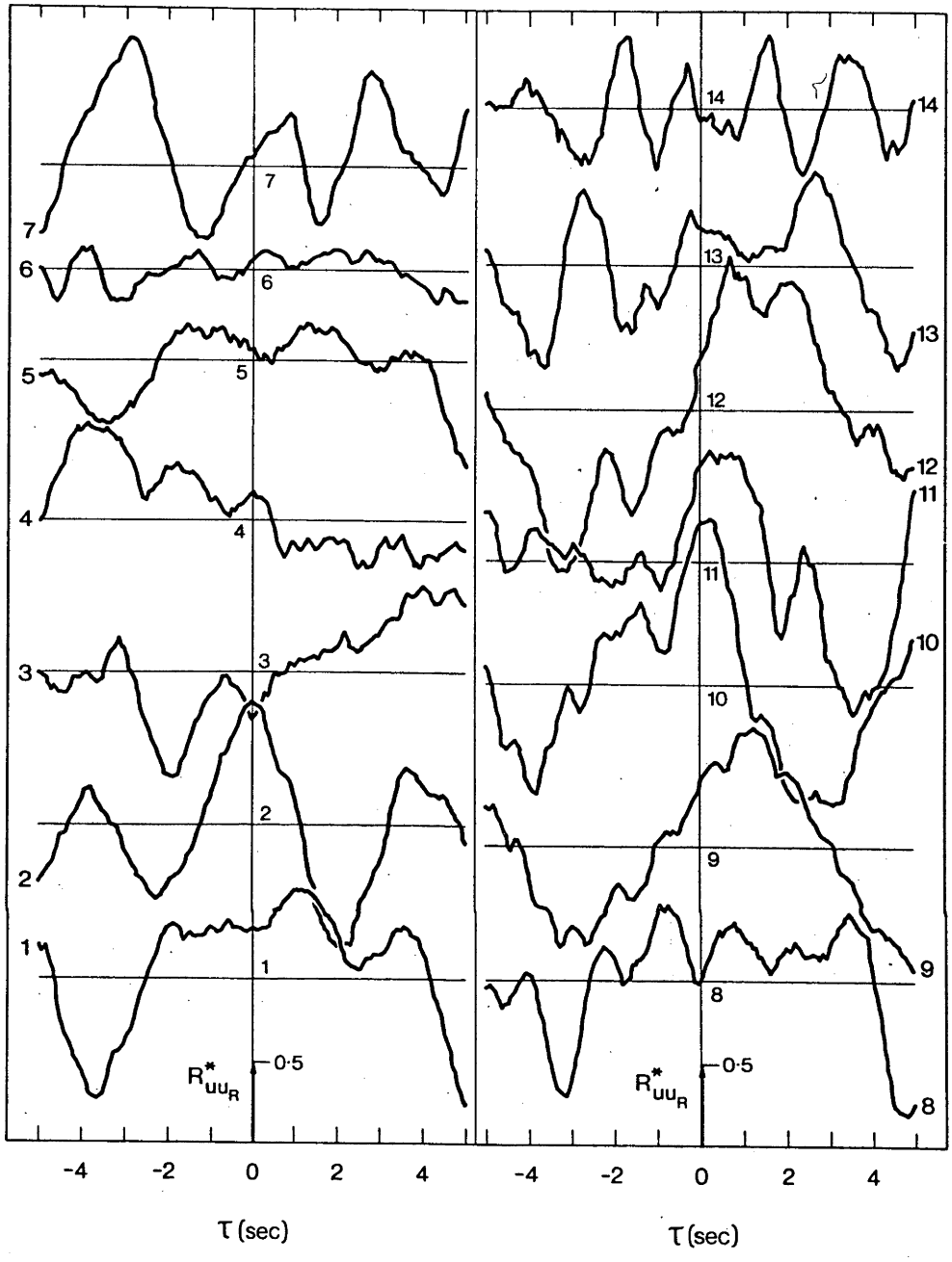

Fig. 13. Series of short period space-time correlations, $R^*_{uu_R}$, for successive ten second intervals of R2; z = 1.0 m. Correlations are numbered consecutively.

(a)

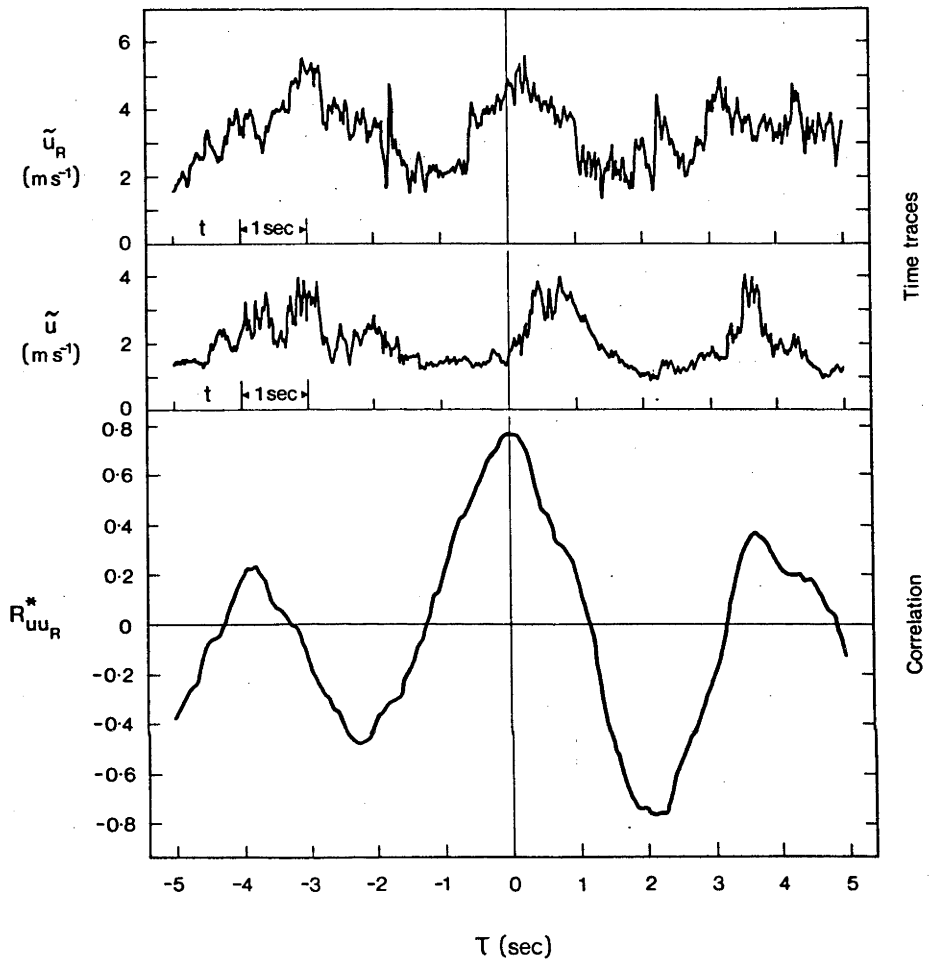

Fig. 14. Comparison of two short period space-time correlations with the corresponding ten second time traces of $\tilde{u}$ and $\tilde{u}_R$ versus time. From R2, (a) z = 1.0 m, (b) z = 1.5 m.

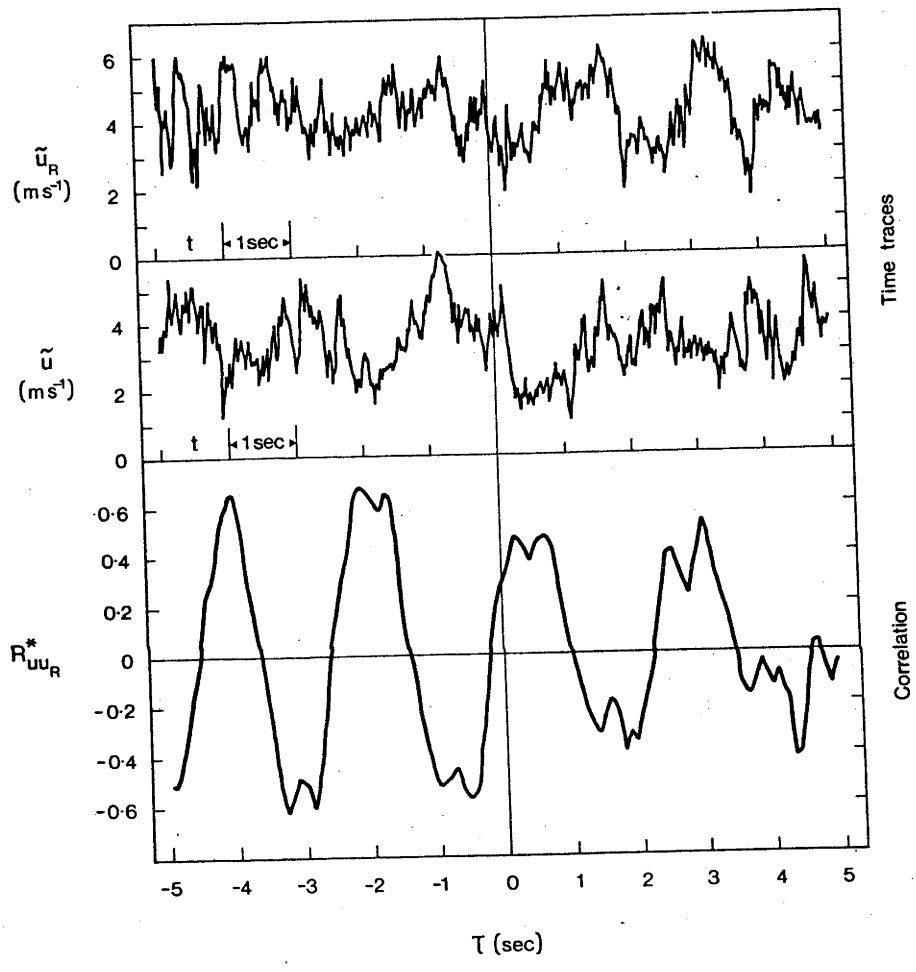
$\tilde{u}_R$ (ms^{-1})
6
4
2
0
t
1sec
$\tilde{u}$ (ms^{-1})
4
2
0
t
1sec
Time traces
$R^*_{uu_R}$
0·6
0·4
0·2
0
-0·2
-0·4
-0·6
Correlation
-5
-4
-3
-2
-1
0
1
2
3
4
5
τ (sec)

Fig. 14b.

$R^*_{uu_R}$ from the series of correlations from R2 at 1.0 m and 1.50 m are compared with the corresponding 10 second intervals of their time traces. The periodicity in the two signals which has been picked out by the correlations is obvious. The 'filtering' effect of R^* can be appreciated by comparing the smoothness of the R^* traces in Figure 14 with the time series from which they were derived. By counting the number of intervals when periodicity of one frequency or the other was dominant in the sequences of $R^*_{uu_R}$ for each height, Figure 15 was constructed; here the fraction of the total time when periodicity of one frequency was detected at both wires is plotted against height. Ten second intervals when $R^*_{uu_R}$ was aperiodic or the frequency of the periodicity was equivocal were rejected, but occasionally both frequencies were clearly present. On average, 30% of the ten second traces were rejected.

We can see from Figure 15 that periodic gust arrival occupies about 40% of the total time irrespective of the position of the lower probe. The time occupied by waving frequency fluctuations, on the other hand, shows a definite increase with height. This is partly a result of the observed shift to higher and lower frequencies of the wave motion impressed upon the air as it is convected from the centre of waving at the top of the stalks to higher and lower levels respectively. As ω_1 and ω_2 move apart, $R^*(\tau)$ decreases in magnitude [see equation (4)]. It is apparent, however, that over a significant fraction of the total time, periodic velocity fluctuations can be discerned from a height of 2 m, through the canopy to the ground, and that a large fraction of the gusts arriving at 2 m are felt directly throughout the canopy.

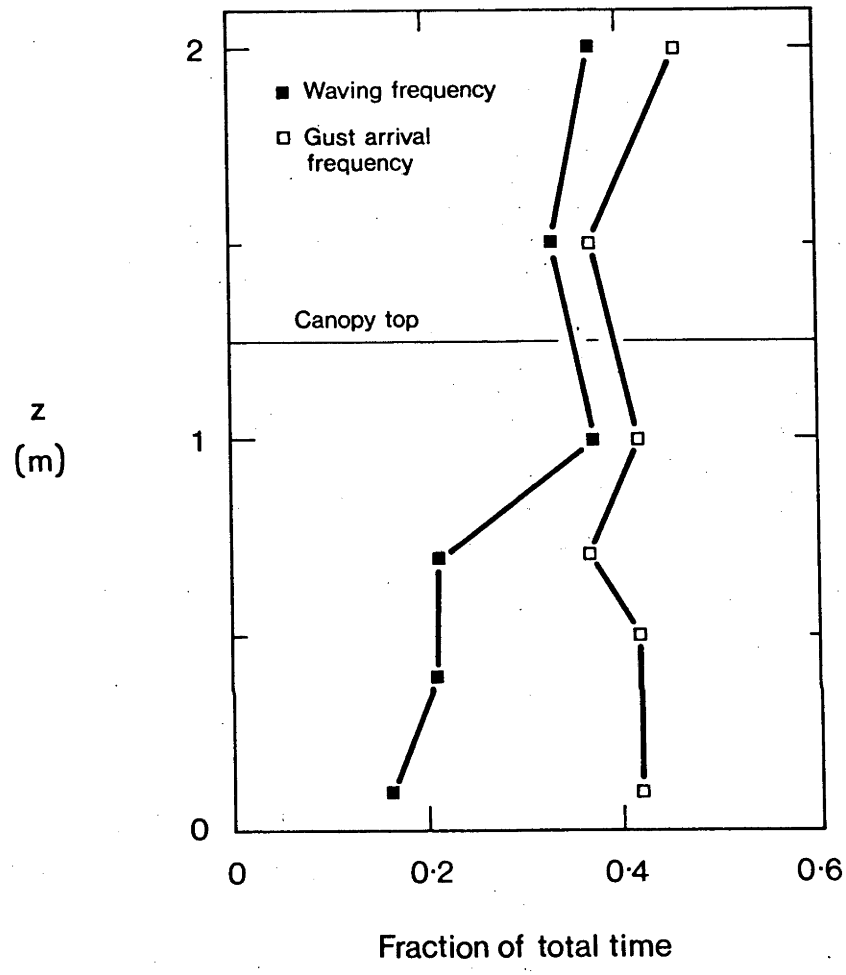

Fig. 15. Fraction of total time that periodic signal of same frequency was present in $\tilde{u}$ and $\tilde{u}_R$ versus height.

3.4 PRESSURE VELOCITY CORRELATIONS

Because of technical problems the pressure sensor, strain gauged wheat stalk bridges and hot wires were only operated in conjunction during the two recorded points of R5. The power spectra of surface pressure and stalk displacement had peaks at precisely the same frequency, 0.7 Hz, while the waving frequency velocity fluctuations, measured by the hot wires, showed a progressive decrease of frequency with height, the measured frequency just above the ground being only about 80% of its value at 1.0 m (see Part I). The pressure and velocity fluctuations are linked by a Poisson's equation (see Burton, 1971) which in its integral form shows that pressure fluctuations at a point are the result of velocity fluctuations over all space and need not be well correlated with those immediately nearby. The experimental results of Burton (1971),obtained in a rough wall turbulent boundary layer, and the theoretical work of Mulhearn (1975), who calculated pressure-velocity correlations in a uniform shear flow using rapid distortion theory, both indicate that R_{pu} approaches zero at zero separation and time delay.

The long time pressure velocity correlation, R_{pu}, from R5 at z = 1.2 is presented in Figure 16. The trace is strongly periodic at the waving frequency. Although the 1.2 m correlation has contributions of longer time scales superimposed upon it, the dominant periodicity argues for the belief that the waving motion is the prime inducer of surface pressure fluctuations. It was pointed out in Part I that the ratio of the r.m.s. pressure fluctuations to the shear stress, $(\overline{p^2})^{\frac{1}{2}}/\rho u_*^2$, at z = 1.2 m is about 4 times greater than that in any other rough wall boundary layer available for comparison.

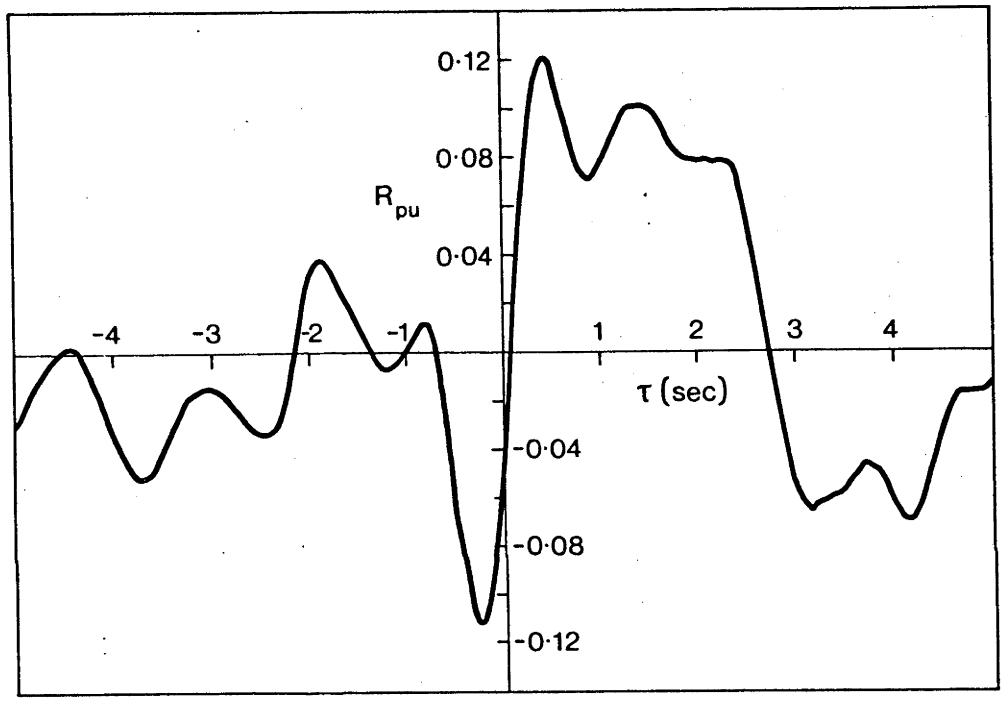

Fig. 16. Pressure velocity correlation coefficient, $R_{pu}(\tau)$, versus time delay, τ, from R5; z = 1.2 m.

The periodicity of R_{pu} suggests that this 'extra pressure' might be a direct result of the coherent waving which would add to the correlation resulting from passage of large eddies and the random small scale turbulence which must also be present.

Figure 17 presents the correlation between strain gauge output and velocity, R_{sgu}, for R5, z = 1.2 m. The correlation is strongly periodic, of course, since the stalk vibration is harmonic and well correlated with the neighbouring velocity. The maximum correlation corresponds to a time delay of 0.15 s, the stalks' motion slightly lagging the velocity fluctuation. The pressure-strain gauge correlation R_{psg}, of Figure 18 is purely periodic, a reflection of the stalks' behaviour in acting as a mechanical 'narrow band filter' for the velocity. The time delay of zero correlation is now the sum of the velocity-pressure and strain gauge-velocity time delays.

4. Conclusions

Examining the simultaneous time traces of streamwise velocity at a reference height of 2 m and at various heights above and within a wheat canopy suggested a direct connection between times of high reference velocity and periods of turbulence within the canopy. Conditional averaging of mean velocity and shear stress within the canopy revealed qualitatively different velocity and shear stress profiles during gusts and times of low wind. Strong winds penetrated much more effectively into the canopy. In the middle region of the canopy, the shear stress contribution during a gust was an order of magnitude greater than when winds were low.

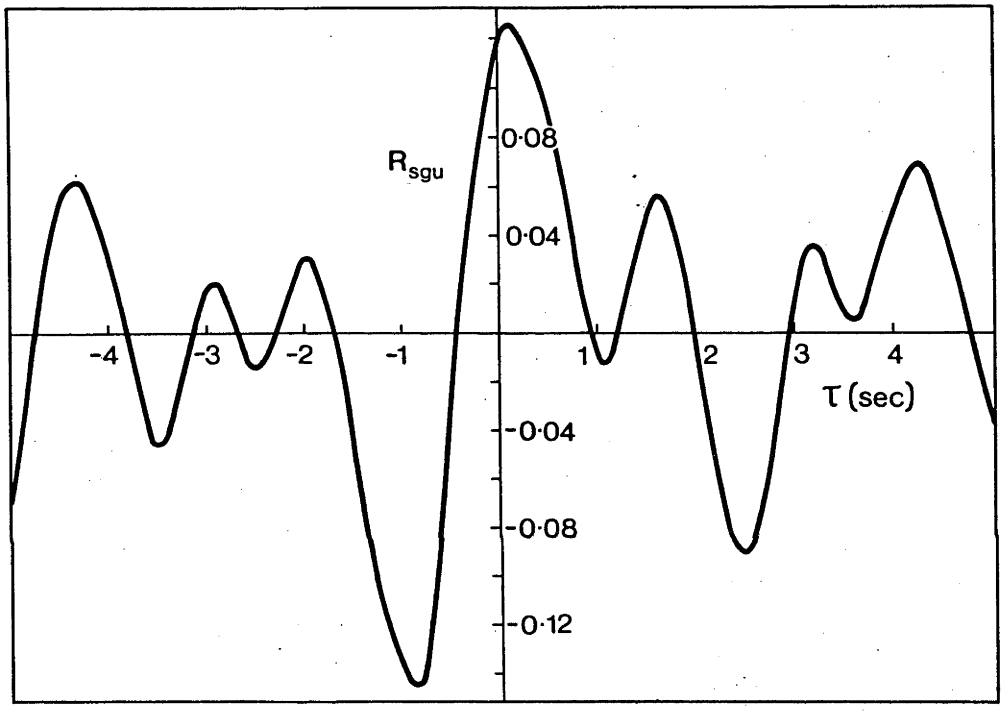

Fig. 17. Strain gauge output - velocity correlation, R_{sgu}, from R5; z = 1.2 m.

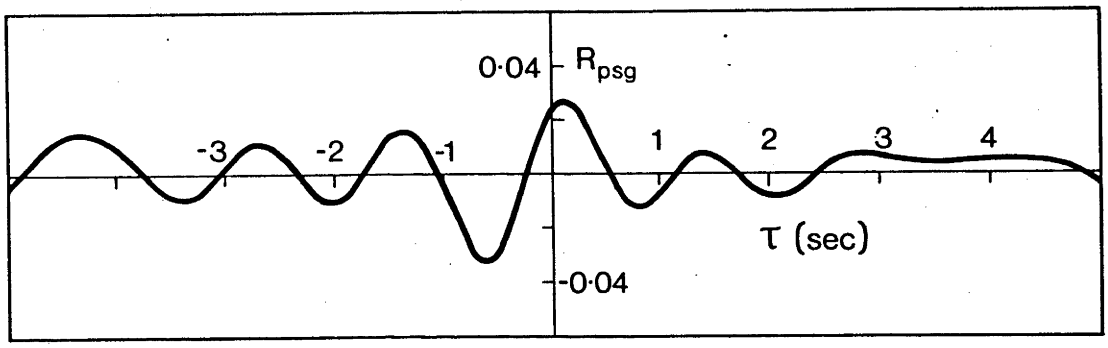

Fig. 18. Pressure - strain gauge correlation, R_{psg}, from R5; z = 1.2 m.

Decomposing the contributions to Reynolds stress into four quadrants and a 'hole' region, after the manner of Lu and Willmarth (1973), enabled the relative importance of different aspects of the velocity field in momentum transfer to be assessed. Above the canopy, the contribution of gusts or sweeps was predominant, while within the middle regions of the crop, outward interactions became almost as large, the resultant shear stress being the difference of the two. This result is assumed to be caused by the wavelike particle path superimposed upon the turbulent fluid by waving stalks in the aftermath of a gust. Above the canopy, bursts appeared to gain in importance and the relative magnitudes of the four quadrants appeared to approach the situation observed in a rough wall channel flow by Nakagawa and Nezu (1977). The only comparable results in the atmosphere, those of Weiss and Allen (1976) over vine rows, confirm the predominance of gusts in momentum transfer close to the surface.

Space-time correlations of u_R and u(z) allowed a definite vertical propagation velocity of maximum correlation to be derived. This velocity decreased as the lower wire entered the canopy, suggesting a progressive deceleration of the large eddies which are assumed to be responsible for the R_{uu_R} as they interact with the canopy. It is perhaps superfluous to point out here, in view of the other evidence for the presence of the large eddies, that the rate of vertical propagation of a shear wave, which is propagated by eddy diffusion with an eddy diffusivity, ε, given by $-\overline{uw} = \varepsilon \partial U/\partial z$, can be calculated using the model of Tan and Ling (1961). The time delay derived from their calculation for the 2 m separation is 2.88 s, more than twice the observed time lag.

It was realized that the long averaging period, 150 s, of the velocity correlations would obscure any intermittent features of the flow which might have a high correlation over a shorter time but which would be cancelled out by their random phase relationships in the course of a long average. Accordingly, successive short period space-time correlations were formed with time delays of ± 5 s in a ten second interval. Many of these short time averages were observed to be periodic in time delay at the waving frequency or the average frequency of gust arrival. It can be shown that a short time average of the form defined in equation (3) is a sensitive test of intervals when the two signals being correlated are periodic with the same frequency. It could be shown by counting the ten second intervals when a certain frequency dominated the correlation, that for run R2, during 40% of the time, gusts were present in periodic trains penetrating the whole canopy and that velocity fluctuations caused directly by stalk waving were sensed by both wires for about 20% of the time when the lower wire was at the bottom of the canopy but for 40% of the time it was in the upper layers.

The pressure-velocity correlation, R_{pu}, has a strongly periodic appearance despite the long time average. The pressure fluctuations at the ground surface are apparently caused by the velocity fluctuations at the top of the canopy, and the coherent nature of the wavelike velocity fluctuations is assumed to account for a value of $(\overline{p^2})^{\frac{1}{2}}/\rho u_*^2$, about 4 times that observed in other rough wall boundary layers.

Acknowledgements.

The author thanks Dr E.F. Bradley, Dr A.R.G. Lang, and Dr C.J. Barnes of this laboratory for much helpful discussion and particularly Dr P.J. Mulhearn of the Royal Australian Naval Research Laboratory, Sydney, whose enthusiasm and guidance made this work possible.

References

Allen, L.H. Jr.: 1968, 'Turbulence and Wind Speed Spectra within a Japanese Larch Plantation', J. Appl. Meteorol. 7, 73-78.

Brown, G.L. and Thomas, A.S.W.: 1976, Large Structure in a Turbulent Boundary Layer, Univ. of Adelaide, Dept. of Mech. Eng. Report TN16/76.

Burton, T.E.: 1971, On the Generation of Wall Pressure Fluctuations for Turbulent Boundary Layers over Rough Walls, Acoustics and Vibration Lab. Report No. 70208-4, Massachusetts Institute of Technology.

Corrsin, S.: 1974, 'Limitations of Gradient Transport Models in Random Walks and Turbulence', Adv. Geophys. 18A, 25-59.

Cowan, I.R.: 1968, 'Mass, Heat and Momentum Exchange between Stands of Plants and their Atmospheric Environment', Quart. J. Roy. Meteorol. Soc. 94, 523-544.

Dorman, C.E. and Mollo-Christensen, E.: 1973, 'Observation of the Structure on Moving Gust Patterns over a Water Surface ("Cat's Paws")', J. Phys. Oceanogr. 3, 120-132.

Finnigan, J.J.: 1978, 'Turbulence in Waving Wheat. I. Mean Statistics and Honami', Boundary-Layer Meteorol. (submitted for publication).

Grass, A.J.: 1971, 'Structural Features of Turbulent Flow over Smooth and Rough Boundaries', J. Fluid Mech. 50, 233-255.

Hoerner, S.F.: 1965, Fluid-dynamic Drag, published by the author.

Inoue, K., Uchijima, Z., Horie, T. and Iwakiri, S.: 1975, 'Studies of Energy and Gas Exchange within Crop Canopies. (10) Structure of Turbulence in Rice Crop', J. Agric. Meteorol. (Japan) 31, 71-82.

Isobe, S.: 1972, 'A Spectral Analysis of Turbulence in a Corn Canopy', Bull. Nat. Inst. Agric. Sci. (Japan) Ser. A, No. 19, 101-112.

Laufer, J.: 1972, 'Recent Developments in Turbulent Boundary Layer Research', 1st Naz. Alta Mat., Symp. Math. 9, 299.

Lu, S.S. and Willmarth, W.W.: 1973, 'Measurements of the Structure of the Reynolds Stress in a Turbulent Boundary Layer', J. Fluid Mech. 60, 481-511.

Maki, T.: 1975a, 'Interrelationships between Zero-plane Displacement, Aerodynamic Roughness Length and Plant Canopy Height', J. Agric. Meteorol. (Japan) 31, 7-15.

Maki, T.: 1975b, 'Wind Profile Parameters of Various Canopies as Influenced by Wind Velocity and Stability', J. Agric. Meteorol. (Japan) 31, 61-70.

Mulhearn, P.J.: 1975, 'On the Structure of Pressure Fluctuations in Turbulent Shear Flow', J. Fluid Mech. 71, 801-813.

Nakagawa, H. and Nezu, I.: 1977, 'Prediction of the Contributions to the Reynolds Stress from Bursting Events in Open Channel Flows', J. Fluid Mech. 80, 99-128.

Seginer, I. and Mulhearn, P.J.: 1978, 'A Note on Vertical Coherence of Streamwise Turbulence inside and above a Model Plant Canopy', Boundary-Layer Meteorol., in press.

Shaw, R.H.: 1977, 'Secondary Wind Speed Maxima Inside Plant Canopies', J. Appl. Meteorol. 16, 514-521.

Tan, H.S. and Ling, S.C.: 1961, A Study of Atmospheric Turbulence and Canopy Flow, Therm Advanced Research Division, Report No. TAR-TR 611, Ithaca, New York.

Thom, A.S.: 1972, 'Momentum, Mass and Heat Exchange of Vegetation', Quart. J. Roy. Meteorol. Soc. 98, 124-134.

Townsend, A.A.: 1976, The Structure of Turbulent Shear Flow. Cambridge Univ. Press.

Weiss, A. and Allen, L.H. Jr.: 1976, 'The Flux-angle Distribution of Momentum as Determined from Propellor Anemometer Measurements', Quart. J. Roy. Meteorol. Soc. 102, 775-779.

Willmarth, W.W.: 1975, 'Structure of Turbulence in Boundary Layers', in Yih, C.-S. (ed.), Advances in Applied Mechanics, Vol. 15, Academic Press, New York, pp. 159-254.

CHAPTER 4

MODELLING WAVING CROPS IN A WIND TUNNEL

J.J. FINNIGAN and P.J. MULHEARN

This paper was published in Boundary-Layer Meteorology, volume 14, pp. 253-277 (1978).

Abstract. Analysis of movie films of a field of barley, combined with observations of the motions of individual plants, show that single stalks oscillate at a well-defined natural frequency even when stimulated by turbulent winds. Treating single stalks as resonant cantilevers allows the use of standard engineering methods to determine their elastic properties. Armed with these values, the application of similarity analysis to the equation of motion of a single stalk leads to criteria for aeroelastic modelling of wheat plants in the wind tunnel. A representative value for the spacing of stalks in a small section of model wheat field was calculated by referring to published data on momentum absorption in a variety of real and model canopies. Preliminary measurements of first and second moments of velocity in the model appear to confirm the importance of including elastic properties in wind-tunnel simulations of airflow in flexible crops.

SYMBOLS

t	time
x	length co-ordinate measured along stalks from base to ear
y	deflection of stalk normal to x co-ordinate
$\hat{y}$	amplitude of stalk vibration
ω	radian frequency of stalk vibration
f	circular frequency
L	stalk length or canopy height
d	stalk diameter
F	force applied to deflect stalk
m	mass/unit length of wheat stalk
M	mass of ear
$\delta(x)$	width of plant or model stalk
c	viscous damping coefficient of stalk
$\tilde{u}$	streamwise horizontal velocity
$\tilde{w}$	vertical velocity
U	time mean streamwise velocity
W	time mean vertical velocity
u	$\tilde{u} - U$
w	$\tilde{w} - W$
U_L	value of U at z = L, the top of the canopy
a	projected area/unit volume of canopy elements
ρ	air density
p'	fluctuating static pressure
i_u, i_w	turbulence intensity
$U*$	friction velocity

τ_w	surface shear stress
z_o	roughness length
D	zero plane displacement
κ	Von Karman's constant (= 0.41)
ν	kinematic viscosity
C	dimensionless drag coefficient
T	time scale
$S_{uu}(f)$	power spectrum of horizontal velocity vector
$S_s(f)$	power spectrum of stalk bending
Φ_{uu}	power spectrum of u component of velocity
Φ_{ww}	power spectrum of w component of velocity
Φ_{uw}	cross spectrum of u and w
θ	phase velocity of Honami waves
θ_n	eigenvalues of stalk waving equation

1. Introduction

The advantages of modelling atmospheric airflows in wind tunnels are many, and much effort has been devoted to this facet of micrometeorology. Canopy flows in particular have received a great deal of attention because of the peculiar difficulties involved in making accurate measurements of fluctuating velocities among real plants. The normal laboratory tool for studies of turbulent flow is the hot-wire anemometer, a particularly fragile instrument, and consequently most field work has relied upon cruder tools such as Hastings heated-thermocouple anemometers, which cannot separate the orthogonal components of the wind vector. Recent experiments by Shaw et al. (1974), however, using a split-film anemometer, indicate the kind of instrumentation necessary to obtain more detailed results.

Measurements among stylized canopies of rods and pegs, by, for instance, Thom (1971) and Kawatani and Meroney (1970), have provided information about the characteristic mean velocity profile of canopy flow, and the dependence of such parameters as turbulence intensity upon plant spacing. A more recent detailed study by Seginer et al. (1976) attempted to separate the effects of turbulence generated by the model stalks alone from that characteristic of the total flow. Higher moments of velocity fluctuations were also measured, providing more insight into the detailed structure of canopy turbulence.

To date, however, no one has attempted to include the elastic properties of real plants in their simulations. Arrays of rigid cylinders are normally employed, or, on the rare occasions when the model elements are flexible, such as in the work of Ito (1968) and

Meroney (1968), the flexural characteristics of the elements are quite arbitrary. This could be an important oversight, particularly in the case of flexible cereal crops, such as wheat, rice, and barley, whose waving in strong winds is such a striking phenomenon.

To illustrate this we can write the drag force per unit length upon a waving wheat plant as

$$F = \tfrac{1}{2}\rho\, C\delta(x)\left(\tilde{u} - \frac{dy}{dt}\right) \left| \tilde{u} - \frac{dy}{dt} \right|$$

where ρ is air density, C is the dimensionless drag coefficient, $\delta(x)$ is the width of the plant intercepting the air flow at a station x measured along the stalk and includes contributions from ear, leaves and stalk, $\tilde{u}$ is the instantaneous wind speed, and y is the displacement of the stalk from its mean position.

Making the simplifying (and in general untrue) assumption that $\tilde{u} - \frac{dy}{dt} > 0$ at all times, we can expand the expression above and take its time average to obtain the time mean expression for the drag force per unit length

$$\overline{F} = \tfrac{1}{2}\rho\, C\delta(x)\left[U^2 + \overline{u^2} + \overline{\left(\frac{dy}{dt}\right)}^2 - 2u\,\overline{\frac{dy}{dt}}\right]$$

where $\tilde{u}$ has been split up into its mean and fluctuating parts, U and u respectively.

Assuming a longitudinal turbulent intensity, i_u, of 0.4 within the canopy where $i_u = \sqrt{\frac{\overline{u^2}}{U}}$, and an amplitude of stalk waving equal to one half the stalk height, other values being defined in Table I, the sizes of the contributions to the time-mean drag at the top of the canopy can be estimated as: $U^2 \sim 16\ m^2\ s^{-2}$; $\overline{u^2} \sim 2.56\ m^2\ s^{-2}$; $\overline{\left(\frac{dy}{dt}\right)}^2 \sim 1.2\ m^2\ s^{-2}$; $2u\,\overline{\frac{dy}{dt}} \sim 3.5\ m^2\ s^{-2}$. Using this very crude procedure, which assumes perfect correlation between the fluctuating quantities, the orders of

magnitude of the terms dependent upon stalk waving are seen to be comparable to other terms in the expression for mean drag, and given the large scale and coherent nature of canopy waving, we might expect its effect on the diffusion of momentum and scalar quantities to be pronounced.

In the following sections we will discuss the various observations and measurements of the properties of waving plants which form a basis for dynamic modelling. Criteria will be derived for preserving the elastic behaviour of single stalks in a wind-tunnel model and empirical results used to calculate the density of elements in such a model canopy. Finally, some preliminary results from a small model wheat field will be discussed.

2. Honami and Waving Plants

One of the most striking examples of the interaction between the atmospheric boundary layer and the air flow within a plant canopy is the phenomenon of Honami. This word, coined by Inoue (1955), describes the regular, ocean-like waves which appear in cereal canopies on windy days. To investigate Honami, the authors took 8 mm movie films of a field of 80-cm high green barley, under windy conditions. The waving plants were filmed at 54 frames/sec and the film was played back at a lower speed for analysis. The resonant frequencies of individual plants and the mean wind speed at the top of the canopy were also measured.

Upon analysis the field was seen to be divided into patches of coherent waving, elongated downstream with abrupt and arbitrary phase differences between adjacent patches. Within patches individual plants vibrated at a fixed frequency, but a small but smoothly varying phase difference between adjacent plants gave the impression of waves moving through the canopy. The individual patches were roughly 20 stalk heights in downwind extent by about 5 stalk heights crosswind (16 m × 5 m) and retained their identity for about 5 seconds on average. The wavelength of the Honami waves was of the order of 8 m, so about three distinct crests would be seen in any patch. During the passage of waves, individual stalks vibrated at the same frequency as when deflected and allowed to oscillate in isolation. For the stalks tested this was 0.68 ± 0.04 Hz.

The distribution of phase velocity of the waves, θ, (that is, the passage velocity of wave crests in a patch of coherent waving) is

shown in Figure 1 for a 70 second period when the mean velocity at the top of the canopy was 1.6 m/s. The average phase velocity is 8 m/s but the measured points show a considerable spread. Since the frequency with which crests pass a point in space is determined by the frequency of vibration of individual stalks - a frequency we observed to be fixed at the resonant value independent of phase velocity - then the distribution of phase velocity in Figure 1 implies a complementary distribution of wavelengths.

The large phase velocities suggest that Honami waves are records of the passage of gusts of air with high streamwise momentum which sweep down to the surface from an outer part of the boundary layer, bending over a succession of stalks in their downwind passage. These then spring back and vibrate with a streamwise phase difference. Downsweeps of this kind have been observed by Grass (1971) in a rough wall turbulent boundary layer and by Nakagawa and Nezu (1977) in a rough walled channel. Honami waves appear to be analogous to 'catspaws' on open water with the additional property of the plants' elasticity conferring persistence and regularity on the waves.

Results presented by Schwerdtfeger et al. (1975) of measurements in barley and ryecorn permit a similar interpretation.

To investigate in greater detail the proposition that individual stalks behave as resonant cantilevers when forced by a random wind, the following simple experiment was performed. Two strain gauges (Philips PR 9833K/01) were cemented close to the base of a single tiller of a wheat plant (Triticum aestivum L. em. Fiori et Parl cv. Gabo 3), growing in a plant pot. This was placed on short grass amongst widely spaced small trees and bushes on a windy day and about 12 other similar

pot grown wheat plants arranged around it. The mean horizontal velocity of the wind at the height of the ear was 2 m/s and the turbulence intensity was 15%. A DISA hot-film anemometer probe (type 55A81) was mounted vertically at the height of the ears and connected to a DISA constant temperature bridge (type 55D01). The strain gauge output, which was proportional to the stalk bending and therefore the deflection of the ear, and the hot film output, linearized on an EAI TR20 analogue computer, were recorded on an analogue tape recorder (Hewlett Packard type 3955). The experimental set up is detailed in Figure 2. The two records were later digitized and processed on the CSIRO CYBER 76 computer to obtain power spectra of velocity and stalk deflection. These are plotted in Figure 3. The vertical scales have been adjusted so that the curves are directly comparable.

Although the spectral function of velocity, $S_{uu}(f)$, falls away steadily with increasing frequency, f, the spectrum of stalk deflection $S_s(f)$, shows a strong peak at 2 Hz, the fundamental resonant frequency of the strain-gauged stalk, after which it falls away much more rapidly. A second peak at 13 Hz is probably associated with the second harmonic but it is insignificant compared with the main peak. The results of this rather artificial set up have now been confirmed by strain gauge measurements on stalks in a real wheat canopy. These later results will be published separately.

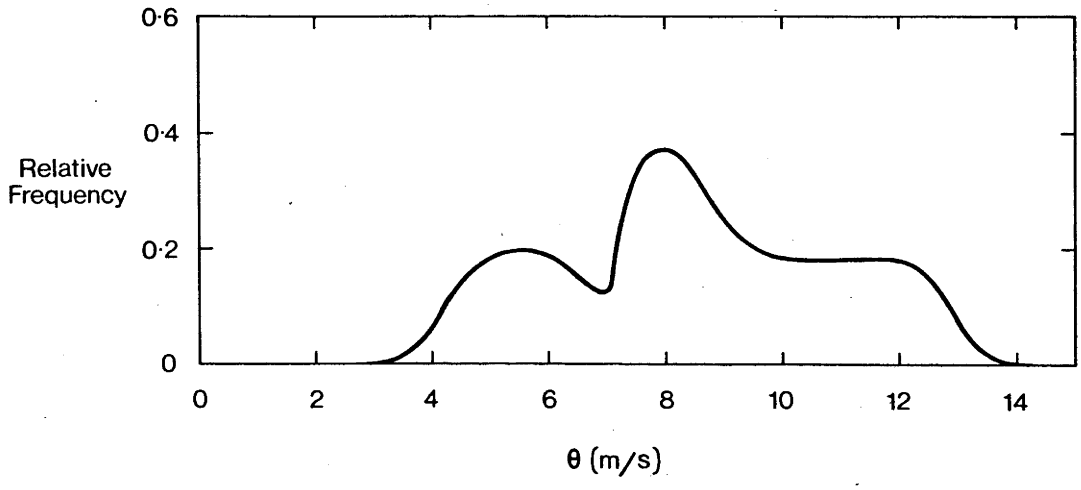

Fig. 1. Frequency distribution of Honami-wave phase velocities.

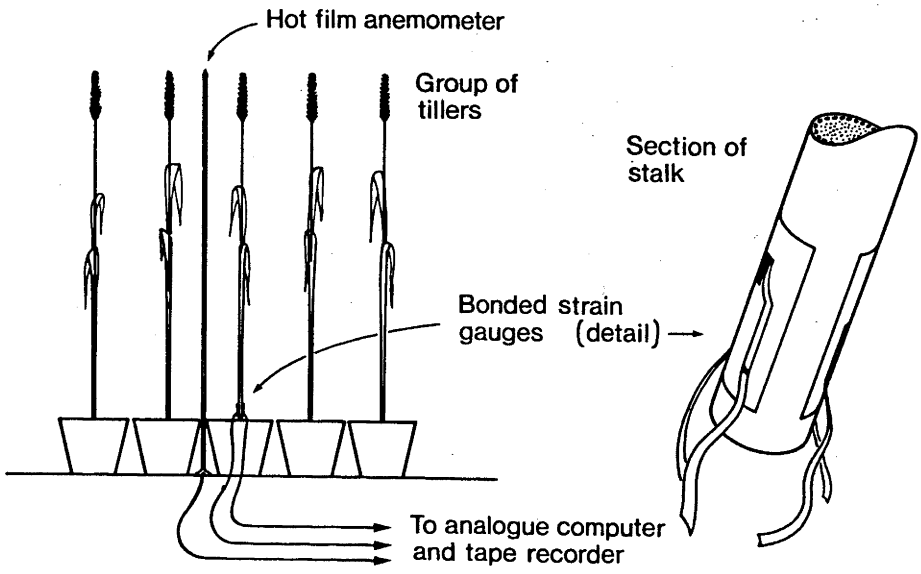

Fig. 2. Experimental arrangement of strain gauged wheat stalk.

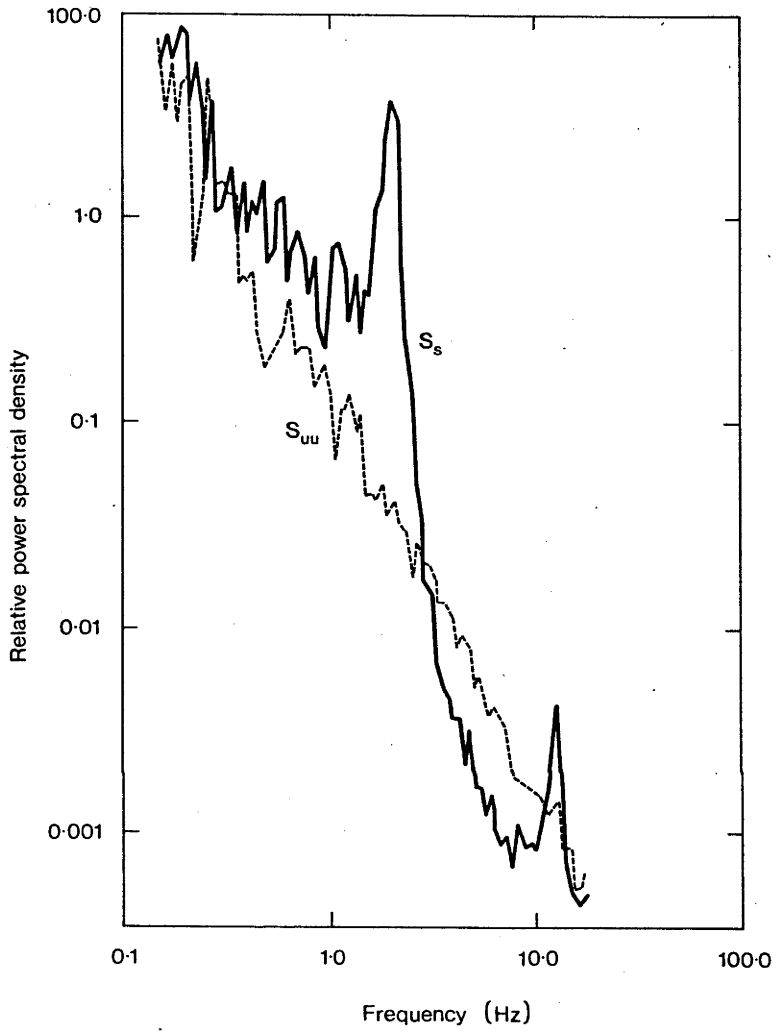

Fig. 3. Spectra of strain gauge output and wind speed.

3. Mechanical Properties of Wheat Stalks

In order to determine the physical constants which define the dynamic properties of single stalks, tests were carried out on a sample of twelve wheat tillers grown in an artificial environment and upon ten stalks of wheat grown under natural conditions. The same strain of wheat was used as in the strain gauge experiments, but we believe that the results obtained will be applicable to cereal crops in general. The measurements on the artificially grown sample were carried out on young green plants with a water content of 78% by weight in the stalks and 45% in the ears. The naturally grown plants were measured just before harvesting and contained only 10% of water in the stalks and 8% in the ears.

If the deflection of the stalk for a given horizontal load is measured, then its flexural rigidity or stiffness, J, is given by the small deflection theory of beams as:

$$J = \frac{FL^3}{3y_L} , \qquad (1)$$

where y_L is the stalk deflection at $x = L$, x being measured along the stalk. F is the force applied normally at $x = L$ to deflect the stalk.

The expression above neglects the effect of the distributed mass of the stalk compared to the applied force. The formula also assumes that the flexural rigidity, J, is a constant along the stalk and we are therefore measuring a kind of average value where the details of stalk structure are smoothed out.

The flexural rigidity for the two samples differed by over an order of magnitude, being 7.6×10^{-3} Nm^2 for the green plants and 13.8×10^{-2} Nm^2 for the dry sample. The natural frequency of isolated stalks,

however, varied much less, from 4.4 radians/sec for the green stalks to 6.1 radians/sec for the dry stalks, the increase in stiffness being largely offset by increased stalk length and mass of the ear as the plants grew.

We can express the internal viscous damping of the stalk as a force proportional to the stalk velocity, and we define the damping coefficient, c, in the following expression

$$y_L = \hat{y}_L \exp(-\frac{c}{2m} t)\cos\omega t \qquad (2)$$

where m is the mass per unit length of the stalk, $\hat{y}_L$ is the undamped amplitude of vibration, and t is time. Despite the complex internal structure of real stalks, curves of normalized maximum amplitude y_L/L, of the damped vibration against time, obtained by photographing the oscillating stalk, show an excellent agreement with equation (2). The curves for two artificially grown stalks are presented in Figure 4. When the ears and leaves of the test specimens were removed and a small lead weight, of equal mass but much smaller aerodynamic drag than the ear and flag leaf, was attached to the tip, the damping coefficient was reduced by only 6%. At certain stages of growth of a dense canopy, however, most of the damping may well be caused by the mutual interference of adjacent plant leaves. In a real canopy, this will have the effect of further reducing the variation of waving frequency as the older, stiffer stalks, with a potentially higher frequency, will also have more entangling leaf growth and a higher apparent damping coefficient.

Values of flexural rigidity, damping coefficient, natural frequency, and mass of ear and stalk and other relevant dimensions have been obtained by averaging the two groups of measurements. These are set out in Table I.

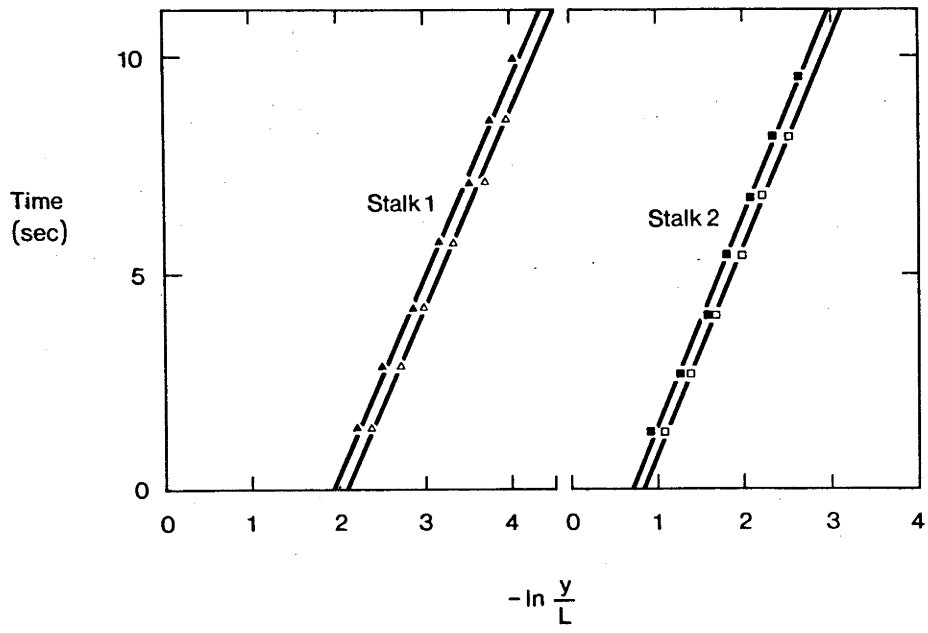

Fig. 4. Examples of viscous damping curves for two wheat stalks.

TABLE I

The numerical values of parameters used in section 4 are set out here. Those constants which define the dynamic behaviour of single wheat stalks are the results of a series of measurements on plants of the strain Triticum aestivum L. em. Fiori et Parl, cv. Gabo 3, which were grown in the CSIRO phytotron, 'CERES' and at the Ginninderra experimental farm.

Parameter	Meaning	Value
A. Prototype wheat stalk		
U_L	Mean velocity at crop height, L	4 m s^{-1}
L	Length of wheat stalk or canopy height	0.7 m
M	Mass of ear	2.31×10^{-3} kg
m	Mass/unit length of stalk.	5.07×10^{-3} kg m^{-1}
J	Flexural rigidity	$6.9 \times 10^{-2} \pm 5\%$ Nm^2
g	Acceleration due to gravity	9.81 m s^{-2}
ω	Natural frequency of wheat stalk	4.4 radians sec^{-1}
c	Damping coefficient	2.4×10^{-2} kg m^{-1} sec^{-1}
δ	Aerodynamic width of wheat plant	3×10^{-2} m
C	Dimensionless drag coefficient	0.5
B. Nylon model stalks		
m	Mass/unit length of stalks	7.03×10^{-5} kg m^{-2}
J	Flexural rigidity	1.6×10^{-6} N m^2
d	Stalk diameter	0.25×10^{-3} m
L	Stalk length	5×10^{-2} m
c	Damping coefficient	2.46×10^{4} kg m^{-1} sec^{-1}
ω	Natural frequency of model stalk	220.0 radians sec^{-1}

4. Criteria for an Aeroelastic Model

Following the previous section, we can characterize a waving wheat stalk as an elastic cantilever, carrying at its tip the mass of the ear and flag leaf, experiencing internal viscous damping and excited by an aerodynamic force as the wind in the canopy is intercepted by the ear, leaves and stalk. With the neglect of rotary inertia and transverse shear deformation, the equation of motion of such a structure can be written as

$$J\frac{\partial^4 y}{\partial x^2} + m\frac{\partial^2 y}{\partial t^2} + c\frac{\partial y}{\partial t} + mg\frac{\partial y}{\partial x} = \tfrac{1}{2}\rho\, C\, \delta(x)\left(\tilde{u} - \frac{\partial y}{\partial t}\right)\left|\tilde{u} - \frac{\partial y}{\partial t}\right| \qquad (3)$$

where x is the distance along the stalk, measured in a positive direction from the root, y is the displacement of the stalk from its vertical mean position, c is the viscous damping coefficient, m is the mass per unit length of the stalk, g is the acceleration due to gravity, C is the dimensionless drag coefficient of the plant, $\delta(x)$ represents the effective 'width' of the plant at any x as it intercepts the airflow, and $\tilde{u}$ is the instantaneous streamwise velocity. For convenience J, the flexural rigidity, is assumed to be constant along the stalk.

To complete Equation (3) we must add appropriate boundary conditions to take account of the cantilever root mounting and the mass of the ear plus flag leaf, M. The effect of the concentrated masses of the other leaves has been ignored as reference to Table II shows that their effect is not significant.

Rewriting Equation (3) in dimensionless form we obtain

$$\frac{d^4\eta}{d\xi^4} + \left[\frac{mL^4}{JT^2}\right]\frac{\partial^2\eta}{\partial t'^2} + \left[\frac{cL^4}{JT}\right]\frac{\partial\eta}{\partial t'} + \left[\frac{mgL^3}{J}\right]\frac{\partial\eta}{\partial\xi} = \left[\tfrac{1}{2}\rho\,\frac{C\,L^5\delta}{JT^2}\right]\left(\left[\frac{UT}{L}\right]u' - \frac{\partial\eta}{\partial t'}\right)^2 \qquad (4)$$

TABLE II

Average values of masses and mass moments from a sample of tillers of Gabo 3.

	Weight of component as a percentage of total plant weight	Mass moment about base of stem as % of moment of ear plus stalk alone
Flag leaf	8	7
Next leaf	6.5	4
Stalk	48.0	35
Ear	37.5	54

where $\eta = y/L$; L is the length of the stalk

$\xi = x/L$

$t' = t/T$; T is some time scale

$u' = \tilde{u}/U_L$; U_L is the mean streamwise velocity at the height of the ear.

The boundary condition at the tip now involves M/mL.

When the right hand side of Equation (4) is set equal to 0, we have an equation describing the unforced vibration of the cantilever. Its motion, $\eta(\xi,t')$, can be represented as the superposition of a series of dimensionless deflected shapes or 'modes' of vibration, $\eta_n(\xi)$, each with its associated frequency. The frequencies are defined by the values of θ_n where $\theta_n^4 = \frac{mL^4\omega_n^2}{J}$. ω_n is the frequency of the nth mode of vibration and the sequence $\theta_{1,2 \ldots n}$ is defined by the boundary conditions. The form of the corresponding mode of vibration is found by substituting the appropriate θ_n into the solution of Equation (4) which takes the form $\eta_n(\xi) = \text{Function } (\theta_n,\xi)$.

Under the influence of a distributed force, the motion can still be represented as the superposition of the same modes and frequencies, but their relative magnitudes now depend upon the frequency and distribution of the imposed force. In particular, if the applied force depends on the stalk motion, as is the case for damping or aerodynamic drag, then the response of one mode depends upon the interaction of all other modes with the force.

If all of the dimensionless coefficients of Equation (4) and the boundary condition M/mL are kept constant between the prototype and model, the dimensionless deflection of the stalk, $\eta(\xi,t')$, will be faithfully reproduced. Unfortunately with the reduction in scale necessary for most wind tunnel tests, exact similarity of geometry and mass distribution is a practical impossibility. In most cases we would wish to replace the complex real plants by uniform cantilevers.

Changing the mass distribution or boundary conditions between prototype and model means in general that none of the mode shapes and only one frequency can be correctly scaled. For the particular case of interest where a weighted cantilever is replaced by a uniform unweighted one, their frequencies in a chosen mode can be made to correspond by adjusting the mass per unit length of the uniform cantilever (or its length or flexural rigidity) but the shapes of the matched modes will differ in detail and the other modes and frequencies will bear different relationships to the matched pair for each cantilever. This is illustrated in Figure 5, where the first three mode shapes of the stylized wheat stalk defined in Table I are drawn, together with those for a uniform cantilever whose mass per unit length has been adjusted so that its fundamental frequency corresponds to the weighted stalk.

Faced with the problem of matching only one frequency between prototype and model, the details of the interaction between the plant and the aerodynamic force must be taken into account. In the case of waving wheat stalks it is apparent from Figure 3 and from measurements made by Finnigan in a wheat canopy (Chapters 2 and 3) that both the stalk's motion and its interaction with the wind are predominantly in the fundamental mode. This may not be true for all canopies however. Waving of trees in a conifer plantation, for instance, is probably a result of excitation in higher harmonic modes as well.

If the geometry of the individual plants and their spacing in the canopy were accurately scaled, and the Reynolds number of the flow around them reproduced, similarity of the airflow would ensure correctly scaled aerodynamic forces on the model. Unfortunately this is impossible and we

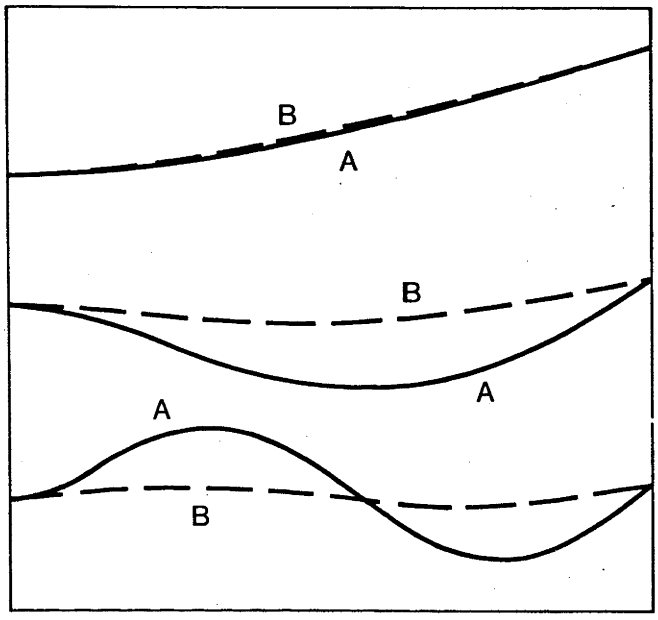

Fig. 5. Dimensionless modes of vibration and associated frequencies for two cantilevers A and B, which have the same fundamental vibrational frequency.

A: Tip mass = 2.31×10^{-3} kg; Mass/unit length = 5.07×10^{-3} kg m^{-1}.

B: Tip mass = 0; Mass/unit length = 18.6×10^{-3} kg m^{-1}.

A corresponds to the prototype wheat stalk.

try instead to model the overall aerodynamic force by adjusting C and δ. At the Reynolds number based on δ, $\frac{U_L \delta}{\nu}$ (where ν is the kinematic viscosity of air), appropriate to atmospheric conditions, to a good approximation C does not vary with velocity although it is quite sensitive to stalk spacing, r (Seginer et al., 1976). In reproducing the features of a fully turbulent atmospheric boundary layer we automatically ensure that the flow around individual roughness elements is fully turbulent and the drag coefficients of prototype and model will be equal. For uniform cantilevers, δ_{model} is the cross stream width or, in the case of a circular cylinder, the diameter.

Within a reasonably dense canopy, mean streamwise velocity increases rapidly with height, usually following an approximately exponential curve. In a wheat crop where Honami was taking place, Denmead and Bradley (1973) observed a profile of the form

$$U = U_L \exp\left[-2.6\left(1 - \frac{z}{L}\right)\right] \qquad (5)$$

where U_L is velocity at height L, the top of the canopy, and z is the vertical co-ordinate measured up from the ground surface.

Assuming this profile and taking into account the areas of ear, flag leaf, and stalk we can write

$$F(90 - 100) \; : \; F(80 - 90) \; : \; F(70 - 80) \equiv 1.0 \; : .198 \; : \; .110,$$

where F(90 - 100) is the aerodynamic force on the top 10% of the plant, and so on.

In the case of wheat, then, it seems reasonable to take a value of δ corresponding to the net width of ear and flag leaf as representative of the whole plant. In mature wheat canopies the leaf area index is approximately constant with height in the upper two thirds of the canopy so this will not be a bad approximation.

Since we are matching modes of vibration, the time scale T in Equation (4) becomes $\frac{1}{\omega}$ where ω is the frequency of the matched mode, in the present case the fundamental. Substituting $T = \frac{1}{\omega}$ into Equation (4) we obtain

$$\underset{D1}{\phantom{\left[\frac{mL^4\omega^2}{J}\right]}} \quad \underset{D2}{\phantom{\left[\frac{mL^4\omega^2}{J}\right]}} \quad \underset{D3}{\phantom{\left[\frac{mL^4\omega^2}{J}\right]}} \quad \underset{D4}{\phantom{\left[\frac{mL^4\omega^2}{J}\right]}}$$

$$[1] \quad \frac{\partial^4\eta}{\partial\xi^4} + \left[\frac{mL^4\omega^2}{J}\right]\frac{\partial^2\eta}{\partial t'^2} + \left[\frac{cL^4\omega}{J}\right]\frac{\partial\eta}{\partial t'} + \left[\frac{mgL^3}{J}\right]\frac{\partial\eta}{\partial\xi}$$

$$\underset{D5}{\phantom{\left[\frac{C L^5\delta^4\omega^2}{J}\right]}} \quad \underset{D6}{\phantom{\left[\frac{U_L}{L\omega}\right]}}$$

$$= \left[\tfrac{1}{2}\rho\,\frac{C\,L^5\delta^4\omega^2}{J}\right]\left(\left[\frac{U_L}{L\omega}\right]u' - \frac{\partial\eta}{\partial t'}\right)^2 \qquad (6)$$

The actual magnitudes of the dimensionless coefficients to the wheat stalk defined by the values of Table I are:

D1	D2	D3	D4	D5 x $D6^2$
1.0	1.32	0.53	0.96	0.639

(In calculating these values we have scaled x by L but y by L/2 since this would normally be an upper limit on stalk deflection.)

All of the terms in Equation (6) appear to be of the same order of magnitude and it is instructive to consider the dimensionless coefficients individually.

D2 $\left[\frac{mL^4\omega^2}{J}\right]$ As we have already pointed out, the values of D2 are fixed by the forms of the prototype and model cantilevers which determine in each case the sequence $\theta_{1,2\ \ldots\ n}$. If the numerical value of D2 differs very much between the prototype and model, it is worth calculating the relevant mode shapes as we have done in Figure 5 to check that the discrepancy is acceptable.

D3 $\left[\frac{cL^4\omega}{J}\right]$ It is difficult to predict, from engineering data, the internal damping of a model stalk made from an arbitrary material. In

a real canopy, as we have already mentioned, at certain stages of plant growth, much of the damping might come from mutual interference of adjacent leaves and stems rather than from true internal viscous dissipation of energy. The best way to preserve similarity of group D3 is to incorporate some means of adjusting the damping of the stalks empirically. In the model described in section 5, this is achieved by varying the clamping pressure on their bases.

D4 $\left[\frac{mgL^3}{J}\right]$ If the model stalks are to be homogeneous cantilevers, then groups D2 and D4 cannot be satisfied simultaneously. A reduction in scale is automatically compensated for in D2 by an increase in ω but no such effect comes to the rescue of D4. It can be observed, however, that the frequency of vibration of a single stalk held horizontally is at the most 6% greater than the same stalk held vertically. In the first instance, gravitational attraction should not affect the stalk's motion, whereas in the second case it must. We conclude from this that the natural frequency of the stalk is relatively insensitive to D4 and the main effect of gravitational attraction is upon the form of the deflected curve. For the kind of aerodynamic interactions we are interested in modelling, this will be of only secondary importance.

D6 $\left[\frac{U_L}{L\omega}\right]$ The ratio of the velocity scales of the air and the waving motion, often called the reduced frequency, is essentially a geometric condition. Preservation of D6 ensures that the wavelength of Honami waves and canopy height bear the same relation in the real crop and the model.

The problem of modelling individual wheat stalks then is one of making model cantilevers of a material and size such that $\left[\frac{mL^4\omega^2}{J}\right]$ does

not differ too much between the prototype stalk and the uniform model cantilever, ensuring that $\left[\frac{1}{2}\rho \frac{CL^5\delta\omega^2}{J}\right]$ and $\left[\frac{U_L}{L\omega}\right]$ are the same for prototype and model, taking into account the properties of the wind tunnel, and finally providing enough adjustment in the model to preserve $\left[\frac{cL^4\omega}{J}\right]$ unchanged. The general question of aeroelastic modelling of complex structures is dealt with in many texts (for example Bisplinghoff et al., 1957) and the reader is referred to these for more detailed discussion of the problem.

Turning from individual stalks to the properties of the crop as a whole, we wish to reproduce the momentum absorption of the canopy by spacing the model stalks with some particular density. Snyder (1972) suggests that equality of z_o/L is an appropriate boundary condition for the airflow above the canopy, where z_o is the roughness length defined by the logarithmic velocity profile:

$$\frac{U}{U^*} = \frac{1}{\kappa} \ln \left(\frac{z - D}{z_o}\right) \quad . \tag{7}$$

κ is Von Karman's constant (= 0.41); $U^* = \left(\frac{\tau_w}{\rho}\right)^{\frac{1}{2}}$ is the friction velocity, where τ_w is the surface shear stress; D is the height above the ground ($z = 0$) of the origin of the logarithmic profile, and $\ln z_o$ is the intercept at $U = 0$ on the z axis. z_o is usually taken to be a measure of the momentum absorption character of a canopy.

Seginer (1974) has correlated the variation of z_o/L with the drag per unit volume of roughness elements and this provides us with a means of deciding upon an appropriate spacing for the model stalks. He presented the results of eleven workers for various types of rough surface as plots of CaL versus z_o/L (Figure 6), where a is the projected area/unit volume of the roughness elements. The appropriate value of CaL for a desired z_o/L will determine the spacing of the model elements

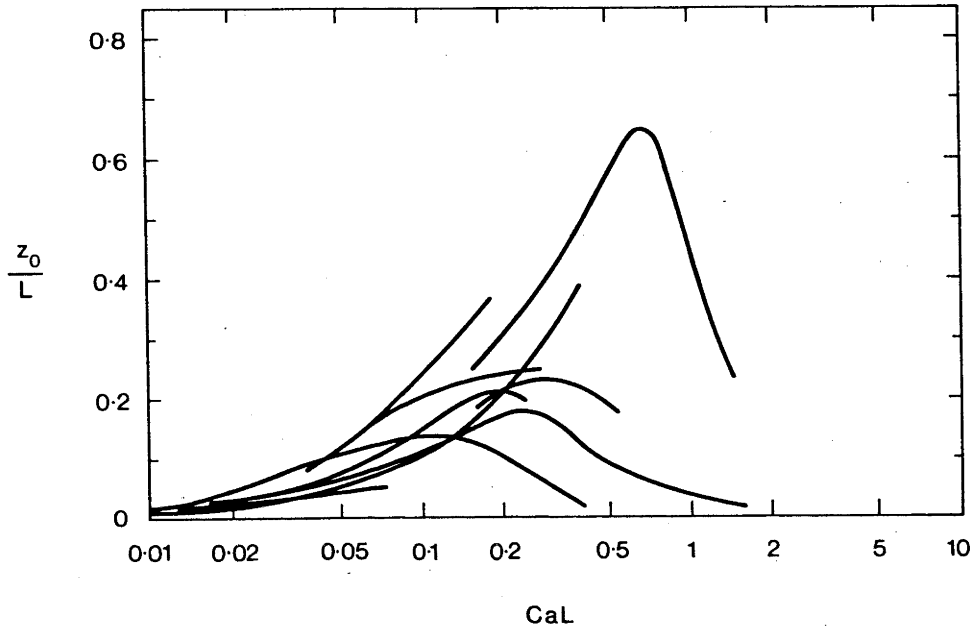

Fig. 6. Curves of CaL versus z_o/L for various rough surfaces (after Seginer, 1974).

although care should be taken since some of the drag coefficients used to obtain Figure 6 are too high, and the whole curve should perhaps be shifted slightly to the left.

At the moment, we have insufficient information to estimate the effect of elasticity on the airflow some distance above the canopy - this is after all one of the main reasons for making an aeroelastic model - but equality of group D6 ensures geometric similarity of the wavy surface which defines the canopy height.

Within a model crop, the Reynolds number of the airflow will commonly be an order of magnitude smaller than in the real world, being approximately $\sim 5 \times 10^2$ rather than $\sim 5 \times 10^3$. Simulation of z_o/L will set a lower limit upon the wind-tunnel speed, however, and ensure that the drag coefficients of real and model stalks are similar. The highly turbulent nature of canopy flow makes this more certain and we can be confident that the real and model within-canopy flows will be qualitatively similar.

The use of z_o/L as a scaling criterion automatically assumes the existence of a logarithmic velocity profile, representative of an equilibrium atmospheric boundary layer, in the wind-tunnel. The general criteria for simulating the atmospheric boundary layer are discussed in detail by Snyder (1972) and will not be pursued further here.

5. Experimental Apparatus and Procedure

A small section of model wheat field 52 cm long by 40 cm wide was constructed to model the prototype defined by the values in Table I. The material chosen for the model stalks was cylindrical, monofilament nylon fishing line. Each stalk was 5 cm long and 0.25 mm in diameter. The ratio of $D5_{model}$ to $D5_{real\ canopy}$ was 0.7, and $D6_{model}$ could be made equal to $D6_{real\ canopy}$ with a wind tunnel speed of 15 m/s.

In the model canopy CaL = CndL, where n is the number of stalks per unit horizontal area. A typical value of z_o/L for wheat is 0.2 and reference to Figure 6 reveals that this corresponds to a CaL of 0.15. With a model stalk height of 5 cm and a stalk diameter of 0.025 cm, CaL = 0.15 when n = 4 stalks/cm^2. Further reference to Seginer (1974) shows that a CaL value of 0.15 corresponds to D/L of 0.6, an acceptable value for wheat.

The stalks were spaced on a square grid of 5 mm side and the clamping pressure on the bases of the stalks varied by adjusting the tension on the threaded steel rods until $D3_{model} = D3_{real\ canopy}$. The damping was measured by photographing the decay of an impulsively started vibration with the aid of a stroboscope as the stalks had a natural frequency of about 30 Hz. The measured damping coefficient was $2.46 \times 10^4 \pm 15\%$ kg m^{-1} sec^{-1}. Details of the model construction are shown in Figure 7. The model was placed in the working section of the CSIRO Division of Environmental Mechanics wind tunnel, an open return circuit tunnel driven by an upstream centrifugal fan. The working section is 12 m long, 0.61 m high, and 1.83 m wide. A full description of the wind tunnel can be found in Mulhearn et al. (1976). A thick turbulent boundary layer was developed in the tunnel by placing 1.2 m of smooth surface followed by 4.28 m of a very rough

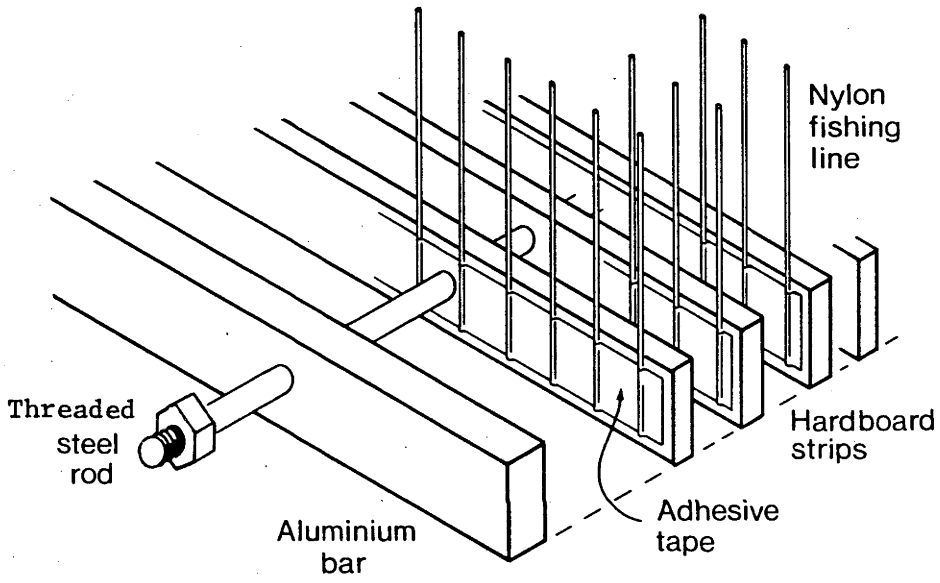

Fig. 7. Method of constructing model wheat crop.

surface upstream of the model canopy. The rough surface was formed by pieces of gravel, whose average diameter was 14 mm, glued in a random pattern to sheets of 1.2 cm thick particle board. The model base was 2.5 cm thick and a ramp section, 10 cm long, was used to fair the rough surface into the model section. The space between the model side and the tunnel walls was filled by more rough surface, level with the bottom of the canopy. The details of the installation of the model are shown in Figures 8 and 9.

Streamwise and vertical components of both mean and fluctuating velocity were measured with a DISA 55P61 X-wire probe connected to two channels of Thermo Systems Inc. Model 1050 hot-wire anemometry. Records were also made of the output of a 12.5 mm diameter microphone (Bruel and Kjaer type 4133 plus type 2615 cathode follower). The microphone was connected to a 3.18 mm diameter hole in the model ground surface via a conical chamber. The hole was on the model centreline, 39 cm from its leading edge (Figure 8). The outputs of both hot wires and the microphone were filtered with Rockland model 1042F four pole filters set to pass frequencies below 100 Hz. The signals were scaled and biased to vary between ± 5 V d.c. on an Electronic Associates Inc. TR20 Analogue Computer and then digitized and recorded on magnetic tape on a Digital Equipment Corp. PDP11/40 computer where all the results were later processed. Calibration of the hot wires for both yaw and velocity was done with the probe on the traverse gear, first raising it into the region of uniform flow which existed above the surface boundary layer.

Profiles of mean and turbulence statistics are presented for vertical traverses of the hot wire at three streamwise stations on the tunnel centreline. The characteristics of the boundary layer upstream

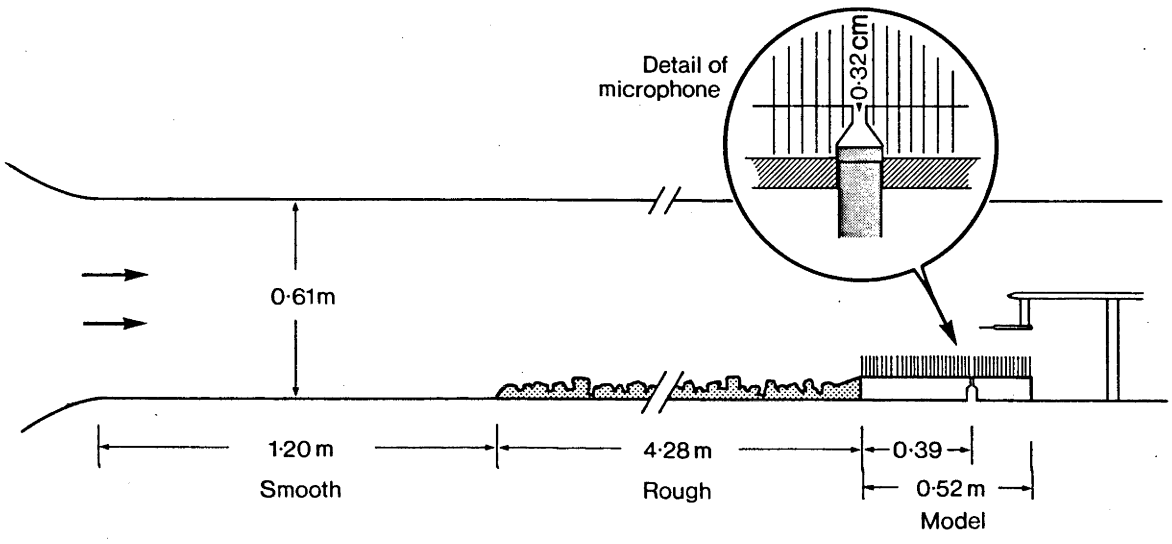

Fig. 8. Arrangement of model wheat field in wind tunnel.

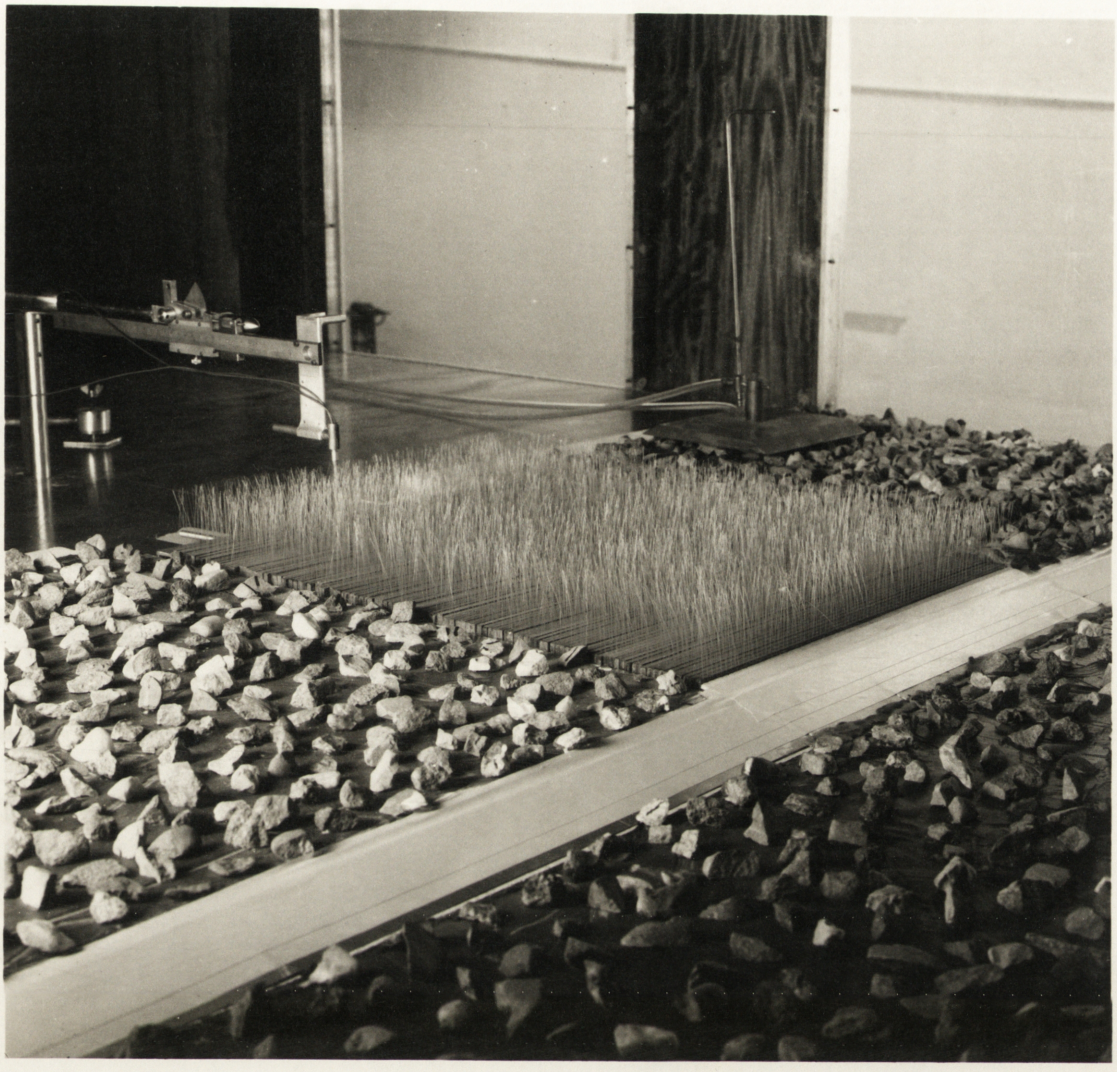

Fig. 9. Model wheat field in wind tunnel

of the model canopy were obtained by removing the model section and replacing it with a sheet of smooth particle board. The traverse was then made above this smooth section about 20 cm downstream of the end of the rough surface. Vertical traverses with the model in position were made above the microphone (39 cm from the start of the canopy) and 1 cm downstream of the model. For the traverse within the canopy, six stalks were removed from around the probe - three from each of the two rows immediately in front of the wires - to prevent the wires or prongs being hit by a flailing stalk. The outputs of the two wires were sampled for 200 sec at a rate of 500 Hz per channel at each vertical station, in order to calculate the first, second, and joint moments of $\tilde{u}$ and $\tilde{w}$. These results are presented in Figures 10-15. Despite the precautions noted above, the upstream 'within canopy' results are incomplete because of a series of broken wires, and the profiles above $z = 4.4$ cm must be inferred from the downstream results.

Spectra of pressure and velocity variance were obtained from the same records which had been used to compute the mean moments. Over sixteen thousand points (2^{14}) were transformed for each spectrum using a fast fourier transform (FFT) algorithm developed by Fraser (1978). Before transformation, the data time series was tapered by a cosine bell or 'Hanning window' function to reduce leakage. The raw spectrum after transformation was smoothed by sideways averaging around each point with a bandwidth of 3 Hz.

6. Results

6.1 MEAN QUANTITIES

The mean velocities plotted in Figure 10 reveal that the flow is accelerating at the rear of the model, an effect commonly observed in forest clearings and at the edges of various canopies. Measurements by Kawatani and Meroney (1970) in canopies of rigid pegs, and by Meroney (1968) in a model forest, reveal that profiles of mean velocity and turbulence intensity are still adjusting more than 20 canopy heights downstream of the leading edge of their models. Since the present model is only 10 canopy heights in extent, equilibrium flow conditions will never be achieved and comparisons with other published results must be treated with caution. The mean velocity profiles appear to be approaching a constant, non-zero value in the lower regions of the canopy. This observation has not yet been satisfactorily explained but the same behaviour is apparent in the rigid model canopy of Seginer et al. (1976) and in unpublished measurements made in a field of waving wheat by one of the present authors. The effect cannot be explained by the rectifying property of hot wires which produces spuriously high mean velocity readings in highly turbulent flows (Tutu and Chevray, 1975). Apart from this, the profiles are the familiar concave shape of canopy flows. The variation of Reynolds stress, $-\overline{uw}$, with height is shown in Figure 11. Shear-stress values behind the canopy are higher than within, but both curves approach a maximum at the top of the stalks. This behaviour is identical to that reported by Seginer et al. (1976) in a canopy of rigid rods. It was clear that the amplitude of stalk vibration within a few centimetres of the edge of the canopy was much larger than in the central portion and we would expect turbulent fluctuations to be larger in this region.

Profiles of streamwise and vertical turbulence intensity, i_u and i_w, where $i_u = (\overline{u^2})^{\frac{1}{2}}/U$ and $i_w = (\overline{w^2})^{\frac{1}{2}}/U$, are shown in Figure 12. Of particular interest is the fact that i_u increases with height

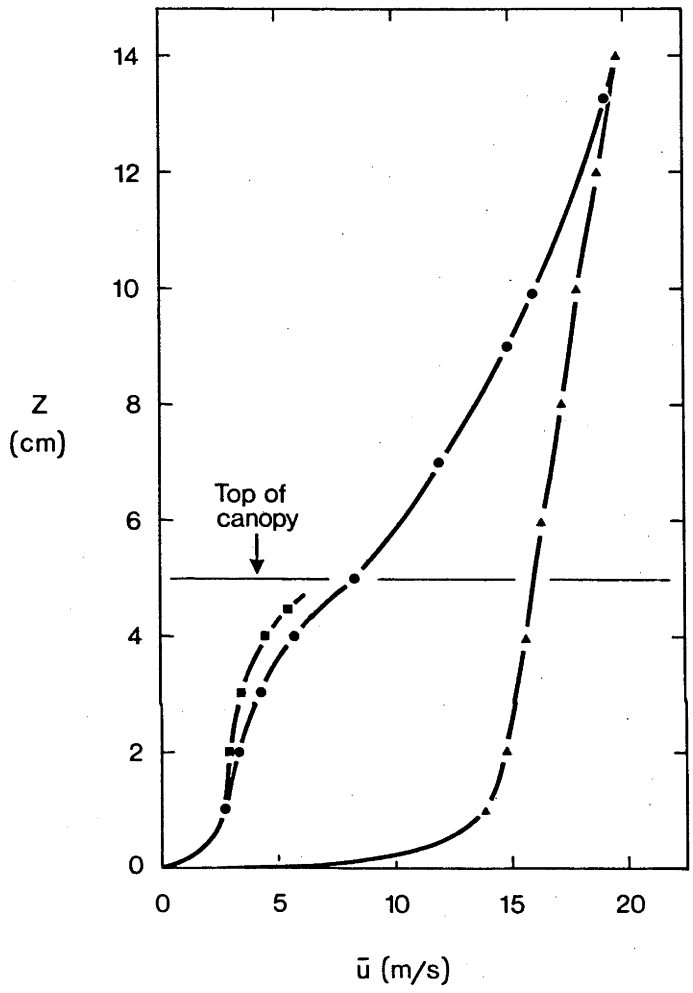

Fig. 10. Mean velocity profiles: ■, within canopy; ●, behind canopy; ▲, upstream.

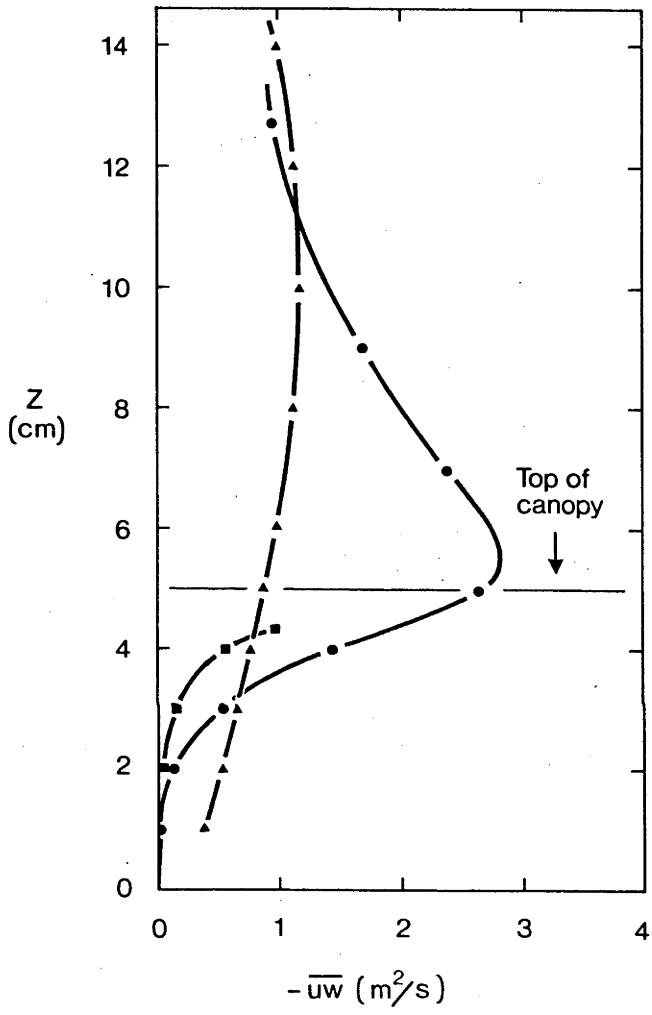

Fig. 11. Reynolds shear stress profiles: symbols as previous figure.

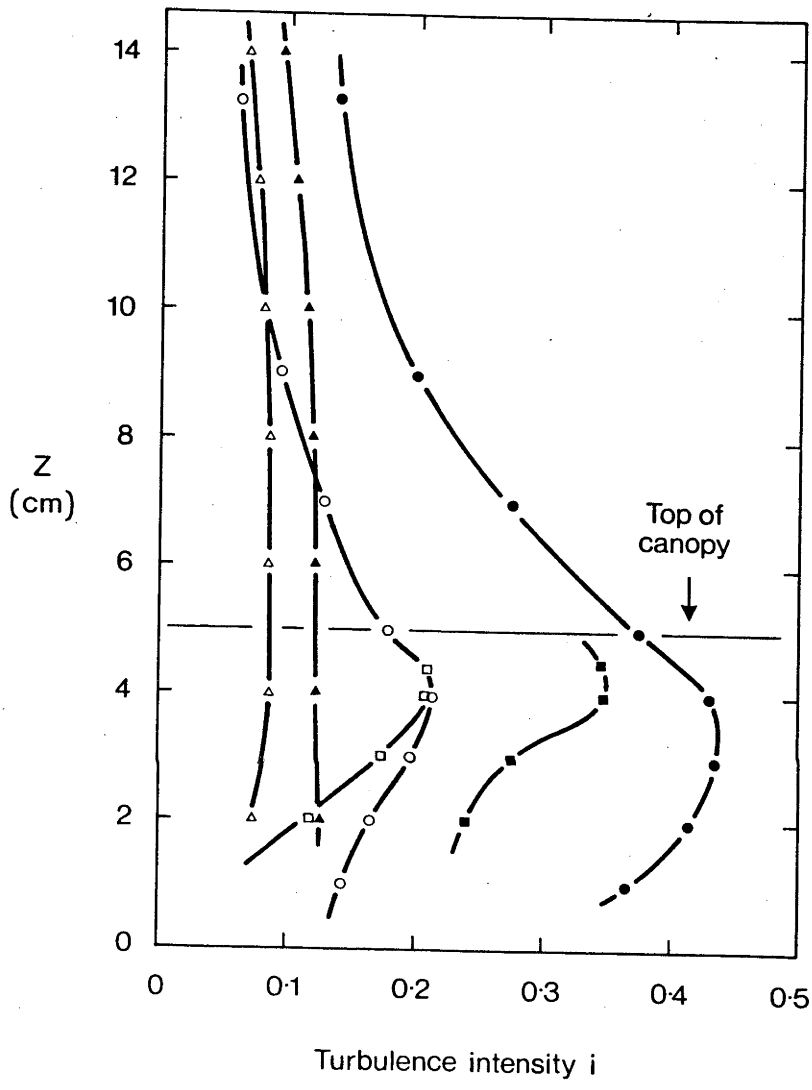

Fig. 12. Profiles of turbulence intensities, i_u and i_w: ▲, i_u upstream; △, i_w upstream; ■, i_u within canopy; □, i_w within canopy; ●, i_u behind canopy; ○, i_w behind canopy.

in the canopy to a maximum value just below the top. Cionco (1972) collected data on turbulence intensities in many canopies and concluded that for 'ideal' canopies, that is canopies whose projected area/unit volume was constant with height, i_u is essentially constant also. Results of Seginer et al. (1976) confirm this. However, data of Inoue, Lemon, and Denmead obtained in a wheat crop and reported in Cionco (1972) and by personal communication showed that, when large scale disturbances passed through the canopy, causing strong waving or Honami , the vertical profile of turbulence intensity changed from being constant to showing a strong increase with height. The authors have been unable to find other published data which would throw more light on this behaviour but recent measurements by one of the present authors in a field of waving wheat have confirmed this phenomenon. The effect of waving upon i_u is usually obscured by the practice of taking ensemble averages over many different runs and is further confused by the dependence of i on local leaf area density. The vertical variation of i_w is observed in rigid model canopies (e.g. Seginer et al., 1976) and does not appear to be particularly enhanced in the present case by the waving motion. The upstream profiles of U, $-\overline{uw}$, i_u, and i_w are included in the foregoing figures for purposes of comparison.

6.2 SPECTRA

The distribution of fluctuating pressure at the model ground surface is shown in Figure 13 and has been corrected for the frequency response characteristics of the Bruel and Kjaer microphone. The spectrum of background noise, obtained with the tunnel motor running at operating speed but the fan inlet vanes closed so that the wind speed was zero, is also shown on this plot. The spectrum shows a strong peak at 31 Hz which is, as closely as can be determined by 'freezing' the

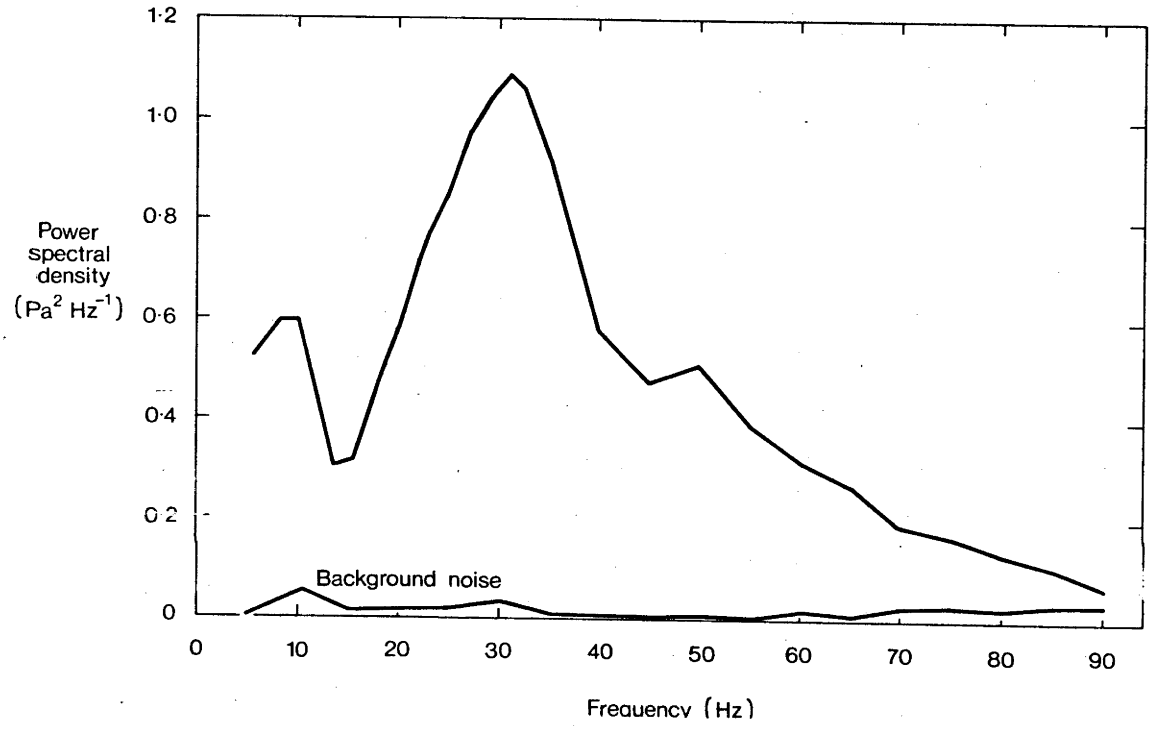

Fig. 13. Surface pressure spectra within canopy.

stalks' motion with a stroboscope, the natural frequency of stalk vibration. With the assumption of incompressible flow, it can be shown that the order of magnitude of pressure fluctuations developed in the vicinity of the top of the canopy by the waving stalks is of order $\rho\ U\ \omega\hat{y}/\sqrt{2}$, where the stalks vibrate sinusoidally with an amplitude $\hat{y}$. The acoustic pressure signals generated by this same motion are of order $\rho\ c\ \omega\ \hat{y}/\sqrt{2}$ where c is the speed of sound. In estimating the size of the acoustic signals we have, of course, allowed the fluid to become compressible again but this rough procedure provides some basis for comparison of the two effects. The ratio of the variances of pressure signal resulting from the two effects is therefore $(c/U)^2$ which is of order 10^3. Since the amplitude of stalk vibration close to the model floor approaches zero, we assume that the largest contribution to the variance of p' shown in the spectrum is acoustic. If this is so, the pressure spectrum should be a good indicator of the actual waving frequency, its sharp peak tending to support the assumption that all the stalks are waving with a common and well-defined frequency of 31 Hz.

Power and cross spectra of u and w, Φ_{uu}, Φ_{ww}, and Φ_{uw} are shown for z = 2.5 cm in Figure 14 a and b and z = 4.4 cm in Figure 15 a and b. In all of these plots, the most prominent feature is a large peak close to the natural frequency of 31 Hz. In the spectrum of streamwise fluctuations at 4.4 cm, this peak, although prominent, is overshadowed by the power at lower frequencies, but well within the canopy at z = 2.5 (Figure 14) it is more important. Spectra of vertical fluctuations show the effects of waving even more clearly as they are not masked by a large background streamwise component. In this case it is the spectrum at z = 4.4 cm which shows the larger

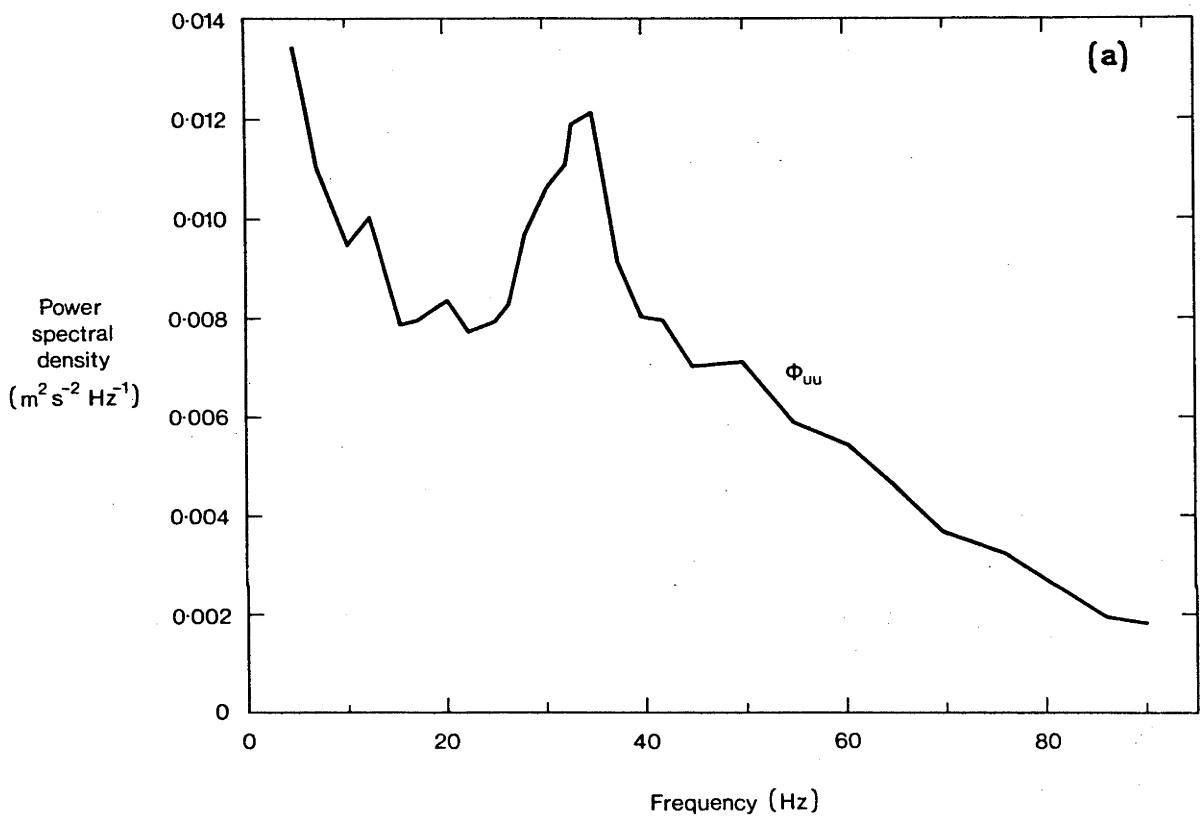

Fig. 14. (a) and (b). Power and cross spectra of velocity, Φ_{uu}, Φ_{ww}, Φ_{uw}, at z = 2.5 cm within canopy.

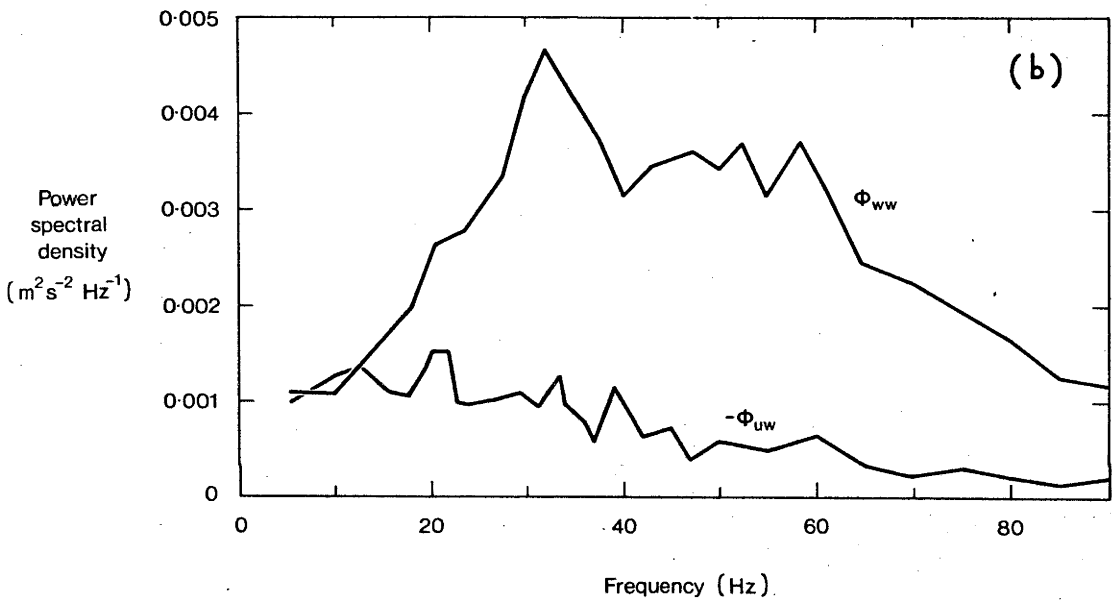
0·005
0·004
0·003
0·002
0·001
0
Power spectral density ($m^2 s^{-2} Hz^{-1}$)
(b)
Φ_{ww}
$-\Phi_{uw}$
0
20
40
60
80
Frequency (Hz)

Fig. 14 (b)

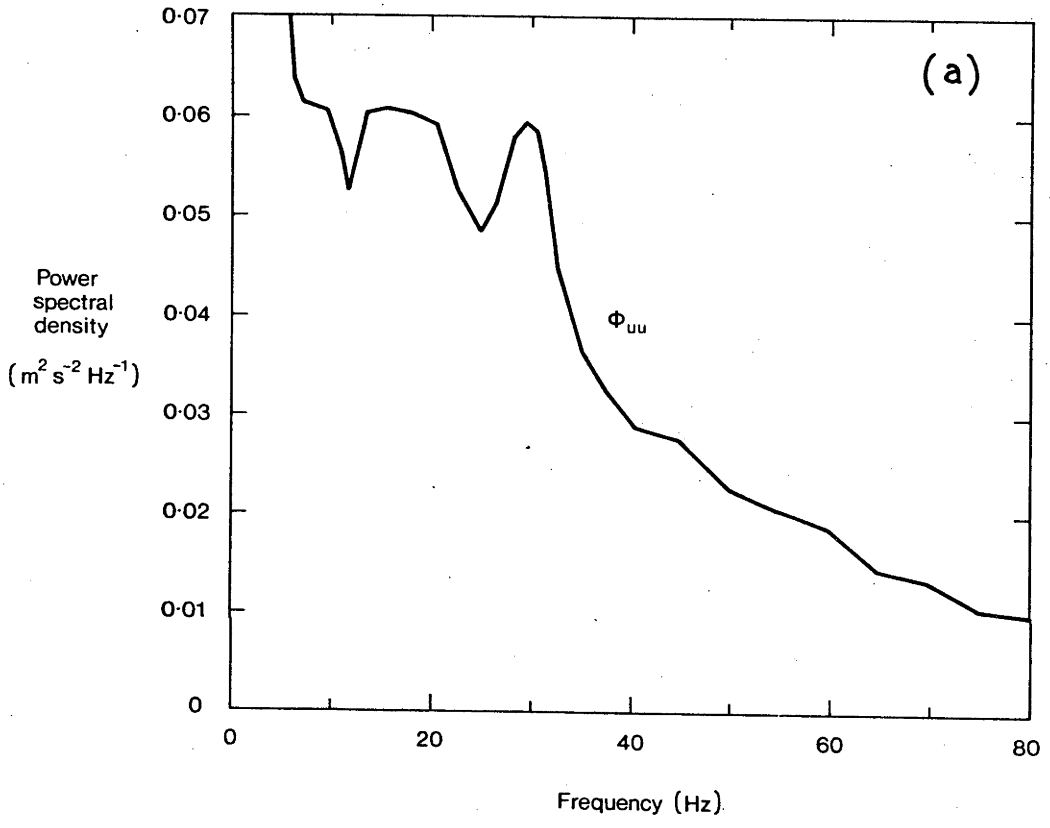

Fig. 15. (a) and (b). Power and cross spectra of velocity, Φ_{uu}, Φ_{ww}, Φ_{uw}, at z = 4.4 cm within canopy.

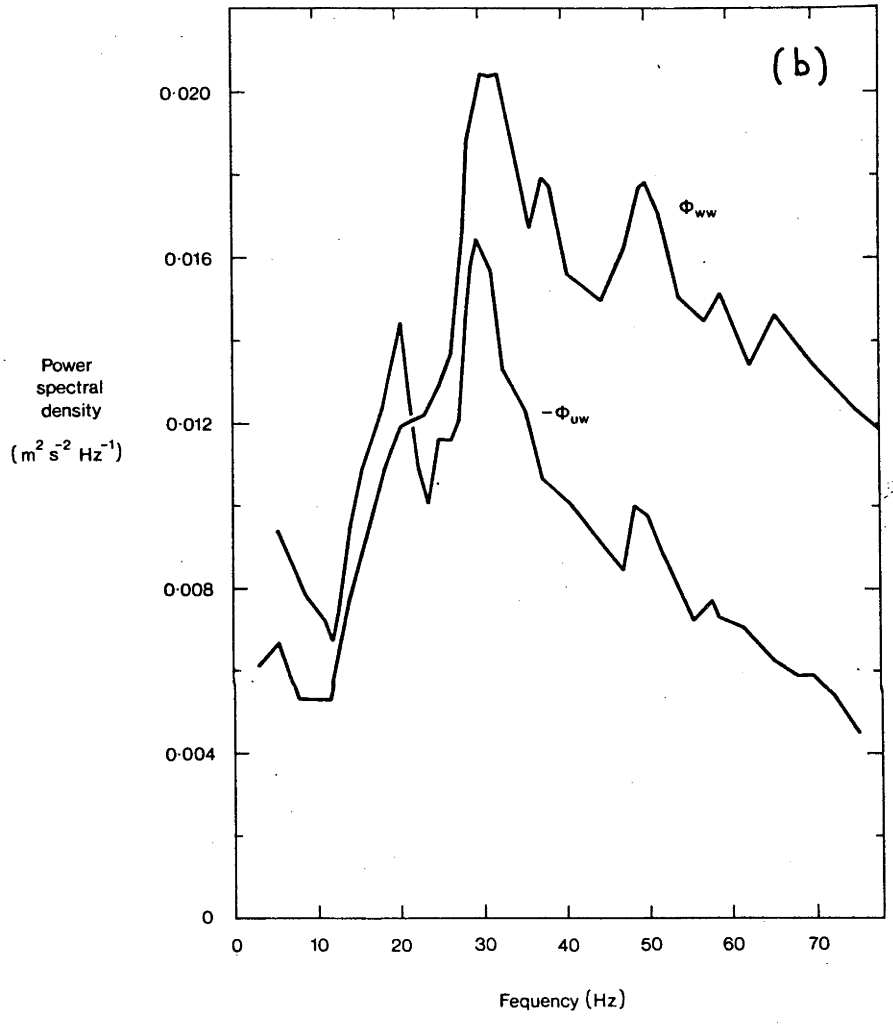
(b)
0·020
0·016
0·012
0·008
0·004
0
Power spectral density
(m² s⁻² Hz⁻¹)
Φww
−Φuw
0
10
20
30
40
50
60
70
Fequency (Hz)

Fig. 15 (b)

effect. Other peaks are also prominent in Φ_{ww} between 50 and 60 Hz at both vertical positions but these cannot be identified with second harmonics nor would we expect this as the stalks vibrate predominantly in their fundamental mode. Of particular interest for studies of diffusion in the waving canopy are the cross spectra of u and w, the spectrum of Reynolds shear-stress. At z = 4.4 cm Φ_{uw} shows the effect of waving particularly strongly. At z = 2.5 this peak is much reduced but, as reference to Figure 9 reveals, shear stress at this level is already practically negligible. Finally, one can observe a shift in the position of the main peak to a higher frequency as one goes from z = 4.4 cm to z = 2.5 cm. This is particularly marked in the plot of Φ_{uu}. This behaviour is so far unexplained.

7. Conclusions

Careful studies of Honami and the motion of individual wheat and barley stalks lead to the conclusion that even though they are excited by a turbulent wind, single stalks vibrate at a particular and well-defined natural frequency. This property enables them to be treated as resonant cantilevers, whose elastic properties can be measured by well-established engineering techniques.

Canopies made up primarily of collections of single stalks with a fairly well-defined common frequency of vibration, such as wheat, rice, or barley, can be represented by uniform cantilevers without sacrificing any important aspects of their elastic or aerodynamic properties. These uniform cantilevers can then be scaled down in an aeroelastic model constructed in accordance with certain conditions which can be derived quite simply by similarity analysis of the equation of motion of a single stalk. The dimensionless groups, which must be kept constant between the real canopy and the model, represent the ratios of the inertial, damping and aerodynamic forces to the elastic force on the stalk, and the ratio of the velocity scales of the waving motion and the windspeed. In the case of a wheat canopy the gravitational force on the stalk was shown to have little effect on waving frequency, although this may not be true for all canopies.

By referring to a large number of empirical results collected by Seginer (1974) it proved possible to predict the spacing of stalks in a model canopy which would reproduce the bulk momentum absorption of a dense wheat crop, specifically preserving the correct values of z_o/L in the model. A small prototype section of simulated crop was

constructed according to the foregoing criteria and measurements made of first and second moments of fluctuating wind speed and surface pressure. The effect of waving was seen in the vertical profiles of streamwise turbulent intensity, which increased with height, unlike the situation in rigid canopies of the same geometry, and in the power and cross spectra of the fluctuating parameters. A strong peak in the surface static pressure spectrum at the waving frequency is believed to be mainly acoustic noise, but peaks in the velocity spectra at the waving frequency are also prominent. Of particular interest is the fact that much of the Reynolds stress, $-\overline{uw}$, at the top of the canopy, is centred around the waving frequency.

Because of the short fetch of model surface, equilibrium conditions could not be achieved in the boundary layer above and within the canopy. This prevents any conclusions being drawn at this stage about the effect of the waving upon such parameters as z_o and d although the detailed structure of the turbulent flow obviously depends strongly upon the waving motion. A larger section of model canopy is now under construction so that equilibrium flow conditions can be developed and studied.

REFERENCES

Bisplinghoff, R.L., Ashley, H. and Halfman, R.L.: 1957, 'Aeroelasticity', Addison-Wesley Inc., Reading, Massachusetts.

Cionco, R.M.: 1972, 'Intensity of turbulence within canopies with simple and complex roughness elements', Boundary-Layer Meteorology 2, 453-465.

Denmead, O.T. and Bradley, E.F.: 1973, 'Heat, Mass and Momentum transfer in a wheat crop', Paper presented to First Australasian Conference on Heat and Mass Transfer. Melb. Aust.

Fraser, D.: 1978, 'An optimised mass storage FFT', Assoc. of Comp. Mach. Trans. on Math. Software. (in press)

Grass, A.J.: 1971, 'Structural features of turbulent flow over smooth and rough boundaries', J. Fluid. Mech. 50, 233-235.

Inoue, E.: 1955, 'Studies of the phenomena of waving plants ("HONAMI") caused by wind. Part 1. Mechanism and characteristics of waving plants phenomena', J. Agric. Met. (Japan) 11, 18-22.

Ito, S.: 1968, 'Inner and outer flow velocity distributions through tall simulated vegetation', Technical Report (CER67-68JEC61), Fluid Dynamics and Diffusion Laboratory, Colorado State University.

Kawatani, T. and Meroney, R.N.: 1970, 'Turbulence and wind speed characteristics within a model canopy flow field', Agr. Meteorol. 7, 143-158.

Meroney, R.N.: 1968, 'Characteristics of wind in and above model forests', J. Appl. Meteorol. 7, 780-788.

Mulhearn, P.J., Banks, H.J., Finnigan, J.J., and Annis, P.G.: 1976, 'Wind forces and their influence on gas loss from grain storage structures', J. Stored Prod. Res. 12, 129-142.

Nakagawa, H. and Nezu, I.: 1977, 'Prediction of the contributions to the Reynolds stress from bursting events in open-channel flow, J. Fluid Mech. 80, 99-128.

Schwerdtfeger, P., Radok, U., Bennet, J., van Meurs, B., Piggin, I., Ussher, A., and Wu, A.: 1975, 'The physical environment of plants', in L.P. Smith (ed), Progress in Biometeorology - Division C, Progress in Plant Biometeorology, pp. 11-20, Swets and Zeitlinger, B.V., Amsterdam.

Seginer, I.: 1974, 'Aerodynamic roughness of vegetated surfaces', Boundary Layer Meteorol. 5, 383-393.

Seginer, I., Mulhearn, P.J., Bradley, E.F., and Finnigan, J.J.: 1976 'Turbulent flow in a model plant canopy', Boundary-Layer Meteorol. 10, 423-54.

Shaw, K.J., Silversides, R.H. and Thurtell, G.W.: 1974, ' Some observations of turbulence and turbulent transport within and above plant canopies', Boundary-Layer Meteorol. 5, 430-449,

Snyder, W.H.,: 1972, 'Similarity Criteria for the application of Fluid Models to the study of Air Pollution Meteorology', Boundary-Layer Meteorol. 3, 113-134.

Thom, A.S.: 1971, 'Momentum absorption by vegetation', Q.J.R. Meteorol. Soc. 97, 414-428.

Tutu, N.K. and Chevray, R.: 1975, 'Cross-wire anemometry in high intensity turbulence', J. Fluid Mech. 71, 785-800.

Postscript to Chapter 4

The more detailed investigation into the wavelike structure of the velocity field in the real wheat canopy, discussed in Chapters 2 and 3, has clarified two of the points which arose in the discussion of results obtained in the prototype model canopy of Chapter 4. Firstly, the observed shift of the spectral peak in ϕ_{uu} between $z = 2.5$ cm and $z = 4.4$ cm is in the opposite direction to that observed in the real wheat field. Furthermore the prominent, high frequency peak in the ϕ_{ww} spectrum for $z = 4.4$ cm is at approximately 50 Hz rather than twice the frequency of the waving peak. However, the prototype canopy is too small in extent for equilibrium flow conditions to be established, and an abrupt change of surface level coincides with its leading edge. It is certain that the mean streamline through $z = 2.5$ cm at the measuring station will not have been parallel to the model ground surface so that the hot wire at 2.5 cm may be sensing frequencies characteristic of a higher level, while the large acceleration accompanying the distorted mean flow field will affect any imposed velocity wave in unpredictable ways.

The second point concerns the order of magnitude arguments which were used to suggest that the pressure fluctuations at the ground surface were an acoustic effect. A more detailed (but still very approximate) calculation of the acoustic power of the waving stalks was carried out using Lighthill's theory of aerodynamic sound generation. The waving stalks were regarded as acoustic dipoles with an instantaneous dipole strength, $P(x,t)$, where $P(x,t) = P' \exp 2\pi i(x-\theta t)$. P' is the r.m.s. fluctuating force on the top 25% of the stalk, $i = \sqrt{-1}$, and θ is the phase velocity of the honami wave as defined in Chapters

2 and 3. Lighthill's (1962) formula for the pressure perturbation caused by a dipole at a point in the near field was used, and the mean square fluctuation in pressure at the sensor was calculated by time averaging the integrated pressure field resulting from dipoles throughout the whole of the model canopy. θ was taken as $\theta = 1.8\ U(H)$ (see Chapter 2). The r.m.s. acoustic field at the pressure sensor was found to be 0.545 Pa^2. This is approximately 1.5% of the measured value, a result in direct contradiction to that derived from the cruder dimensional arguments advanced in Chapter 4. The conclusions of Chapters 2 and 3, that the pressure at the surface is a consequence of the velocity field at the top of the canopy, means however that the position of the peak of the pressure spectrum can still be taken as a measure of the stalk waving frequency.

Reference

Lighthill, M.J.: 1962, 'Sound Generated Aerodynamically', Proc. Roy. Soc. A267, 147-182.

CHAPTER 5

A SIMPLE MATHEMATICAL MODEL OF AIRFLOW IN WAVING PLANT CANOPIES

J.J. FINNIGAN and P.J. MULHEARN

This paper was published in Boundary-Layer Meteorology, volume 14, pp. 415-431 (1978).

Abstract. A simple mathematical model is proposed, which combines the effects of mean wind speed, plant spacing and the drag coefficients of individual plants to calculate the fluctuating airflow within a waving crop canopy. The model is non-linear and is only amenable to analytical treatment when linearized; however, the full non-linear version can be solved on an electronic analogue computer.

The linear and non-linear results show unexpectedly good agreement, and the success of the linearization allows clear conclusions to be drawn about the relationship between the elasticity, geometry and mean wind speed through a stand of plants and the fluctuating components of airflow and stalk motion.

Finally, the analytical results are in qualitative agreement with wind tunnel results from two model canopies with different characteristics.

1. Introduction

The relationship between the distribution of plants in a living canopy and the mean properties of the turbulent atmospheric boundary layer above has received a great deal of attention in recent years. Measurements in real canopies and wind tunnel models have provided a basis for several mathematical models of momentum transfer in canopies (e.g. Cionco, 1965; Cowan, 1968; Thom, 1971). These models, in general, have attempted to predict the mean properties of turbulent canopy flow from a consideration of the local plant geometry and the mean velocity. Interpretations of wind tunnel and field experiments have tended to follow the same pattern.

Wind tunnel measurements by the present authors in an aeroelastic model of a wheat field (Finnigan and Mulhearn, 1977) and in a real wheat canopy (Chapters 2 and 3) show, however, that in flexible waving crops, the structure of turbulent velocity fluctuations can be dominated by the waving motion. In these cases the elastic as well as the geometric properties of the plants should be taken into account when predicting or interpreting results.

Seginer (1974) has collected results from many workers which enable the mean momentum absorption properties of stands of plants or wind-tunnel models to be inferred from the spacing and individual drag coefficients of the canopy elements. His results, however, give no clue as to how the spacing and drag coefficients of waving plants might affect the velocity fluctuations. It seemed useful to the present authors to set up a simple mathematical model to investigate this dependence.

In contrast to the work of Cionco, Cowan and Thom, the model to be

described makes no attempt at a general description of turbulent momentum transfer within a canopy; its aims are much more limited. By investigating how the drag and element density of a collection of rods, vibrating in phase, affects their interaction with the air around them, we hope merely to draw some qualitative conclusions about the relationship between velocity and vibration in the analogous situation of the upper regions of a waving wheat crop. This will, we hope, help to clarify the interactions and aid the interpretation of future measurements.

2. The Mathematical Model

Imagine a uniform two dimensional array of rigid circular cylinders or rods, free to move in a plane normal to their axes but restrained by a spring force proportional to their displacement. The motion of each rod is also damped by a force proportional to its velocity. When an external pressure gradient is applied to the whole system, the rods, and the air in the spaces between them, move in the direction of the negative gradient and, if this gradient is periodic, after some time the whole system will be in periodic motion with a constant amplitude. This system is sketched in Figure 1. If the diameter of the rods is small compared with the length scale of the pressure gradient, so that the static pressure force on any rod can be neglected compared to its aerodynamic drag, and if we are outside the boundary layer and near wake of an individual rod, then the motion of the air between the rods and far from their ends is described by the one dimensional momentum equation in the streamwise direction,

$$\frac{d\tilde{u}}{dt} = -\tilde{k}(t) - \beta\left(\tilde{u} - \frac{d\tilde{y}}{dt}\right)\left|\tilde{u} - \frac{d\tilde{y}}{dt}\right| , \qquad (1)$$

where $\tilde{u}$ is the instantaneous streamwise velocity; $\tilde{k} = \frac{1}{\rho}\frac{dp}{dx}(t)$ is the streamwise kinematic pressure gradient, where p is static pressure,

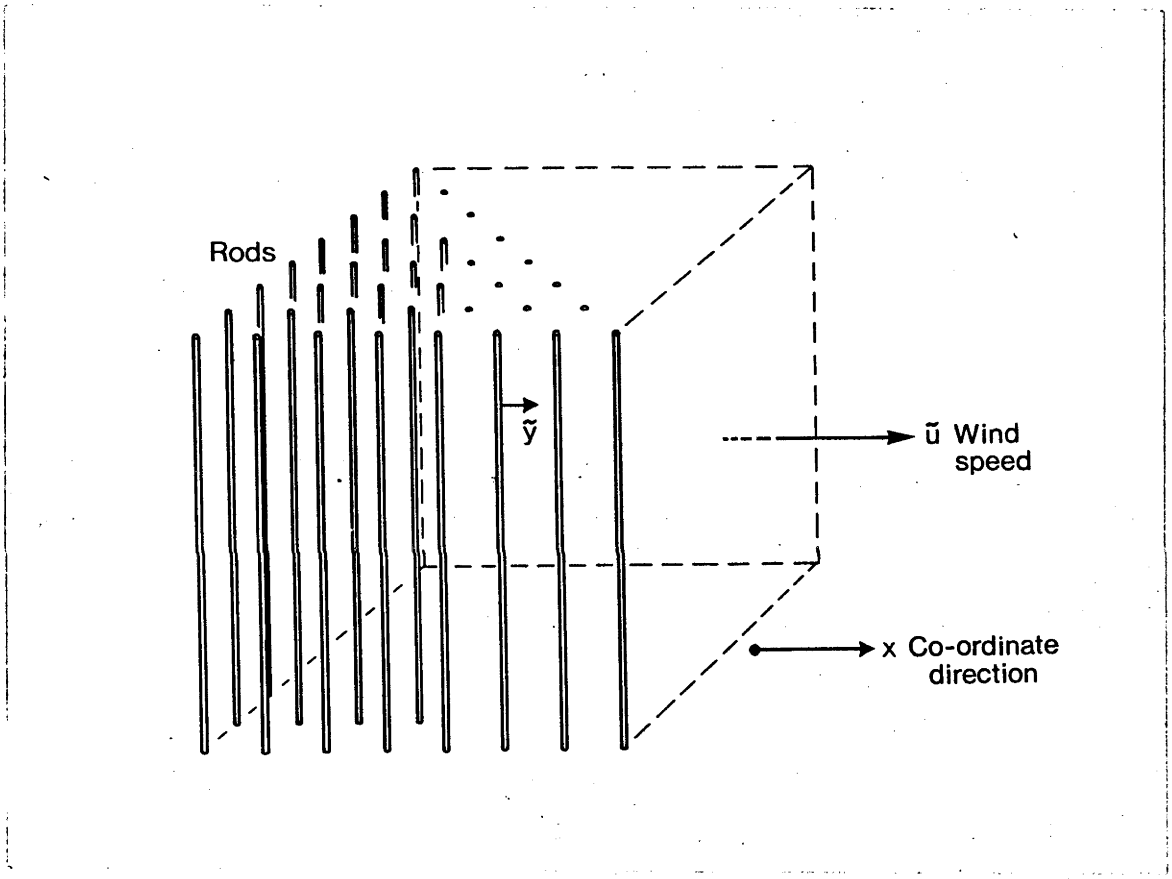

Fig. 1. Schematic view of the essentials of the present model.

ρ is air density, t is time and x is the streamwise co-ordinate of length, and $\tilde{k}$ is considered to be a function of time only; $\beta = \frac{1}{2}CA$, where A is the projected area of rods per unit volume of space and C is the appropriate dimensionless drag coefficient; $\tilde{y}$ is the streamwise displacement of any rod from its zero position so that $(\tilde{u} - \frac{d\tilde{y}}{dt})$ is the wind speed relative to the rod. Notice particularly that the sign of $(\tilde{u} - \frac{d\tilde{y}}{dt})$ is retained even though it appears as its square.

The motion of an individual rod is represented by the equation of a damped harmonic oscillator, forced by the fluctuating aerodynamic drag,

$$\frac{d^2\tilde{y}}{dt^2} + \xi \frac{d\tilde{y}}{dt} + \omega_n^2 \tilde{y} = \alpha(\tilde{u} - \frac{d\tilde{y}}{dt}) \left| \tilde{u} - \frac{d\tilde{y}}{dt} \right| , \qquad (2)$$

where ω_n is the natural frequency of the rod, whose mass is m, in free, undamped oscillation; and ξ, which equals c/m, is the damping coefficient per unit mass. This is defined by the equation for the decay in amplitude, y_o, of the vibration after an impulsive displacement:

$$y_o(t) = y_{o_{max}} \exp\left[-t(c/2m)\right] .$$

$\alpha = \frac{1}{2} \rho Ca/m$, where a is the area, projected normally to the airstream, of a single rod.

The idealizations involved in applying this model to arrays of real plants are obvious. The motion of the rods is normal to their axes and they remain a fixed distance apart. For a plant canopy we consider the spring stiffness, $S(=m\omega_n^2)$, to be provided by the flexural rigidity of the stalks which we approximate by the value for a uniform cantilever, $S = 3J/L^3$, where L is the length of the stalk and J its flexural rigidity. Equations (1) and (2) are linked by their aerodynamic drag terms.

The two equations are perhaps best regarded as describing the region just below the top of a wheat canopy, where the ear and flag leaf wave in the airflow and are restrained by the springy stalk (Figure 2). In real canopies, mean velocities increase approximately exponentially with height and mean square fluctuations have strong peaks around the top of the plants. The data in Figure 3, obtained in a field of waving wheat (Finnigan, unpublished results), are typical.

Perhaps a more fundamental departure from reality, however, is that $\tilde{k}$, the fluctuating pressure gradient, which we regard as the forcing function, is independent of the system response. This is a consequence of the one dimensional nature of the model. In practice, pressure, velocity and waving are interdependent; but since we are most interested in velocity and vibration, quantities which can be measured experimentally and with which we can compare our model, the pressure gradient is chosen as the external input.

Noting that α and β have dimensions of length^{-1}, we define the following dimensionless quantities

$$u' = \tilde{u}\,\frac{\beta}{\omega_n}\ ;\quad y' = \tilde{y}\beta\ ;\quad \tau = t\,\omega_n\ ;\quad k' = \tilde{k}\,\frac{\beta}{\omega_n^2}\ ;\quad \xi' = \frac{\xi}{\omega_n}\ .$$

Substituting for $\tilde{u}$, $\tilde{y}$, t, $\tilde{k}$ and ξ in Equations (1) and (2), we obtain:

$$\frac{du'}{d\tau} = -\,k' - (u' - \frac{dy'}{d\tau})\ \left|\ u' - \frac{dy'}{d\tau}\ \right| \qquad (3)$$

$$\frac{d^2y'}{d\tau^2} + \xi'\,\frac{dy'}{d\tau} + y' = \gamma\ (u' - \frac{dy'}{d\tau})\ \left|\ u' - \frac{dy'}{d\tau}\ \right|\ , \qquad (4)$$

where $\gamma = \frac{\alpha}{\beta}$.

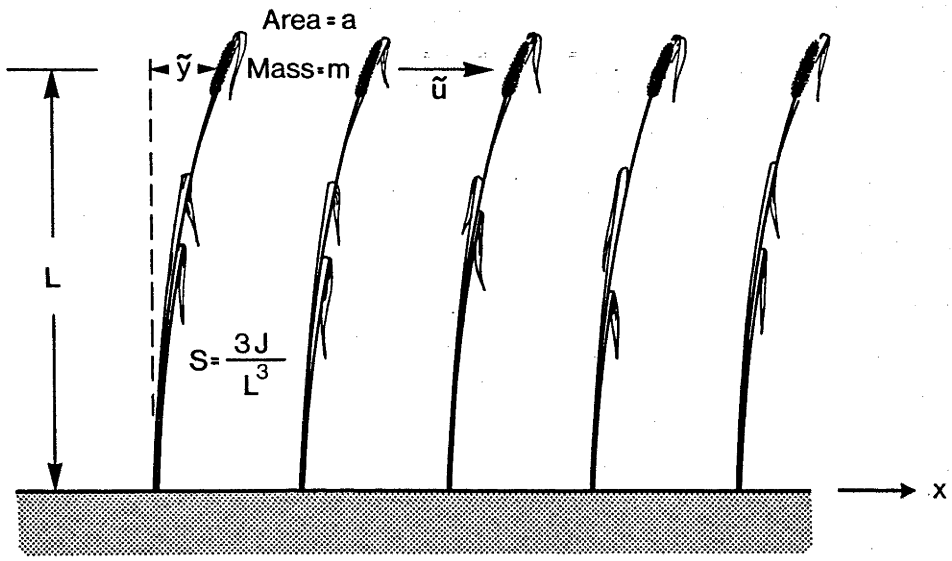

Fig. 2. Relationship of the co-ordinates of the present model to a real canopy.

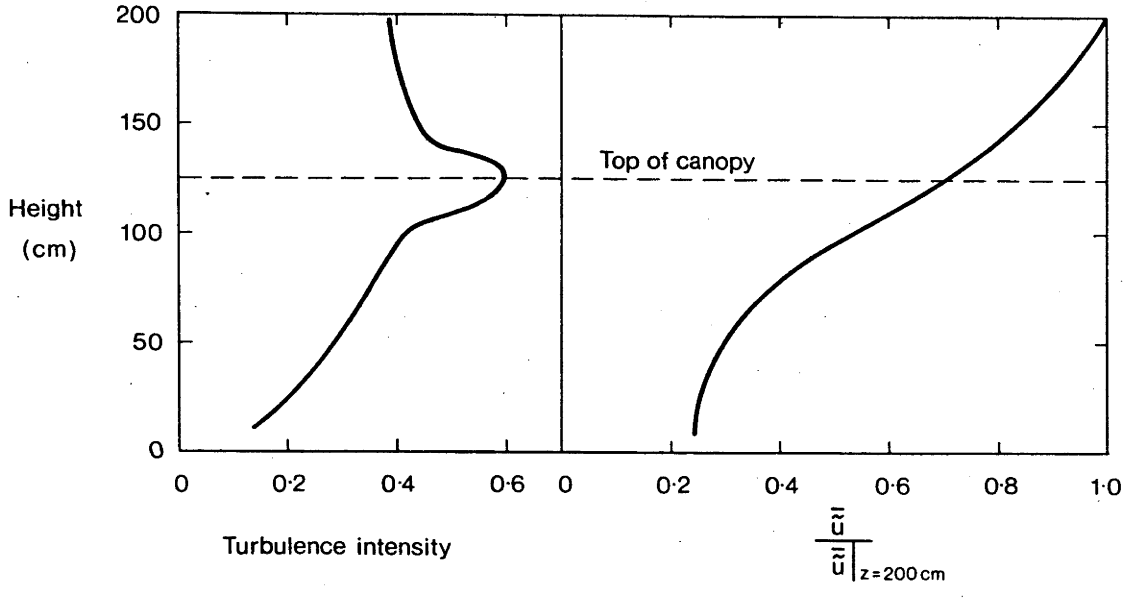

Fig. 3. Streamwise turbulence intensity, i_u [$i_u = \frac{[(\tilde{u} - \bar{\tilde{u}})^2]^{\frac{1}{2}}}{\bar{\tilde{u}}}$], and normalized mean velocity profiles measured in a waving wheat canopy at Ginninderra, Canberra, 1976.

Equations (3) and (4) form a system of second order, non-linear, ordinary differential equations, whose analytical solution is made particularly difficult by the awkward nature of the non-linear term, $(u' - \frac{dy'}{d\tau}) \mid u' - \frac{dy'}{d\tau} \mid$. They can however be linearized.

We separate all time dependent variables into their mean and fluctuating parts:

$$u' = U + u \; ; \quad k' = K + k \; ; \quad y' = Y + y \; . \tag{5}$$

Substituting these expressions into Equations (3) and (4) and making the further assumption that $U \gg u$ and $U \gg \frac{dy'}{d\tau}$, we obtain, after neglecting the squares of small quantities,

$$\frac{du}{d\tau} = - (K + k) - [U^2 + 2U(u - \frac{dy}{d\tau})] \tag{6}$$

$$\frac{d^2y}{d\tau^2} + \xi' \frac{dy}{d\tau} + (Y + y) = \gamma \, [U^2 + 2U(u - \frac{dy}{d\tau})] \; , \tag{7}$$

and after taking the time average of (6) and (7) we obtain the following equations for the mean quantities:

$$\text{from (6)} \quad 0 = - K - U^2 \tag{6a}$$

$$\text{from (7)} \quad Y = \gamma U^2 \; . \tag{7a}$$

Finally, subtracting (6a) from (6) and (7a) from (7) results in linear equations for the fluctuating variables:

$$\frac{du}{d\tau} = - k - 2U(u - \frac{dy}{d\tau}) \tag{8}$$

$$\frac{d^2y}{d\tau^2} + \xi' \frac{dy}{d\tau} + y = 2\gamma U(u - \frac{dy}{d\tau}) \; . \tag{9}$$

Since we are seeking periodic solutions of Equations (8) and (9), and regard $k(\tau)$ as the external input to the system, we assume the following functional forms for the variables:

$$k = \pi e^{i\omega\tau} \quad , \quad u = \hat{u}e^{i\omega\tau} \quad , \quad y = \hat{y}e^{i\omega\tau} \quad , \tag{10}$$

where π is real, $\hat{u}$ and $\hat{y}$ are complex time independant amplitudes, and $i = \sqrt{-1}$.

Substituting Equations (10) into (8) and (9) we obtain,

from (8) $$i\omega\hat{u} = - \pi - 2U(\hat{u} - i\omega\hat{y}) \tag{11}$$

and from (9) $$-\omega^2\hat{y} + i\omega\xi'\hat{y} + \hat{y} = 2\gamma U(\hat{u} - i\omega\hat{y}) \tag{12}$$

and after some algebra we obtain Equations (13) and (14):

$$\frac{\hat{u}}{\pi} = - \frac{1}{\zeta} \quad , \tag{13}$$

where

$$\zeta = \left[(i\omega + 2U) - \frac{4i\gamma\omega U^2}{(-\omega^2 + i\omega\xi' + 2i\gamma\omega U + 1)} \right] ;$$

and $$\frac{\hat{y}}{\pi} = - \frac{2\gamma U}{\theta\zeta} \quad , \tag{14}$$

where $$\theta = (-\omega^2 + i\omega\xi' + 2i\gamma\omega U + 1).$$

From (13) and (14) it is a simple matter to compute the amplitudes of the periodic variables u and y for any frequency as ratios of the forcing function, k, as well as their phase relationships and the way in which all of these quantities vary with γ, u and ξ'.

We can form a comparative estimate of the effect of the stalks' elasticity upon the airflow by comparing the results obtained from Equation (13) with the case where the stalks are held rigid; that is, where y, $\frac{dy}{d\tau}$ and $\frac{d^2y}{d\tau^2}$ are zero. In this case Equation (12) disappears, and Equation (13) becomes:

$$\frac{\hat{u}}{\pi} = \frac{-1}{2U + i\omega} \quad . \tag{13a}$$

Similarly the ratio of the fluctuating drag terms, R, where

$$R = \frac{2U(u - dy/d\tau)}{2Uu} \;\Big|\; \begin{matrix} \text{stalks waving} \\ \text{stalks fixed} \end{matrix} \tag{15}$$

can be calculated from Equations (13), (13a) and (14).

It is more realistic, however, to consider the ratio of the root mean square fluctuating velocities relative to the stalks in the rigid and waving cases. This ratio is given by:

$$R_{total} = \frac{\left[\int_o^\infty |(\hat{u} - i\omega\hat{y})|^2 \, d\omega\right]^{\frac{1}{2}}}{\left[\int_o^\infty |(\hat{u})|^2 \, d\omega\right]^{\frac{1}{2}}} \;\Big|\; \begin{matrix} \text{stalks waving} \\ \text{stalks fixed} \end{matrix} \tag{16}$$

R_{total} can be regarded as the ratio of the fluctuating components of the drag force averaged over all frequencies in the two cases.

The full non-linear equation system, (3) and (4), can be set up on an analogue computer and readily solved. No assumptions need be made about the relative sizes of the mean and fluctuating velocities. The response of the equation system to a forcing function of given frequency and amplitude can then be found by injecting the appropriate pure sinusoid. To do this for every frequency of interest, however, would be a very tedious business. A much more convenient method (and since the system is non-linear, a more realistic approach) is to represent k, the pressure gradient, by Gaussian White Noise. The ratio of the mean square outputs, y and u, to the input, k, can then be found for all frequencies by obtaining the Fourier transform of the three signals.

3. Theoretical Results

Before we discuss the results which are obtained from Equations (13) and (16) and the analogue computer model, it is worth interpreting some of the parameters of these equations in terms of real canopies.

α is the total drag coefficient of an individual stalk or rod, whereas β represents the drag on the air of the distribution of stalks in unit volume of space. α then can be regarded as representing the momentum intercepting qualities (the size, roughness or leafiness) of the plant in question, while β reflects the momentum absorption of the whole canopy. γ, the ratio of α to β, decreases as the plants in the canopy are packed closer together and increases with increasing spacing or decreasing plant mass. For a given real wind speed, increasing γ implies a decrease in U, the dimensionless mean velocity, as β decreases, or in the case of decreasing m, as ω_n increases.

Typical values of γ have been calculated for a strain of wheat whose elastic and aerodynamic properties have been carefully measured. The mass, m, appropriate to our model was determined using Rayleigh's energy method for the vibration of elastic cantilevers (Thomson, 1965). This simple procedure enables one to calculate the magnitude of a point mass on the end of a light cantilever which will vibrate at the same natural frequency and have the same stiffness as the prototype heavy, weighted cantilever which we use to represent the real wheat stalk

with its heavy ear, leaves and stem. The values used to calculate γ are set out in Table I.

Three values of γ (0.4, 0.2, 0.1) represent sparse, medium and dense plantings of wheat respectively. ξ' was calculated from measurements of the damped vibrations of single stalks. The decay in amplitude of waving after an impulsive displacement was measured photographically. In real canopies, particularly dense ones, most of the damping may well come from mutual interference of adjacent leaves and stems, which could well be much higher than the internal viscous damping measured for single stalks. It was observed however that the present model is relatively insensitive to ξ' in any practical range, as the coefficient of $\frac{dy'}{d\tau}$ in the aerodynamic terms tends to be much larger than ξ'.

Results from the linearized mathematical model for the cases of $\xi' = 0.2$; $\gamma = 0.4, 0.2, 0.1$ are presented in Figures 4, 5a and 6, respectively. For each value of γ, the calculation was performed for three values of dimensionless mean velocity, $U = 0.25; 0.5; 0.75$.

The full non-linear equations were patched up on an Electronic Associates Inc. TR20 analogue computer and the white noise input was provided by a General Radio Model 1381 Random Noise Generator. The white noise input, k', and the system output, u', were sampled simultaneously and the resultant time series stored in a Digital Equipment Corporation PDP 11/40 digital computer where both records were subsequently transformed using a FFT algorithm developed by Fraser (1977). The results are plotted in Figures 5b, 7b and 8b as the ratio of the power in the dimensionless velocity fluctuations, $|u'|^2$, to the power in the dimensionless forcing function, $|k'|^2$.

Figures 4, 5a and 6 show, for the linearized case, that the effect of increasing γ at constant U is to increase the effect of the waving

TABLE I

Values used in the calculation of the parameters α, β, γ, ξ'.

Real canopies (These values correspond to a strain of wheat, Triticum Aestivum L. em. Fiori et Parl, cv. Gabo 3; see Finnigan and Mulhearn, 1977.)

$A = 2.0\ m^2/m^3$: sparse crop	β =	0.5
$A = 4.0\ m^2/m^3$: medium crop		1.0
$A = 8.0\ m^2/m^3$: dense crop		2.0
$a = 2.33 \times 10^{-3}\ m^2$	α =	0.2
$m = 3.5 \times 10^{-3}$ Kg		
$c = 3.0 \times 10^{-3}$ Kg/sec	ξ' =	0.2
$\omega_n = 4.4$ radians/sec		
$C = 0.5$		

Model canopies

$A = 1.88\ m^2/m^3$ sparse case	β =	0.47
$A = 4.372\ m^2/m^3$ dense case		1.183
$a = 8.0 \times 10^{-6}\ m^2$ (only top 60% of stalk is used to form a)	α =	2.407
$m = 8.26 \times 10^{-7}$ Kg		
$c = 12.3 \times 10^{-2}$ Kg/sec	ξ' =	$6.8\ 10^{-2}$
$\omega_n = 220$ radians/sec		
$C = 0.5$		

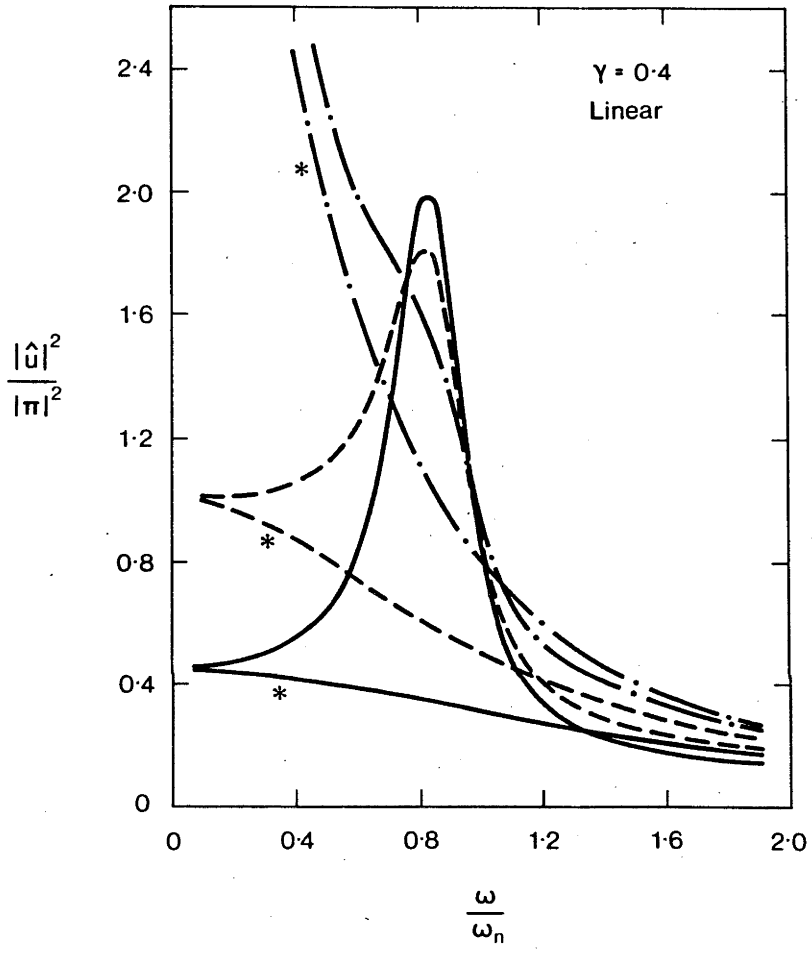

Fig. 4. Results of the linearized model (equations 13 and 13a) for $\gamma = 0.4$. $-\cdot-$ U = 0.25; --- U = 0.5; —— U = 0.75.
* Stalks fixed.

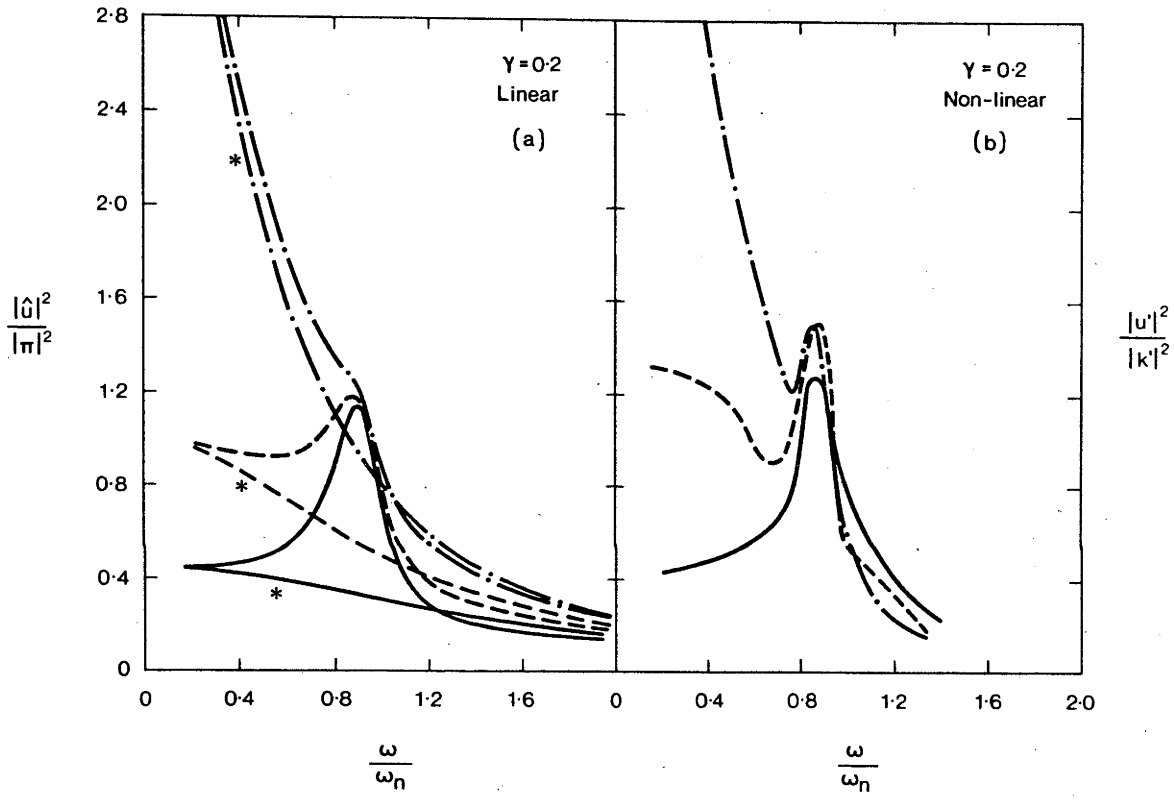

Fig. 5. a. Results of the linearized model for $\gamma = 0.2$

$-\cdot-$ U = 0.25; --- U = 0.5; —— U = 0.75.

* Stalks fixed.

b. Analogue computer solution of the non-linear equations for the same values of U and γ.

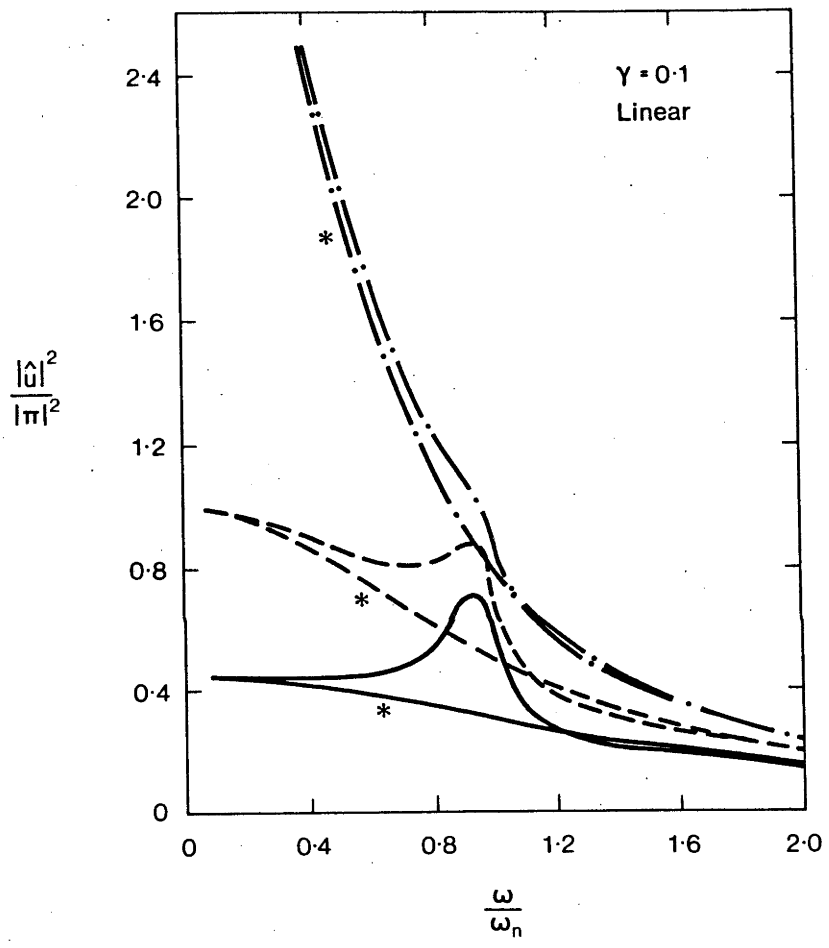

Fig. 6. Results of the linearized model for $\gamma = 0.1$.

—·— U = 0.25; — — —U = 0.5; ——— U = 0.75.

* Stalks fixed.

motion at resonance upon the velocity fluctuations. The effect is clearly seen by comparing the departure of the curves from the 'stalks fixed' result in each case. Decreasing β at constant α means an increase in γ: the canopy gets thinner. At the same time decreasing β at constant U implies an increase in real mean velocity ($U = \frac{\bar{u}\beta}{\omega_n}$). In other words, despite the sparser crop, the increase in wind speed enhances the effect of the waving motion on the airflow.

Increasing γ at constant β is equivalent to reducing the stalks' inertia, and they follow the fluctuations in velocity more readily. At the same time, their resonant frequency ω_n ($\omega_n = \sqrt{S/m}$) decreases; thus a constant U implies an increase in $\bar{u}$, again resulting in an increased influence of the waving stalks upon the airflow at resonance.

Figures 7a, 5a and 8a present curves for γ = 0.1, 0.2 and 0.4 respectively, while the mean velocity, $\bar{u}$, has been held constant. γ has been increased by decreasing β, and U has been adjusted accordingly; i.e. the crop has been progressively thinned while the real mean wind speed remained constant. The effect of the waving motion increases with canopy density although the increased momentum absorption of the denser canopies reduces the net response of the system. Figures 7b, 5b and 8b present the results from the non-linear analogue computer model, for comparison with the corresponding linear cases 7a, 5a and 8a. The agreement is surprisingly good.

Figure 9 shows, in the linear case, the increasingly strong functional dependence of $\frac{\hat{u}}{\pi}$ upon U as γ gets larger, which is predicted by Equation (13). Values of γ of this order can only really be achieved in wind tunnel models and this property emphasizes the importance of picking the correct velocity scale in aeroelastic model canopies.

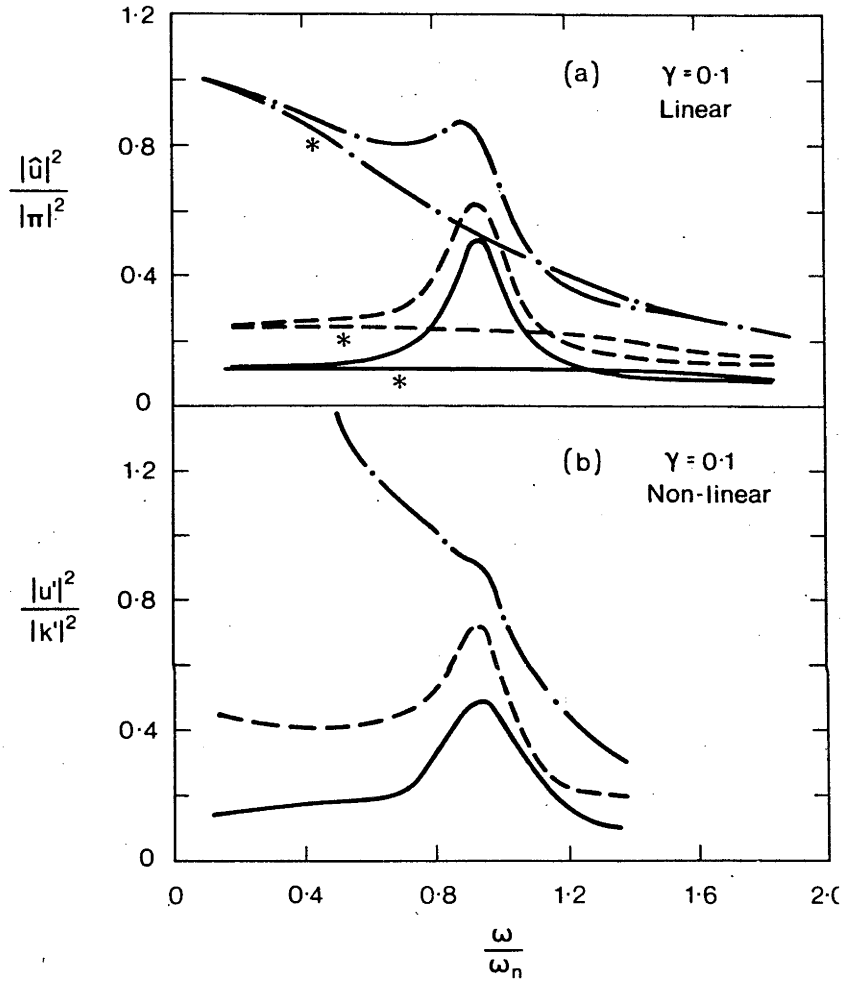

Fig. 7. a. Results of the linearized model for $\gamma = 0.1$.
$-\cdot-$ U = 0.5; ---- U = 1.0; —— U = 1.5.
* Stalks fixed.
b. Corresponding non-linear results.

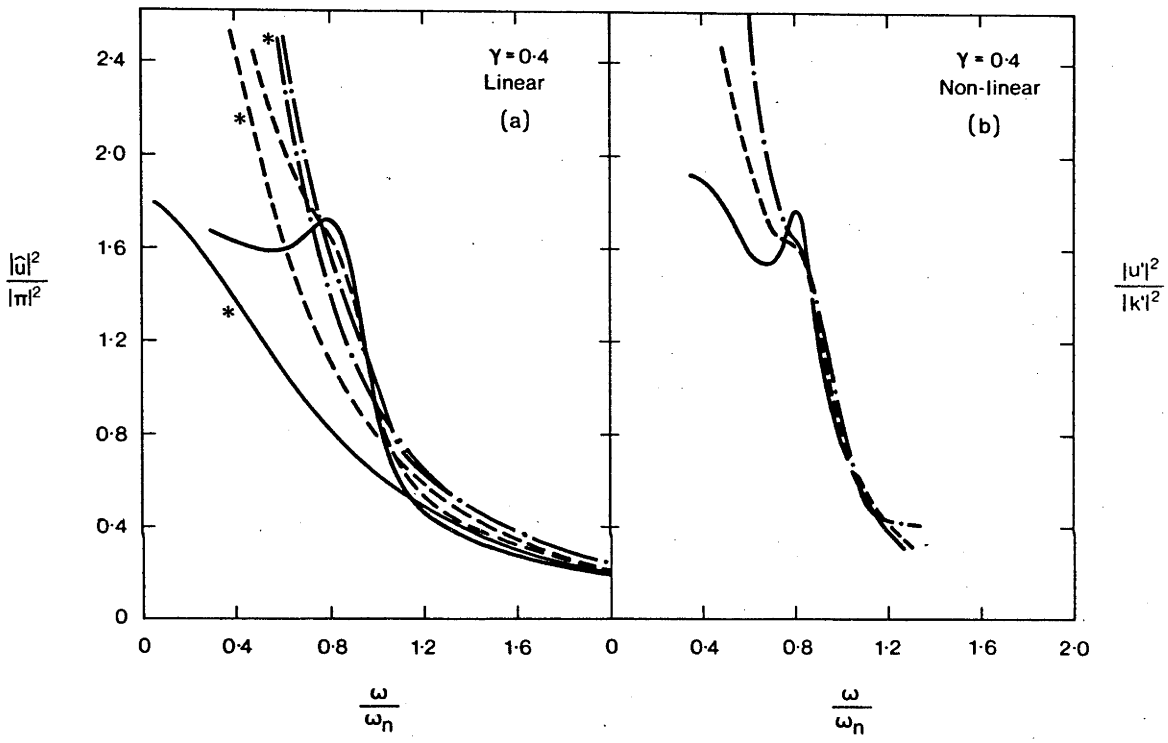

Fig. 8. a. Results of the linearized model for $\gamma = 0.4$.
— · — U = 0.125; --- U = 0.25; —— U = 0.375.
* Stalks fixed.
b. Corresponding non-linear results.

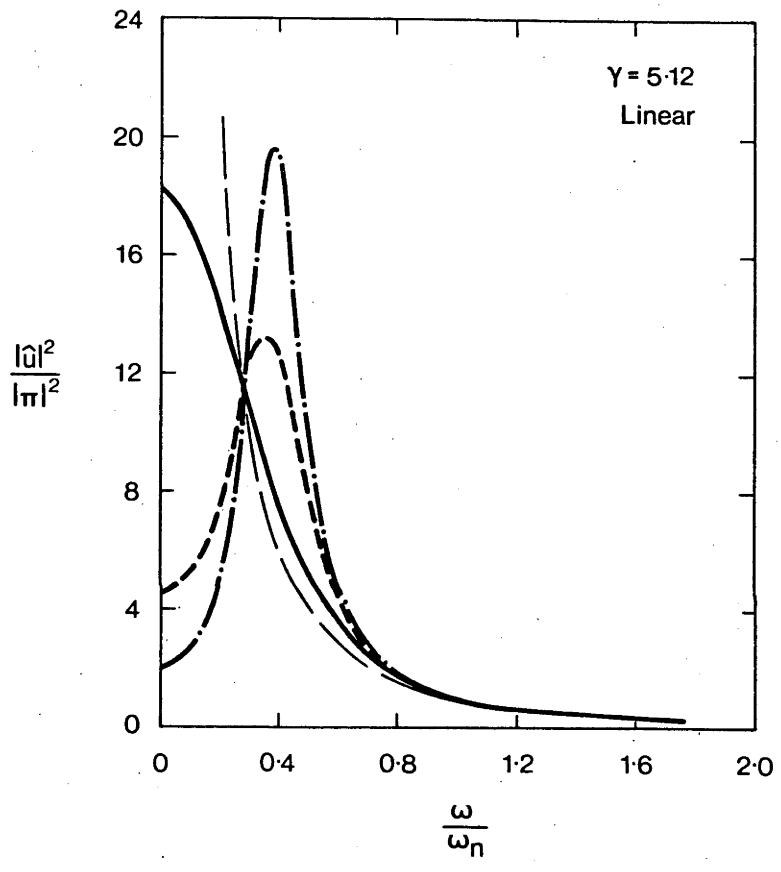

Fig. 9. Results of the linearized model for $\gamma = 5.12$.

— — — U = 0.0235; ——— U = 0.1175; --- U = 0.235;

— · — · — U = 0.3525.

From Equation (13) we can see that for very large and very small values of γ, the peak of the u/π vs. ω/ω_n curve approaches $\omega = 0$. In the case of very large γ this is a consequence of increased aerodynamic damping and its effect can be seen in Figure 9 in the reduction of the resonant peak to $\omega/\omega_n \simeq 0.5$.

Finally in Figure 10 we see the relationship of the root mean square relative velocities of the air past the stalks when they are waving and when they are fixed; that is the fluctuating parts of the linearized drag. This ratio decreases with increasing wind speed (as expected from the foregoing results) and has a minimum value which moves towards smaller values of γ as U increases. The effect of increasing canopy density is more clearly seen in the trajectories of increasing β, with α and $\bar{u}$ held constant. These indicate a rapid decrease in the ratio, $\frac{u-dy/d\tau}{u}\Big|_{\text{stalks fixed}}^{\text{stalks waving}}$ as β increases, the trend being most marked at small values of γ.

Linearization

A particularly intriguing feature of these results is the close correspondence between the linear and non-linear solutions, particularly at the higher values of U or lower values of γ. This correspondence continues even when the non-linear cases have turbulence intensities as high as 70% where the linearizing assumptions are completely violated. This is a consequence of the peculiar nature of the aerodynamic term, $(u' - \frac{dy'}{d\tau})\left| u' - \frac{dy'}{d\tau} \right|$, which acts to suppress higher harmonics.

We can illustrate this effect by letting $u - \frac{dy'}{d\tau}$ equal $\sin \tau$; then

$$(u' - \frac{dy'}{d\tau}) \left| u' - \frac{dy'}{d\tau} \right| \equiv (U + \sin \tau) \left| U + \sin \tau \right| . \qquad (15)$$

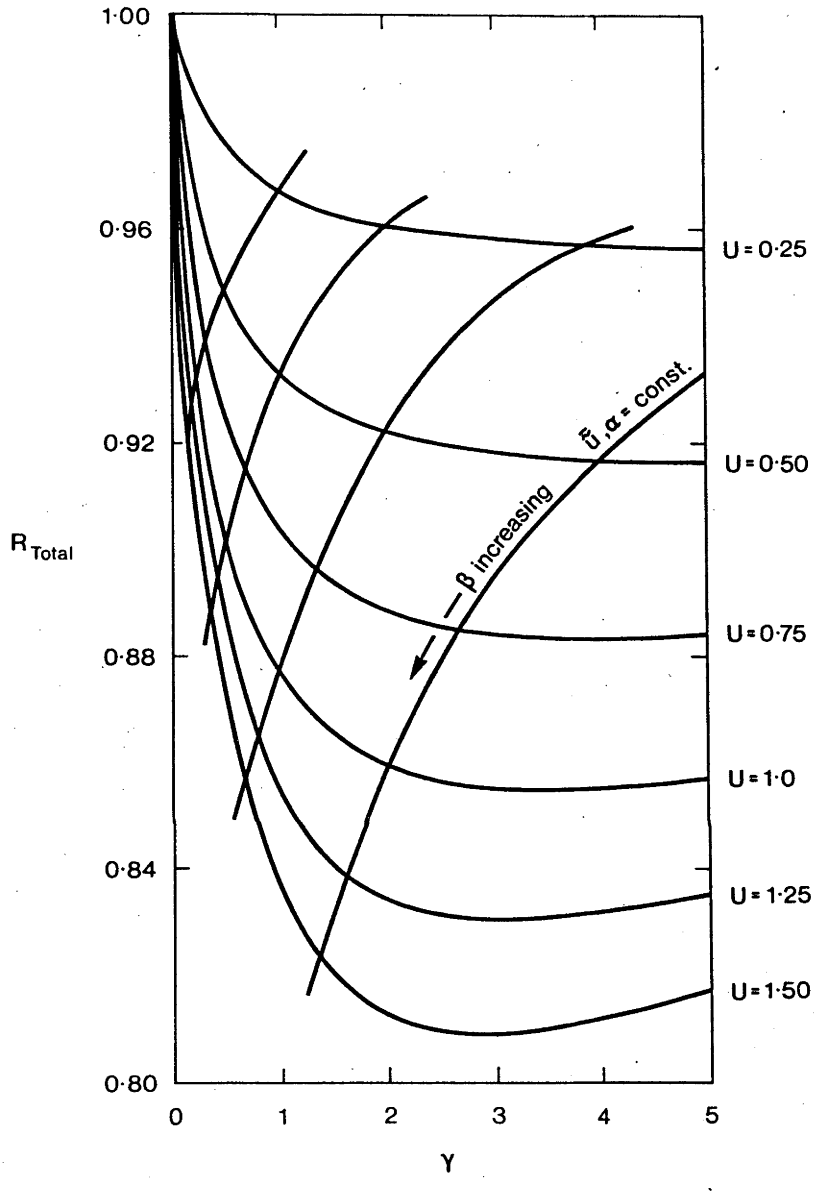

Fig. 10. Ratio of the fluctuating parts of the linearized drag term with the stalks fixed and free to wave.

If we form the Fourier series $F(\tau)$ of the right hand side of Equation (15), then

$$F(\tau) = a_0 + \sum_{n=1}^{\infty} \left[a_n \cos n\tau + b_n \sin n\tau \right] = (U + \sin \tau) \left| U + \sin \tau \right| \qquad (16)$$

In Table II we present the power contained in the first three higher harmonics, $(a_n^2 + b_n^2)\big|_{n = 2, 3, 4}$ divided by the power of the first harmonic, $(a_1^2 + b_1^2)$ for values of U between 0 and 0.9. For the cases considered, the power in any higher harmonic is at most 11% of the power in the fundamental.

4. Comparison with Wind Tunnel Results

In order to test the predictions of this idealized model against the behaviour of some actual waving canopies, we have calculated values of α and β appropriate to two wind tunnel model flexible canopies. The canopies are aeroelastic models of wheat fields and the criteria used to define their size, density and flexibility are discussed in Finnigan and Mulhearn (1978).

Both wind tunnel models consisted of stalks of nylon, 5 cm high and 0.025 cm in diameter, and individual stalks vibrated with a frequency of about 31 Hz. The stalks were arranged in a square grid with their bases clamped between strips of hardboard. The clamping pressure could be varied to adjust the damping. The density of stalks in the two canopies was 1 and 2 stalks/cm^2 for the sparse and dense cases respectively.

The models were tested in the CSIRO Division of Environmental Mechanics wind tunnel where an atmospheric boundary layer had been simulated. A full description of the tunnel and the present experimental set up can be found in Mulhearn et al. (1976) and Finnigan and Mulhearn (1978) respectively. The arrangement of the dense model canopy in the wind tunnel is shown in Figure 11.

TABLE II. Ratio of power in nth Fourier coefficient of $(U - \sin\tau)|U - \sin\tau|$ to the power in the fundamental.

U	$\frac{(a_2^2 + b_2^2)}{(a_1^2 + b_1^2)}$	$\frac{(a_3^2 + b_3^2)}{(a_1^2 + b_1^2)}$	$\frac{(a_4^2 + b_4^2)}{(a_1^2 + b_1^2)}$
0	0	0.0402	0
0.1	9.6×10^{-3}	0.037	3.7×10^{-4}
0.2	0.034	0.029	1.2×10^{-3}
0.3	0.064	0.0194	1.75×10^{-4}
0.4	0.089	0.011	1.75×10^{-3}
0.5	0.103	5.1×10^{-3}	1.27×10^{-3}
0.6	0.107	1.85×10^{-3}	6.7×10^{-4}
0.7	0.101	4.7×10^{-4}	2.3×10^{-4}
0.8	0.090	6.5×10^{-5}	4.2×10^{-5}
0.9	0.076	2.1×10^{-6}	1.8×10^{-6}

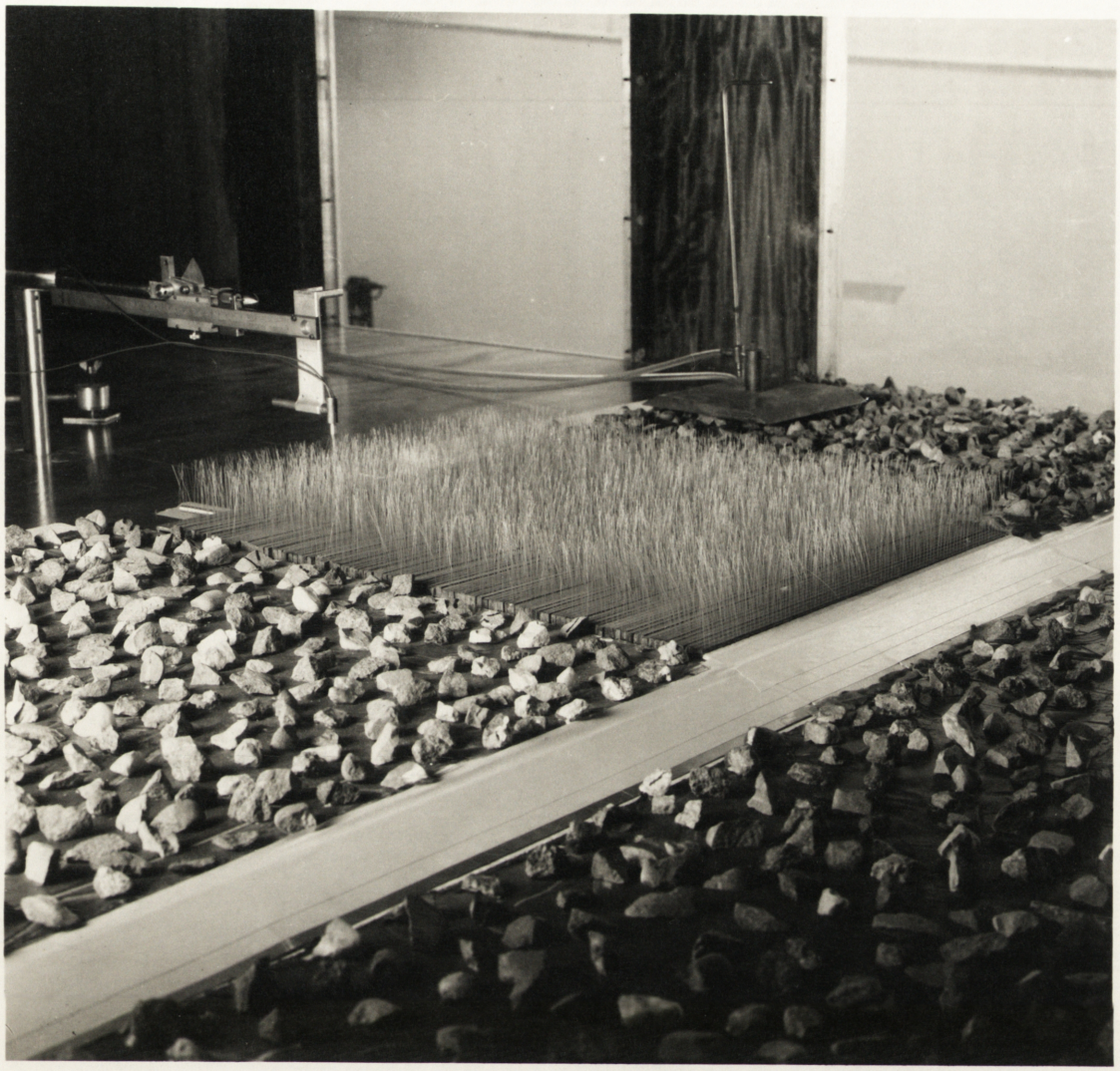

Fig. 11. Model canopy in the wind tunnel.

Power spectra of streamwise velocity fluctuations in the two canopies were obtained by using DISA model 55P61 hot wire 'X' probes connected to two channels of Thermo-Systems Inc. model 1050 anemometry and linearizing and transforming the velocity time records obtained with the digital computer system described in Section 3.

Power spectra of streamwise fluctuations in the two models are plotted in Figure 12. The measurements were made 5 mm below the top of the canopies and the mean velocity at the stalk height was 7 m/s in each case. In the dense model canopy the influence of the waving stalks is immediately obvious in the strong peak at the waving frequency but this is completely absent in the case of the sparse model. Figure 13 shows the results of solving the linearized equations, (8) and (9), with the values of γ, ξ' and $\bar{U}$ corresponding to the two models. Although the simple mathematical model cannot produce representative spectra, the qualitative agreement is satisfactory.

5. Conclusions

A simple one-dimensional mathematical model has been developed to give a qualitative measure of the effect of plant spacing, flexibility, leafiness and mean wind speed upon the fluctuations in airflow within a living canopy. The fluctuations in velocity per unit kinematic pressure gradient as a function of frequency for various practical values of plant spacing, drag coefficients and mean velocity can be calculated from the analytical solutions of the linearized equations.

An increase in either mean wind speed or plant density enhances the effect of the stalks' waving upon the velocity, although increased canopy density also leads to a greater overall attenuation of the fluctuations at all frequencies. Increasing the leafiness or drag coefficient (or decreasing the mass) of individual plants in a stand of

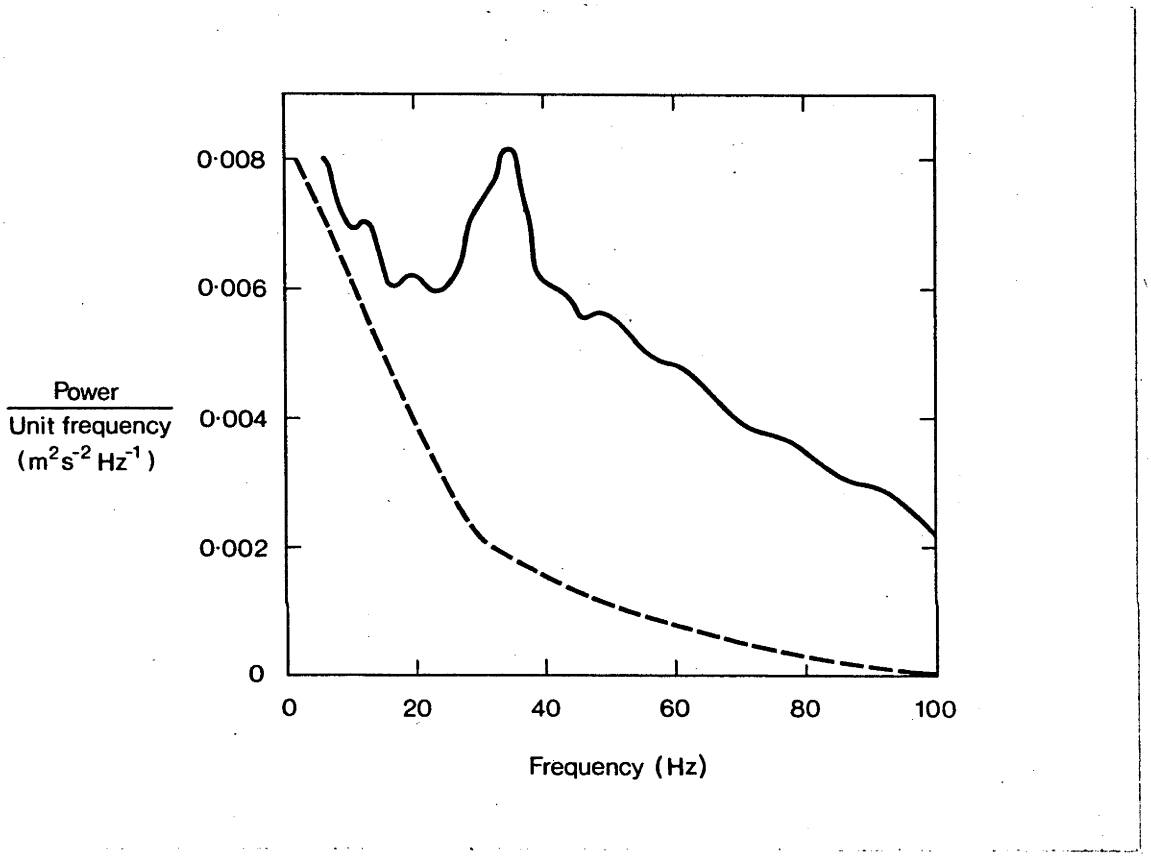

Fig. 12. Power spectra of streamwise velocity in two aeroelastic model canopies of different density. ——— dense; — — — sparse.

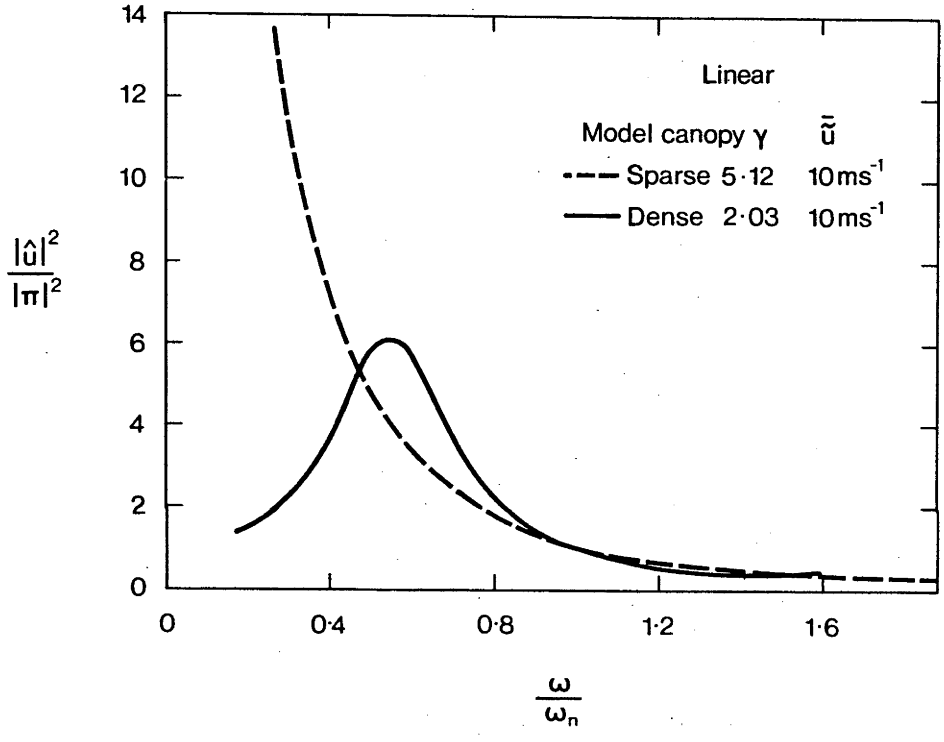

Fig. 13. Results from the linear model corresponding to the two canopies in Figure 12.

constant density greatly increases the influence of waving on the airflow, but the dependence of this effect upon the mean velocity becomes much stronger. The increased aerodynamic damping of individual plants causes a large reduction in the resonant frequency of the system. The results from the non-linear and the linearized equations are similar, even when the linearizing assumptions are grossly violated; this is a result of the nature of the aerodynamic drag term which acts to suppress higher harmonics.

Finally, comparing the predictions of the linearized theory with measurements upon two aeroelastic wind tunnel model canopies, with different stalk spacings, we obtain a satisfactory agreement which tends to support the use of the model for qualitative predictions. Any property of a canopy which might be directly affected by the interaction between the waving and the airflow, for instance, the overall momentum absorption or the turbulence intensities in the upper parts of a canopy, should exhibit a stronger dependence upon mean wind speed as the canopy density decreases.

References

Cionco, R.M.: 1965, 'A mathematical model for airflow in a vegetative canopy', J. Appl. Meteorol. 4, 517-522.

Cowan, I.R.: 1968, 'Mass, heat and momentum exchange between stands of plants and their atmospheric environment', Q.J.R. Meterorol. Soc. 94, 523-544.

Finnigan, J.J. and Mulhearn, P.J.: 1978, 'Modelling waving crops in a wind tunnel', Boundary-Layer Meteorol. 14, 253-277.

Fraser, D.: 1978, 'An optimised mass storage FFT, Assoc. of Comp. Mach.', Trans. on Math. Software (in press).

Mulhearn, P.J., Banks, H.J., Finnigan, J.J., and Annis, P.G.: 1976, 'Wind forces and their influence on gas loss from grain storage structures', J. Stored Prod. Res. 12, 129-142.

Seginer, I.: 1974, 'Aerodynamic roughness of vegetated surfaces', Boundary Layer Meteorol. 5, 383-393.

Thom, A.S.: 1971, 'Momentum absorption by vegetation', Q.J.R. Meteorol. Soc. 97, 414-428.

Thomson, W.T.: 1965, Vibration Theory and Applications, George Allen and Unwin Ltd., London.

CHAPTER 6

PRELIMINARY WIND-TUNNEL MEASUREMENTS IN A LARGE, AEROELASTIC MODEL CANOPY

Abstract. A large aeroelastic model canopy has been constructed in accordance with the design criteria advanced in Chapter 4. It was installed in the CSIRO Division of Environmental Mechanics wind tunnel and preliminary tests have been performed. Measurements of turbulent velocity fluctuations with an X wire indicate that over the rear one-third of the canopy, approximately equilibrium flow has been established at all but the highest windspeeds.

1. Introduction

Following the apparent success of the prototype model canopy, described in Chapter 4, in simulating some of the features of a real wheat field, a larger model was constructed so that equilibrium flow conditions could be achieved. The measurements in the real wheat field stress the importance of correctly modelling the boundary layer above the canopy before attempting to study the flow within. To investigate further the phenomena described in Chapters 2 and 3 and to test the predictions of the mathematical model of Chapter 5, the wind tunnel simulation must also extend over an adequate range of wind speed.

The problems of exploiting the analogy between fully developed rough wall turbulent boundary layers and the lower part of the atmospheric boundary layer have been discussed by several authors, for example Cermak and Arya (1970). Equilibrium atmospheric boundary layers in neutral conditions (z/L small, where L is the Monin-Obhukov length) and where Coriolis forces are negligible are well represented by the inner region of fully developed turbulent boundary layers over aerodynamically rough surfaces. Neutral conditions in the atmosphere are the exception rather than the rule, but on days of strong wind over a rough surface such as a wheat field, a logarithmic profile at least 5 m in depth might be expected, even during times of strong insolation (Lumley and Panofsky, 1964). In neutral conditions the log region would be at least 20 m in depth over such terrain.

Because of the lower limit on the size of a wind tunnel model canopy imposed by the requirements of fully turbulent flow around the

stalks, and the purely practical details of construction, a relatively thick tunnel boundary layer is needed, if the logarithmic layer is not to be disproportionately thin relative to the canopy height. Measurements in fully developed turbulent layers over very rough walls by Blake (1970) and Burton (1971) show that the logarithmic region occupies about 15-20% of the total boundary layer thickness. In some wind tunnels, sufficient fetch is available to allow thick boundary layers to grow naturally. This is certainly the best strategy to adopt if practical and has been used by Meroney (1968), Kawatani and Meroney (1970), Hsi and Nath (1970) and Plate and Quraishi (1968) in the very large Colorado State University Wind Tunnel.

More often though, faced with a limited extent of wind tunnel working section, it is necessary to artificially thicken the boundary layer in the hope that it will then come to equilibrium with the model surface within the fetch available. Practical solutions to this problem have been proposed by, amongst others, Counihan (1969, 1970, 1973), Cook (1973) and Teunissen (1975). In the present case, a modification of the scheme, successfully used for flow over a very rough random surface of stones by Mulhearn and Finnigan (1978), is used. Measured turbulence statistics will be presented to demonstrate the development and final form of the boundary layer over the model.

2. Experimental Arrangement

The model canopy was installed in the CSIRO Division of Environmental Mechanics wind tunnel, an open return-circuit tunnel with a working section

1.83 m wide, 11 m long and 0.6 m high at the end of the contraction. The roof height is adjustable so that a zero pressure gradient can be maintained in the working section, despite the growing boundary layer. Static pressure tappings are spaced every .92 m along the roof centreline to measure the pressure gradient. A more detailed description of the wind tunnel can be found in Mulhearn et al. (1976) and Wooding (1968).

The model canopy was constructed in exactly the same way as the prototype described in Chapter 4. The canopy was 1.83 m wide (spanning the working section) and 3.35 m in streamwise extent. The model stalks, of 0.25 mm diameter nylon line, were 5 cm high and had a natural frequency of vibration of about 30 Hz. The model canopy was placed in the tunnel, 3 m downstream of the end of the contraction and was preceded by 3 m of very rough surface, consisting of pieces of gravel roughly 1.5 cm in diameter, glued to wooden boards in a random pattern. 1.4 m of this same rough surface were placed downstream of the canopy and the canopy floor and the surface of the 'gravel' boards were adjusted to the same level. A 5 cm high, solid aluminium fence was placed across the floor of the tunnel just before the first section of rough surface to initiate the formation of a thick turbulent layer. The experimental setup with exact dimensions is drawn in Figure 1a.

A traverse gear which could be placed at any streamwise station and traversed both vertically and horizontally was used to obtain turbulence profiles. The sensor used was a Disa type 55P63 X wire anemometer probe, connected to two channels of Thermo-Systems Inc. model 1050 hot wire anemometry. Signals were low pass filtered below 500 Hz, and sampled digitally at 1 kHz by a PDP 11/40 computer where

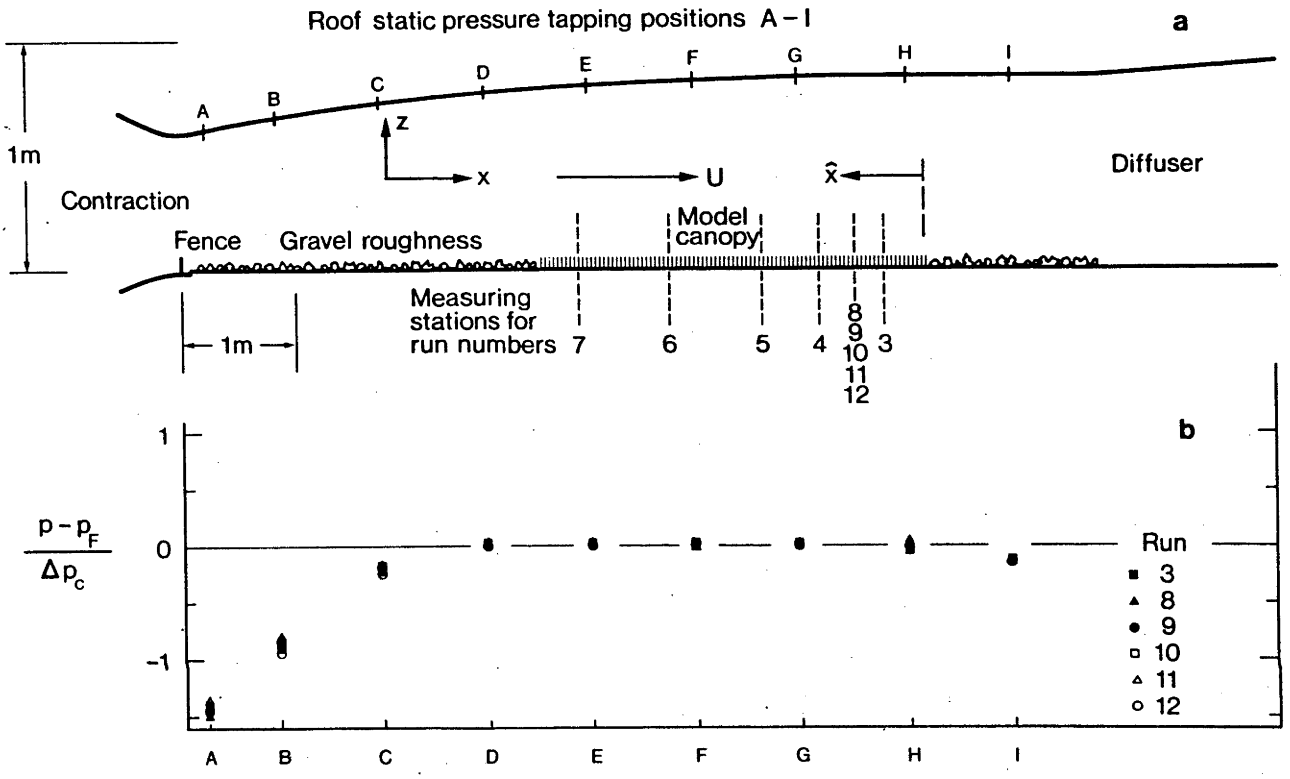

Fig. 1. (a) Schematic view of experimental arrangement showing positions of measuring stations and static pressure tappings; (b) Variation of static pressure along working section, normalised with pressure drop across the contraction. Horizontal co-ordinates correspond to 1a.

they were linearized using predetermined calibration data and subsequently processed.

Static pressures were measured by a Betz manometer with a resolution of 0.025 Pa. General views of the wind tunnel setup are presented in Figure 2.

3. Results and Discussion

All turbulence profiles were measured on the wind tunnel centreline. x and z co-ordinates are defined in Figure 1a; $\tilde{u}$ is the instantaneous velocity parallel to x and $\tilde{w}$ parallel to z. $\tilde{u} = U + u$ where $U = \overline{\tilde{u}}$ and $\overline{\ }$ denotes a time average. Similarly $\tilde{w} = W + w$. Run numbers 3, 4, 5, 6 and 7 refer to profiles measured at $\hat{X}$ = .35, .85, 1.35, 2.10, and 2.85 m respectively, where $\hat{X}$ is measured positive upwind from the rear edge of the canopy. Runs 8 - 12 inclusive were all made at $\hat{X}$ = .60 m.

Before any traverses were made, the height of the roof was adjusted to give a zero pressure gradient over the canopy. The pressure difference between pressure hole, F, one third of the way down the canopy (see Figure 1a) and the other holes, non-dimensionalised with the pressure drop across the contraction, Δp_c is presented in Figure 1b. Data are plotted for Runs 3, 8, 9, 10, 11 and 12. It was realised that the solid and wake blockage of the traverse gear would affect downstream holes during Runs 4, 5, 6 and 7 but spot checks during these runs revealed no measurable change in the gradient upstream of the measuring station. The results were normalised with the contraction pressure drop since this

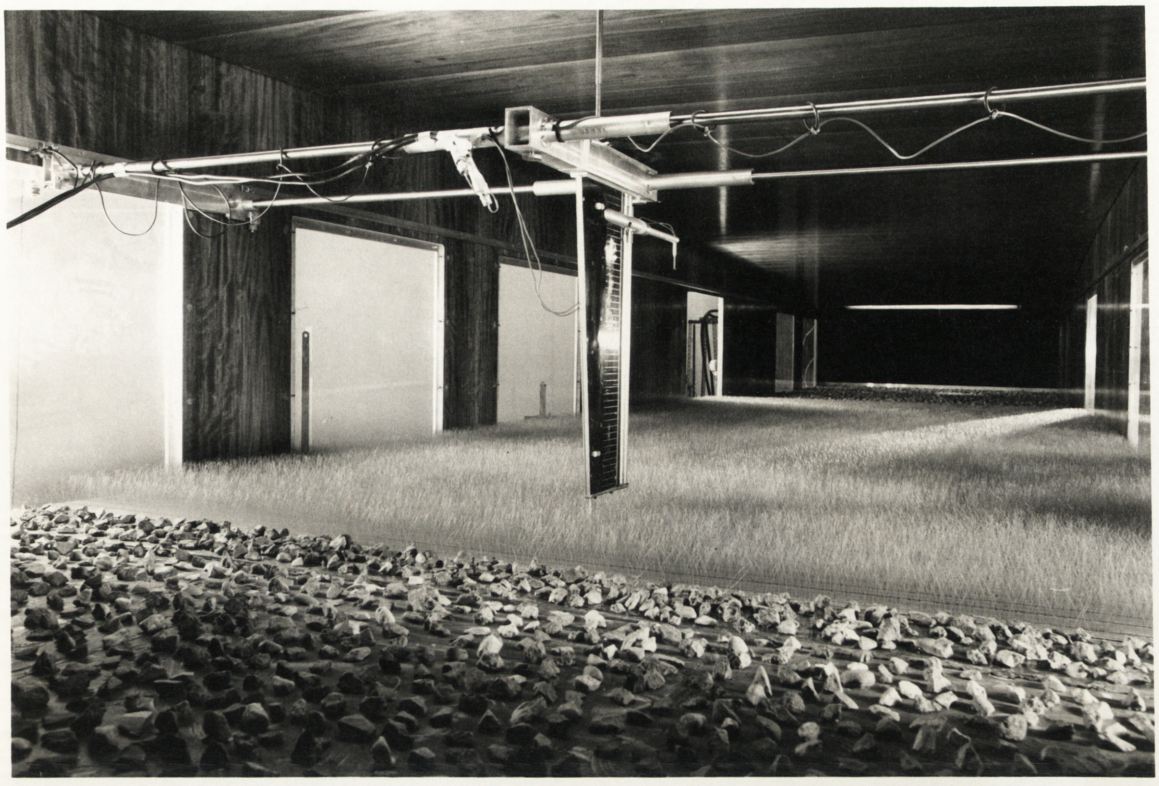

Fig. 2. General views of canopy in the wind tunnel illustrating traverse gear.

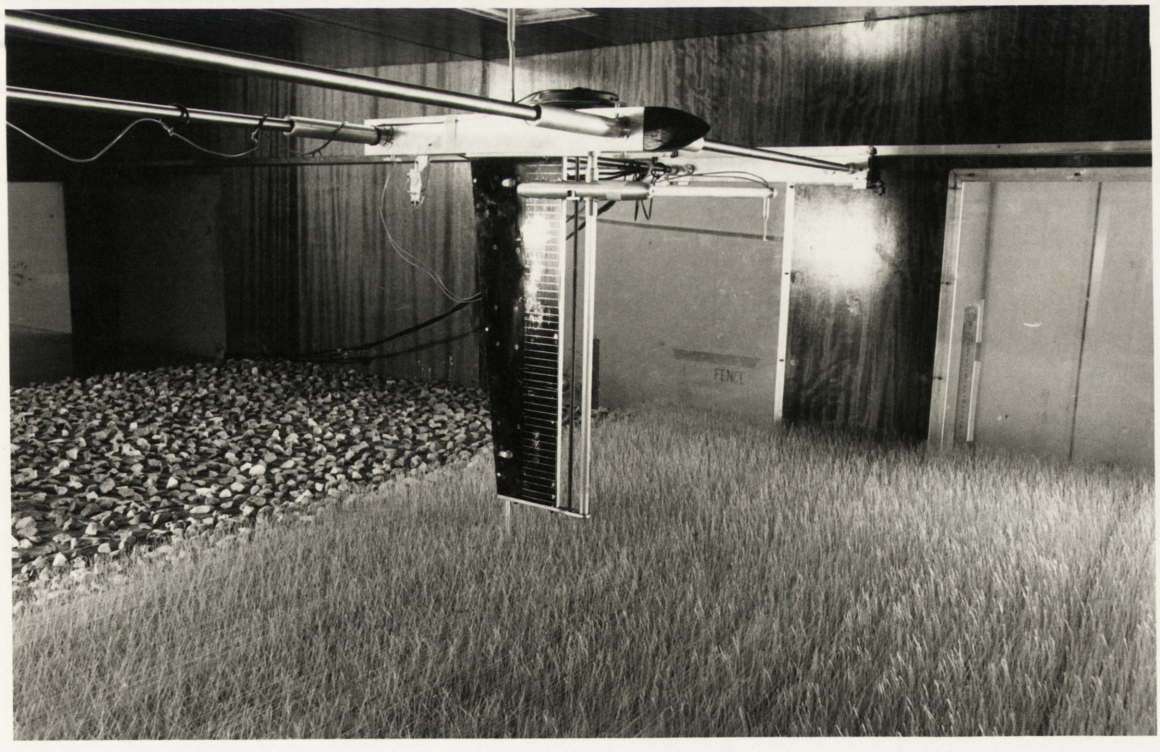

measurement was unaffected by the streamwise position of the traverse gear. In Figure 3, the variation of Δp_c with $\frac{1}{2}\rho U^2(42)$ where U(42) is the mean velocity measured by the X wire, .42 m above the wind tunnel floor, is plotted. $d[\frac{1}{2}\rho U^2(42)]/d\ \Delta p_c$ is approximately 1.40. It can be seen from Figure 1b that, over the extent of the canopy, the static pressure variation is less than .5% of the dynamic head at .42m. The deviation at hole I is presumably a result of blockage by the traverse mechanism.

In the initial part of the working section the airflow encounters a strong adverse pressure gradient. Combined with the upwind fence and the rough surface, this causes a rapid thickening of the boundary layer. The measurements of Bradshaw and Ferris quoted by Tani (1968) in a flat plate turbulent boundary layer after a change from an initial sharp adverse pressure gradient to a zero gradient, showed perturbations to shear stress and streamwise turbulence intensity profiles more than 10 boundary layer thicknesses downwind of the change. In the present case, however, it was hoped that the increased mixing in the rough wall layer would more rapidly remove the effect of the initial region. The results of Perry and Joubert (1963) in a rough wall turbulent layer with an adverse pressure gradient suggest that, close to the wall, the effect of the pressure gradient is not felt directly, the velocity profile there continuing to scale on wall variables. The results of Bradshaw and Ferris, however, quoted in Bradshaw (1976), showed that after the removal of the adverse pressure gradient, the turbulent energy balance in the outer part of the flow was perturbed long after the inner layer had returned to equilibrium.

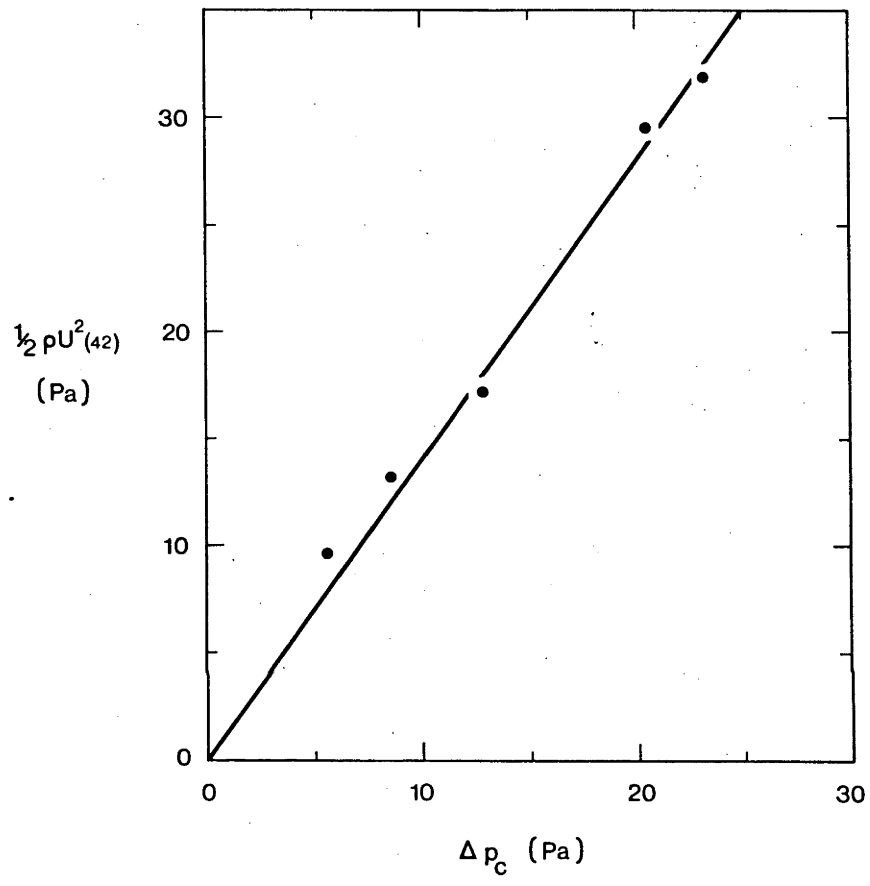

Fig. 3. Variation of dynamic head at z = .42 m with pressure drop across contraction from Runs 8-12.

The development of the mean velocity profiles over the canopy at successive $\hat{X}$ stations is shown in Figure 4 from Runs 3 - 7. The shape of the curves is apparently quite insensitive to streamwise position. The profiles of Reynolds stress, $-\overline{uw}$, at the same $\hat{X}$ stations are plotted in Figure 5. They are much more indicative of the state of the boundary layer as it adjusts to the new surface. At z = .42 m, $-\overline{uw}$ remains unchanged from its upstream value. Close to the top of the canopy however, $-\overline{uw}$ decreases from a value of 3.32 m^2 s^{-2} at $\hat{X}$ = 2.85 m, to 2.4 m^2 s^{-2} at $\hat{X}$ = .85 and .35 m, suggesting that the characteristic 'overshoot' of shear stress upon encountering a surface of different roughness has occurred. This phenomenon has been noted by Tani (1968) for both smooth-rough and rough-smooth changes and can be seen in the data of Antonia and Luxton (1971a) after a smooth-rough transition.

The last two profiles at $\hat{X}$ = .35 and .85 m are within ± 5% of their mean value of 2.4 m^2 s^{-2} for about three canopy heights above the top of the stalks.

A new measuring station was selected therefore, midway between the last two at $\hat{X}$ = .60 m, and a series of five profiles was taken at different velocities (Runs 8-12 inclusive). Streamwise and vertical turbulence intensities, $[(\overline{u^2})^{\frac{1}{2}}/U, (\overline{w^2})^{\frac{1}{2}}/U]$ and normalized friction velocity, u_*/U $[u_* = (-\overline{uw})^{\frac{1}{2}}]$ from these traverses are plotted in Figure 6. The mean velocity at z = .42 m for each profile is included on the plot. It is obvious from the excellent collapse of i_u, i_w and u_*/U, that the flow is fully turbulent down to the lowest windspeed and that the general characteristics of the turbulence are identical in each case.

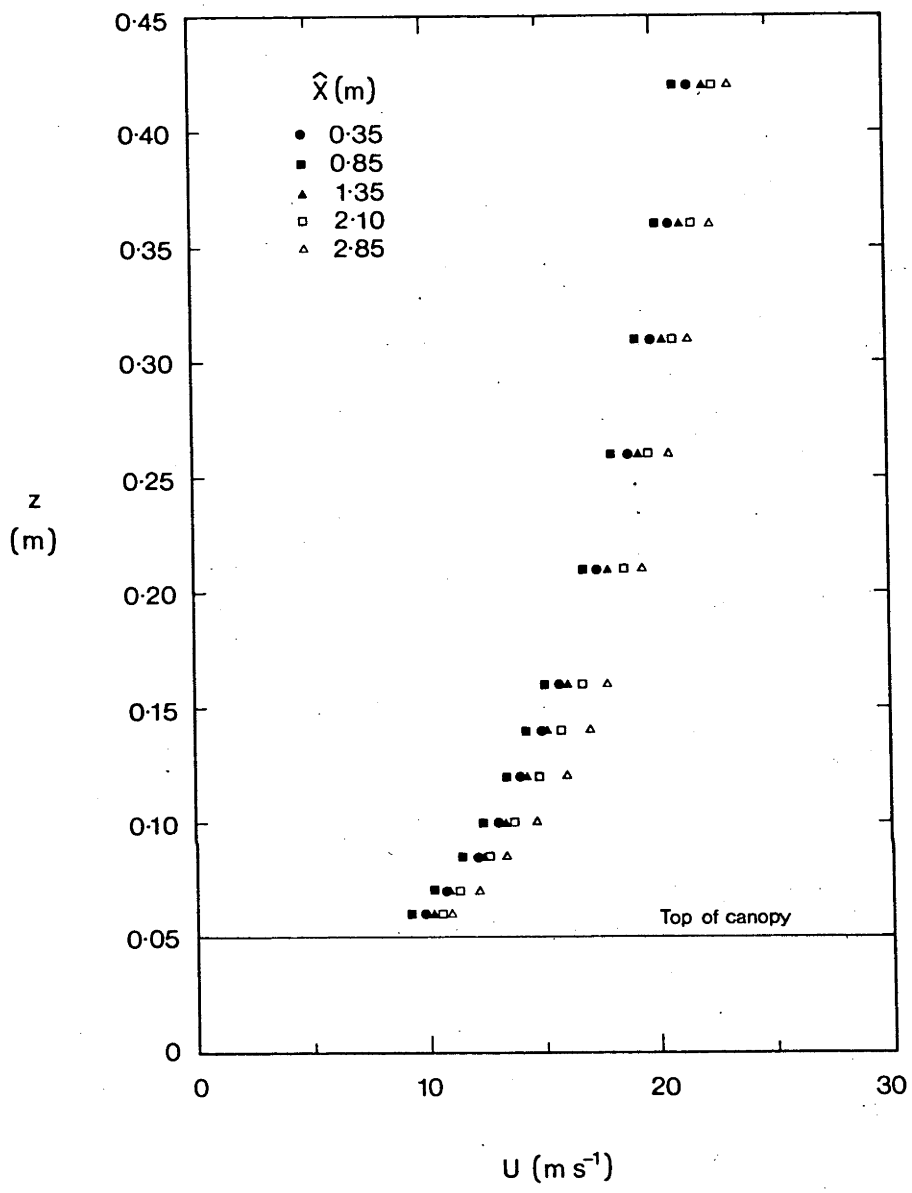

Fig. 4. Mean velocity profiles at various $\hat{X}$ stations from Runs 3, 4, 5, 6, 7. Δp_c = 20.5 Pa.

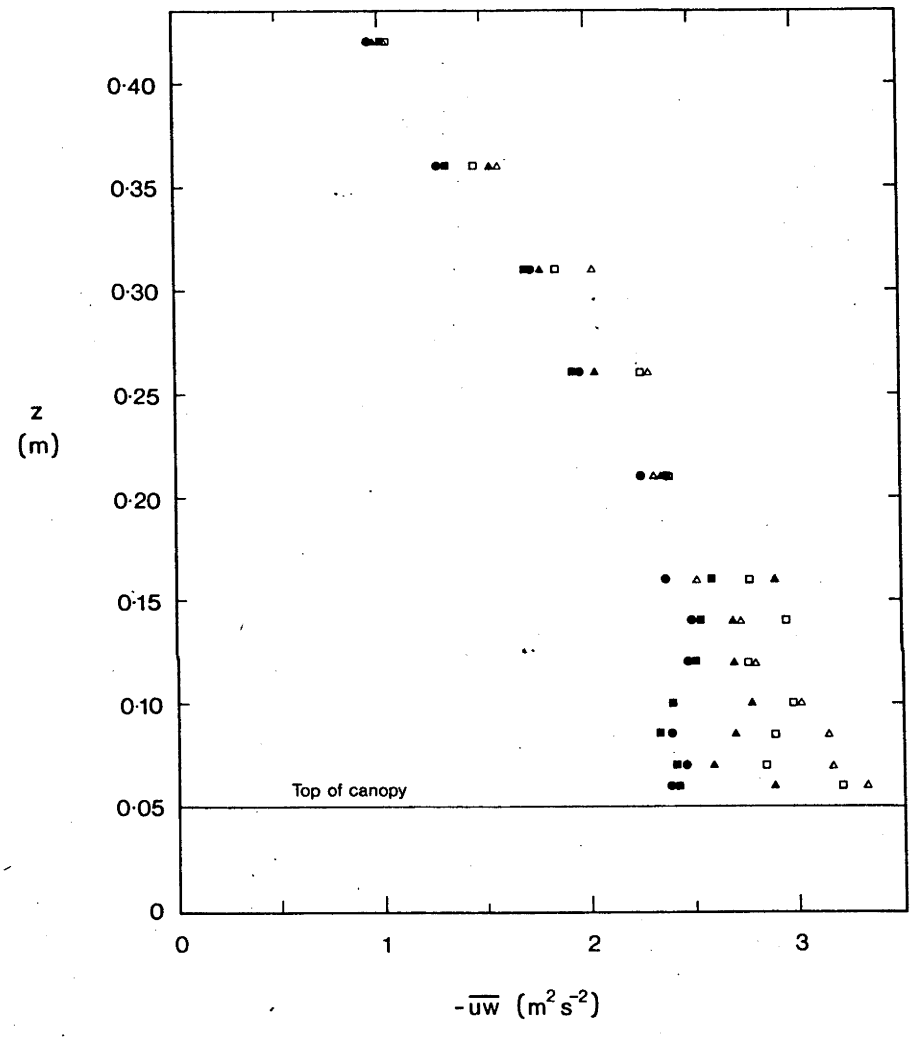

Fig. 5. Profiles of shear stress, $-\overline{uw}$ at various $\hat{X}$ stations from Runs 3-7. Symbols as in Figure 4.

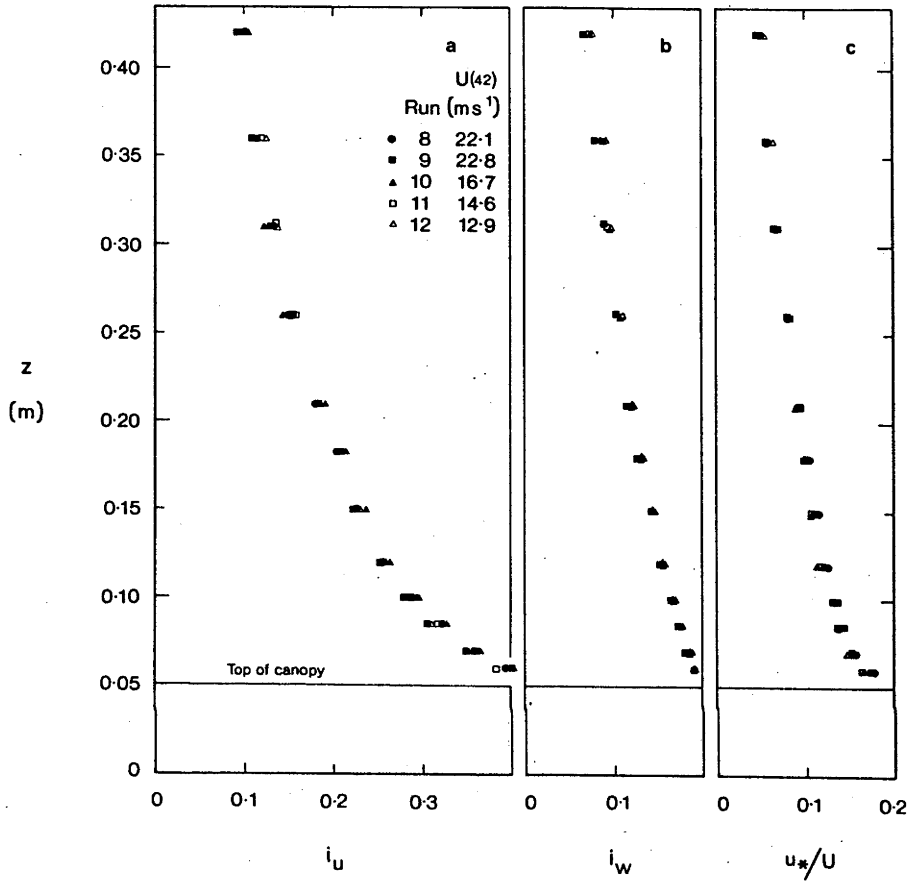

Fig. 6. (a) Profiles of streamwise turbulence intensity, i_u at various mean velocities from Runs 8-12. $\hat{X}$ = 0.6 m; (b) Vertical turbulence intensity, i_w; (c) Normalised friction velocity, u_*/U.

The profiles of shear stress, $-\overline{uw}$, for the same runs, plotted in Figure 7, show a similar depth of 'constant' stress layer at each windspeed. The three lower speed profiles show less relative variation in $-\overline{uw}$ up to a height of .21 m than do the higher speed runs, 8 and 9.

Plots of $\overline{u^2}$ and $\overline{w^2}$ from Run 10 are presented in Figure 8. The profile of $-\overline{uw}$ is included for comparison. It has been generally stated that $\overline{w^2}$ is constant in the lower atmosphere (Panofsky, 1974) but Dr. E.F. Bradley (private communication) reports that over a pine forest, $\overline{w^2}$ increases by about 40% between tree top level (16 m above ground) and a level 24 m above ground. The present data show an initial increase in $\overline{w^2}$ of about 30% between one and two canopy heights above the surface. $\overline{w^2}$ is then roughly constant to the top of the constant stress region where it starts to decrease. The decrease with height of $\overline{u^2}$ agrees, at least qualitatively, with atmospheric measurements (Panofsky, 1974).

In the same review, Panofsky states that typical atmospheric estimates for the ratios $i_u : i_w : u_*/U$ are 2.5 : 1.25 : 1 with a fair degree of uncertainty in the first two estimates. Taking $z = .16$ m, the middle of the constant region of $\overline{w^2}$, as a representative height, the present results give 2.08 : 1.34 : 1. The ratio $i_w : u_*/U$ is a little high but these estimates are well within the scatter of the atmospheric data. Furthermore the present measurements are closer to the underlying rough surface than most atmospheric results.

The vertical profile of mean velocity in the constant stress region of a boundary layer over tall roughness and in neutral stability has the form

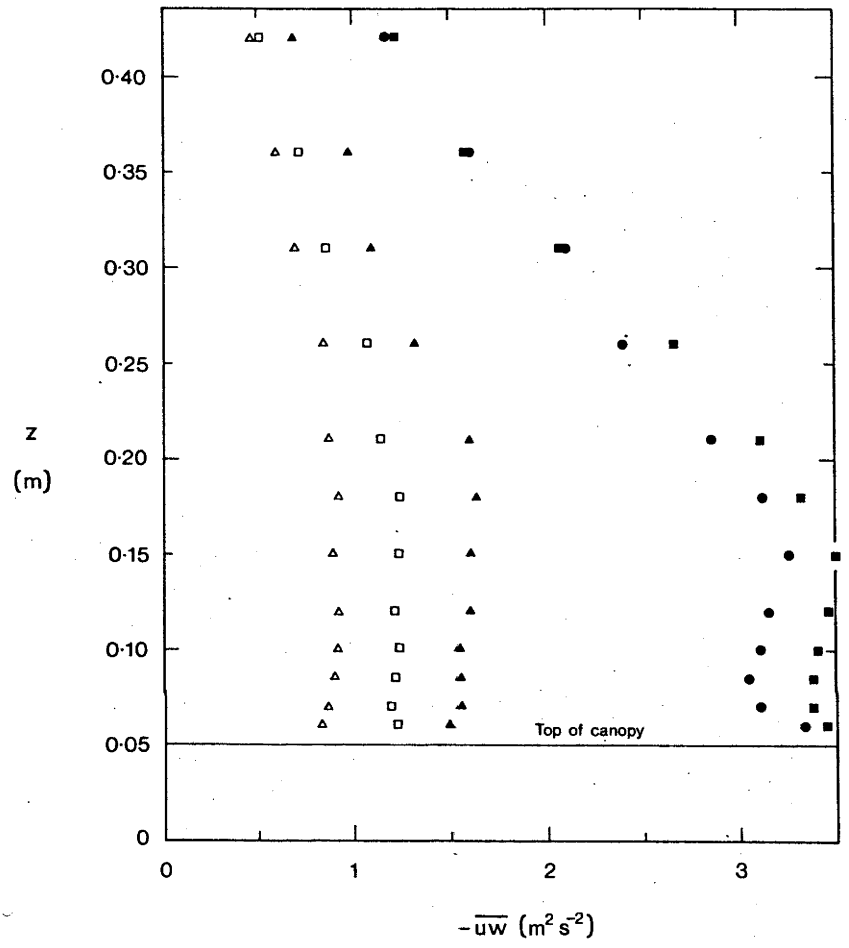

Fig. 7. Profiles of shear stress, $-\overline{uw}$, from Runs 8-12. Symbols as in Figure 6.

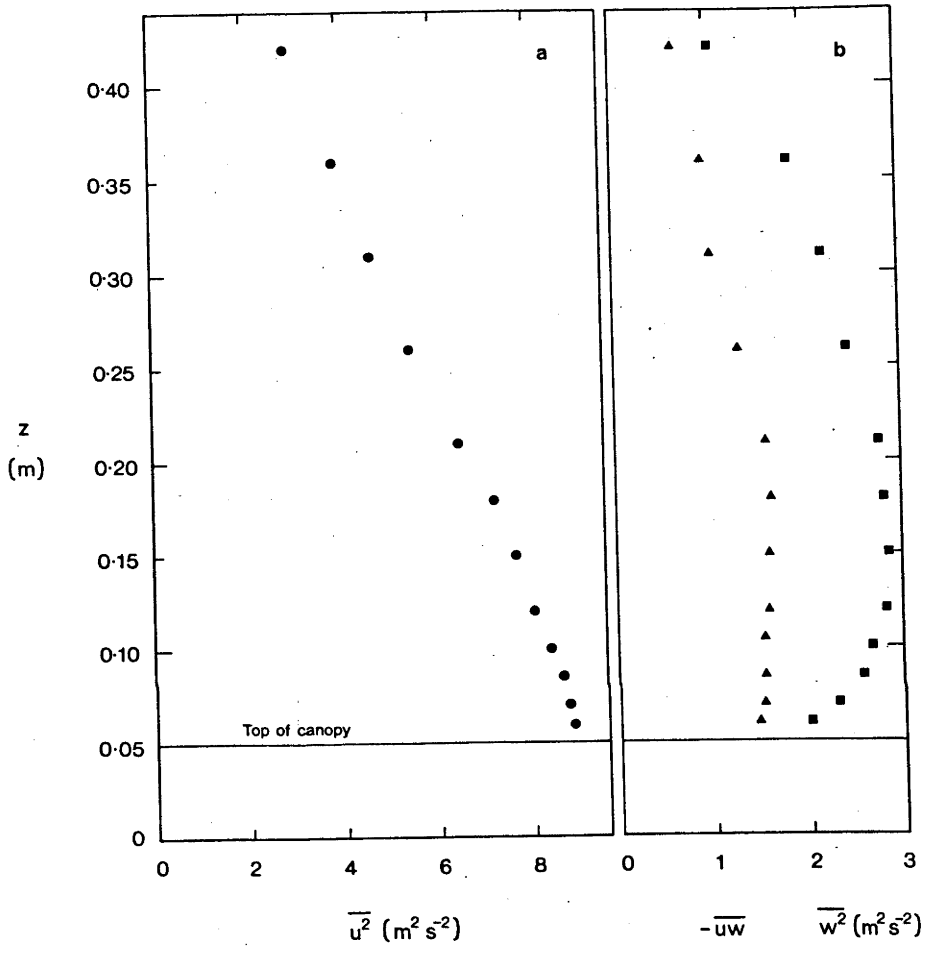

Fig. 8. (a) Profile of mean square streamwise fluctuations, $\overline{u^2}$, from Run 10; (b) Profiles of mean square vertical fluctuations, $\overline{w^2}$, and shear stress, $-\overline{uw}$, from Run 10. ▲, $-\overline{uw}$; ■, $\overline{w^2}$.

$$U = \frac{u_*}{\kappa} \ln \left[\frac{z-d}{z_o}\right] \qquad (1)$$

where z_o is the roughness length and d the displacement of the origin of the log profile from the surface. κ, Von Kármán's constant, has been taken as 0.4 in the present study. The velocity profiles from Runs 8 - 12 at $\hat{X}$ = .6 m have been plotted in logarithmic form in Figure 9. The departure of the profiles from logarithmic dependence on z - d coincides with the top of the constant stress region for Runs 10, 11 and 12 but occurs somewhat earlier in Runs 8 and 9 which were at a higher wind speed. The shape of the profiles is typical of measurements made in fully developed rough wall turbulent layers. See for example the results of Blake (1970) and Burton (1971).

To obtain Figure 9, the value of d, the zero plane displacement, was varied until the points lying in the constant stress region fell upon a reasonable straight line. No weight was given to the point closest to the canopy. z_o and u_* could then be determined from the intercept at U = 0 and the slope, dU/d [ln(z-d)]. Values of u_* derived in this way are compared with u_* from the X wire measurements in Table I. z_o and d are included in the table.

Runs 10, 11 and 12 show a satisfying agreement between the measured and inferred values of u_* and give values of z_o/H and d/H of 0.63 and 0.06 where H is the canopy height, 5 cm. d/H is close to the design intention of 0.6 but z_o/H is somewhat low compared to the intended value of 0.2. Both values, however, are within the scatter of field measurements. Profiles 8 and 9, however, do not agree well with the other runs. Equally good straight lines could

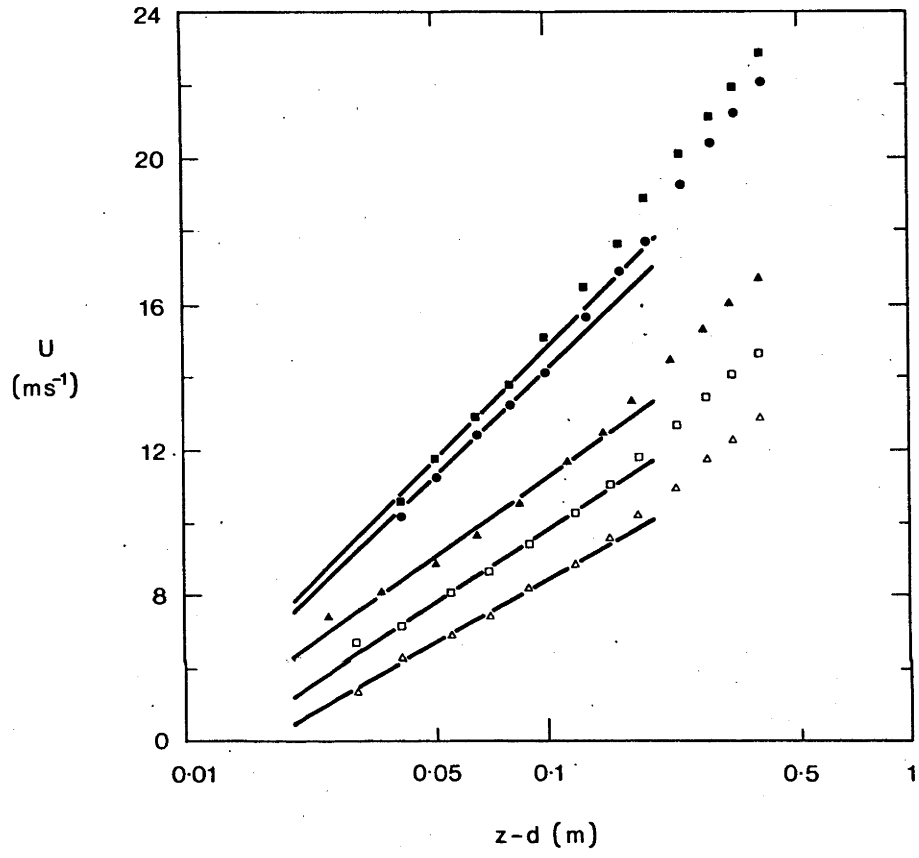

Fig. 9. Logarithmic plot of U against z - d from Runs 8-12. Symbols as in Figure 6.

be fitted through the data with u_* equal to 1.66 or 1.29 m s^{-1} for Run 8 and 1.74 or 1.38 m s^{-1} for Run 9. In the first case values of z_o and d were unacceptably low, whereas in the second there is a large discrepancy in u_* measured by X wire and log plot (see the asterisked values for 8 and 9 in Table I). The relatively large variation in $-\overline{uw}$ in the 'constant stress' regions of profiles of 8 and 9 compared to 10, 11 and 12 has already been remarked upon and it seems that equilibrium conditions may not be properly established at the higher wind speeds.

The measurements of Mulhearn and Finnigan (1978) in a boundary layer developed over a long fetch of the gravel surface, allow a direct comparison of the aerodynamic roughness of the upstream gravel and the canopy. If an approximate skin friction coefficient is defined as $C_f = -2\ \overline{uw}/U^2$ (42) for the present results and an analogous quantity derived from the gravel results (the comparison is not exact since in neither case is the highest velocity measured completely outside the boundary layer), then C_f(canopy) = 1.19 x 10^{-2} whilst C_f(gravel) = 0.85 x 10^{-2}. C_f(canopy) is an average value for Runs 8 - 12.

The gravel is apparently not quite as rough as the canopy but the difference is not great. Under these circumstances the main readjustment taking place in the flow over the canopy may well be a result of the abrupt change of effective surface level. In fully developed flow over the gravel, d = 1.2 cm while z_o = 0.38 mm.. Using the value of d from Runs 10 - 12, the effective change in surface level is 1.8 cm. In a future series of measurements, the effect of raising the upstream gravel surface to make this difference zero will be investigated.

TABLE I

Parameters of the logarithmic profile derived from Figure 9 and X wire results

Run No.	u_* (m s^{-1}) from X wire	u_* (m s^{-1}) from log plot	z_o (cm)	d (cm)
8	1.76	1.66	0.1	0.8
9	1.85	1.74	0.1	0.8
10	1.25	1.25	0.26	3.3
11	1.10	1.15	0.32	2.8
12	0.95	0.99	0.32	2.8
8^*	1.76	1.29	0.33	3.3
9^*	1.85	1.38	0.34	3.3

8, 8^*, 9 and 9^* are parameters for Runs 8 and 9 respectively, derived from Figure 9 with different values of z_o and d.

It is interesting to note that the profiles of $-\overline{uw}$ from Runs 8 - 12, which are plotted in Figure 7, are reasonably constant down to 1 cm above the top of the canopy. Mulhearn and Finnigan (1978) report an increase in $-\overline{uw}$ with height over the gravel surface, the depth of the region of appreciable $\partial(-\overline{uw})/\partial z$ being about twice the average stone spacing. Antonia and Luxton (1971b) found similar behaviour over their rough surface of two dimensional bars. In the case of the model canopy, two horizontal roughness length scales are possible. Applying the criterion of a region of finite $\partial(-\overline{uw})/\partial z$ of two times roughness spacing, the stalk spacing, 0.5 cm, would allow variation over a depth of only 1 cm. The average wave length, λ, of honami waves in the canopy can be estimated from the results of Chapter 2 as $\lambda \simeq 1.8\ U(H)/f$, where H is the canopy height and f the frequency of stalk vibration, giving $\lambda \simeq 0.6$ m. The random superposition of honami waves at a fixed point in the canopy however, should ensure that instantaneous perturbations to $\partial(-uw)/\partial z$, caused by varying surface geometry, would disappear in a long time average.

4. Conclusions

The developing boundary layer exhibits a reasonably thick constant stress region over roughly the last third of the model canopy. Profiles of streamwise and vertical turbulence intensities and u_*/U are identical for a range of windspeeds at a measuring station .60 m before the rear edge of the canopy, indicating essentially

identical turbulent processes at each wind speed. The mean velocity profiles show a well defined logarithmic dependence on z -d in the constant stress region at the three lower windspeeds. Values of u_* taken from the log plots agree well with u_* from X wire measurements. d and z_o averaged 0.63 H and 0.06 H respectively, the value of d being close to the design intention but z_o being somewhat low.

Plotting the mean velocities from Runs 8 and 9 in logarithmic form gave somewhat anomalous results. Equally good straight lines could be fitted to the data when d was either 0.8 cm or 3.3 cm. In the first case, u_* was close to the X wire measurement but the value of d was unreasonably low, whereas when d = 3.3 cm u_* was only 70% of the X wire value. The implication is that local energy equilibrium has not been established at the higher wind speeds and the logarithmic law does not apply.

A skin friction coefficient calculated from the X wire measurement was only about 20% higher than that measured in equilibrium conditions over the gravel roughness. Since this means that the shear stress balance will not undergo a drastic change on encountering the canopy, raising the upstream surface so that its effective zero plane corresponds with the canopy may speed up the establishment of equilibrium flow over the model at all wind speeds.

Future measurements will allow calculation of autocorrelation coefficients so that integral length scales may be compared with atmospheric values. Terms in the turbulent energy budget will also be computed to establish the nature of the energy

balance over the complex surface of the canopy and as a sensitive test of the approach to local equilibrium or self preservation of the developing boundary layer.

Acknowledgement

The author would like to thank Mr. Colin Hazelton of the CSIRO Division of Environmental Mechanics who designed and built the precision traverse gear which greatly facilitated these measurements and Mr O.A. Simakoff who constructed the model canopy.

References

Antonia, R.A. and Luxton, R.E.: 1971a, 'The Response of a Turbulent Boundary Layer to a Step Change in Surface Roughness. Part 1. Smooth to Rough', J. Fluid Mech. 48, 721-761.

Antonia, R.A. and Luxton, R.E.: 1971b, 'Energy Balance in a Turbulent Boundary Layer on a Rough Wall', Phys. Fluids 14, 1027-1029.

Blake, W.K.: 1970, 'Turbulent Boundary-layer Wall-pressure Fluctuations on Smooth and Rough Walls', J. Fluid Mech. 44, 637-660.

Bradshaw, P.(Ed): 1976, Topics in Applied Physics: Turbulence, Springer-Verlag: Berlin, 335 pp.

Burton, T.E.: 1971, On the Generation of Wall Pressure Fluctuations for Turbulent Boundary Layers over Rough Walls, Acoustics and Vibration Lab. Report No. 70208-4, Massachusetts Institute of Technology.

Cernak, J.E. and Arya, S.P.S.: 1970, 'Problems of Atmospheric Shear Flows and their Laboratory Simulation,' Boundary-Layer Meteorol. 1, 40-60.

Cook, N.: 1973, 'On Simulating the Lower Third of the Urban Adiabatic Boundary Layer in a Wind Tunnel', Atmos. Environ. 7, 691-705.

Counihan, J.: 1969, 'An Improved Method of Simulating an Atmospheric Boundary Layer in a Wind Tunnel', Atmos. Environ. 3, 197-214.

Counihan, J.: 1970, 'Further Measurements in a Simulated Atmospheric Boundary Layer', Atmos. Environ. 4, 259-275.

Counihan, J.: 1973, 'Simulation of an Adiabatic Urban Boundary Layer in a Wind Tunnel', Atmos. Environ. 7, 673-689.

Hsi, G. and Nath, J.H.: 1970, 'Wind Drag Within Simulated Forest Canopies', J. Appl. Meteorol. 9, 592-602.

Kawatani, T. and Meroney, R.N.: 1970, 'Turbulence and Wind Speed Characteristics Within a Model Canopy Flow Field', Agr. Meteorol. 7, 143-158.

Lumley, J.L. and Panofsky, H.A.: 1964, The Structure of Atmospheric Turbulence, Wiley-Interscience, New York. 239 pp.

Meroney, R.N.: 1968, 'Characteristics of Wind in and above Model Forests', J. Appl. Meteorol. 7, 780-788.

Mulhearn, P.J., Banks, H.J., Finnigan, J.J., and Annis, P.C.: 1976, 'Wind Forces and their Influence on Gas Loss from Grain Storage Structures', J. Stored Prod. Res. 12, 129-142.

Mulhearn, P.J. and Finnigan, J.J.: 1978, 'Turbulent Flow over a Very Rough, Random Surface', Boundary Layer Meteorol. (in press).

Panofsky, H.A.: 1974, 'The Atmospheric Boundary Layer Below 150 Meters', Ann. Rev. Fl. Mech. 6, 147-177.

Perry, A.E. and Joubert, P.N.: 1963, 'Rough-Wall Boundary Layers in Adverse Pressure Gradients', J. Fluid Mech. 17, 193-211.

Plate, E.J. and Quraishi, A.A.: 1965, 'Modelling of Velocity Distributions Inside and Above Tall Crops', J. Appl. Meteorol. 4, 400-408.

Tani, I.: 1968, 'Review of Some Experimental Results on the Response of a Turbulent Boundary Layer to Sudden Perturbations', In S.J. Kline, M.J. Morkovin, G. Sovran and D.J. Cockrell (eds), Proc. Computation of Turbulent Boundary Layers. AFOSR-IFP-Stanford Conference.

Teunissen, H.W.: 1975, 'Simulation of the Planetary Boundary Layer in a Multiple Jet Wind Tunnel', Atmos. Environ. 9, 145-174.

Wooding, R.A.: 1968, A Low-Speed Wind Tunnel for Model Studies in Micrometeorology, CSIRO Div. Plant Ind. Tech. Paper No. 25, 39 pp.

CHAPTER 7

CONCLUDING REMARKS

The results set out in Chapters 2 and 3 clearly show the primary role played by large gusts in determining the turbulence structure amongst the plants. The turbulence is in fact quite intermittent since only the stronger gusts penetrate effectively into the middle regions of the canopy. There is no reason why this behaviour should not apply to canopies in general and not just to waving cereal crops. This observation illustrates the basic difficulty of turbulent transport models based on mean quantities. When the velocity field is intermittent, or less restrictively, when it has a large turbulence intensity, the time average of any transfer process, which depends upon a power of velocity other than the first, cannot be expressed in terms of the mean velocity without obscuring the nature of the process. Obvious examples are aerodynamic drag, which varies with powers of $\tilde{u}$ between 3/2 and 2, and heat transfer, which expressed as Nusselt Number, varies like $\tilde{u}^n$ where $n \simeq 0.75$. With the physical details of the process hidden in derived coefficients, extension from particular experiments to general applications is unlikely to be very successful.

The turbulence generated close to a rough surface must reflect to some degree the character of that surface and a good deal of effort has been expended in attempting to relate the individual drag coefficients of surface roughness elements to the mean drag as expressed in, for instance, the parameters of the logarithmic profile, d and Z_o. Seginer (1974) presents a brief review of some of these theories. Their application is invariably limited to the particular type of roughness considered. The fact that the drag coefficient of bluff bodies in unsteady flow can be dominated by effects which disappear in steady flow, even steady flow with a component of small scale turbulence, is

always ignored. The waving canopies treated in this thesis represent an extreme example of this behaviour, the elastic stalks responding to the gusts by imposing a further, well defined length scale, the honami wavelength, onto the turbulent flow.

Within crops of only moderate height, such as cereal canopies, the effects of atmospheric stability are usually considered to be unimportant in all but the lightest winds. Because the plants are only about one or two metres in height, the ratio z/L, where L is the Monin-Obhukov stability length, is usually small. If the gustiness of the boundary layer flow some way above the crop is affected by stability however, we would expect this to be reflected in the canopy flow field. The 'gustiness' of the turbulent wind is expressed by the kurtosis of the velocity fluctuations, $\overline{u^4}/(\overline{u^2})^2$. Unfortunately, obtaining this quantity involves measuring the fourth moment of velocity and Lumley and Panofsky (1962) have shown that, for Gaussian velocity distributions, to determine fourth order moments to the same accuracy as second order moments, requires more than five times the averaging period. Referring to the discussion in Chapter 2, we can see that an averaging time of more than 1500 s is required to determine fourth order moments to 14% accuracy in the canopy, while some way above the surface where integral time scales are longer, the averaging periods required soon become prohibitive.

Lumley and Panofsky (1962) report that the ratio of r.m.s. streamwise velocity to friction velocity, u'/u_* increases with instability while Inoue et al.(1975), have measured similar behaviour at a height of 2.5 m above a field of rice, but no measurements of kurtosis are available. One aspect of the question can be pursued

in the wind tunnel aeroelastic model however, by making use of the fact that the gust arrival frequency scales on mean wind speed. Furthermore the elastic behaviour of the flexible canopy gives us a convenient means of relating wind tunnel velocities to those in the real canopy. This is the 'reduced frequency', U/fL, where U is the mean velocity, L the stalk's length and f its waving frequency. This dimensionless group can be interpreted as the condition for geometric similarity between real crop and model of the waves in canopy height. From the measured values of f and L in the real and model canopy we can say that a windspeed of U_M in the model is equivalent to a speed of $\frac{U_M \cdot f_{model} \cdot L_{model}}{f_{real\ crop} \cdot L_{real\ crop}} \simeq 1.7U_M$.

In constrast to times of instability, we might expect the turbulence amongst the plants to be least intermittent when stabilizing temperature gradients are accompanied by moderate to strong winds. These (admittedly rare) conditions might also be the times when we would expect gradient transport models, despite their shortcomings, to be most successful.

References

Inoue, K., Uchijima, Z., Horie, T. and Iwakiri, S.: 1975, 'Studies of Energy and Gas Exchange within Crop Canopies (10) Structure of Turbulence in Rice Crop', J. Agric. Meteorol. (Japan) 31, 71-82.

Lumley, J.L. and Panofsky, H.A.: 1964, The Structure of Atmospheric Turbulence, Wiley-Interscience, New York.

Seginer, I.: 1974, 'Aerodynamic Roughness of Vegetated Surfaces', Boundary-Layer Meteorol. 5, 383-393.